On the Role of Receptor Downregulation and Costimulation in Shaping the T Cell Response



Philipp Kruger

Sir William Dunn School of Pathology

Exeter College

A thesis submitted for the degree of

Doctor of Philosophy

Trinity term 2018

Acknowledgements

The last four years have been a time of tremendous personal growth and countless opportunities for me and I am indebted to many people who contributed to this wonderful experience.

First to my supervisor Dr Omer Dushek who deserves much of the credit for making me the scientist I am today. Having jumped head-first into a mathematical modelling project without any prior experience, his continued guidance allowed me to explore the new field and build confidence and I truly enjoyed the intellectually stimulating and uniquely collaborative work in his interdisciplinary group. Furthermore, Omer has entrusted me with many responsibilities over the years that I now see as important milestones for my professional development, including the supervision of student projects, co-authoring grant applications, and managing collaborations.

My thanks also go out to all past and present members of the Dushek, Van der Merwe and Brown labs for a most friendly and supportive work environment, for helpful comments and advice during lab meetings, and for sharing their reagents and helping with experiments. More broadly, I could not have wished for a better research department and would like to thank all those Dunn School students, academics and staff who invested time and effort to create such a social and supportive atmosphere, particularly Dr Patty Sachamitr and Professor Matthew Freeman for starting this trend.

I greatly appreciate the advice received from the assessors of my *Transfer to DPhil Status* report and my *Confirmation of DPhil Status* report, Professors Simon Davis, Helen Byrne, Michael Dustin, and Vincenzo Cerundolo, and from my examiners, Dr John James and Professor Michael Dustin, and all those who commented on the work during meetings in Oxford and at conferences.

I gratefully acknowledge the financial support without which this work would not have been possible: The Hugh and Dorothy Usher Cunningham Scholarship from Exeter College Oxford and the Dunn School Departmental Studentship funded by the Edward Penley Abraham Trust. I am also grateful to the Cellular Immunology Unit Trust for providing a postdoctoral extension award that will allow me to continue the work over the next few

months. The work of the lab was further supported by the Wellcome Trust, the Royal Society and Cancer Research UK. Reagents for this project have been kindly provided by our collaborators Professors Simon Davis, Christoph Renner, Marion H. Brown, and Adaptimmune Ltd.

Many thanks also to my friends and family who have provided a healthy social life as an important balance to the research and particularly to Jana for proofreading this whole thesis without understanding a single sentence and finding (hopefully) all the typos.

Finally, I would like to extend my heartfelt thanks to the contractors carrying out the building works on our accommodation for the consideration they showed by delaying the start of the works from February to October 2018, just after I had finished writing.

Contributions

Work in the Dushek lab is extremely collaborative with multiple people working on different aspects of the same project. This means that this thesis includes some work that was performed by other researchers in order to present a complete picture. In addition, I have supervised multiple short student projects which have generated data that was also included here. All the contributions from other people are listed below to provide an overview (Table 0.1), and are again indicated in the corresponding figure legends.

The costimulation work described in chapter 3 forms part of a larger project involving multiple researchers. I have initiated this project and performed many of the pilot experiments for CD28, CD2 and CD6 costimulation. Johannes Pettmann has generated some of the relevant CD2 data presented herein under my supervision when he started as a rotation student, and some of it independently as part of his DPhil project.

Figure	**Contributor**	**Contribution**
Figure 2.2	Nicola Trendel	generated and analysed all the data.
Figure 2.5	Nicola Trendel	same data as in Figure 2.2.

Figure	Contributor	Contribution
Figure 2.6	Nicola Trendel	same data as in Figure 2.2.
Figure 3.10	Johannes Pettmann	generated all the data. I performed the analysis.
Figure 3.11	Johannes Pettmann	generated all the data. I performed the analysis.
Figure 3.13	Johannes Pettmann	generated the CD2 data under my supervision. I performed the analysis.
Figure 3.13	Jake Thomas	generated the CD28 data under my supervision. I performed the analysis.

Tab. 0.1: Contributions from other lab members to figures in this thesis.

The mathematical modelling for this project was even more collaborative and given that the aim of our work is essentially to derive one model that can explain the experimental data from different projects in the lab, it is not surprising that the resulting model must always be the result of a group effort. The final model presented in chapter 2 has been developed over years with major contributions from Omer Dushek, Nicola Trendel, John Nguyen and myself. The parameters for this model were determined by Nicola Trendel and Omer Dushek using an Approximate Bayesian Computation - Sequential Monte Carlo (ABC-SMC) algorithm developed by Nicola Trendel. I have performed the mathematical analyses and parameter modulations presented in chapter 3.

Some of the work presented in this thesis has been included in a manuscript for publication. Almost all the data and much of the text in chapter 2 and two figures in chapter 4 appear in a modified form in (Trendel et al., 2019). This is indicated in the corresponding figure legends. All the text included here that is identical or similar to the paper has been originally written by me. There are some references in chapter 2 to our previous work (Lever et al., 2016) which I have also co-authored, but no data or writing from this publication have been included here.

To Jana, my love,
for making everything in life
seem easy and wonderful

Abstract

T cells are critical decision-makers in the immune system and their activation determines whether a cell or molecule constitutes a threat to the body and needs to be eliminated or whether it should be ignored and tolerated by the immune system. Many molecules that play a role in T cell activation and their interactions with each other have been identified, but an overall understanding of the decision-making processes that lead to changes in T cell behaviour remain enigmatic. We are studying human T cell activation through a combination of *in vitro* experimental stimulation experiments and mathematical modelling. Our minimal experimental platform allows us to systematically vary the input signals the T cell receives by modulating antigen dose, antigen affinity, stimulation time and costimulatory ligands, and by stimulating through either a TCR or a CAR. We show here that T cell activation (measured as cytokine production) shows an adaptation phenotype in response to all antigen doses and affinities. A detailed study of TCR downregulation and the incorporation into a mathematical model revealed that TCR downregulation is sufficient to explain this adaptation. The intrinsic inactivation of the T cells is context-dependent and the cells can be re-activated with a higher affinity ligand. Furthermore, we show that the inactivated cells can be re-activated when a non-stimulating pMHC is presented together with a costimulatory ligand. We generated a similar dataset for CAR T cells and showed that they can equally get desensitised by antigen and that the CAR is also downregulated depending on antigen dose and affinity, suggesting that a similar model may apply. We used the resulting mathematical model of T cell activation to predict the potential effects of costimulatory molecules on the dose response profiles, including, for example, adhesion effects or signal amplification. We then systematically stimulated T cells with ligands to CD2 and CD28 and compared the responses to the model predictions. We found that CD28 primarily lowers the threshold for T cell activation downstream of the TCR whereas CD2 showed a more complex phenotype with a strong adhesion effect combined with amplifying effects on downstream signalling.

Contents

Acknowledgements I
Contributions II
Abstract V
Contents VI

1. Introduction 1

1.1 Initiation of an Immune Response 2
1.2 The T Cell's Role in the Immune System 3
1.2.1 Challenges 4
1.3 Molecular Details of T Cell Activation 5
1.3.1 The T Cell Receptor Complex 5
1.3.2 T Cell Receptor Triggering 6
1.3.3 The Immunological Synapse 8
1.3.4 T Cell Receptor Signalling 9
1.3.5 Costimulation 10
1.3.6 T Cell Effector Functions 11
1.4 T Cell Tolerance 12
1.4.1 Clonal Deletion 12
1.4.2 Anergy and Adaptation 13
1.4.3 Regulatory T Cells 14
1.5 T Cell Cancer Therapy 14
1.5.1 Reversing the Suppressive Microenvironment 15
1.5.2 Tumour Antigens 16
1.5.3 Enhancing Antigen Recognition 16
1.5.4 Redirecting T Cells Towards New Antigens 17
1.6 The Phenotypic Modelling Approach 18
1.7 Aim 20

2. Tuning of TCR Expression Levels to Antigen Strength Limits T Cell Responses 21

2.1 Introduction to TCR Downregulation 22

2.1.1 Mechanisms of TCR Downregulation 22
2.1.2 Downregulation of Non-engaged Bystander TCRs 23
2.1.3 TCR Recycling 24
2.1.4 TCR Downregulation as a Mechanism of T Cell Adaptation 26
2.2 Results 27
2.2.1 Adaptation of T Cell Responses to Antigen Dose and Affinity . . . 27
2.2.2 TCR Downregulation Dynamics 28
2.2.3 Building a Mathematical Model of TCR Downregulation 31
2.2.4 TCR Downregulation Model Reproduces T Cell Adaptation 36
2.2.5 T Cells Adapted to a Low-Affinity Antigen are Re-activated with a Higher-Affinity Antigen 39
2.2.6 T Cell Adaptation to Antigen is Overcome by Costimulation 41
2.3 Discussion 44
2.3.1 Function of Peripheral T Cell Adaptation 44
2.3.2 Mechanisms of Peripheral T Cell Adaptation 45
2.3.3 Model Limitations 47
2.3.4 Comparison to Our Previous Model 48
2.3.5 Other Models of TCR Downregulation 51

3. Quantitative Effects of CD28 and CD2 Costimulation on CD8$^+$ T Cell Activation 55

3.1 Introduction to Costimulation 56
3.1.1 Effects of CD28 Costimulation on T Cell Activation 56
3.1.2 Effects of CD2 Costimulation on T Cell Activation 57
3.2 Results 60
3.2.1 Simulation of Costimulatory Effects on T Cell Activation 60
3.2.2 Expression of Costimulatory Receptors on Human CD8$^+$ T Cells 68
3.2.3 Quantitative Effects of CD28 Costimulation on TCR Downregulation 68
3.2.4 Quantitative Effects of CD28 Costimulation on Cytokine Production 71
3.2.5 Effects of CD28 Costimulation on T Cell Surface Markers 73
3.2.6 Modelling CD28 Costimulation 75

3.2.7 Quantitative Effects of CD2 Costimulation on TCR Downregulation 77
3.2.8 Quantitative Effects of CD2 Costimulation on Cytokine Production 79
3.2.9 Modelling CD2 Costimulation 81
3.2.10 Costimulatory Receptor Up- and Downregulation 84
3.2.11 Quantitative Effects of CD6 Costimulation 86
3.2.12 Effect of CD86 Immobilisation on pMHC Detection 90
3.3 Discussion 94
3.3.1 Costimulatory Effects in Context 94
3.3.2 Limitations 96

4. CAR T Cells are Desensitised by Receptor Downregulation 99
4.1 Introduction to CAR T Cells 100
4.1.1 General CAR Design 100
4.1.2 Clinical Trial Results 101
4.1.3 The Optimal CAR Design 103
4.1.4 CAR Downregulation 104
4.2 Results 106
4.2.1 A Novel CAR T Cell Stimulation System 106
4.2.2 Effects of CAR Signalling on CAR Downregulation 109
4.2.3 CAR T Cells Get Desensitised by Antigen 112
4.2.4 Extrinsic Costimulation Overrides CAR T Cell Desensitisation . . 114
4.3 Discussion 116
4.3.1 Implications of CAR T Cell Adaptation 116

5. Conclusion 119
5.1 Summary 120
5.2 Future Directions 122
5.2.1 The Role of Adaptation 122
5.2.2 Model Refinement 122
5.2.3 Extended Costimulation Project 123
5.2.4 Optimising CAR T Cells 125

6. Materials and Methods 127

6.1 Reagent Suppliers and Brands 128

6.2 List of Reagents 130

6.3 Molecular Biology 137

6.3.1 Polymerase Chain Reaction 137

6.3.2 Agarose Gel Electrophoresis 138

6.3.3 DNA Extraction 139

6.3.4 Restriction Enzyme Digest 139

6.3.5 In-Fusion® Reaction 139

6.3.6 Bacterial Cell Transformation 140

6.3.7 Colony PCR 140

6.3.8 DNA Extraction from Bacterial Cultures 141

6.3.9 DNA Quantification 141

6.3.10 DNA Sequencing 141

6.3.11 Receptor Constructs 141

6.4 Protein Production 142

6.4.1 pMHC Refolding 142

6.4.2 Fluorescent pMHC Tetramers 143

6.4.3 Nickle/NTA Column Protein Purification 143

6.4.4 Biotinylation 144

6.4.5 Fast Protein Liquid Chromatography 144

6.5 Culture of Cell Lines 145

6.5.1 Incubation 145

6.5.2 Jurkat 145

6.5.3 HEK293T 145

6.5.4 CHO 145

6.5.5 Freezing and Thawing 146

6.5.6 Cell Counting 146

6.6 Isolation and Culture of Primary T Cells 147

6.6.1 Blood Collection 147

6.6.2 HLA Typing 147

6.6.3 T Cell Isolation 148

6.6.4 T Cell Expansion 148
6.6.5 Measuring Receptor Expression 149
6.7 HEK293T Transfection 150
6.7.1 Polyethylenimine Transfection 150
6.7.2 X-tremeGENE™ HP Transfection for Lentivirus Production 151
6.8 Lentiviral Transduction 151
6.9 T Cell Stimulation 151
6.9.1 Ligand Immobilisation on Streptavidin-coated Plates 151
6.9.2 Quantification of Ligand Immobilisation 152
6.9.3 T Cell Incubation with Small Molecule Inhibitors 153
6.9.4 T Cell Stimulation 154
6.9.5 Transfer Experiments 154
6.9.6 Flow Cytometry 155
6.9.7 ELISA 155
6.10 Analysis 156
6.10.1 Data fitting 156
6.10.2 Data Normalisation 157
6.10.3 Statistical Analysis 158
6.11 Mathematical Modelling 158

Appendix XI

Abbreviations XI
List of Figures XVI
List of Tables XVII
References XVIII

"On fait la science avec des faits comme une maison avec des pierres; mais une accumulation de faits n'est pas plus une science qu'un tas de pierres n'est une maison."

Henri Poincaré (1854-1912)

Science is built up with facts, as a house is with stones. But a collection of facts is no more a science than a heap of stones is a house.

1 Introduction

1.1 Initiation of an Immune Response

The body's immune response against invading pathogens starts with the recognition of conserved Pathogen-associated Molecular Patterns (PAMPs) by Pattern Recognition Receptors (PRRs) of the innate immune system. These include soluble molecules like complement components or C-reactive protein and receptors expressed on the surface and inside of innate immune cells, such as Toll-like Receptors (TLRs). Some of the first cells to recognise a threat would be tissue-resident macrophages and dendritic cells. Both of these cell types are professional phagocytes, i.e. they have the ability to ingest microbes or their parts, but their functional roles differ. Macrophages are mainly responsible for pathogen clearance and initiating an inflammatory response through mediators like TNF-α. They also play a critical role in wound healing and tissue homeostasis. Dendritic cells are specialised for the activation of T cells. In their immature state, they constantly sample their environment until an inflammatory stimulus or the recognition of PAMPs by PRRs induces their maturation and migration to the T cell zone of the draining lymph node. Examples include the recognition of bacterial lipopolysaccharide or flaggelin by cell surface TLR4 and TLR5, respectively, or the recognition of viral nucleic acids in endosomes by TLR3, TLR7, TLR8, and TLR9. In addition to distinct PAMPs, innate immune cells can also recognise danger signals that derive from cellular stress or tissue damage (Iwasaki and Medzhitov, 2015). The ingested pathogen components will be processed by the dendritic cell to be presented on the cell surface to T cells in the lymph node. Proteins are digested by the proteasome in combination with specialised proteases that generate peptide fragments which can then be displayed by a complex antigen-presentation machinery (Rock et al., 2016) on major histocompatibility complex (MHC) class I and class II molecules on the dendritic cell surface (Zinkernagel and Doherty, 1974). The term maturation summarises several processes that confer full T cell activation potential on the dendritic cell. This includes the further upregulation of MHC molecules and of ligands such as CD80 and CD86 for T cell costimulatory receptors, as well as the production of a range of cytokines. It is important to note that an immature dendritic cell which does not express these costimulatory ligands will induce immunological tolerance when a T cell recognises the presented peptide-MHC (pMHC) (Reis e Sousa, 2006).

CD = cluster of differentiation, TNF = tumour necrosis factor

1.2 The T Cell's Role in the Immune System

T cells are leukocytes of the adaptive immune system that play a central role in the defence against various threats, including infectious diseases and cancer. After their development in the bone marrow and thymus, naïve T cells circulate through the body, screening it for signs of infection or malignancy. Each T cell clone carries a randomly generated T cell receptor (TCR) that binds to a subset of all pMHC complexes ("antigens"). This endows the T cell with a certain specificity, but on the other hand, each TCR must bind to a large number of pMHCs in order for the T cell repertoire to cover all antigens that can theoretically occur in nature (Mason, 1998). When naïve T cells get activated by mature dendritic cells in lymph nodes, they undergo clonal expansion and differentiation into various types of effector cells, some of which eventually become long-lived memory cells. T cells can be further divided into two main subsets, classified by the expression of the co-receptors CD4 and CD8. $CD4^+$ T cells are a heterogeneous group of cells that contains different subsets of helper T cells and regulatory T cells. Helper T cells serve many different functions in the immune system, most of which involve activating other cell types such as B cells and macrophages, to facilitate more effective immune responses. The type of T cell response initiated depends on the cytokines produced by the activating dendritic cell which is itself determined by the initial PAMP stimulus. Hence, different pathogens induce different T cell responses which then lead to different immunological effects (Iwasaki and Medzhitov, 2015).

Cytotoxic $CD8^+$ T cells are the main subset studied in this thesis. They are also initially activated by dendritic cells, but require additional help from $CD4^+$ T cells for full activation (Tham et al., 2002; van Mierlo et al., 2004; Su et al., 2009; Ahrends et al., 2017). Their main functions are the production of pro-inflammatory cytokines and the direct elimination of infected or malignantly transformed host cells. $CD8^+$ T cells constantly screen the body for signs of infection or malignancy by scanning the peptides that are displayed by all nucleated cells on MHC class I molecules on their surface (Zinkernagel and Doherty, 1974). The peptides are sampled from all the proteins in the cytosol including, for example, viral proteins during an infection or proteins that are expressed in cancer cells, such

as NY-ESO-1 (Chen et al., 1997). A $CD8^+$ T cell will ignore the target cell if it only presents peptides derived from self-proteins (self-pMHC), but it will kill it if it detects foreign peptides, for example from a virus.

1.2.1 Challenges

T cells face a number of unique challenges due to their biological role as versatile decision makers (as discussed by Van der Merwe and Dushek (Van der Merwe and Dushek, 2011)). The T cell must be able to:

1) **recognise structurally diverse ligands**. Unlike most other receptors, the TCR binds to a range of pMHC ligands, each of which will have a different binding interface and affinity. The interface is determined by the MHC allele, the presented peptide and the hypervariable CDR loops of the TCR that mediate most of the contact with the antigen (Davis and Bjorkman, 1988). However, evidence from crystal structures suggests that different TCRs share a common binding orientation diagonal to the MHC (Rudolph et al., 2006).

2) precisely **measure the affinity of the TCR-pMHC bond** and translate this information into biologically different responses (Courtney et al., 2018). Examples for this include selection in the thymus where a low-affinity interaction of a newly generated TCR with self-pMHC results in a survival signal and the positive selection of the developing T cell, whereas a high-affinity interaction with a self-pMHC results in a death signal and negative selection (Kappler et al., 1987; Kisielow et al., 1988). In addition, there is evidence that mature T cells rely on low-affinity interactions with self-pMHC for their homeostatic survival in the periphery (Tanchot et al., 1997), while binding to a high-affinity pMHC during an infection would cause the same cells to respond with clonal expansion and differentiation into effector cells.

3) **recognise minute amounts of its cognate pMHC**. This is necessary because intracellular pathogens and cancer cells have evolved immune evasion mechanisms that downregulate antigen processing and presentation pathways (Gewurz et al., 2001; Tobar et al., 2004; Sahin et al., 2017). Some studies suggest that T cells can recognise

NY-ESO = New York esophageal squamous cell carcinoma, CDR = complementarity-determining region

and at least partially respond to one single pMHC complex (Sykulev et al., 1996; Irvine et al., 2002; Purbhoo et al., 2004). This striking sensitivity is all the more remarkable given that TCR binding affinities are generally quite low (in the micromolar range (Aleksic et al., 2012)) compared to other receptor-ligand interactions and particularly compared to B cell receptors that undergo somatic hypermutation to increase their affinity.

4) **discriminate between self and non-self**. The few foreign pMHC complexes that the T cell should respond to will be presented on the APC surface alongside hundreds of thousands of self-pMHCs (Irvine et al., 2002). This raises the question how the T cell is able to display such a high sensitivity for foreign peptides while ignoring the self-pMHCs and avoiding autoimmune reactions. T cells discriminate between antigens based on their affinity and a high antigen concentration cannot compensate for low affinity (Altan-Bonnet and Germain, 2005; Dushek et al., 2011). It was originally shown by McKeithan that such a phenotype can be achieved through a kinetic proofreading mechanism (Mckeithan, 1995), but the molecular mechanisms that mediate this process are still unclear.

1.3 Molecular Details of T Cell Activation

1.3.1 The T Cell Receptor Complex

The subject of this thesis is the $\alpha\beta$ T cell receptor complex which consists of multiple polypeptide chains. The binding interface that interacts with the pMHC complex is formed by the TCRα and TCRβ chains linked through a disulfide bond, but their minimal intracellular tails have no known signalling capacity. The complex further contains a disulfide-linked CD3ζ homodimer, a CD3γ-CD3ϵ heterodimer and a CD3δ-CD3ϵ heterodimer (Samelson et al., 1985; Call et al., 2004; Alcover et al., 2018). However, due to the lack of a complete crystal structure of the complex, the exact arrangement of the chains is unknown (Alcover et al., 2018).

The ligand-binding TCRα and TCRβ chains are generated independently during T cell development in the thymus through genetic rearrangement. They each consist of a variable and a constant domain. The variable part of the receptor interacts with the pMHC

and is assembled randomly from V, D and J gene fragments, ensuring that each TCR has distinct binding properties. The diversity created through the recombination of the three fragments (or two for the α chain that does not contain a D fragment) is further increased by the random insertion and deletion of nucleotides at the junctions. The variability is concentrated mostly in the hypervariable CDR1, 2 and 3 loops of which CDR3 is thought to interact mostly with the peptide (Davis and Bjorkman, 1988). This process ensures that a broad repertoire of unique TCRs is generated.

1.3.2 T Cell Receptor Triggering

All the CD3 chains mediate TCR signalling via immunoreceptor tyrosine-based activation motifs (ITAMs) in their intracellular tails (Reth, 1989). CD3ζ contains three ITAMs, whereas CD3ϵ, γ and δ contain one ITAM each. The reversible phosphorylation of the tyrosine residues within the ITAMs by Src family kinases like Lck is considered the first step in the signalling cascade downstream of the TCR (Courtney et al., 2018), but it is still unclear how the initial pMHC binding event triggers ITAM phosphorylation and the subsequent signalling from the multi-subunit TCR complex. This has long been one of the major open questions in T cell biology and multiple mechanisms for TCR triggering have been proposed. Each is based on experimental evidence and each is more or less controversial, but it is worth noting that these mechanisms are not necessarily mutually exclusive (Minguet et al., 2007; Van der Merwe and Dushek, 2011; Courtney et al., 2018).

The **oligomerisation of multiple TCRs into clusters** upon antigen binding could explain how a downstream signal is generated, but such models have difficulty explaining the T cell sensitivity to very low ligand doses (Van der Merwe and Dushek, 2011). As a solution, several models have been proposed that postulate the formation of a TCR cluster in response to only one pMHC ligand, for example by assuming that self-reactive TCRs form clusters together with the foreign-peptide specific TCR (Irvine et al., 2002; Krogsgaard et al., 2005), or that TCRs already exist in nanoclusters on resting T cells (Pageon et al., 2016; Martin-Blanco et al., 2018). The experimental evidence for this is still conflicting because some investigators have found pre-existing TCR clusters (Scha-

Lck = lymphocyte-specific protein tyrosine kinase

mel et al., 2005; Sherman et al., 2011; Lillemeier et al., 2009; Pageon et al., 2016) while others have found the TCR to be almost exclusively monomeric on resting cells (James et al., 2007; Brameshuber et al., 2018).

A **conformational change** in the TCR would be an obvious mechanism to explain how binding of a single pMHC can trigger downstream signalling. It has been argued that conformational changes could be the consequence of pulling and shearing forces during T cell-APC interactions that arise from the movement of the cells and the actin cytoskeleton (Sun et al., 2001; Li et al., 2010). There is experimental evidence for a conformational change in the constant domain of the TCRα chain (Kjer-Nielsen et al., 2003; Beddoe et al., 2009) and in CD3ϵ (Martínez-Martín et al., 2009; Wang et al., 2009) and mutation of either of the involved motifs abrogates TCR signalling. However, any conformational change model would need to take into account the immense structural diversity of the TCR-pMHC binding interface (discussed above) and it still not clear how a conserved mechanism might initiate such a change. One mechanism that has been proposed based on the structure of the CD3ϵ-CD3γ heterodimer can be described as a "piston-like" displacement of the CD3 chains upon TCR binding (Sun et al., 2001; Kim et al., 2010). Such changes could increase the accessibility of the CD3 chains as some of them have been reported to be closely associated with membrane lipids in resting TCRs (Xu et al., 2008; Lee et al., 2015). Others have argued that conformational changes might occur mostly on the level of entire TCR complexes and induce the dimerisation or oligomerisation of TCRs (Minguet et al., 2007; Kuhns et al., 2010) or indeed the heterodimerisation of the TCR with its co-receptor (Palmer and Naeher, 2009).

The **Kinetic Segregation Model** (Davis and Van Der Merwe, 1996, 2006) posits that the TCR is constitutively phosphorylated by membrane-associated kinases like Lck and dephosphorylated by transmembrane phosphatases like CD45. Phosphatase activity dominates in a resting T cell and prevents TCR signalling. However, once the T cell comes into contact with an APC, the TCR binds to pMHC and this interaction creates an intermembrane distance of around 15 nm (Rudolph et al., 2006), which sterically excludes the bulky extracellular domain of CD45 (Irles et al., 2003; Chang et al., 2016). This passive process is further promoted by other receptor-ligand pairs of similar size, like

CD2-CD58 and CD28-CD86, which are discussed in more detail in chapter 3. The shifted kinase-phosphatase balance means that within the close contact, the TCR ITAMs will be phosphorylated even when the TCR is not engaged. However, the kinetic segregation model assumes that unbound TCRs will diffuse out of the close contact before they can initiate downstream signalling. The binding to a pMHC ligand will slow this diffusion and retain the TCR out of the reach of phosphatases for long enough to trigger downstream signalling and activate the T cell. The exclusion of CD45 from the TCR-pMHC binding regions can be readily observed by microscopy when T cells interact with APCs (Leupin et al., 2000; Stinchcombe et al., 2001; Douglass and Vale, 2005; Varma et al., 2006), and this segregation as well as T cell signalling can be abrogated when CD45 is truncated or the pMHC ligand is elongated (Irles et al., 2003; Choudhuri et al., 2005; James and Vale, 2012).

1.3.3 The Immunological Synapse

When a T cell comes into contact with an APC that presents the cognate antigen, the two cells will form a highly structured cell-cell interface that involves the physical reorganisation of receptors, membranes and the cytoskeleton. The bound TCRs form microclusters together with signalling molecules like Lck and PKC-θ in the periphery of the interface which then move towards the centre of the synapse where they form a central supermolecular activation cluster (cSMAC) (Monks et al., 1998; Grakoui et al., 1999; Leupin et al., 2000; Stinchcombe et al., 2001; Potter et al., 2001; Douglass and Vale, 2005). The integrin LFA-1, an adhesion molecule important for T cell activation, forms a ring around the cSMAC that is termed peripheral SMAC (pSMAC) (Irvine et al., 2002; Purbhoo et al., 2004). During synapse formation, the actin cytoskeleton is reorganised to open up the centre of the synapse and accumulate outside of the pSMAC (Stinchcombe et al., 2006; Douglass and Vale, 2005). The microtubule-organising centre is recruited to the centre of the synapse where, in $CD8^+$ T cells, it mediates the delivery of cytotoxic granules to the membrane (Stinchcombe et al., 2001, 2006). TCR signalling derives from the microclusters in the periphery of the synapse and is terminated through receptor downregulation once they reach the cSMAC (Varma et al., 2006). Functionally, the formation of a structu-

PKC = protein kinase C, LFA = lymphocyte function-associated antigen

red immunological synapse has been suggested to provide the antigen-dependent stop signal for T cell migration (Grakoui et al., 1999), to contribute to T cell antigen discrimination (Grakoui et al., 1999), the exclusion of transmembrane phosphatases (Douglass and Vale, 2005; Varma et al., 2006), the concentration of receptors and signalling molecules (Lee et al., 2003; Douglass and Vale, 2005; Grakoui et al., 1999) and to the eventual abrogation of signalling through receptor downregulation in the cSMAC (Lee et al., 2003; Varma et al., 2006). TCR downregulation is discussed in more detail in chapter 2.

1.3.4 T Cell Receptor Signalling

The signalling cascades that follow TCR triggering have been extensively studied and hundreds of protein interactions have been reported to take place (Roncagalli et al., 2014; Courtney et al., 2018). However, the function of this stunning complexity remains largely elusive. Different signalling modules and feedback loops will likely contribute to antigen discrimination, signal amplification, diversification, ultrasensitivity, or provide integration points for other signalling pathways, but very few such functional modules have been identified to date and I will therefore only summarise the known biochemical interactions briefly.

The phosphorylation of the CD3 ITAMs by Lck is usually considered the first step in TCR signalling, although Lck is itself regulated through phosphorylation and dephosphorylation by Csk and CD45, respectively (James and Vale, 2012). Lck asociates with the plasma membrane either through myristoylation and palmitoylation or through association with the co-receptor CD4 or CD8 (Veillette et al., 1988). It has been suggested that the main function of the co-receptors is to bind the pMHC and thereby bring Lck into close proximity with the TCR ITAMs (Artyomov et al., 2010). The phosphorylated ITAMs then serve as docking sites for the tandem SH2 domains of ZAP70 which is itself also activated by Lck and through trans-autophosphorylation (Chan et al., 1992). Active ZAP70 in turn phosphorylates the adaptor proteins LAT and SLP76 which nucleate the LAT signalosome, a complex that contains a vast number of enzymes and adaptor proteins

Csk = C-terminal Src kinase, SH2 = Src homology region 2, ZAP70 = Zeta chain-associated protein of 70 kDa, LAT = linker for activation of T cells, SLP76 = SH2 domain-containing leukocyte protein of 76 KDa, PLC = phospholipase C, NFAT = nuclear factor of activated T cells, NFκB = nuclear factor 'kappa-light-chain-enhancer' of activated B cells

and initiates almost all further TCR signalling (Roncagalli et al., 2014). The phosphorylation of PLC-γ1 results in the activation of two signalling pathways: A calcium-dependent pathway that culminates in the nuclear translocation of the transcription factor NFAT, and the activation of PKC which triggers the NFκB signalling pathway and can also activate c-jun, a subunit of the transcription factor AP-1. Other components of the LAT signalosome trigger the activation of WASp which is responsible for actin remodelling and cytoskeletal rearrangements. The LAT signalosome also triggers the MAPK signalling pathway that culminates in activation of ERK and transcription of c-fos, the second component of AP-1. Thus, all three major transcription factors that characterise T cell activation, NFAT, NFκB and AP-1, are induced by the LAT signalosome (Courtney et al., 2018).

1.3.5 Costimulation

T cell costimulation is defined as a second signal beside the TCR which modulates or amplifies TCR signalling. It is required for full T cell activation but cannot activate the T cell on its own. The two-signal hypothesis of lymphocyte activation was first proposed for B cells in 1970 (Bretscher and Cohn, 1970) and extended to T cells in 1975 (Lafferty and Cunningham, 1975). The theory was then confirmed experimentally in a series of *in vitro* experiments and CD28 was shown to be the receptor that mediates the second signal that is required for full T cell activation, particularly for the activation of naïve $CD4^+$ T cells (Mueller et al., 1989; June et al., 1987; Harding et al., 1992). However, the view of the second signal to be absolutely essential for T cell activation has been challenged and costimulation is now seen more as a quantitative and qualitative modulator of T cell activation (Bachmann et al., 1996; Deenick et al., 2003; Skånland et al., 2014; Esensten et al., 2016). A multitude of different receptors have been described to costimulate T cells, including members of the CD28 family of receptors (e.g. CD28, ICOS), the TNF receptor family (e.g. CD27, 4-1BB), and the CD2/SLAM family. In addition, T cells express many receptors that can inhibit T cell activation, for example, PD-1, CTLA-4 or BTLA. Expression of all these receptors on the T cell is tightly regulated by the

AP = activator protein, WASp = Wiskott–Aldrich Syndrome protein, MAPK = mitogen-activated protein kinase, ERK = extracellular-signal regulated kinase, ICOS = inducible T cell costimulator, SLAM = signalling lymphocytic activation molecule, PD-1 = programmed cell death protein 1, CTLA = cytotoxic T lymphocyte-associated protein, BTLA = B and T lymphocyte attenuator

environment and the T cell's activation and differentiation state (Chen and Flies, 2013). However, beyond a binary classification into activating and inhibitory receptors, we know very little about the functional roles of individual receptors. Costimulation through the two receptors studied in this thesis, CD2 and CD28, is discussed in more detail in chapter 3. CD28 costimulation generally needs to be presented together with the TCR ligands to be effective whereas some cytokines that contribute to the differentiation of naïve $CD4^+$ T cells into different helper cell subsets can still act after the TCR signal has subsided (Iezzi et al., 1999).

1.3.6 T Cell Effector Functions

Downstream of the signalling network, activation of the three main transcription factors AP-1, NFAT and NFκB results in wide-ranging phenotypic changes in the T cell including the upregulation of cell surface receptors such as CD69, 4-1BB and PD-1, metabolic changes, cytokine production, cell division and, in the case of cytotoxic $CD8^+$ T cells, direct target cell killing through upregulation of Fas ligand or through secretion of perforin and granzymes. The exact outcome of T cell activation depends on the T cell subset, the antigenic stimulus and many modulating factors like the cytokine environment and costimulatory signals.

Most importantly for this thesis, $CD8^+$ T cells produce several effector cytokines, including TNF-α, IFN-γ, GM-CSF, RANTES, MIP-1α and MIP-1β (Kristensen et al., 2004; van den Berg et al., 2013; Jenkins et al., 2015). They also produce IL-2 upon initial activation, but later depend on $CD4^+$ T cells for the supply of this critical survival and proliferation factor (Tham et al., 2002). TNF-α and IFN-γ have been shown to be important effector molecules for $CD8^+$ T cell-mediated tumour and infection control in mouse models (Prévost-Blondel et al., 2000; Hausmann et al., 2005; Allie et al., 2013; Ligocki et al., 2015). In humans, however, the physiological role of $CD8^+$ T cell-derived cytokines is less clear, mostly because the same cytokines can also be produced by other cell types like $CD4^+$ T cells or natural killer (NK) cells. In the extreme cases of patients with a deficiency in perforin-mediated killing, $CD8^+$ T cells fail to disengage from their target

Fas = first apoptosis signal, IFN = interferon, GM-CSF = granulocyte-macrophage colony-stimulating factor, RANTES = regulated on activation, normal T cell expressed and secreted, MIP = macrophage inflammatory protein

cell and produce more IFN-γ, TNF-α and IL-2 (Jenkins et al., 2015) and this contributes to systemic inflammation. However, this result is confounded by the fact that NK cells are similarly affected by this deficiency and show an even stronger increase in the production of these cytokines. Indeed, the patients affected by this disease often develop life-threatening cytokine release syndrome in the first few weeks of life when the $CD8^+$ T cell compartment is not yet fully developed (Jenkins et al., 2015).

1.4 T Cell Tolerance

As discussed above, the T cell receptor binding domains for new T cells are generated during thymic development through genetic recombination. The randomness of this process means that T cells will also recognise self-peptides that should not elicit an immune response. Subsequently, T cells that bind to self-antigens presented on medullary thymic APCs with too high an affinity receive a death signal ("negative selection") (Kappler et al., 1987; Kisielow et al., 1988). This deletion process prunes the T cell repertoire of the most strongly self-reactive clones and establishes "Central Tolerance", but it is not perfect. Only a subset of all possible self-peptides are expressed by medullary thymic APCs (Derbinski et al., 2005) and even if the antigen is expressed, some T cells might be just below the affinity threshold for deletion and could potentially respond to self-antigen in peripheral organs. Thus, T cells can elicit unwanted immune responses against self-antigens which can lead to severe autoimmune disorders like type 1 diabetes mellitus (Roep and Peakman, 2012) or multiple sclerosis (Riedhammer and Weissert, 2015). Consequently, in order to ensure immune tolerance to self, T cell recognition and responsiveness is tightly regulated by multiple different processes in the periphery.

1.4.1 Clonal Deletion

Self-reactive T cell clones can be subjected to apoptotic cell death upon TCR signalling in the periphery under some conditions, particularly as a result of chronic antigen stimulation (Kurts et al., 1997; Hernandez et al., 2001; Redmond et al., 2005; Singh et al., 2006). This is mediated by immature or tolerogenic APCs that express low levels of costimulatory ligands, but it is not entirely clear which factors determine whether a T

cell receives a death signal or is merely inactivated (see next section) (Redmond et al., 2005; Singh et al., 2006).

1.4.2 Anergy and Adaptation

During thymic development, positively selected T cell precursors are known to undergo a "tuning" or "adaptation" process via upregulation of CD5 that is believed to set their TCR signalling thresholds depending on how strongly they interact with self-antigens presented by thymic APCs (Azzam et al., 2001; Wong et al., 2001). Similar adaptation processes take place in the periphery, but a multitude of different underlying mechanisms have been reported including upregulation of CD5 and downregulation of the TCR (Schönrich et al., 1991; Tafuri et al., 1995; Smith et al., 2001; Stamou et al., 2003; Singh and Schwartz, 2003; Hawiger et al., 2004; Ryan et al., 2005; Chiodetti et al., 2006; Lees et al., 2006; Han et al., 2010). Continuous T cell tuning in the periphery has long been appreciated as an important process to prevent autoimmunity while retaining self-reactive T cells which might be important to cover the microbial peptide repertoire (The Tunable Activation Threshold model (Grossman and Paul, 1992)). Human tumour-specific $CD8^+$ T cells appear to be able to re-adjust their adaptation level and become responsive again towards their respective antigen, compared to peripheral blood T cells from the same individual (Dorothee et al., 2005). The term "clonal anergy" was initially introduced to describe the intrinsic unresponsive state observed when B or T cells are stimulated with their cognate antigen without appropriate costimulatory signals for full activation. This is believed to constitute an alternative fate for self-reactive T cells that establishes peripheral tolerance without deletion of the cells. However, as Ronald Schwartz, one of the pioneers in this field of research, wrote, the literature on this topic soon became difficult to navigate. Due to a lack of understanding of the underlying mechanisms driving this unresponsiveness, "the term anergy was used to describe almost any tolerance phenomenon in which the lymphocytes survived and appeared to be functionally unresponsive" (Schwartz, 2003). This assessment applies to the studies mentioned above some of which refer to the reported unresponsive state as anergy, others as adaptation, adaptive tolerance, calibration or desensitisation. While there are almost certainly different pathways in existence that can intrinsically inactivate self-reactive T cells in the

periphery, it is far from clear whether two studies that use different terminology are actually discussing two different phenomena. Conversely, it is very likely that many studies that used the same terminology actually reported on distinct functional states.

T cells can also undergo a process called "exhaustion", but this unresponsive state is usually not suggested to be a mechanism of peripheral tolerance to self-antigen but rather a process that limits excess T cell activation in response to foreign antigen, for example during chronic infections. Its molecular pathways are relatively well understood and involve the upregulation of multiple inhibitory receptors and epigenetic changes in the T cells (Wherry, 2011).

1.4.3 Regulatory T Cells

Regulatory T cells (Tregs) are specialised T cells that inhibit a broad range of processes in the immune system, most importantly the activation and effector functions of other T cell subsets. The best characterised Treg population is a subset of $CD4^+$ T cells that express the transcription factor FoxP3 and express high levels of CD25. These cells can originate from the thymus (Itoh et al., 1999) where they are believed to have recognised self-antigens with higher affinity than their effector $CD4^+$ T cell cousins (Jordan et al., 2001), but they can also be generated in the periphery (Apostolou and von Boehmer, 2004). Patients that lack FoxP3 suffer from severe systemic autoimmune reactions early in life and provide clear evidence for the Tregs' critical role in peripheral tolerance (Bacchetta et al., 2016). However, they employ a multitude of different effector mechanisms (reviewed in (Schmidt et al., 2012)) and a detailed discussion of their functions would go beyond the scope of this thesis.

1.5 T Cell Cancer Therapy

The Cancer Immunosurveillance Hypothesis was first proposed by Paul Ehrlich in 1908 (Ehrlich, 1909) and states that within multicellular organisms, abberant cells are constantly generated and would grow into tumours if they were not kept under control by the immune system. We know today that the immune system has various ways of recognising

FoxP3 = forkhead box P3

and eliminating cancerous cells, including the specific recognition of tumour antigens by T cells. The central question in the research field of cancer immunotherapy is how to fully activate the endogenous capacity of the immune system to eliminate cancer cells. Ideally, the response initiated by such a therapy would be restricted to the tumour tissue and create a long-lasting immune memory to protect the patient from a relapse. T cells are antigen-specific, have the potential of tumour homing, clonal expansion, long-term persistence and immune memory and they directly lyse tumour cells, rendering them ideal effectors for cancer immunotherapy. However, a tumour that leads to a clinical diagnosis has by definition escaped control by the immune system. For example, tumour cells often downregulate MHC molecules to render themselves invisible to T cells (Sahin et al., 2017). Additionally, many solid tumours actively establish an immunosuppressive microenvironment to inhibit anti-tumour immune responses.

1.5.1 Reversing the Suppressive Microenvironment

The most successful cancer immunotherapy approach to date has been the application of checkpoint inhibitors, antibodies that block immune-inhibitory pathways and thereby release the endogenous anti-tumour immune response. The first checkpoint inhibitor was Ipilimumab, an antibody against the inhibitory receptor CTLA-4 that is expressed on T cells (Krummel and Allison, 1995; Leach et al., 1996). Ipilimumab is now clinically approved for use against multiple different types of cancer and a recent meta analysis of clinical trial data for melanoma showed a plateau in the survival curves from around three years after treatment, i.e. the 20 % of patients who survived for three years were still alive at the ten year follow-up (Schadendorf et al., 2015). Other checkpoint inhibitors that target the inhibitory receptor PD-1 or its ligands have achieved even more impressive clinical results and the combination with Ipilimumab increases the three-year survival of melanoma patients to 58 %, but also leads to severe autoimmune side effects in many patients (Wolchok et al., 2017). Many other immune-inhibitory receptors are currently under pre-clinical and clinical investigation as targets for potential checkpoint inhibitors.

Another way of shifting the tumour microenvironment towards a more inflammatory mil-

lieu would be to provide immune-activating or inflammatory stimuli. For example, these could be Toll-like receptor agonists (Sagiv-Barfi et al., 2018), stimulating antibodies that target T cell costimulatory receptors (Berman et al., 2015; Sagiv-Barfi et al., 2018) or pro-inflammatory cytokines (Hu et al., 2017; Chmielewski and Abken, 2017; Avanzi et al., 2018).

1.5.2 Tumour Antigens

Cancer arises from the malignant transformation of healthy cells which means that the vast majority of the antigens expressed by a tumour cell will be self-antigens. Consequently, it is not obvious which antigens drive the T cell response against a tumour. Tumour antigens can be broadly classified into two groups:

1) **Neoantigens** which are altered peptides that arise from mutations in the tumour cell genome and - when presented by the MHC - are recognised as completely tumour-specific non-self antigens (Monach et al., 1995; Coulie et al., 1995). This can also include viral antigens if the tumour has a viral aetiology. Recent evidence suggests that neoantigens are the main targets of the T cell response elicited by checkpoint inhibitor therapy (Gubin et al., 2014; Rizvi et al., 2015).

2) **Tumour-associated antigens** which groups together everything that is not truly tumour-specific, including proteins that are highly overexpressed by tumour cells (for example carbonic anhydrase IX (Lamers et al., 2013) or ErbB2 (Morgan et al., 2010)), organ- or lineage-specific proteins like CD19 (Davila et al., 2014; Maude et al., 2018) and proteins that are expressed only in cancer cells and normally during development or in immune-privileged sites (NY-ESO (Chen et al., 1997), MAGE-A3 (Linette et al., 2013)).

1.5.3 Enhancing Antigen Recognition

Different cancer immunotherapy strategies have been designed to improve the endogenous anti-tumour T cell response either by increasing the number and activation state of the relevant T cell clones or by introducing higher-affinity TCRs. One strategy to increase T cell numbers is the isolation of tumour-infiltrating lymphocytes (TILs) from resected

MAGE = melanoma-associated antigen

tumour tissue which are mostly specific for neoantigens. The TILs are then expanded *in vitro* before they are re-infused into the patient's blood stream. It has been shown that they can home to the remaining tumour sites and completely eradicate the cancer in some cases (Zacharakis et al., 2018), but the *in vitro* cell expansion is not always reliable and many patients do not respond at all. A number of other approaches can be summarised as "cancer vaccinations". These generally aim to introduce tumour antigens into the patient, mostly together with some form of adjuvant to improve the immune response. A dendritic cell vaccine is already approved for clinical use in prostate cancer (although it is controversial whether it provides any benefit) (Huber et al., 2012) and recent clinical results indicate that neoantigen vaccines delivered either as mRNA or as peptide cocktails can trigger polyclonal T cell immune responses in patients (Sahin et al., 2017; Ott et al., 2017).

Tumour-associated antigens are self-antigens and the responding T cells can therefore be subject to negative selection in the thymus (Träger et al., 2012). This means that tumour-specific TCRs generally exhibit a lower binding affinity for their target antigen than TCRs that recognise foreign antigens (Aleksic et al., 2012). However, tumour-specific TCRs can be genetically modified to increase their binding affinity and this approach has been taken in studies with adoptively transferred patient T cells carrying the new TCR (Rapoport et al., 2015) and with soluble TCRs that were connected to an anti-CD3 antibody (ImmTACs®) (Liddy et al., 2012). Some clinical studies report promising anti-tumour activity (Rapoport et al., 2015), but the high-affinity TCRs can also respond to low-level antigen expression on healthy cells or exhibit unpredictable crossreactivity which has resulted in fatal toxicities (Linette et al., 2013).

1.5.4 Redirecting T Cells Towards New Antigens

The adoptive transfer of autologous T cells that are genetically modified to express chimeric antigen receptors (CARs) is a novel approach to antigen-specific cancer immunotherapy. The CAR strategy employs the antigen diversity and specificity of antibodies for the redirection of T cells against cell surface tumour-associated antigens independent of MHC molecules. A CAR is an engineered receptor that is introduced genetically into the

ImmTAC = immune mobilising monoclonal TCRs against cancer

T cells of a cancer patient. The CAR T cells are then re-infused into the patient's blood stream where the CAR recognises the tumour antigen and delivers a T cell activation signal which results in the killing of the tumour cell and the production of cytokines. CAR design and clinical results are discussed in more detail in chapter 4.

A similar approach has led to the development of bi-specific T cell engagers, engineered antibodies which recognise a tumour antigen with one arm and a CD3 chain with the other. They also redirect T cells towards the tumour cell and activate them regardless of their endogenous TCR specificity, but in contrast to CARs, they are soluble molecules and not patient-specific. They have shown remarkable clinical activity in leukaemia which has led to clinical approval (Topp et al., 2012).

1.6 The Phenotypic Modelling Approach

The work presented in this thesis combines T cell stimulation experiments with mathematical modelling to better understand T cell activation quantitatively. Biological systems can be simulated at different levels of detail, ranging from models that encompass whole ecosystems to atom-level molecular dynamics simulations of a single protein subunit. However, it is important to note that even the most detailed model is still only a model of the real system and therefore incomplete and simplified. On the other hand, even a very coarse-grained model can make useful predictions about the behaviour of a system, for example the simple model of the spread of an infectious disease by Kermack and McKendrick which underlies the concept of herd immunity, i.e. it predicts that an epidemic can only occur when a certain minimal fraction of the population is susceptible to the disease (Kermack and McKendrick, 1927).

The system we are trying to understand is a single cell, or more specifically, the process of how this cell responds to input signals with changes in behaviour. For such cellular models, the most common modelling approach is to explicitly include in the model the individual proteins that have been found biochemically to play a role in the respective pathway. In the case of T cells, an immensely complex signalling network has been identified, but how this complexity leads to the phenotype of T cell activation is still poorly understood. This is due to the fact that mathematical models at this level of detail are as-

sociated with a high degree of uncertainty because the accuracy of their predictions relies on too many parameter values that are difficult to determine (protein concentrations, reaction rates, etc.). The model of immunological synapse formation, TCR downregulation and signalling produced by Lee et al. is a good example of this modelling approach (Lee et al., 2003). In this study, a large number of signalling interactions was incorporated into a complex model, not because they were necessary to explain the experimental findings, but because those interactions had been reported previously. Examples include sequential ITAM phosphorylation by Lck, TCR recycling, and positive and negative feedback loops between Lck, ERK and the phosphatase SHP-1 (Lee et al., 2003). The resulting model is associated with high uncertainty, because its predictions depend on reliable estimates for all the parameters. A second disadvantage of such a complex model is that it is much more difficult to understand the contribution of different processes in the model to the outcome and therefore, to develop an intuitive understanding of the mechanisms underlying the observed behaviour.

We are employing a phenotypic modelling approach that primarily aims to explain the observed input-output relationship of the system, its behaviour, rather than its biochemical architecture. Such an approach is particularly useful for the study of decision-making processes in T cell activation because of the extreme complexity of the signalling network (Gett and Hodgkin, 2000; Lever et al., 2016; Proulx-Giraldeau et al., 2017). A consequence of this approach is that we are trying to find the simplest possible model that can explain the data. This allows us to identify the minimal set of reactions necessary to achieve a certain behaviour or phenotype, without making any assumptions about the underlying processing machinery. This means that we can identify motifs, for example a positive feedback loop, and understand their function in the pathway. However, such a results cannot be interpreted as positive feedback between two proteins that activate each other, but rather as more abstract modules that might consist of multiple proteins (and other molecules) within the cell. In other words, the resulting model cannot be directly mapped onto the known biochemical pathways, but its limited complexity makes it more intuitive.

SHP = Src homology region 2 domain-containing phosphatase

1.7 Aim

The overall aim of this thesis is to contribute to a better understanding of the processes that govern T cell activation.

In chapter 2, we investigate the role of TCR downregulation in limiting primary human T cell responses. We systematically analysed T cell activation in response to different antigen doses and affinities over time and found that T cells show an adaptation phenotype during stimulation and quickly downregulate their TCRs. Based on this data, we built a mathematical model of T cell activation that incorporates TCR downregulation dynamics. It shows that TCR downregulation alone is sufficient to explain T cell adaptation at all antigen doses.

The results presented in chapter 3 represent part of a larger project that aims to contribute to a better understanding of the functional differences between different T cell accessory receptors beyond a binary classification. Using a similar approach as in chapter 2, T cells were stimulated systematically with different pMHC doses and affinities together with ligands for CD28 and CD2. The effects those costimulatory receptors have on the pMHC dose response curves were then compared to predictions the mathematical model from chapter 2 makes for defined mechanisms such as adhesion effects, a decreased T cell activation threshold, or an amplification of existing signals.

Finally, chapter 4 describes the first data on CAR T cell function from a newly developed experimental system. By using large variations in antigen dose and affinity without the involvement of adhesion molecules, costimulatory or inhibitory receptors, this system can provide quantitative insights into CAR T cell activation. Combined with mathematical models, this systematic data can then be used to predict improvements to CAR design in the future. We show here that CAR downregulation upon antigen engagement correlates with antigen strength and with T cell activation, as it does for TCRs. We further show that, similar to the TCR in chapter 2, first-generation CAR T cells are limited by adaptation in response to antigen.

2 Tuning of TCR Expression Levels to Antigen Strength Limits T Cell Responses

2.1 Introduction to TCR Downregulation

The downregulation of the TCR is known to take place upon antigen encounter (Reinherz et al., 1982; Zanders et al., 1983; Schönrich et al., 1991; Valitutti et al., 1995; Cai et al., 1997) but its functional significance remains controversial. In early work it was thought that TCR downregulation was a measure of T cell activation because it correlated strongly with activation markers and was similarly modulated by antigen affinity and dose (Valitutti et al., 1995; Viola and Lanzavecchia, 1996; Cai et al., 1997; Itoh et al., 1997; Martin and Bevan, 1998; Bachmann et al., 1997b). However, subsequent work has shown that TCR downregulation can take place in the absence of TCR signalling (e.g. by blocking tyrosine kinases) and must therefore be distinct from T cell activation (Cai et al., 1997; Salio et al., 1997; San Jose et al., 2000; Monjas et al., 2004). It was also shown to be independent of CD28 costimulation (Cai et al., 1997; Bachmann et al., 1997a; Iezzi et al., 1998).

2.1.1 Mechanisms of TCR Downregulation

At least two clearly distinct pathways of TCR downregulation have been identified, one constitutive and one induced by ligand binding (Lauritsen et al., 1998; Dietrich et al., 2002; von Essen et al., 2002, 2006). Receptor downregulation in general is often linked to ubiquitination via E3 ubiquitin ligases and ultimately leads to degradation of the receptors via the lysosomal pathway (Frank and Fuchs, 2008). At least for ligand-induced downregulation, the same seems to apply to the TCR (Valitutti et al., 1997; D'Oro et al., 1997; Lauritsen et al., 1998; Liu et al., 2000; Naramura et al., 2002; Lee et al., 2003) and different E3 ubiquitin ligases have been implicated in the process, including Cbl-b (Bachmaier et al., 2000; Jeon et al., 2004; Naramura et al., 2002), c-Cbl (Murphy et al., 1998; Naramura et al., 1998, 2002) and GRAIL (Nurieva et al., 2010). A more mechanistic study found that Cbl is recruited to the TCR via direct binding to ZAP70 and can then ubiquitinate CD3ζ, but there was also residual recruitment and ubiquitination in ZAP70-deficient cells (Wang et al., 2001) which is more in line with the findings by multiple groups that the ligand-induced downregulation pathway can still proceed when Lck is blocked (Cai

Cbl = casitas B-lineage lymphoma proto-oncogene, GRAIL = gene related to anergy in lymphocytes

et al., 1997; Salio et al., 1997; San Jose et al., 2000; Monjas et al., 2004).

Constitutive TCR downregulation is mediated by a CD3γ di-leucine motif (DxxxLL) (Dietrich et al., 2002) which is bound by the adaptor proteins AP-1 and AP-2, thereby linking the TCR to the clathrin-mediated endocytosis machinery (Dietrich, 1997). Baseline TCR expression is increased in CD3γ di-leucine mutated transgenic mice compared to wild-type controls (Dietrich et al., 2002; Bonefeld et al., 2008). This process leads to a slow constitutive turnover of TCRs in resting T cells but it is dramatically amplified by PKC phosphorylation of CD3γ Ser^{126} (Dietrich et al., 1994, 2002; von Essen et al., 2002, 2006; Bonefeld et al., 2008). This means that although constitutively active, this pathway is further amplified by TCR signalling and can even be triggered by phorbol esters that activate PKC without TCR engagement (Dietrich et al., 2002; von Essen et al., 2006; Bonefeld et al., 2008; Torres et al., 2003). This is consistent with work showing that constitutively active Lck, PKC-α or PKC-θ increase basal TCR downregulation (D'Oro et al., 1997; von Essen et al., 2006).

2.1.2 Downregulation of Non-engaged Bystander TCRs

If TCR signalling increases the basal TCR downregulation rate, it follows that signalling from active TCRs upon ligand binding will result in the downregulation of non-engaged bystander TCRs. This process has been observed experimentally (San Jose et al., 2000; Bonefeld et al., 2003; Monjas et al., 2004; von Essen et al., 2006; Fernández-Arenas et al., 2014) and it is further supported by the finding that bystander downregulation is reduced when PI3K, PKC or Src family kinases are inhibited, or CD3γ is mutated (San Jose et al., 2000; Bonefeld et al., 2003; von Essen et al., 2006). Interestingly, inhibition of Lck prevents downregulation in response to weak stimuli (by inhibiting the signalling-dependent bystander pathway) but does not prevent downregulation in response to strong stimuli (the signalling-independent pathway is not affected) (San Jose et al., 2000; Monjas et al., 2004). This dependence on the strength of the stimulus explains why some investigators that did not do a detailed ligand titration found that tyrosine kinase inhibition completely blocked TCR downregulation (D'Oro et al., 1997; Martin and Bevan, 1998; Bonefeld et al., 2003), while others found that it had no effect (Cai et al.,

PI3K = phosphoinositide 3-kinase

1997; Salio et al., 1997). This suggests that bystander TCRs are downregulated by a TCR signalling-dependent amplification of the same molecular mechanisms that mediate constitutive TCR turnover. However, San Jose et al. and Monjas et al. stimulated T cells through a TCR and observed the comodulation of non-engaged CD3ζ chimeric molecules that did not include any CD3γ motifs, suggesting that other motifs in CD3ζ or completely different pathways of downregulation also play a role in bystander downregulation (San Jose et al., 2000; Monjas et al., 2004), one of which could be the recently described binding of β-Arrestin-1 to unphosphorylated TCR ITAMs (Fernández-Arenas et al., 2014).

2.1.3 TCR Recycling

There is evidence that TCRs that are internalised via the constitutive or bystander route are not immediately degraded and can recycle back to the cell surface (Krangel, 1987; Liu et al., 2000; Dietrich et al., 2002; Bonefeld et al., 2003; von Essen et al., 2006). It has been suggested that the internalisation of bystander TCRs is used by T cells as a way to deliver those TCRs to the immunological synapse (Das et al., 2004; Finetti et al., 2009; Fernández-Arenas et al., 2014). The molecular pathways involved in this process include the phosphorylation of β-Arrestin-1 by PKC which then binds to bystander TCRs and leads to their internalisation and transfer to the immunological synapse (Fernández-Arenas et al., 2014).

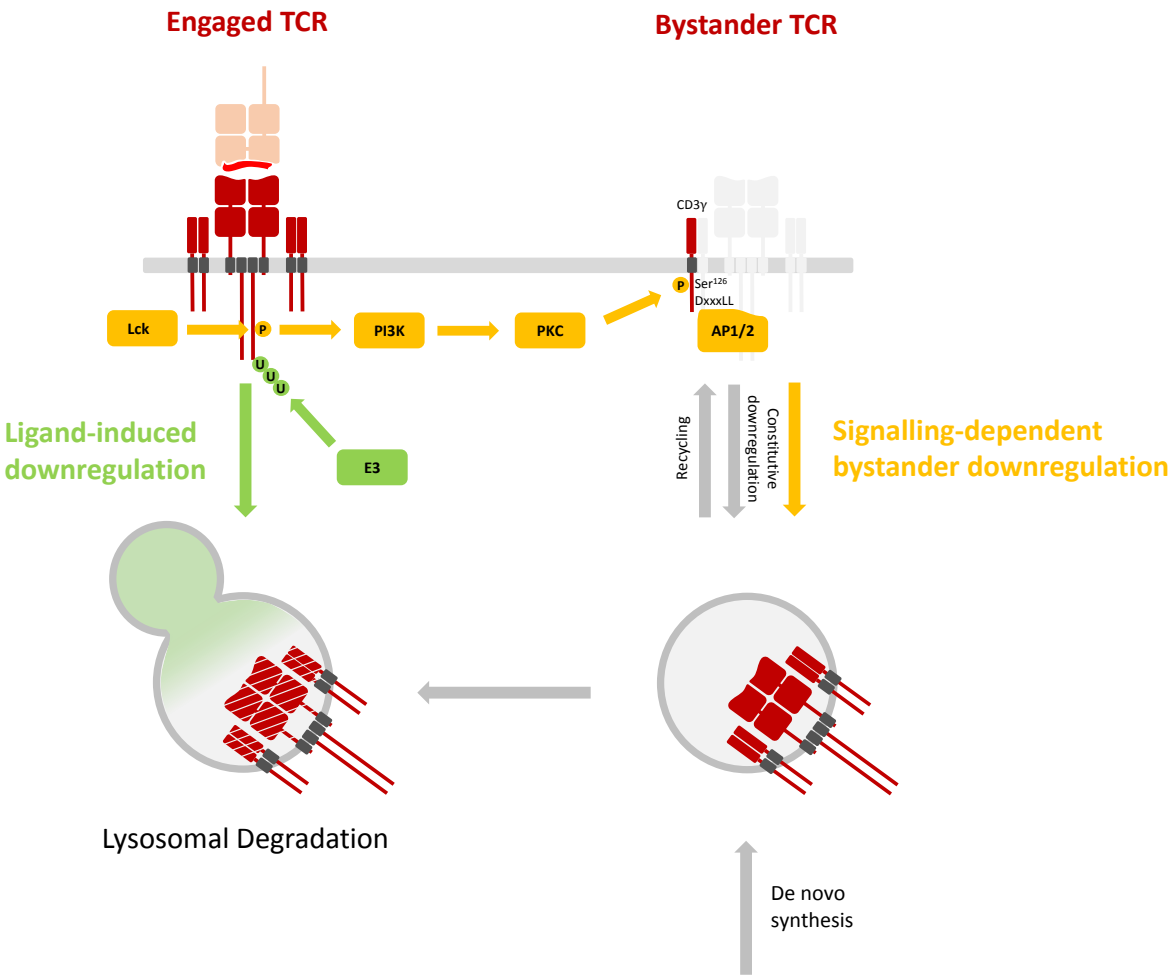


Fig. 2.1: Schematic of TCR downregulation pathways. Schematic summarising the emerging consensus from the literature on TCR downregulation. Downregulation proceeds via two pathways: One is ligand-dependent, but does not depend on signalling, the other is the signalling-mediated downregulation of non-engaged bystander TCRs. TCR signalling is drastically simplified to show only the relevant molecules that have been implicated in the process experimentally. Lck phosphorylates the CD3 ITAMs after antigen engagement. This leads to a signalling cascade which ultimately activates PI3K and PKC. PKC then phosphorylates the Serine at position 126 in CD3γ of a non-engaged TCR. This phosphorylation increases the rate of constitutive clathrin-mediated TCR downregulation which is initiated by AP1/2 binding to the DxxxLL motif in CD3γ. TCRs downregulated via this route can be recycled back to the cell surface instead of being degraded. Downregulation of the engaged TCRs is mediated by E3 ubiquitin ligases and leads to lysosomal degradation.

2.1.4 TCR Downregulation as a Mechanism of T Cell Adaptation

Receptor downregulation upon ligand binding is well-known to take place in many different contexts and generally thought to serve as a mechanism to prevent excessive signalling, for example for hormone receptors (Frank and Fuchs, 2008). Even in the earliest reports showing downregulation of the TCR upon antibody triggering and later upon antigen engagement, the possibility was introduced that TCR downregulation might play an important physiological role in limiting T cell activation in response to self-antigens for which the T cell might have a low affinity (Reinherz et al., 1982; Zanders et al., 1983; Schönrich et al., 1991; Cai et al., 1997). This concept is still not generally accepted, but it is worth noting that near-complete downregulation of the TCRs has been identified as a mechanism of peripheral tolerance in transgenic mouse models (Schönrich et al., 1991; Ferber et al., 1994; Tafuri et al., 1995; Martin and Bevan, 1998; Stamou et al., 2003). More recently, it was reported that TCR downregulation could contribute to T cell-APC disengagement in lymph nodes (Bohineust et al., 2018). In line with those findings, T cell tolerance is lost in transgenic mice that are deficient for the E3 ubiquitin ligases Cbl-b (Bachmaier et al., 2000; Jeon et al., 2004), c-Cbl (Murphy et al., 1998; Naramura et al., 1998) and GRAIL (Nurieva et al., 2010) and this was directly correlated with impaired TCR downregulation (Nurieva et al., 2010; Naramura et al., 2002) or with increased baseline TCR expression levels on positively-selected thymocytes (Murphy et al., 1998; Naramura et al., 1998). More mechanistic *in vitro* investigations showed that impaired TCR downregulation leads to more sustained early TCR signalling (Lee et al., 2003; Naramura et al., 2002). However, other investigators using similar model systems concluded that TCR downregulation did not play a role in tolerising T cells because no overt downregulation was observed (Singh and Schwartz, 2003; Hawiger et al., 2004; Ryan et al., 2005; Lees et al., 2006; Han et al., 2010).

2.2 Results

2.2.1 Adaptation of T Cell Responses to Antigen Dose and Affinity

We used an established *in vitro* T cell stimulation system where primary human $CD8^+$ T cells are transduced with an affinity-matured 1G4 TCR ($1G4^{Hi}$) and stimulated with plate-immobilised recombinant pMHCs (Lever et al., 2016). We used the 9V mutant of the NY-$ESO_{157\text{-}165}$ peptide as our index peptide, because it is more stably bound to HLA-A2 than the wild type 9C and has little effect on TCR binding (Chen et al., 2000, 2005). A similar stimulation system with plate-immobilised recombinant pMHC complexes has been piloted by Iezzi et al. (Iezzi et al., 1998) to study the effects of antigenic stimulation on transgenic mouse $CD4^+$ T cells in isolation from costimulatory signals and adhesion receptors. They compared responses of naïve and effector T cells to a large range of pMHC doses with and without costimulation through an anti-CD28 antibody. They also studied the effect of different stimulation times on T cell proliferation and measured CD69 expression and TCR downregulation at 5 h, but did not investigate cytokine production. We analysed T cell responses to twelve doses of pMHC and measured cytokine production after stimulation times of 1-8 h by ELISA. We found that T cells stop producing TNF-α after the first 4-5 h of stimulation (Figure 2.2 A) even though antigen was still present. This phenotype where a system is presented with a constant input signal but the output ceases after a certain stimulation time is formally termed "adaptation" (Ma et al., 2009). T cells adapted to antigen at all pMHC doses, but higher doses showed a sharper decrease in production which led to optimal production in response to an intermediate dose of pMHC ("bell-shaped" dose response, Figure 2.2 A), as we have previously described (Lever et al., 2016).

Given that this adaptation was observed in response to a pMHC ligand with supra-physiological affinity ($K_D = 7.07 \times 10^{-5}$ μM), we wondered whether it also takes place when T cells are presented with a pMHC with physiological affinity. We have confirmed the adaptation phenotype with a low-affinity pMHC variant (4A8K, K_D = 1.78 μM) and observed similar temporal dynamics (Figure 2.2 B). As expected for a lower-affinity in-

HLA = human leukocyte antigen, K_D = dissociation constant, ELISA = enzyme-linked immunosorbent assay

teraction, the T cells were only activated and started TNF-α production at higher ligand doses.

There are multiple potential reasons for the cells to stop cytokine production while the antigen is still present, including activation-induced cell death (Lees et al., 2006; Bonefeld et al., 2008), negative feedback mechanisms that switch off the signalling (Honda et al., 2014; Stefanová et al., 2003; Hawiger et al., 2004; Altan-Bonnet and Germain, 2005), and TCR downregulation. We excluded activation-induced cell death as a potential reason for the declining TNF-α production, because:
1) We have previously shown that in this experimental system, activation-induced cell death is minimal (less than 10 % of the cells stain positive for Annexin V by 8 h) (Lever et al., 2016).
2) Other cytokines adapt on different time scales. IFN-γ, for example, continues to be produced beyond 8 h of stimulation (Trendel et al., 2019).
3) We show in Figure 2.7 and Figure 2.8 that the adapted cells can be fully re-activated and are still capable of producing large amounts of cytokines.

2.2.2 TCR Downregulation Dynamics

We had previously observed TCR downregulation in our experimental system and given that cytokine production is known to require continuous TCR signalling (Huppa et al., 2003), we hypothesised that TCR downregulation would be sufficient to explain the observed adaptation phenotype. In order to test this, we attempted to build a predictive mathematical model that captures TCR downregulation dynamics and cytokine production. This required a detailed analysis of TCR downregulation.

In the same time course experiments discussed above, we stained for surface TCR expression with fluorescent pMHC tetramers to quantify TCR levels by flow cytometry. We found that TCR levels reach their steady-state already after 1 h of stimulation (or less) at all doses and affinities tested (Figure 2.2 C and D), consistent with the rapid downregulation observed in previous studies (Reinherz et al., 1982; Valitutti et al., 1995; Lauritsen et al., 1998; Dietrich et al., 2002; von Essen et al., 2002; Utzny et al., 2006). Interestingly, the TCR is not downregulated further over time, even at intermediate doses that

have only induced partial downregulation (Figure 2.2 C and D). This partial downregulation could be a result of only a fraction of cells downregulating the TCR, but we observed that the whole population of $1G4^{Hi}$ TCR-positive T cells downregulated their TCRs to intermediate levels (Figure 2.2 E).

Steady TCR levels in the presence of antigen can be achieved either by a dynamic balance between continuous TCR expression and pMHC-induced downregulation or by a stop of TCR downregulation. To differentiate between these two possibilities, we induced TCR downregulation for 4 h as described above and monitored TCR recovery after removing the cells from stimulation. We observed that the induced TCR expression levels were relatively stable on the timescale of our stimulation experiments and only recovered on the scale of days (Figure 2.2 F), consistent with other reports (Reinherz et al., 1982; Sousa and Carneiro, 2000). We conclude that TCR re-expression is too slow to account for the observed steady-state, suggesting that TCR downregulation stops.

As expected, we observed the complete loss of the TCR from the surface at high pMHC doses and therefore, this is intuitively consistent with TCR downregulation as the mechanism of adaptation. However, adaptation was observed at all doses and affinities, including intermediate antigen doses where the TCR was only partially downregulated. The observation that there was only incomplete TCR downregulation has previously led investigators to conclude that TCR downregulation is unlikely the mechanism of adaptation in their respective model system (Singh and Schwartz, 2003; Hawiger et al., 2004; Ryan et al., 2005; Lees et al., 2006; Han et al., 2010).

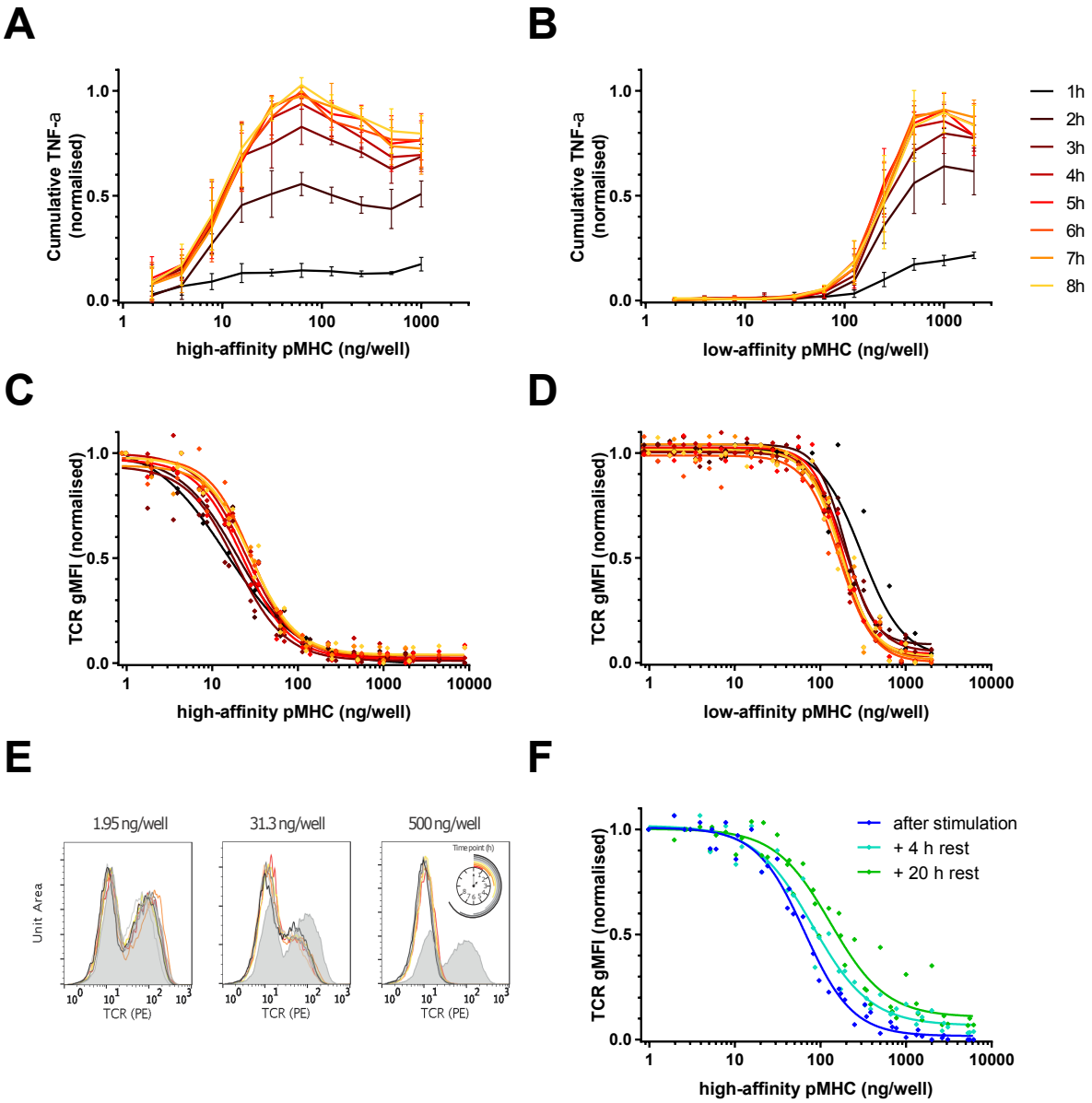


Fig. 2.2: T cell adaptation and TCR downregulation kinetics. Primary human $CD8^+$ T cells carrying the $1G4^{Hi}$ TCR were stimulated with the high-affinity pMHC variant 9V or the physiological-affinity pMHC variant 4A8K. Cumulative cytokine concentrations were measured by ELISA after the indicated stimulation times and TCR expression was determined by tetramer staining and flow cytometry. A) TNF-α production in response to the high-affinity ligand. B) TNF-α production in response to the low-affinity ligand. For averaging between donors, TNF-α was normalised to the maximum response after 6 h of stimulation. Shown are the mean and standard deviation of three independent experimental repeats. TCR downregulation time course with a high- (C) or low-affinity (D) pMHC antigen. E) Representative histograms showing partial TCR downregulation on the whole population of $1G4^{Hi}$ TCR-positive cells at different pMHC doses. F) TCR re-expression time course upon removal of the stimulus following a 4 h stimulation. For averaging TCR downregulation between experiments with different transduction efficiencies, background tetramer staining of the untransduced T cell population was subtracted and the geometric mean fluorescence intensity (gMFI) was normalised to the unstimulated control. Curves represent the mean of three independent experimental repeats (dots). All the data in this figure was produced by Nicola Trendel and included in (Trendel et al., 2019).

2.2.3 Building a Mathematical Model of TCR Downregulation

Based on previous observations and on our quantitative stimulation dataset, we have built a mechanistic mathematical model that simulates TCR downregulation (Figure 2.5). In order to explain the stopping of TCR downregulation, we included cooperative binding between TCR and pMHC which has been observed experimentally (Pielak et al., 2017) and included in previous modelling attempts (Sousa and Carneiro, 2000; Utzny et al., 2006). This leads to a strong dependence of the downregulation rate on TCR and ligand density and as a consequence, the TCR downregulation rate approaches zero once the TCR density falls below a certain threshold. In most models of T cell activation, ligand binding is followed by a modification step (often assumed to be phosphorylation) in order to explain affinity-based antigen discrimination and the fact that antigen dose cannot compensate for low affinity ("kinetic proofreading" (Mckeithan, 1995; Coombs et al., 2002; Utzny et al., 2006; Lever et al., 2016)). Similarly, in our model, bound receptors undergo another phosphorylation-independent modification akin to kinetic proofreading which results in their downregulation. This assumption is based on the observation that TCR downregulation closely correlates with activation in response to different affinities, i.e. it also exhibits antigen discrimination (Valitutti et al., 1995; Viola and Lanzavecchia, 1996; Cai et al., 1997; Itoh et al., 1997; Martin and Bevan, 1998).

This model reproduces the temporal dynamics of TCR downregulation (Figure 2.5), but it assumes TCR downregulation to be completely independent of signalling. However, there are reports in the literature showing effects of TCR signalling on downregulation (D'Oro et al., 1997; Martin and Bevan, 1998; San Jose et al., 2000; Monjas et al., 2004; von Essen et al., 2006). We confirmed this experimentally in a 4 h stimulation experiment where we blocked T cell signalling with the Lck inhibitor A-770041 or the Src family kinase inhibitor PP2, similar to the experiments done by San Jose et al. and Monjas et al. (San Jose et al., 2000; Monjas et al., 2004). In line with their findings, we observed that the result was dependent on the strength of the stimulus. Complete TCR downregulation still ocurred at high antigen doses, but was inhibited at intermediate doses (Figure 2.3). This shows that TCR downregulation does not strictly depend on Lck signalling, but is affected

PP2 = pyrazolopyrimidine 2

by it in a more complex way. Notably, the difference between the downregulation curves becomes apparent mainly through a different shape, but at least for the 4 h time point (for which there were more repeats), there was also a significant difference in the IC_{50} ($p = 0.0002$ for A77 and <0.0001 for PP2, F-test in Prism).

IC_{50} = half maximal inhibitory concentration

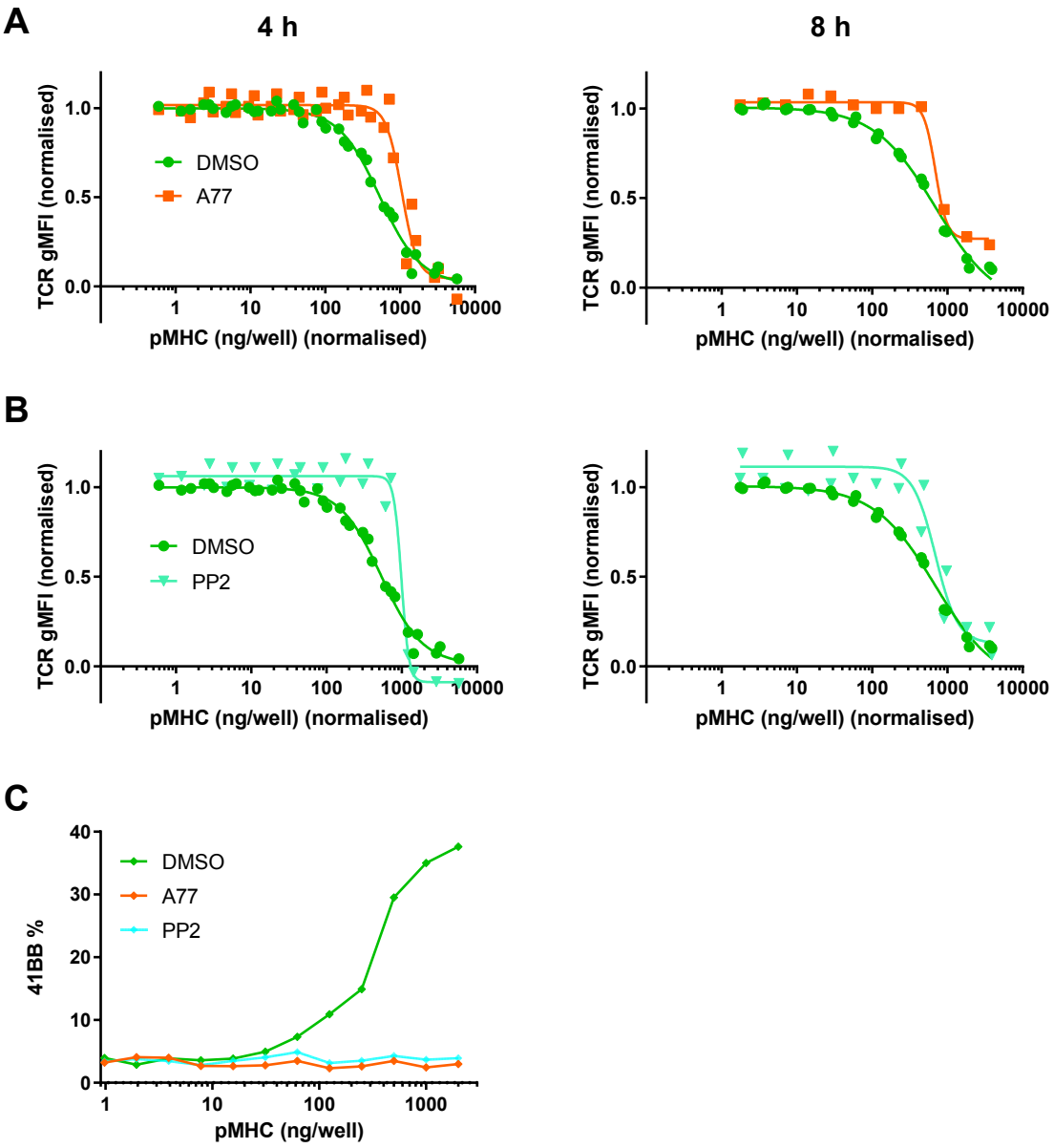


Fig. 2.3: Lck inhibition affects TCR downregulation. Primary human $CD8^+$ T cells carrying the $1G4^{Hi}$ TCR were stimulated for 4 h or 8 h with the physiological-affinity pMHC variant 4A8K. TCRs were stained with pMHC tetramers and expression quantified by flow cytometry. A) Stimulation in the presence or absence of the Lck-specific inhibitor A-770041 (300-500 nM, three donors 4 h, one donor 8 h). B) Stimulation in the presence or absence of the Src family tyrosine kinase inhibitor PP2 (20 µM, two donors 4 h, two donors 8 h). For averaging TCR downregulation between experiments with different transduction efficiencies, the background gMFI of untransduced T cells was subtracted and the gMFI was normalised to the unstimulated control. To account for differences in pMHC immobilisation, the X values for each donor were corrected depending on the IC_{50} of the pMHC-only curve ($X = [pMHC]/(IC_{50}/meanIC_{50})$). That means relative differences between the curves with and without inhibitors are preserved. C) 4-1BB expression after 4 h stimulation with or without inhibitors. Representative data from one donor.

We tested whether different modifications to our model allowed us to reproduce this phenotype in addition to our TCR and TNF-α time course data. The model that emerged (Figure 2.4) includes the signalling-induced downregulation of unbound bystander TCRs. This is in line with the interpretation of similar inhibitor experiments by other investigators who concluded that inhibition of Lck prevents downregulation in response to weak stimuli (by inhibiting the signalling-dependent bystander pathway) but does not prevent downregulation in response to strong stimuli (the signalling-independent pathway is not affected) (San Jose et al., 2000; Monjas et al., 2004). This is consistent with the finding that cell lines with a mutated CD3γ di-leucine motif, Ser^{126}, or PKC inhibition, which are all implicated in the pathway required for bystander downregulation, show the same phenotype as cells with Lck inhibition, i.e. TCR downregulation only with a strong stimulus (Dietrich et al., 2002; von Essen et al., 2002).

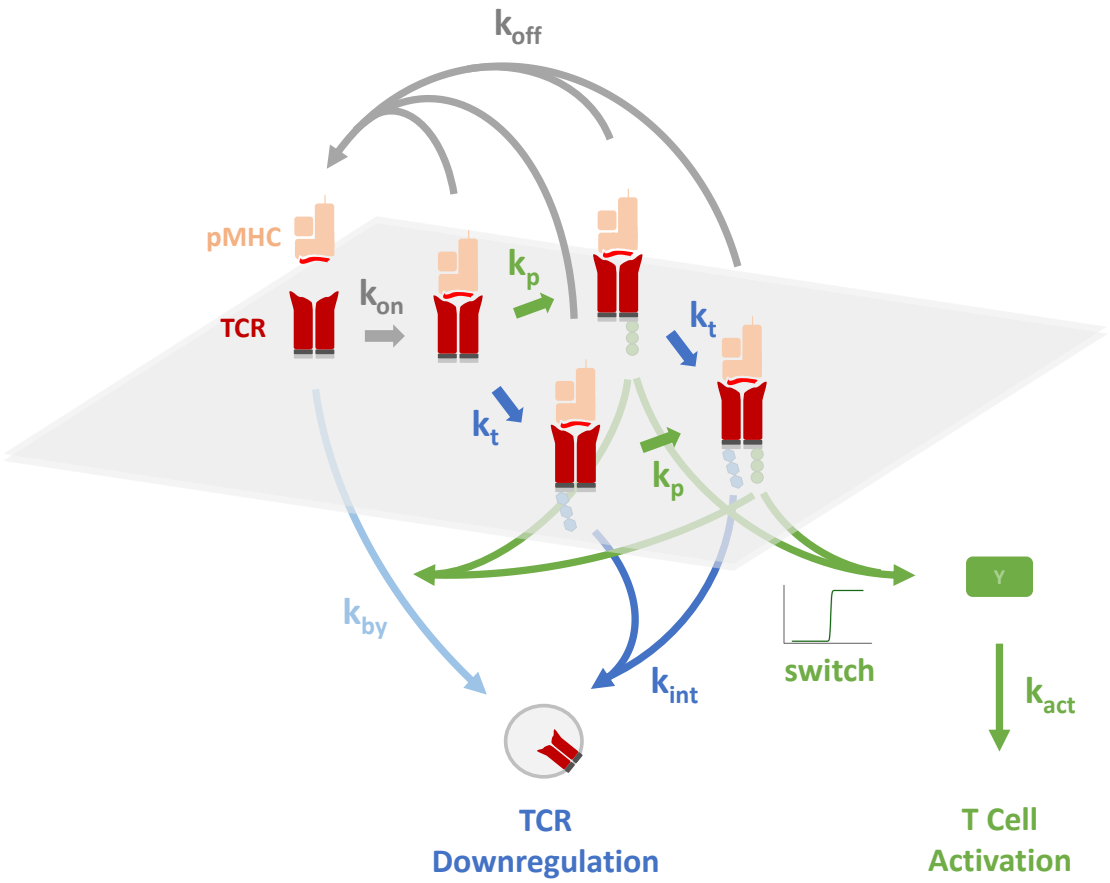


Fig. 2.4: TCR downregulation model schematic. This schematic representation of the mathematical model shows the cell membrane as a gray plane and the different T cell receptor states in red. Reaction rates are depicted as arrows. The process starts with TCR-pMHC binding on the left hand side. This reaction is modelled as cooperative binding with an on-rate and off-rate that depend on the pMHC variant ($\frac{dTCR_{bound}}{dt} = k_{on} * (pMHC * TCR_{free})^{nb} - k_{off} * TCR_{bound}$). The bound TCR can undergo two independent modifications: activation and tagging for downregulation, with rates k_p and k_t, respectively. The activated or tagged TCRs can then also undergo the respective other modification resulting in TCRs that are both tagged and activated. Tagged TCRs are then downregulated with rate k_{int}. Active TCRs initiate downstream signalling that leads to the downregulation of unbound bystander TCRs with rate k_{by} and to cytokine production. The cytokine pathway is modelled with an intermediate node Y which is activated by the TCR in a digital manner ("switch" motif) and exhibits saturation ($\frac{dY}{dt} = k_{fy} * \frac{(TCR_{active}+TCR_{active+tagged})^{ny}}{sy^{ny} + (TCR_{active}+TCR_{active+tagged})^{ny}} * (1 - Y) - k_{ry} * Y$). This reaction is governed by the parameters sy for the threshold of activation, ny for the steepness, and k_{fy} and k_{ry} as forward and reverse rates for the amplitude. Activation of Y is then translated into T cell activation by the linear amplifier k_{act}. We also included a basal downregulation rate of all TCR states and a basal TCR synthesis rate which are not depicted here for clarity. See section 6.11 for all equations and parameters.

The final model was fitted directly to the averaged data from at least three donors and it reproduced the observed TCR downregulation dynamics, i.e. complete downregulation within the first hour of stimulation, and re-expression over the course of days, as well as the effect on the dose-response of Lck inhibition (Figure 2.5). This model is comparable to other attempts to simulate TCR downregulation (Sousa and Carneiro, 2000; Utzny et al., 2006; Lee et al., 2003) (see also section 2.3), although to our knowledge, this is the first time such a model can also explain TCR downregulation with Lck inhibition as well as adaptation in cytokine production (see next section).

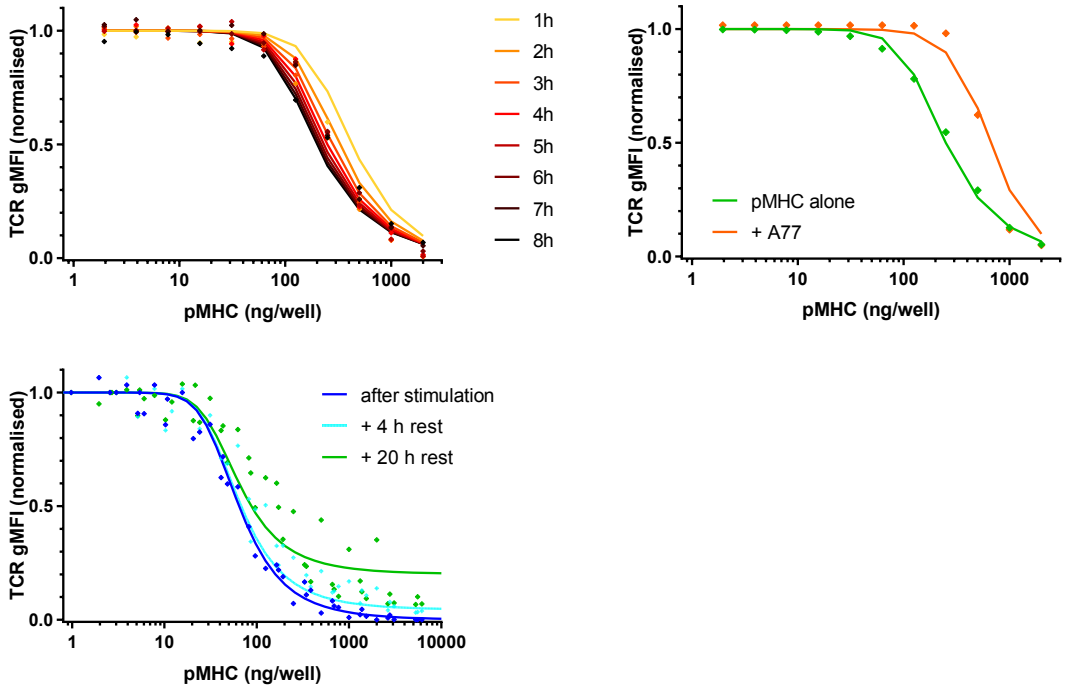


Fig. 2.5: Mathematical model reproduces TCR downregulation dynamics. The model was used to simulate TCR downregulation over 8 h, downregulation with Lck inhibition, and re-expression of the TCR after a 4 h stimulation. Dots show the TCR data from Figure 2.2 that was generated by Nicola Trendel.

2.2.4 TCR Downregulation Model Reproduces T Cell Adaptation

A simulation of a T cell stimulation experiment reveals that TCR downregulation is sufficient to explain adaptation even with minimal changes in TCR levels. Downstream signalling from the activated TCR complexes is followed by digital cytokine production (Huang et al., 2013) once the number of activated receptors exceeds a threshold. We modelled this threshold with a Hill function. This threshold is likely to be quantitatively different for

different cytokines (van den Berg et al., 2013), but we have fitted the model only to our TNF-α data. At low antigen doses and/or affinities, a small change in TCR expression means that the cell enters a regime (few TCRs and few ligands) where it cannot engage enough receptors simultaneously to cross its activation threshold. Importantly, the same applies to the threshold for further TCR downregulation, which means that T cells that have seen low doses of antigen will retain high or intermediate TCR expression levels. In other words, each T cell adjusts its receptor expression exactly to the dose and affinity of antigen. Note that we do not have sufficient data to conclude whether the threshold amount of TCR for downregulation and the threshold for T cell activation are the same or different. Given that downregulation causes the stop in cytokine production, we know that the downregulation threshold cannot be higher than the cytokine production threshold (i.e. downregulation has to stop after cytokine production, otherwise cytokine production would continue). However, it could still be that TCR levels continue to decrease after cytokine production has already stopped which would lead to a "deeper" adaptation state. Thinking about this as a mechanism of peripheral tolerance, we could speculate that upon encountering self-antigen, the T cell might want to adjust its TCR level further than just below the activation threshold at this antigen dose and affinity, because the next APC might be able to present slightly more of the self-antigen.

Furthermore, the model predicts that the time a T cell remains in its activated, cytokine-producing state is dose-dependent. High pMHC doses result in more activation, but also faster TCR downregulation which means that the number of active TCRs on the surface remains above the activation threshold for a shorter time. This explains the bell-shaped dose response curves, because an intermediate pMHC dose with a slower cytokine production rate and a slower TCR downregulation rate can stay above the activation threshold for longer and consequently accumulate more cytokine over time.

In summary, the mathematical model shows that incomplete TCR downregulation is sufficient to explain T cell adaptation. It follows that adaptation is not a cell-intrinsic unresponsive state but rather that adaptation is context-dependent so that the T cell becomes unresponsive to a particular dose/affinity of antigen. This leads to the prediction that the remaining TCR expression should be sufficient for the cell to still be able to respond to a higher dose or affinity.

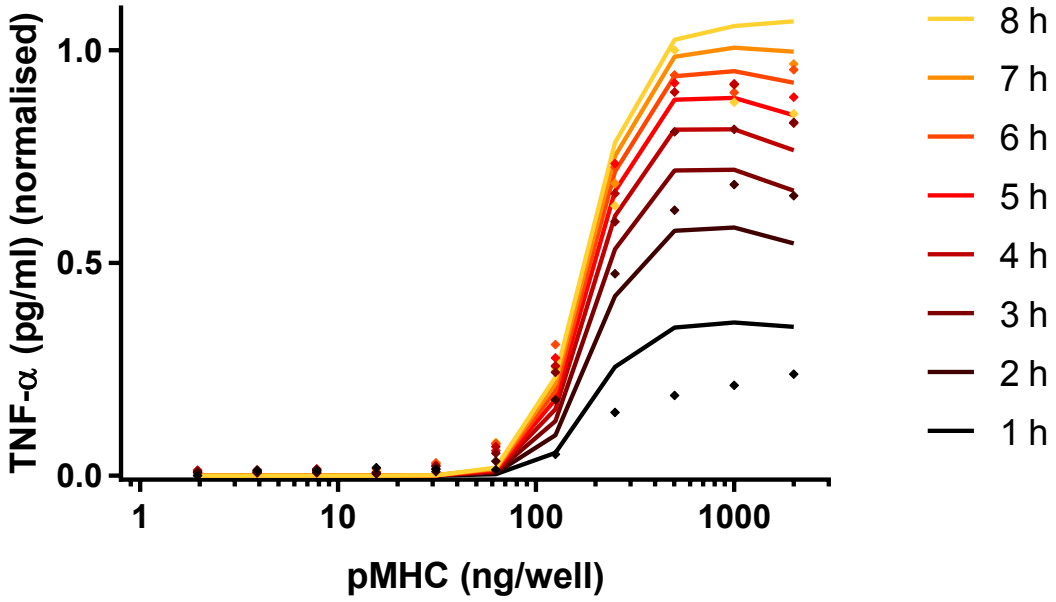


Fig. 2.6: Mathematical model reproduces cytokine production dynamics. Model fitting results (solid lines) for the TNF-α production time course dose response curves from Figure 2.2 (shown as dots) that were generated by Nicola Trendel.

2.2.5 T Cells Adapted to a Low-Affinity Antigen are Re-activated with a Higher-Affinity Antigen

In order to test this prediction, we pre-stimulated T cells with a dose titration of the physiological-affinity pMHC variant 4A8K for 4 h to induce adaptation, rested the cells for 4 h, and then replaced the medium and transferred them to the same pMHC or the high-affinity ligand 9V presented at the same doses for 16 h. Cytokine production during the second round of stimulation was measured by ELISA. We quantified TNF-α production in the second stimulation by fitting a curve to the dose response and comparing the E_{max} of those curves. According to our time course data, the cells should be fully adapted by 4 h and not produce any TNF-α when transferred to the same low-affinity ligand again. Although production did not stop completely, we observed reduced production compared to fresh cells that had not been pre-stimulated with each of four donors (Figure 2.7 A, mean 46.1 %, p = 0.013). We observed that the adaptation was stronger when cells were transferred directly after 8 h of stimulation (see Figure 2.8, mean 13.6 %, p = 0.017), suggesting that the adaptation time might vary between donors which would mean that some have not completely adapted by 4 h.

As predicted by the model, transfer of cells adapted on the low-affinity antigen to a high-affinity antigen at the same dose induced cytokine production (Figure 2.7 B). As expected, the high-affinity ligand produces dose response curves with a higher potency. There was considerable variability, with one donor showing adaptation even with the high-affinity ligand, but this case probably resulted from poor immobilisation of the high-affinity pMHC. For the other three donors, pre-stimulated cells show TNF-α production comparable to fresh cells in response to the high-affinity ligand (Figure 2.7 A, mean: 115.7 %).

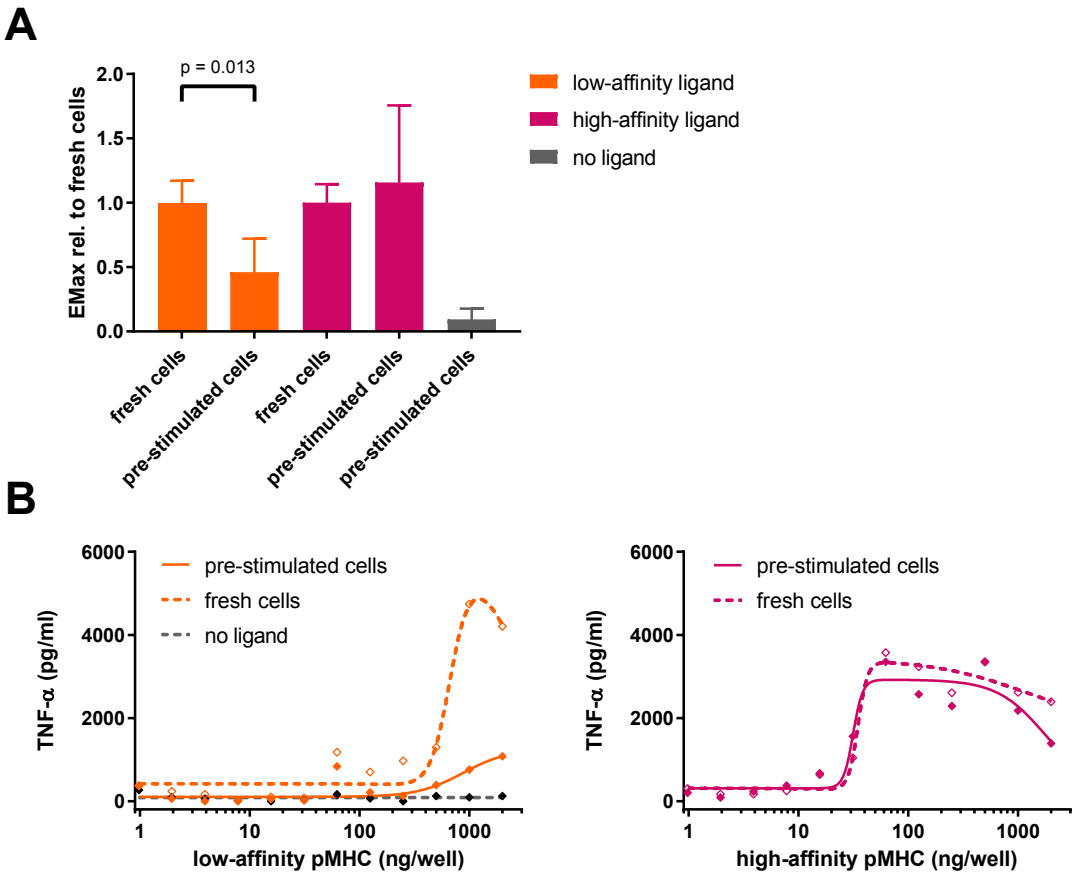


Fig. 2.7: T cells desensitised to a low-affinity antigen can be re-activated with high-affinity ligand. Primary human $CD8^+$ T cells carrying the $1G4^{Hi}$ TCR were stimulated for 4 h with the physiological-affinity pMHC variant 4A8K. The cells were then rested for 4 h and transferred to a second round of stimulation for 16 h on either the same pMHC ligand or the high-affinity ligand 9V. They were compared to fresh cells that were not pre-stimulated. Cytokine concentrations in the supernatant were measured by ELISA. A) E_{max} values from four donors normalised to the mean of each experiment and expressed as a fold-change relative to the mean production across all donors from fresh cells on each ligand. A two-tailed t-test was used for statistical analysis of the adaptation effect (Prism). B) Representative dose response curves from one donor showing responses to the low- and high-affinity ligand.

2.2.6 T Cell Adaptation to Antigen is Overcome by Costimulation

Our data and modelling show that T cells precisely adjust their TCR expression to antigen dose and affinity, but the TCRs remaining on the surface and the downstream signalling machinery are fully functional and can be triggered by a higher-affinity antigen. However, *in vivo*, T cells will encounter their cognate antigen not in isolation, but together with costimulatory ligands on antigen-presenting cells which are known to amplify TCR signals (Murtaza et al., 1999; Michel et al., 2001).

In order to test whether an additional signal through CD28 could override the adaptation phenotype by amplifying signals from the remaining TCRs, we pre-stimulated T cells for 8 h as before and then transferred them to the same pMHC with or without co-immobilised recombinant CD86. Representative dose response curves and the averaged E_{max} values from multiple donors are shown in Figure 2.8. As described in Figure 2.7, the adapted cells produced much less TNF-α (Figure 2.8 B , 13.5 % of maximal production during first stimulation, p = 0.0171). Importantly, adapted cells were strongly re-activated with CD86 and their maximal TNF-α production reached similar levels as during the first stimulation (Figure 2.8 B, first stimulation: 248.4 % of production with pMHC alone, second stimulation: 226.2 %). Importantly, this effect was not only observed with regard to TNF-α production, but also with IL-2, IFN-γ and MIP-1β (Figure 2.8 C), although the adaptation of MIP-1β was less pronounced.

One experiment, where the cells showed almost no response to CD86 costimulation in both the first and second stimulation, was excluded from the analysis on the grounds that the cells were already strongly activated in culture (almost all CD69-positive). Speculatively, this could be due to cross-reactivity of our high-affinity TCR with certain HLA types. We know that binding to HLA-A2 irrespective of the loaded peptide leads to fratricide and activation of the T cells in culture (Tan et al., 2015) which is why we only used HLA-A2-negative donors. However, it is conceivable that the TCR might still bind to some other HLA types that are not recognised by the HLA-A2 antibody, leading to varying degrees of fratricide and T cell activation.

We included a control condition where pre-stimulated cells were transferred to a high dose of CD86 without any pMHC to confirm the well-established finding that CD28 signal-

ling without TCR engagement does not lead to T cell activation and cytokine production (Michel et al., 2001; Huppa et al., 2003). In one experiment, there was no response as expected, but in the other, the cells pre-stimulated with the two highest pMHC doses produced significant amounts of cytokines when transferred to CD86 alone (Figure 2.8 D). We regard this as an outlier most likely brought about by small amounts of pMHC transferred over from the first round of stimulation. Indeed, the increase in potency with CD86 was particularly strong in this experiment, suggesting that a transfer of only one hundredth of the highest pMHC dose would result in the observed response (Figure 2.8 D). However, we cannot formally exclude the possibility that this effect was mediated by CD86 without any pMHC.

In addition to CD28, other costimulatory receptors are known to play an important role in the activation of $CD8^+$ T cells. Others in the group have shown that adapted cells can also be reactivated with the same pMHC co-presented with 4-1BB-Ligand, although the costimulatory effect was not as strong as with CD86 (Trendel et al., 2019).

These findings show that T cell adaptation is context-dependent and can be overcome by costimulatory signals that amplify the remaining TCR signals. This suggests a mechanism by which T cells in contact with an APC can continue to produce cytokines after their TCR expression levels have been adjusted to the presented antigen.

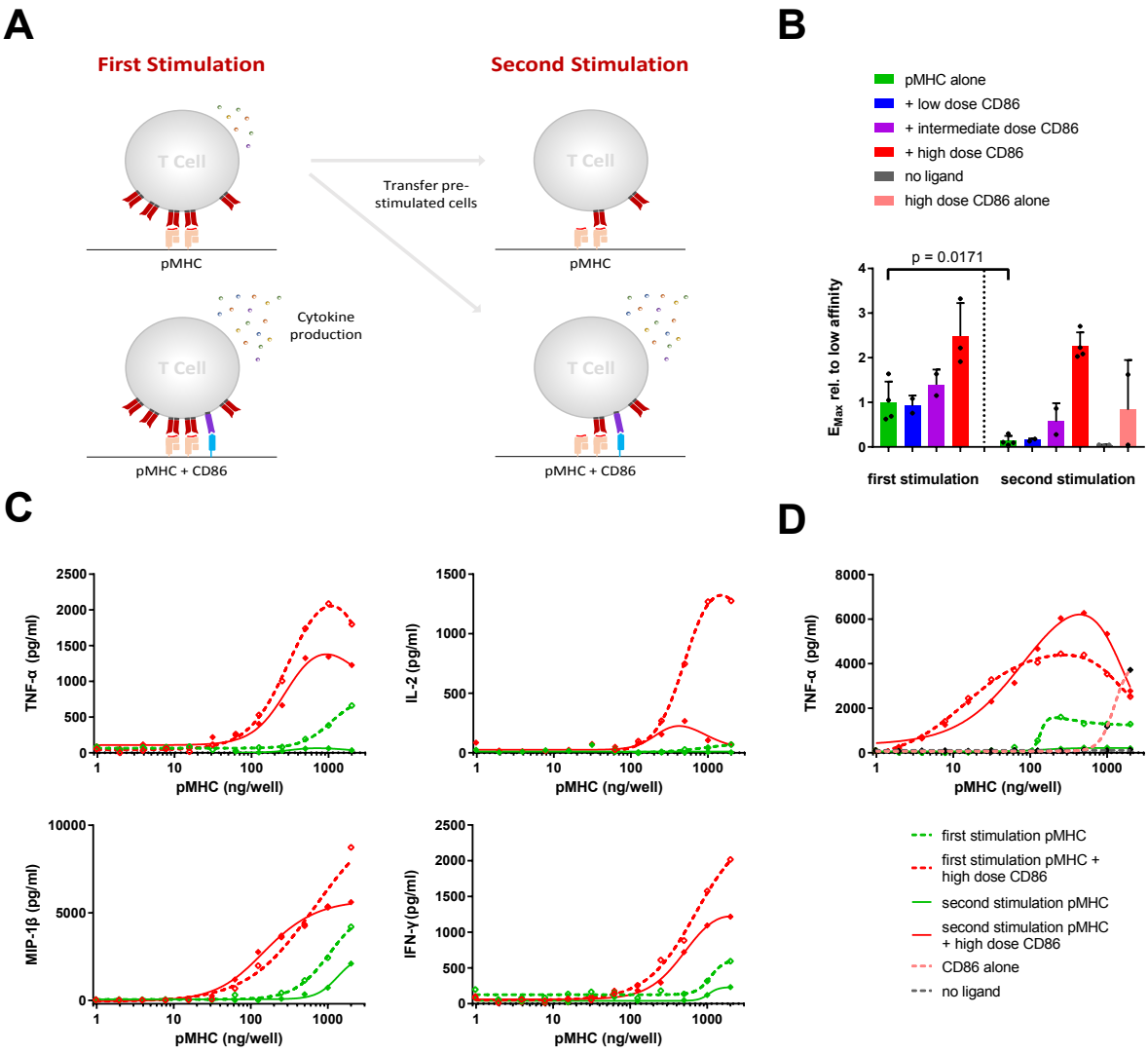


Fig. 2.8: Re-activation of adapted T cells with CD28 costimulation. Primary human $CD8^+$ T cells carrying the $1G4^{Hi}$ TCR were stimulated for 8 h with the physiological-affinity pMHC variant 4A8K with or without different concentrations of CD86. The cells stimulated with pMHC alone were then transferred to a second round of stimulation for 16 h on the same pMHC dose with or without CD86 co-presented on the plate. Cytokine production was measured by ELISA and compared between the first 8 h of stimulation and the second round. A) Schematic of the experiment, not including the controls. B) E_{max} values from multiple donors normalised to the mean of each experiment and expressed as a fold-change relative to the mean production across all donors during the first 8 h in response to pMHC alone. CD86 concentrations varied slightly between experiments and were grouped as follows: low: 25 ng and 50 ng, intermediate: 100 ng and 250 ng, high: 500 ng, 750 ng, and 1000 ng. C) Representative dose response curves from one donor for IL-2, TNF-α, IFN-γ, and MIP-1β production. D) TNF-α dose response curves from another donor. The TNF-α data in this figure was included in (Trendel et al., 2019). For clarity, only the high dose of CD86 is shown as curves. Statistical analysis was performed in Prism using a two-tailed t-test.

2.3 Discussion

We show here that T cells rapidly downregulate their TCRs upon ligand engagement at all doses and affinities of antigen. Even if incomplete, this TCR downregulation leads to T cell adaptation, i.e. a stop in cytokine production. We are able to reproduce this phenotype with a quantitative model that reproduces the temporal dynamics of TCR downregulation as well as cytokine production. This model explains why cytokine production stops and why the cells produce less cytokines at high antigen doses than at intermediate doses. Furthermore, the model predicts that T cell adaptation is not a cell-intrinsic state, but depends on the context of stimulation, and we have been able to confirm the crucial prediction that the adapted cells should get re-activated when presented with a higher-affinity ligand.

2.3.1 Function of Peripheral T Cell Adaptation

Adaptation is a well-known phenomenon in the sensory systems where for example the responses to constant visual or auditory stimuli are reduced over time until the signal stops completely and the constant signal is perceived as the new baseline. Of note, this process is believed to serve a completely different function to what has been proposed for T cells. In the sensory systems, adaptation is used to dramatically increase the dynamic range of the processing system. As an example, the human eye can adapt to see in almost complete darkness when exploring a cave, but is also able to adapt again to a stimulus that is orders of magnitude stronger when stepping outside in bright sunlight (Galizia and Lledo, 2013). Translated to T cell adaptation, this provides an interesting new interpretation regarding the functional consequences of this process. What if peripheral adaptation does not (only) serve the function to inactivate self-reactive T cells to prevent autoimmunity, but also increases the dynamic range of the T cell response? This could explain how the T cell compartment overall remains sensitive to minute amounts of antigen, but can also scale the response during an infection (i.e. distinguish between large and very large amounts of antigen). Indeed, cell-intrinsic adaptation has been reported to limit cytokine production of effector T cells in inflamed tissue. This was suggested to protect the peripheral tissue from damage from overt immune activation when antigen

levels are constant or falling. On the other hand, T cells will continue to respond in this model when the amount of antigen in the tissue is rising, i.e. during an ongoing infection (Honda et al., 2014). However, our data suggests a second mechanism by which the immune system can actively regulate the responsiveness of the adapted T cells without relying on the passive self-regulation in response to the level of antigen presentation. When adapted T cells are presented with costimulation, they can be fully re-activated. If the ongoing infection triggers inflammatory pathways that lead to higher expression of costimulatory ligands on APCs, our model would predict that this would re-activate adapted T cells even if the antigen concentration has not changed. Interestingly, it has been reported that mouse T cells deficient in the E3 ubiquitin ligases that downregulate the TCR lose their dependence on costimulatory signals (Nurieva et al., 2010; Bachmaier et al., 2000). It has also previously been shown that mouse naïve $CD4^+$ T cells require much longer TCR stimulation times to get fully activated than effector T cells (Iezzi et al., 1998). Combined with our model, this could suggest that the requirement for costimulation to activate naïve T cells might be due to the intrinsically limited signalling duration of the TCR. If naïve cells need TCR signalling for 15 hours to get fully activated, they might only be able to achieve this in the presence of a costimulatory signal. However, it is not clear whether the TCR downregulation kinetics are similar for naïve and effector T cells.

2.3.2 Mechanisms of Peripheral T Cell Adaptation

A second point that is interesting about sensory adaptation is that it requires a multitude of different mechanisms that all work together to achieve the phenotype (Galizia and Lledo, 2013). In the case of T cells, many different investigators have reported adaptation and, using different model systems, have come to very different conclusions regarding the mechanism. Given the importance of peripheral T cell tolerance, it is not surprising that multiple mechanisms should exist to ensure that our T cells, which are all self-reactive to some degree (Mason, 1998), remain inactive until a real threat is detected. Continuous T cell tuning in the periphery has long been appreciated as an important process to prevent autoimmunity without deleting self-reactive T cells (Grossman and Paul, 1992). As pointed out above, TCR and co-receptor downregulation have

been reported to serve as mechanisms of T cell adaptation (Schönrich et al., 1991; Ferber et al., 1994; Tafuri et al., 1995; Martin and Bevan, 1998; Stamou et al., 2003), but beyond this, T cells have also been reported to adjust their responsiveness by downregulating signalling intermediates upon activation (Jang and Gu, 2003). Our model is also consistent with work that traced T cell adaptation to an early block in TCR signalling (Chiodetti et al., 2006).

In addition to the downregulation of various factors, it appears that T cells use a variety of different mechanisms to adjust their responsiveness that can collectively be classified as negative feedback. Molecules that have been suggested to be involved in this process include CD5, CTLA-4, PD-1, and SHP-1. PD-1 and CTLA-4 are cell surface receptors that require binding to a ligand for their inhibitory activity. Therefore, they are unlikely to contribute to adaptation in our plate-based stimulation system. However, others have found that PD-1 upregulation can limit the duration of T cell-APC contacts in inflamed skin (Honda et al., 2014). A similar negative feedback mechanism involves the activation and recruitment of the phosphatase SHP-1 by TCR signals which then counteracts further T cell activation (Stefanová et al., 2003; Paster et al., 2015).

While our model does not exclude the possibility that other mechanisms also play a role in adaptation, the more interesting question is why other reports did not consistently identify TCR downregulation as important for adaptation in their transgenic mouse models. Some studies report limited or no difference in TCR levels between adapted and non-adapted cells (Dorothee et al., 2005; Lees et al., 2006; Han et al., 2010; Honda et al., 2014) while others show evidence of TCR downregulation (Singh and Schwartz, 2003; Stamou et al., 2003; Hawiger et al., 2004). Even in those studies that did show differences, the TCRs were mostly only partially downregulated which led the investigators to conclude that TCR downregulation cannot account for the adaptation phenotype. However, as our model shows, the degree of downregulation depends on the strength of the antigenic signal and even minimal downregulation in response to a weak signal can contribute to functional adaptation of the cells towards that same antigen. As discussed, others have reported near-complete downregulation of the TCRs (often together with the co-receptors) on *in vivo*-adapted T cells and interpreted this as the mechanism of adaptation (Schönrich et al., 1991; Ferber et al., 1994; Tafuri et al., 1995; Martin and Bevan,

1998). Interestingly, TCR downregulation has also been suggested to render maternal T cells temporarily tolerant towards paternal antigens during pregnancy (Tafuri et al., 1995) which is a prime example of a state where a temporary context-dependent inactivation of the T cells is required. Again, our model would predict the findings of those groups that did observe TCR downregulation assuming that a stronger antigen was targeted in those studies. This interpretation is supported by the result that further up-regulation of the antigen on the peripheral cells led to further downregulation of the TCR (Ferber et al., 1994). Similar results have been obtained with transgenic $CD8^+$ T cells stimulated *in vitro* with peptides of different affinity. Lower doses of peptide as well as lower affinities elicited less TCR downregulation and this correlated with increased cytolytic capacity (Martin and Bevan, 1998).

Therefore, we conclude that TCR downregulation contributes to peripheral T cell adaptation, but the degree of this contribution varies depending on the dose and affinity of the antigen as well as the expression level and dynamics of the TCR. Our quantitative model shows that even partial TCR downregulation can be sufficient to explain adaptation, but it does not exclude the contribution of other mechanisms which might predominate in some of the experimental systems discussed above. In fact, it has been argued before by others that in their dataset, only the combination of TCR expression levels and CD5 was able to explain the different set points for different transgenic TCRs (Kassiotis et al., 2003).

2.3.3 Model Limitations

It is worth noting that our model simulates the activation of a single average T cell, whereas our data is the product of a population of cells. This approach is commonly taken in modelling studies under the assumption that the response scales linearly with cell number. In other words, we assume that the response of a population of 10,000 cells is the same as the sum of the responses of 10,000 single cells. This is a necessary simplification without which the modelling would not be feasible. Importantly, however, we know that this discrepancy between the model and the data creates one specific problem. Because we model cytokine production as a digital process, the dose response

curve for our average single cell is very steep, whereas our population data is more shallow. We can explain this with population heterogeneity, i.e. small differences between the cells in protein concentrations, metabolic state, etc. These differences are likely to follow a Gaussian distribution, as has been shown for the time to first division after T cell activation (Gett and Hodgkin, 2000). If we model this heterogeneity explicitly as a variation of the threshold for digital cytokine production, the resulting dose response curve for the population becomes shallower (Figure 2.9), showing that the sum of many digitally activated single cells does not result in a digital response on population level (see also (Altan-Bonnet and Germain, 2005)). For the analyses in this chapter, we have not included this modification to the model because modelling it explicitly would require a more in-depth analysis of the effects of such variability on different pMHC affinities and differences between donors. Moreover, there is no reason why there should be intercellular variability only on one parameter and we cannot currently know where exactly this variability would exert the most prominent effects in our model.

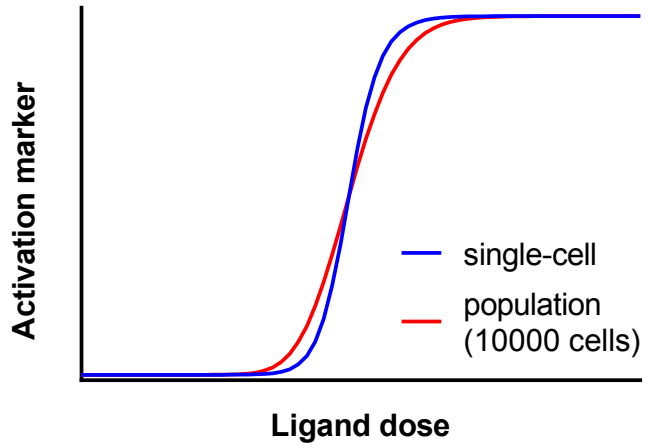


Fig. 2.9: Modelling population heterogeneity. We have used a simplified model of digital T cell activation (Hill-coefficient = 4) without TCR downregulation to illustrate the effect of population heterogeneity. The blue line shows the model output for activation of a single cell as it has been used for all modelling throughout this thesis. The red line shows the result of the same model when the mean of a population of cells is used instead. Each cell in the population has a slightly different activation threshold sampled from a log normal distribution around the default parameter used for the single-cell model (sy = 0.0285, standard deviation = 0.04).

2.3.4 Comparison to Our Previous Model

We have previously generated a model of T cell activation that explained some aspects of the data reported here, for example the bell-shaped dose response curves (Lever et al.,

2016). This model invoked an incoherent feed-forward motif downstream of the active TCR to explain the reduced cytokine production at high antigen doses. However, this previous model was only used to explain T cell responses to antigen dose and affinity collected at one time point. The model was developed based on the assumption that the T cells are in a steady-state. This was based on Jurkat T cell data showing that cytokine production continues at a constant rate. However, as we now show, this is not the case for primary human T cells. In order to explain the more comprehensive dataset presented here, we also had to include the temporal dynamics of TCR downregulation, and we found that modelling this process in detail, TCR downregulation was sufficient to explain the observed adaptation as well as the bell-shaped dose response. This represents a refinement of our more abstract previous model which was based on the assumption that TCR levels would be at steady state and not change over the course of the experiment. Our new model explains the bell-shaped dose response with a similar mechanism, where ligand engagement induces both a positive and a negative signal, the negative arm of which responds more strongly to antigen strength and therefore overtakes activation at high antigen doses and affinities (Figure 2.10). The difference to our previous model is that the mechanism now includes TCR binding and downregulation dynamics. The negative arm of the motif which we assumed to be signalling-mediated, turned out to be the downregulation of the receptor itself.

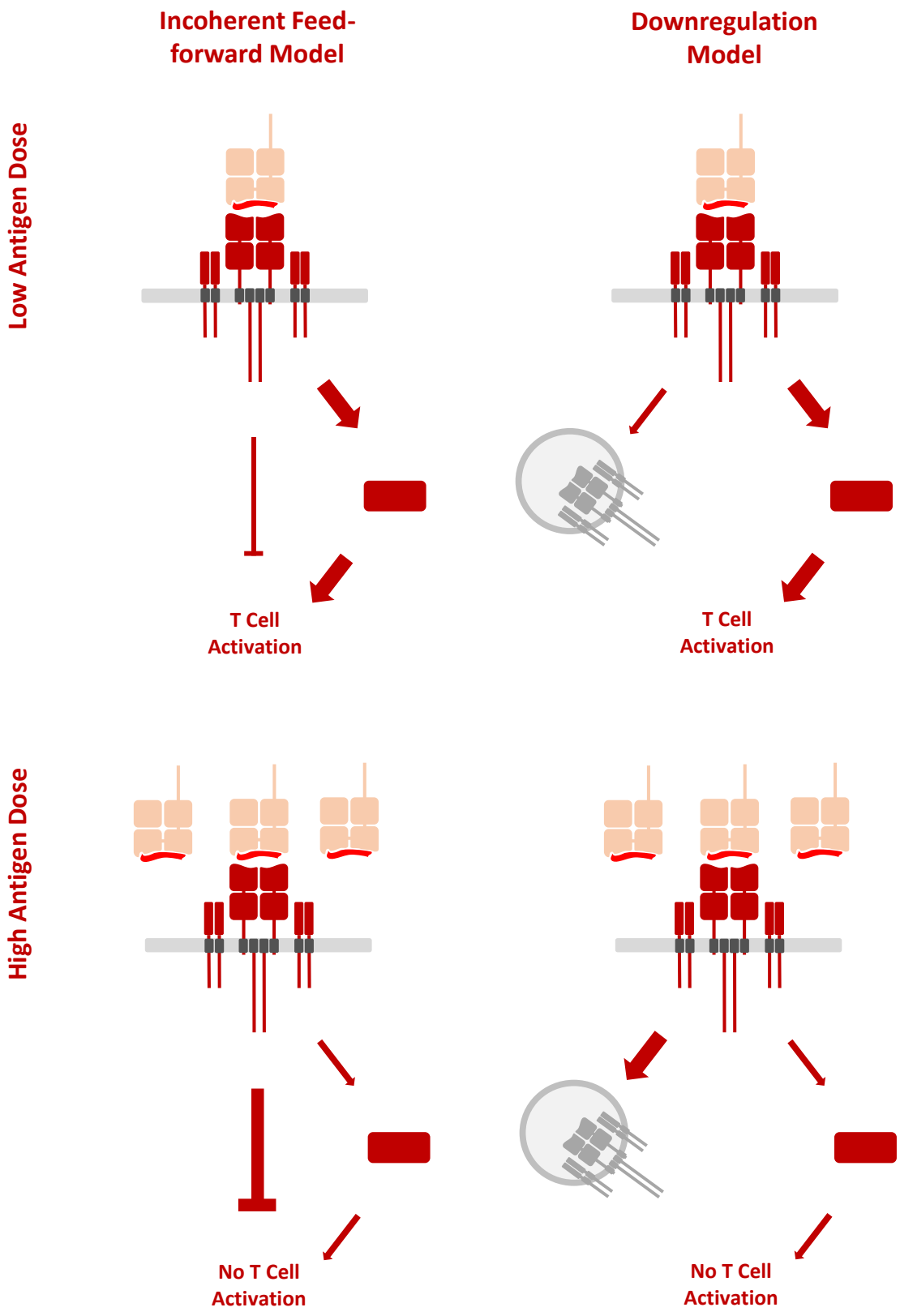


Fig. 2.10: Comparison of incoherent feed-forward model architecture with TCR downregulation model. Simplified schematic representation of our previous model (Lever et al., 2016) and the model presented here. In the incoherent feed-forward motif leads to T cell activation through signalling at low antigen doses, but at high doses, the negative signalling arm is stronger (because the positive arm includes an intermediate node that saturates). The TCR downregulation model also leads to T cell activation via signalling at low antigen doses, but at high doses, TCR downregulation prevents further activation.

2.3.5 Other Models of TCR Downregulation

Our model can be compared to previous attempts at modelling TCR downregulation quantitatively (Sousa and Carneiro, 2000; Coombs et al., 2002; Lee et al., 2003; Utzny et al., 2006) with some interesting differences that require further discussion. Coombs et al. and Lee at al. include kinetic proofreading before TCR downregulation which is consistent with our model, but they do not distinguish between activation of the TCR for signalling and tagging for downregulation. Both groups assume kinetic proofreading to represent phosphorylation of the TCR by Lck (Coombs et al., 2002; Lee et al., 2003). Taken together, this would mean that only phosphorylated TCRs are downregulated, but this is inconsistent with experimental evidence that clearly shows that TCR downregulation does not depend on Lck (Figure 2.3) (Cai et al., 1997; Salio et al., 1997; San Jose et al., 2000; Monjas et al., 2004). Therefore, the two processes, kinetic proofreading before activation and tagging before downregulation, both introduce a similar time delay that discriminates against low-affinity interactions, but they must be independent processes. This is why we have separated them in our model.

Coombs et al. found that they could only explain their data with a model in which TCR can only be internalised after unbinding. This is based on the observation that their highest-affinity ligands did not induce appreciable downregulation. In their view, the longer binding time produced by a high-affinity ligand will actively prevent the TCR from being internalised (Coombs et al., 2002). Our data did not show this effect for high-affinity ligands and therefore, the resulting model must be different. In our model, TCR downregulation proceeds at the same rate even if the binding time of the TCR-pMHC interaction would be much longer. We consider it likely that the downregulation process itself may exert forces that can disrupt the TCR-pMHC bond. Lee et al. also included an affinity optimum for T cell activation in their simulations (without experimental data). They discuss that their high-affinity ligands were bound for too long to be able to trigger multiple TCRs (serial triggering) and therefore, overall activation was reduced. However, TCR downregulation was not affected because it was modelled at a fixed rate, similar to the model we generated (Lee et al., 2003). We have called this mechanism "limited signalling" in our previous work (Lever et al., 2016) but have not included it here because it was not

required to explain the two pMHC affinities that the present work focussed on.

Utzny et al. model TCR bystander downregulation differently from us (Utzny et al., 2006). In their model, activated TCRs get downregulated and take with them either other activated TCRs or unbound TCRs in a cooperative interaction on the cell surface. In our model, unbound TCRs are constitutively internalised at a slow rate which is increased by signalling from activated TCRs, but independent of the downregulation of the activated TCR. It is worth noting that Utzny et al. did not include TCR signalling in their model, but they found that an exponentially decreasing bystander downregulation rate, which is the consequence of signalling-dependent bystander downregulation in our model, produced a better fit for their data (Utzny et al., 2006). There is good experimental support for bystander downregulation to be signalling-dependent (San Jose et al., 2000; Bonefeld et al., 2003; Monjas et al., 2004; von Essen et al., 2006; Fernández-Arenas et al., 2014). Furthermore, Utzny et al. included the serial triggering of clustered TCRs in their model to explain the rapid downregulation of TCRs during the first minutes after antigen encounter (Utzny et al., 2006). Serial triggering of multiple TCRs by each pMHC ligand was first proposed by Valitutti et al. to explain their observation that many more TCRs were downregulated than would be expected by the number of ligands (Valitutti et al., 1995), but Utzny et al. found that this was not enough to explain the rapid downregulation in the first minutes after binding. They further extended the model to include serial triggering as well as bystander downregulation of non-engaged TCRs and both together explained the very fast downregulation kinetics (Utzny et al., 2006). Although our data does not provide information about the TCR downregulation kinetics within the first hour of stimulation, our model includes both serial triggering and bystander downregulation. The possibility that each pMHC can serially bind multiple TCRs is implicit in the way we modelled the binding interactions because it is much more intuitive than the alternative, which would mean that each pMHC is essentially inactivated after one binding event. As discussed above (section 2.2.3), bystander downregulation was included to explain the effect of Lck inhibition on TCR downregulation. Following a phenotypic modelling approach (see section 1.6), we aimed to build the minimal model that is sufficient to explain our data in order to develop an understanding of the fundamental mechanism underlying the observed phenotype. We note that omitting other mechanisms that have been pro-

posed from our model should not be read as a statement that they do not exist, we can only conclude that they were not required to explain our data. One example would be the potential for downregulated TCRs to be re-routed back to the cell surface (Liu et al., 2000; Lee et al., 2003; Das et al., 2004; Fernández-Arenas et al., 2014).

Lee et al. also produced a mathematical model that includes TCR downregulation as well as many signalling interactions. This very complex model (discussed in more detail in section 1.6) leads them to conclude that a "decline of signaling occurs because of TCR degradation" but it is not entirely clear how they arrived at this causal relationship and which parts of the model were required to produce this phenotype (Lee et al., 2003).

3 Quantitative Effects of CD28 and CD2 Costimulation on $CD8^+$ T Cell Activation

3.1 Introduction to Costimulation

3.1.1 Effects of CD28 Costimulation on T Cell Activation

CD28 is the best studied costimulatory receptor and arguably the most important for the initial activation of naïve T cells. It binds to the ligands CD86 or CD80 on antigen-presenting cells which initiates extensive signalling (Esensten et al., 2016; Boomer and Green, 2010; Chen and Flies, 2013). The intracellular tail of the CD28 receptor contains various motifs that have been shown to play an important role in signalling, including proline-rich regions that recruit SH3 domain-containing proteins and a YMNM binding motif that, upon phosphorylation, recruits Grb2 and PI3K via their SH2 domains. The membrane-distal PYAP motif recruits Lck and other proteins. Through a complex signalling cascade that overlaps considerably with TCR signalling, CD28 costimulation leads to a plethora of phenotypic changes in the cell, with effects on proliferation, differentiation, metabolism, survival and cytoskeletal rearrangements, but the links between biochemical events and phenotypic outcomes are largely unclear (Esensten et al., 2016; Boomer and Green, 2010; Chen and Flies, 2013).

In terms of T cell effector function, one of the best-studied outcomes of CD28 costimulation is a strong increase in IL-2 production mediated via transcription factors like NFκB, AP-1 and NFAT as well as the posttranscriptional stabilisation of IL-2 mRNA (Lindstein et al., 1989; Fraser et al., 1991). Interestingly, one study found that the transcriptional increase depended on co-localisation with the TCR, whereas the stabilisation of IL-2 mRNA could also be induced by CD28 costimulation in trans, suggesting two at least partly different signalling pathways (Sanchez-Lockhart and Miller, 2006). IL-2 is the most important factor driving T cell survival and proliferation which means that CD28 costimulation will be critical for T cell clonal expansion. CD28 costimulation also directly increases survival by inducing the upregulation of anti-apoptotic proteins (Boise et al., 1995; Sperling et al., 1996). One study showed that CD28 costimulation decreases the time to first division rather than the division rate which results in a larger T cell population after a few days of expansion (Gett and Hodgkin, 2000).

Grb2 = growth factor receptor-bound protein 2

CD28 costimulation is often described as reducing the threshold for T cell activation towards lower antigen doses. This notion is based on observations that T cells begin to produce cytokines and proliferate in response to antigen at low concentrations or affinities in the presence but not in the absence of CD28 (Murtaza et al., 1999; Bachmann et al., 1996, 1997a). This has been contrasted with the phenotype induced by binding of LFA-1 on T cells to its ligand ICAM-1. LFA-1 is an adhesion molecule that increases TCR-pMHC interactions and therefore induces the T cell to respond to low doses of antigen without affecting the activation threshold downstream of the TCR. CD28 on the other hand does not influence TCR binding, but decreases the downstream threshold and thus also leads to T cell activation at lower antigen doses by a different mechanism to LFA-1 (Bachmann et al., 1997a; Viola and Lanzavecchia, 1996). Similar results were obtained with naïve CD4$^+$ T cells in a lipid bilayer system where T cells adhered to bilayers with the CD2 ligand CD48, but not to bilayers with CD80 (Bromley et al., 2001).

In summary, CD28 costimulation is known to have qualitative and quantitative effects on T cell activation. Biochemical studies have revealed many of the interactions mediating these functional effects, but have not led to a full understanding of the role of CD28 in T cell activation.

3.1.2 Effects of CD2 Costimulation on T Cell Activation

CD2 is expressed on CD4$^+$ and CD8$^+$ T cells and NK cells (Davis and Van Der Merwe, 1996) and more highly expressed on memory T cells (Sanders et al., 1989; Wallace and Beverley, 1990; Lo et al., 2010). The CD2 ligands differ between rodents (CD48) and humans (CD58), but are in both cases expressed broadly on many cell types including APCs (Dustin et al., 1987; Selvaraj et al., 1987; Davis and Van Der Merwe, 1996). On the other hand, the intracellular tail of CD2 is highly conserved between species (Davis and Van Der Merwe, 1996). Surprisingly, CD2 knockout mice only showed a subtle impairment in their immune responses (Killeen et al., 1992; Bachmann et al., 1999), suggesting that the role of CD2 in the immune system might be quite different between mice and humans. This could be explained by the lower affinity of mouse CD48 for CD2 compared to human CD58 (K_D = 60-90 μM vs. K_D = 9-22 μM) (Van der Merwe et al., 1994) or

ICAM = intercellular adhesion molecule

by the competition with another receptor, 2B4, for binding CD48 in the murine system (Clarkson and Brown, 2009). A recent study identified CD58 in zebrafish and suggested that this might provide a better model organism for the investigation of CD2 effects *in vivo* (Shao et al., 2018).

CD2 is a costimulatory molecule that lowers the threshold for T cell activation (Koyasu et al., 1990; Bachmann et al., 1999; Sasada et al., 2002; Milstein et al., 2008) and increases T cell proliferation, differentiation, cytokine production and cytotoxicity (Sanchez-Madrid et al., 1982; Bierer et al., 1988; Chang et al., 1989; Hahn and Bierer, 1993; Sasada et al., 2002; Skånland et al., 2014). The quantitative composition of the induced cytokine profile is distinct from CD28 costimulation (Skånland et al., 2014).

Early work on CD2 identified its signalling-independent role in promoting adhesion of the T cells to target cells and antigen-presenting cells (Bierer et al., 1988; Moingeon et al., 1989). On the molecular level, binding to its ligand CD58 on planar lipid bilayers has been shown to lead to a close alignment of the T cell membrane with the apposing membrane (Dustin et al., 1997; Milstein et al., 2008; Bromley et al., 2001). This creates an intermembrane distance of around 13 nm which is ideal for TCR-pMHC binding and CD2 consequently co-localises with the TCR in the cSMAC (Leupin et al., 2000; Douglass and Vale, 2005). This in turn is consistent with studies showing that CD2 lowers the T cell activation threshold (Koyasu et al., 1990; Bachmann et al., 1999; Sasada et al., 2002; Milstein et al., 2008). In addition to its adhesion role, CD2 exerts a signalling-dependent costimulatory function that further increases T cell activation (Bierer et al., 1988; Chang et al., 1989; Hahn and Bierer, 1993). This costimulatory signalling is dependent on multiple proline-rich regions in the intracellular tail (Chang et al., 1989; Hahn and Bierer, 1993) which were later shown to bind CD2-binding proteins 1, 2 and 3 (Li et al., 1998; Nishizawa et al., 1998; Freund et al., 2002; Tibaldi and Reinherz, 2003; Yang and Reinherz, 2006) as well as Lck (Carmo et al., 1993; Bell et al., 1996) and Fyn (Carmo et al., 1993; Freund et al., 2002). Furthermore, CD2 is connected to the actin cytoskeleton via direct binding of the adaptor molecules CMS and CIN85 via their SH3 domains (Hutchingst et al., 2003; Dustin et al., 1998) and through recruitment of WASp (Badour et al., 2003) and some of the adaptor proteins that bind CD2 recruit members of the Cbl family of E3

CMS = cas ligand with multiple Src homology 3 domains, CIN85 = cbl-interacting protein of 85 kDa

ubiquitin ligases (Tibaldi and Reinherz, 2003; Kirsch et al., 2001).

Initially, CD2 was believed to represent an alternative pathway of T cell activation. CD2 triggering with antibodies can indeed lead to TCR triggering-independent activation of the kinases Syk (Meinl et al., 2000), Lck (Danielian et al., 1992) and subsequently ITK (King et al., 1996). However, it is now clear that for it to lead to full T cell activation (e.g. cytokine production or proliferation), the TCR needs to be expressed on the T cell (Chang et al., 1989; Bockenstedt et al., 1988; Alcover et al., 1988) and Lck and ZAP70 are also required (Meinl et al., 2000; Martelli et al., 2000). This suggests proximal signal integration between CD2 and TCR signalling before activation of ZAP70 which is in line with the observation that CD2 associates with the TCR complex on resting and activated T cells (Brown et al., 1989; Gassmann et al., 1994; Milstein et al., 2008). CD2 costimulation has been shown to induce stronger phosphorylation of TCR proximal signalling molecules such as CD3ζ, ZAP70, and SLP-76 compared to CD28 (Skånland et al., 2014). Consequently, it synergises with the TCR in inducing LAT phosphorylation (Martelli et al., 2000) and the calcium signalling pathway (Espagnolle et al., 2007). More downstream, CD2 signalling leads to strong activation of the MAPK-ERK pathway (Martelli et al., 2000; Skånland et al., 2014) and some NFκB activation, although not as much as CD28 (Skånland et al., 2014). Interestingly, the same pathways were found to be enhanced by CD2 costimulation in human NK cells stimulated through CD16, including phosphorylation of CD3ζ, ZAP70 and ERK (Liu et al., 2016).

Costimulation effects are likely to be T cell subset-dependent. A recent phosphorylation screening after stimulation with an anti-CD3 antibody alone or together with anti-CD2 or anti-CD28 revealed that CD4$^+$ T cells responded more strongly to CD28 signalling than CD8$^+$ T cells, whereas CD8$^+$ T cells responded more strongly to CD2 costimulation (Skånland et al., 2014). This is in line with the observation that the naturally CD28-negative population among human CD8$^+$ T cells relies more on CD2 for their costimulatory signal (Leitner et al., 2015; Lo et al., 2010), as do T cells in a CD28 knockout mouse (Green et al., 2000).

Overall, CD2 clearly has an adhesion role and elicits signalling, but its overall role in T cell activation is not very well understood.

Syk = spleen tyrosine kinase, ITK = interleukin-2-inducible T cell kinase

3.2 Results

3.2.1 Simulation of Costimulatory Effects on T Cell Activation

The TCR downregulation model described in chapter 2 accurately predicts T cell cytokine production in time in response to antigens of different affinity presented at different doses. This allows us to make predictions about how defined perturbations of this network would affect the T cell response. These perturbations are modelled as increases or decreases in the reaction rates in the model and can be understood as modulating effects on the signalling pathways as they would be expected to occur when costimulatory (or inhibitory) receptors are engaged (illustrated in Figure 3.1). In the following, selected parameter perturbations are described that result in distinct simulated T cell activation phenotypes. We have only performed this analysis for costimulatory effects on a low-affinity pMHC ligand.

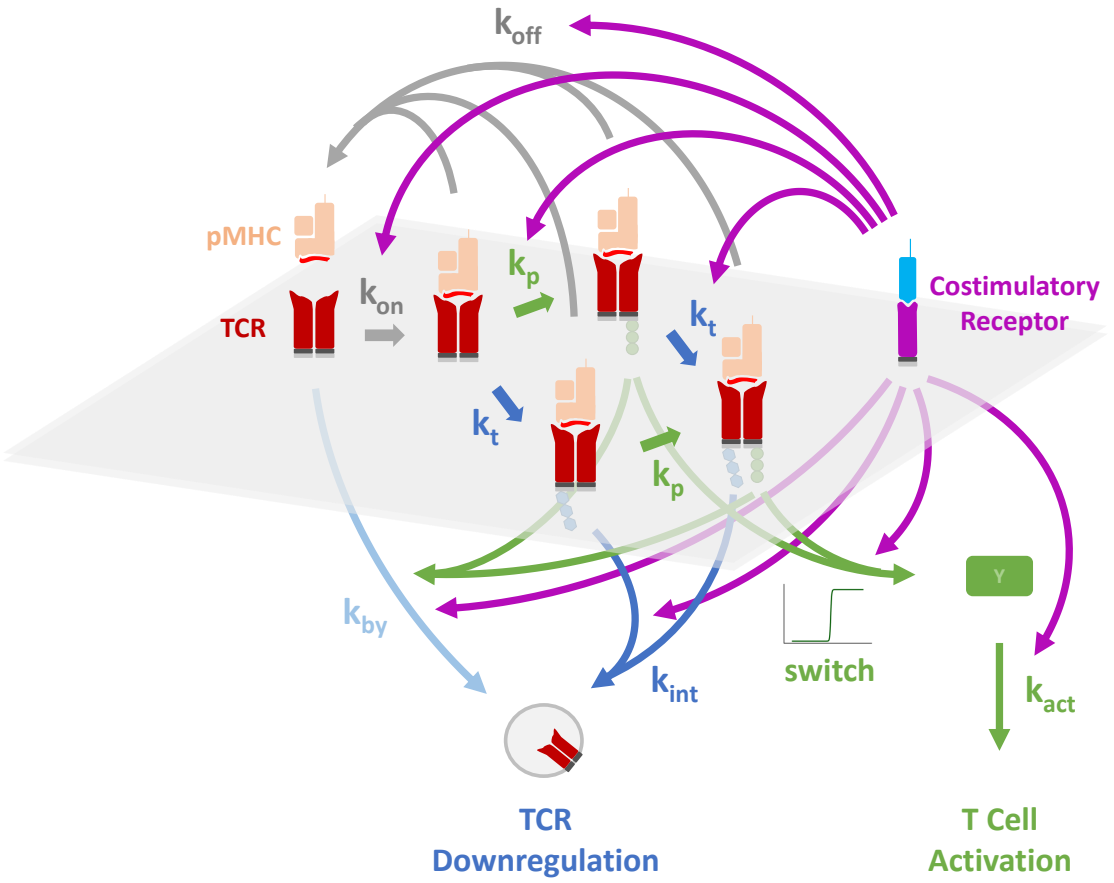


Fig. 3.1: TCR downregulation model schematic. This schematic representation of the mathematical model from chapter 2 shows all the potential integration points for a costimulatory receptor. Costimulation could in principle affect any reaction rate in this model and some costimulatory receptors are likely to have multiple effects.

Amplification of downstream signalling. Our model contains multiple parameters that directly influence cytokine production but have no effect on TCR levels because they act downstream of the active TCR. The default values for these parameters were determined by an Approximate Bayesian Computation-Sequential Monte Carlo (ABC-SMC) fitting algorithm (developed by Nicola Trendel) in chapter 2 and are now increased or decreased 10-fold, 100-fold, or 1000-fold. The simulated cytokine dose response curves after 8 h of stimulation are shown in Figure 3.2. Downstream of the TCR, a switch motif with a threshold parameter (sy) and a steepness parameter (ny) translates the concentration of active TCRs into a downstream signal. The magnitude of this signal is determined by k_{fy} and the degradation rate k_{ry}. Finally, the signal is amplified by k_{act} which leads directly to cytokine production. Consequently, increases in k_{act} directly scale cytokine production without any effect on the EC_{50} (a 1000-fold increase in k_{act} results in a 1000-fold increase in TNF-α production, Figure 3.2 A). The phenotypes for the switch parameters are more complex. The effects of modulations of k_{fy} and k_{ry} were exact opposites and only k_{fy} is shown in Figure 3.2 B. Decreasing this parameter decreases cytokine production without any effect on the EC_{50}. However, increasing k_{fy} leads to an increase in cytokine production that is accompanied by a decrease in EC_{50}. Reducing the steepness parameter ny of the switch function increases cytokine production with a particularly strong effect on low doses, i.e. it generates shallower dose response curves with a much lower EC_{50} but only a 2-fold increase in the E_{max} (Figure 3.2 C). A decrease in the threshold parameter for downstream activation, sy, similarly decreases the EC_{50} with a small (3-fold) increase in maximal cytokine production. Note that all switch parameters exhibit saturation because the switch node is modelled with a function that assumes conservation (e.g. a pool of enzyme that can get activated more and more with increasing signals, but not beyond 100 %):

$$\frac{dY}{dt} = k_{\text{fy}} * \frac{(TCR_{active} + TCR_{active+tagged})^{ny}}{sy^{ny} + (TCR_{active} + TCR_{active+tagged})^{ny}} * (1 - Y) - k_{\text{ry}} * Y$$

EC_{50} = half-maximal effective concentration

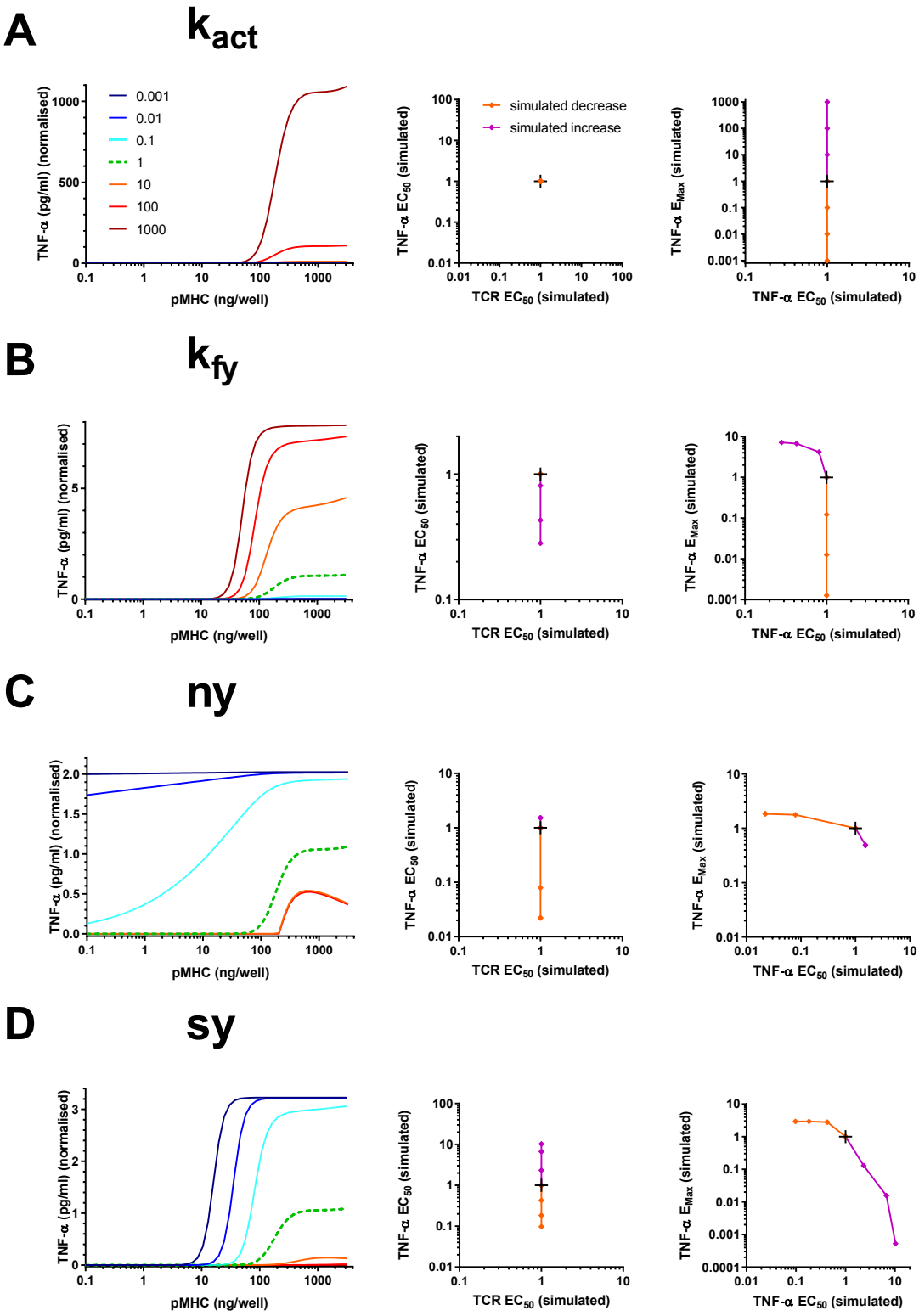


Fig. 3.2: Simulation of modulating effects on downstream signalling parameters. The default parameters from chapter 2 were increased or decreased 10-fold, 100-fold, or 1000-fold (ny only up to 100-fold). The cytokine production dose response curves and the extracted EC_{50} and E_{max} are shown for modulations of the cytokine production rate k_{act} (A), the switch amplitude k_{fy} (B), the switch steepness ny (C) and the switch threshold sy (D) with the respective fold-change indicated in the legend.

Modulating TCR-pMHC binding kinetics. In addition to signalling-mediated effects, costimulatory receptors like CD2 influence adhesion and close-contact formation between a T cell and an APC. We model such effects by modulating the TCR-pMHC binding parameters k_{on} and k_{off}. The default values as determined in chapter 2 were increased or decreased 10-fold, 100-fold, or 1000-fold. The simulated TCR downregulation dose response curves after an 8 h stimulation and the cytokine dose response curves are shown in Figure 3.3 A and B. The two binding parameters have exactly opposite effects on the EC_{50} of cytokine production and on the IC_{50} of TCR downregulation (Figure 3.3 C), but they differ in their effect on the E_{max} of cytokine production (Figure 3.3 C). An increased on-rate slightly increases the E_{max} of cytokine production (<1.5-fold) whereas a decreased off-rate (i.e. longer dwell time) reduces maximal cytokine production and produces much more bell-shaped curves. Importantly, the cytokine EC_{50} and the TCR IC_{50} are affected to exactly the same degree by modifications to the binding parameters (Figure 3.3 C).

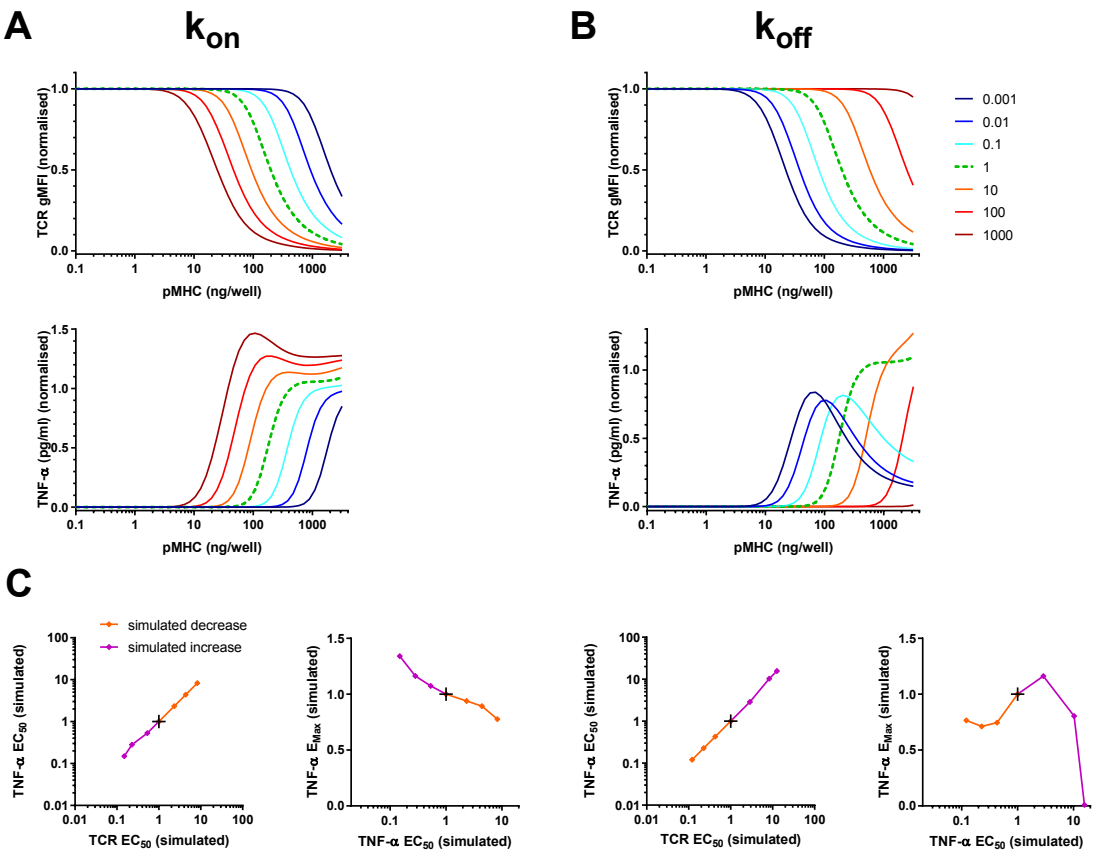


Fig. 3.3: Simulation of modulating effects on TCR-pMHC binding parameters. The default parameters from chapter 2 were increased or decreased 10-fold, 100-fold, or 1000-fold. The resulting TCR downregulation and cytokine production dose response curves are shown for modulations of the TCR-pMHC on-rate (A) and off-rate (B) with the respective fold-change indicated in the legend. C) Extracted EC_{50}, IC_{50} and E_{max} for the curves in A and B.

Modulating TCR downregulation. As discussed above, a costimulatory receptor that has adhesion effects that modulate TCR-pMHC binding kinetics will also change the dynamics of TCR downregulation. However, costimulation could also influence downregulation rates directly through signalling. The resulting dose response curves are shown in Figure 3.4 A and B and the extracted metrics in C. Increasing either of the two downregulation rates results in a shift of the downregulation curves towards lower pMHC doses which is accompanied by a complete abrogation of cytokine production. In this case, TCR downregulation is so quick that the T cells have very little time to produce any cytokines. A reduction in these two rates on the other hand, increases cytokine production because the cells now have more time to produce cytokines (which accumulate in the supernatant). TCR downregulation is not affected much by a reduction in k_{int}, probably because the curves shown here represent the simulation result after 8 h where all TCRs are downregulated even when the downregulation rate is reduced.

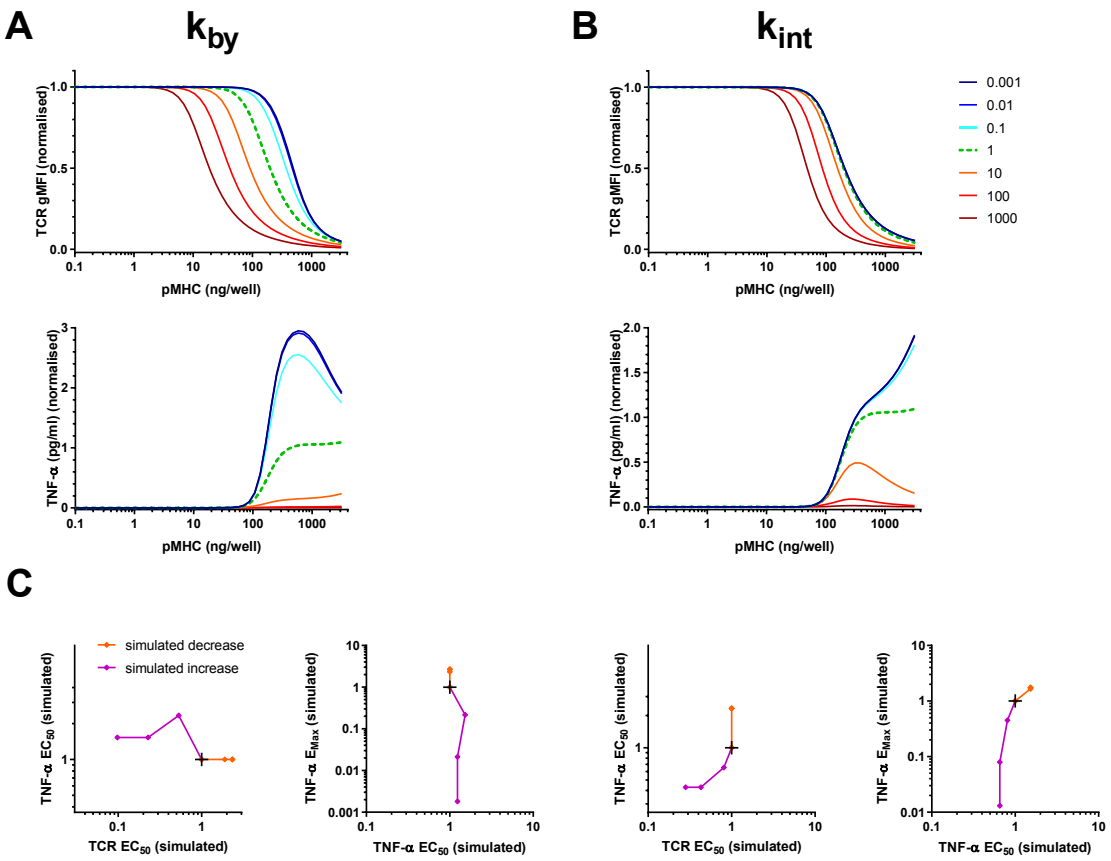


Fig. 3.4: Simulation of modulating effects on TCR downregulation rates. The default parameters from chapter 2 were increased or decreased 10-fold, 100-fold, or 1000-fold. The resulting TCR downregulation and cytokine production dose response curves are shown for modulations of the downregulation rates of non-engaged bystander TCRs k_{by} (A) and engaged TCRs k_{int} (B) with the respective fold-change indicated in the legend. C) Extracted EC_{50}, IC_{50} and E_{max} for the curves in A and B.

3.2.2 Expression of Costimulatory Receptors on Human CD8$^+$ T Cells

In order to compare the above predictions to experimental data for different receptors, we initially wanted to focus on receptors that are constitutively expressed on human CD8$^+$ T cells because receptors that are upregulated upon T cell activation (like 4-1BB or PD-1) will have a more complex phenotype. We confirmed expression of CD28, CD2 and CD6 on primary human CD8$^+$ T cells by flow cytometry (Figure 3.5). It is known that CD28 is expressed on around 50 % of human CD8$^+$ T cells, but also that there is considerable variability between individuals in this number, particularly depending on the donor's age (Esensten et al., 2016).

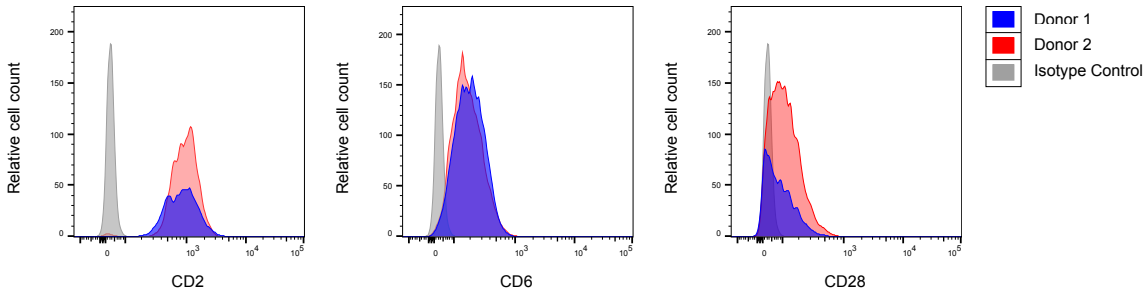


Fig. 3.5: Expression of costimulatory receptors on primary human CD8$^+$ T cells. Five days after removal of the stimulation beads, blasted primary human CD8$^+$ T cells from two donors were stained with antibodies against CD2, CD6 and CD28 and a secondary goat-anti-mouse FITC antibody and analysed by flow cytometry.

3.2.3 Quantitative Effects of CD28 Costimulation on TCR Downregulation

We have stimulated primary human CD8$^+$ T cells carrying the 1G4^{Hi} TCR with plate-immobilised recombinant pMHC as before. For the experiments in this chapter, we used the NY-ESO-1$_{157\text{-}165}$ peptide variant 4A as a high-affinity ligand (K_D = 1.09×10^{-3} μM) and 4A8K as a physiological affinity (K_D = 1.78 μM). In addition, we added a fixed dose of recombinant human CD86 to each pMHC dose response curve. This allowed us to study systematically the effects of CD28 costimulation on T cell activation in response to pMHC ligands of different affinity presented at a broad range of doses. We chose to use CD86 over CD80 because it is present on the cell surface as a monomer, whereas CD80 forms dimers, and the binding preference for CTLA-4 over CD28 is smaller for

FITC = fluorescein isothiocyanate

CD86 than for CD80 (Collins et al., 2002), which translates into preferential recruitment of CD28 by CD86 (Pentcheva-Hoang et al., 2004).

First, we measured TCR downregulation in response to pMHC with and without CD86. Dose response curves from one donor are shown in Figure 3.6 A and B. Curves were fitted to the data using Prism and the averaged effects of four donors are quantified in Figure 3.6 C and D. We made the assumption that all TCR downregulation curves in any one dataset would start at the same baseline (i.e. all cells express the same number of TCRs before stimulation) and would eventually reach the same minimum (complete downregulation) given a high enough pMHC dose. This is based on the model predictions from chapter 2 and on experimental observations with some donors where even the low-affinity pMHC ligand induced complete downregulation. In the example shown in Figure 3.6, immobilisation of the low-affinity ligand was not optimal so that TCR downregulation did not reach the bottom.

The interpretation of this data is affected by another important assumption. As discussed in section 3.2.5, the quantification of surface marker expression is confounded by an upper limit on how much of the protein can be expressed on the cells. This upper bound artificially decreases the EC_{50} or IC_{50}. We have still extracted the IC_{50} values from the TCR downregulation curves here, because our model from chapter 2 explicitly includes TCR downregulation and therefore reproduces the upper and lower bounds for this marker. Notably, TCR downregulation is not used as a marker of T cell activation, because the model assumes (based on the data from chapter 2) that it is a mostly signalling-independent consequence of pMHC binding.

CD86 had no effect on the IC_{50} of TCR downregulation for both the high- and the low-affinity ligand. There was no consistent effect on the Hill coefficients of the high-affinity pMHC curves, but the low-affinity ligand showed a dose-dependent decrease in the Hill number with increasing CD86. We noted some variability between donors particularly with regard to effects on the high-affinity curves, with some showing slight increases in IC_{50} and others slight decreases, but all the effects were small in magnitude. It has been reported before that TCR downregulation is independent of CD28 costimulation (Bachmann et al., 1997a; Cai et al., 1997; Iezzi et al., 1998).

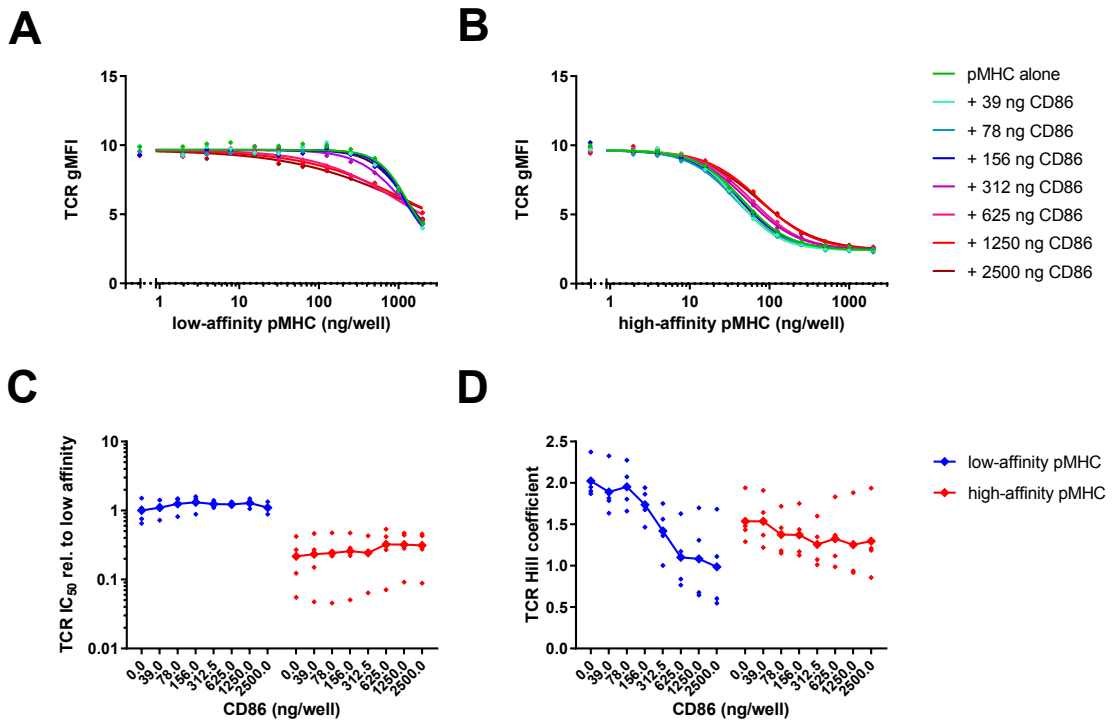


Fig. 3.6: Quantitative effects of CD28 costimulation on TCR downregulation. Primary human CD8$^+$ T cells carrying the 1G4^{Hi} TCR were stimulated for 8 h with the physiological-affinity pMHC variant 4A8K and the high-affinity variant 4A co-presented with a dose titration of recombinant CD86. TCR expression was measured by flow cytometry and curves were fitted using a four-parameter inhibitor dose response curve in Prism under the assumption that all curves start at the same baseline and would reach the same minimum given a high enough dose. A) Representative dose response curves for the low-affinity ligand. B) Representative dose response curves for the high-affinity ligand. C) Averaged IC_{50} values from four donors. The IC_{50} of the dose response curves were normalised to the mean of each dataset and are expressed as a fold-change to the low-affinity pMHC without CD86. D) Averaged Hill numbers from four donors.

3.2.4 Quantitative Effects of CD28 Costimulation on Cytokine Production

In the same stimulation experiments, we assessed the concentration of TNF-α, IFN-γ and IL-2 in the supernatant after 8 h of stimulation. Representative dose response curves from one donor are shown in Figure 3.7 A and B. In order to be able to average data from three donors, we fitted bell-shaped curves to the data in Matlab and extracted the E_{max}, the EC_{50}, and the Hill coefficient (see section 6.10). There was considerable variability between donors in the absolute amounts of cytokines produced, some of which can be explained with differences in transduction efficiency. To be able to compare the effects of costimulation between repeats, we normalised each dataset to its mean. We found that this normalisation reduced variability more than normalising to one arbitrarily chosen curve in the dataset, probably because the E_{max} or EC_{50} of this particular curve could be an outlier in one of the repeats whereas the mean of all curves is more robust. We then averaged the normalised values from all donors. In Figure 3.7 and all subsequent figures, those values are expressed as a more intuitive fold-change compared to the low-affinity pMHC without CD86.

As expected, CD86 leads to a strong dose-dependent increase in cytokine production. The effect is most pronounced for IL-2 (9.9-fold increase compared to 2.9-fold for TNF-α and 3.6-fold for IFN-γ on the low-affinity pMHC) and similar between the high- and low-affinity pMHC (Figure 3.7 C).

Only a small decrease in the EC_{50} was apparent for all three cytokines at higher CD86 doses on the low-affinity pMHC, whereas no change was observed on the high-affinity pMHC (Figure 3.7 D).

In contrast to TCR downregulation, the Hill coefficients did not show any consistent changes with CD86 (Figure 3.7 E). The outliers in the Hill numbers can be attributed to individual poor fits, for example when one outlier datapoint in the ascending part of the curve strongly affected the steepness.

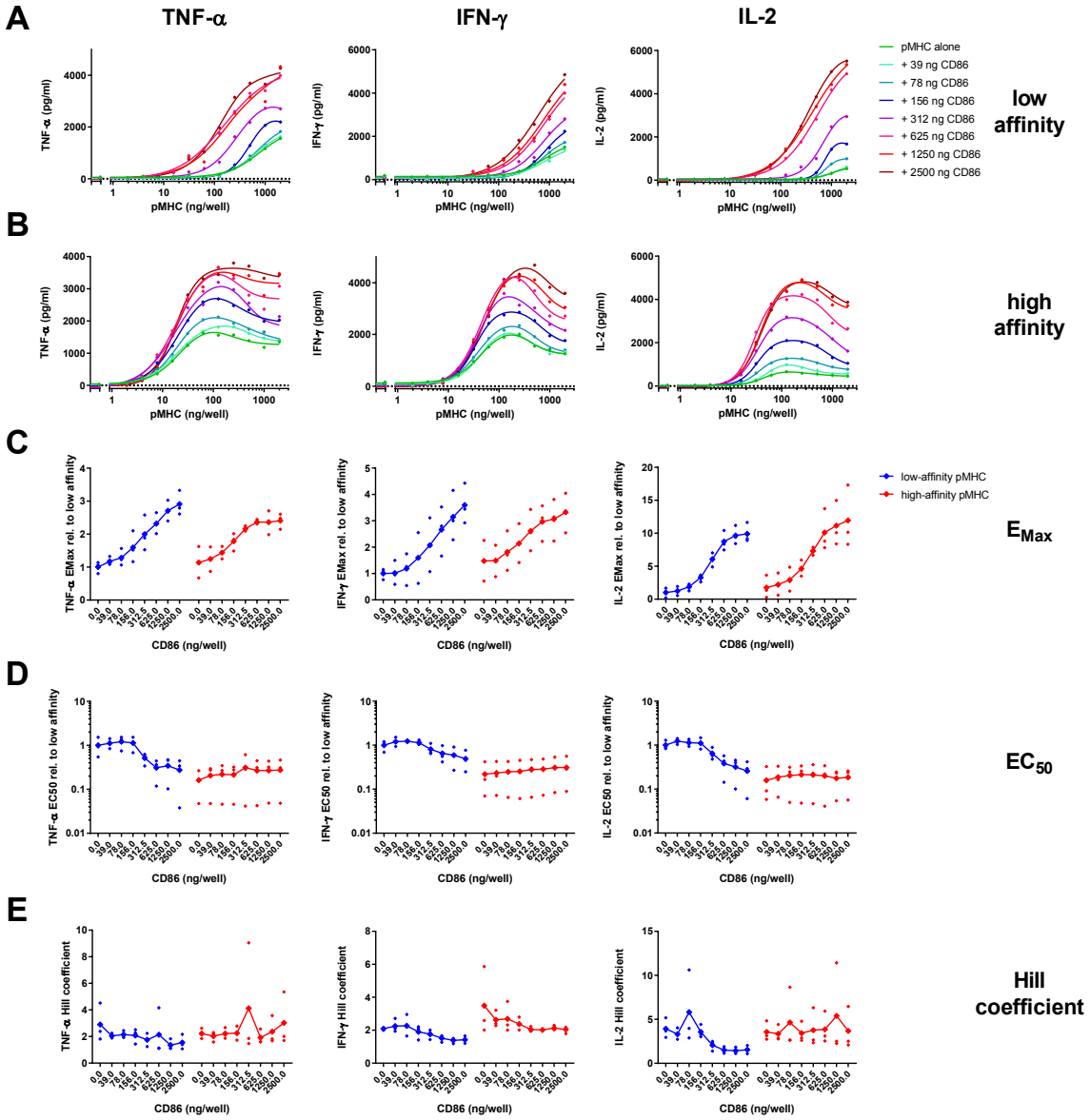


Fig. 3.7: Quantitative effects of CD28 costimulation on cytokine production. Primary human CD8$^+$ T cells carrying the 1G4^{Hi} TCR were stimulated for 8 h with the physiological-affinity pMHC variant 4A8K and the high-affinity variant 4A co-presented with a dose titration of recombinant CD86. Cytokine concentrations were measured by ELISA. A) Representative dose response curves for the low-affinity ligand for TNF-α, IFN-γ and IL-2. B) Representative dose response curves for the high-affinity ligand. C) Averaged E_{max} values from three donors. D) Averaged EC_{50} values from three donors. E) Averaged Hill numbers from three donors. The EC_{50} and E_{max} of the dose response curves were normalised to the mean of each dataset and are expressed as a fold-change to the low-affinity pMHC without CD86.

3.2.5 Effects of CD28 Costimulation on T Cell Surface Markers

We analysed the effects of CD86 on the expression of activation markers on the T cell surface. We saw strong upregulation of CD69 and 4-1BB after 8 h of stimulation, particularly at low doses of pMHC (Figure 3.8). However, we found that surface marker expression in general is difficult to correlate directly with T cell activation. This is due to the fact that the fraction of cells that will express these markers is finite; specifically, it is limited by the 1G4^{Hi} TCR transduction efficiency in any given experiment. In the results shown here, around 60 % of the T cells expressed the TCR (Figure 3.8 A). This upper limit means that the curves with CD86 are not true representations of the effect CD86 has on T cell activation. For example, at the highest dose of pMHC, there is no apparent effect because pMHC alone already induces maximal CD69 and 4-1BB expression, although we know from the cytokine production data that there is a further increase in T cell activation with CD86 at high pMHC doses (section 3.2.4). We have simulated the saturation of an activation marker by including a saturating function as the last term in the model. Figure 3.8 C shows the simulated dose response curve for a modulation of k_{act} which only amplifies maximal activation without any effect on the EC_{50}, as discussed in section 3.2.1. In contrast, the same modulation of k_{act} applied to a saturating activation marker shows an upper limit in the E_{max} and after this is reached, an artificial decrease in the EC_{50}. Note that this simulation is only meant to qualitatively reproduce the phenotype (a shift in the EC_{50}). To fit the surface marker data quantitatively, we would have to find an entirely new set of parameters. We have therefore decided not to quantify the CD86 effect on these curves, because the extracted metrics would be artefacts resulting from the described ceiling effect (e.g. an apparent decrease in EC_{50} with no effect on E_{max}). An alternative measure of surface marker expression is the mean fluorescence intensity which reflects the population average of the amount of CD69 or 4-1BB any single cell can accumulate on its surface. Although this value does scale slightly more with CD86 dose for CD69 (Figure 3.8 B), we believe that similar limitations apply to the maximal amount of these molecules expressed per cell. Surface marker data would therefore be difficult to compare to our model output, because we do not have enough data to model the upper limits of these molecules explicitly. Consequently, we have not used surface markers as quantitative measures of T cell activation in this study.

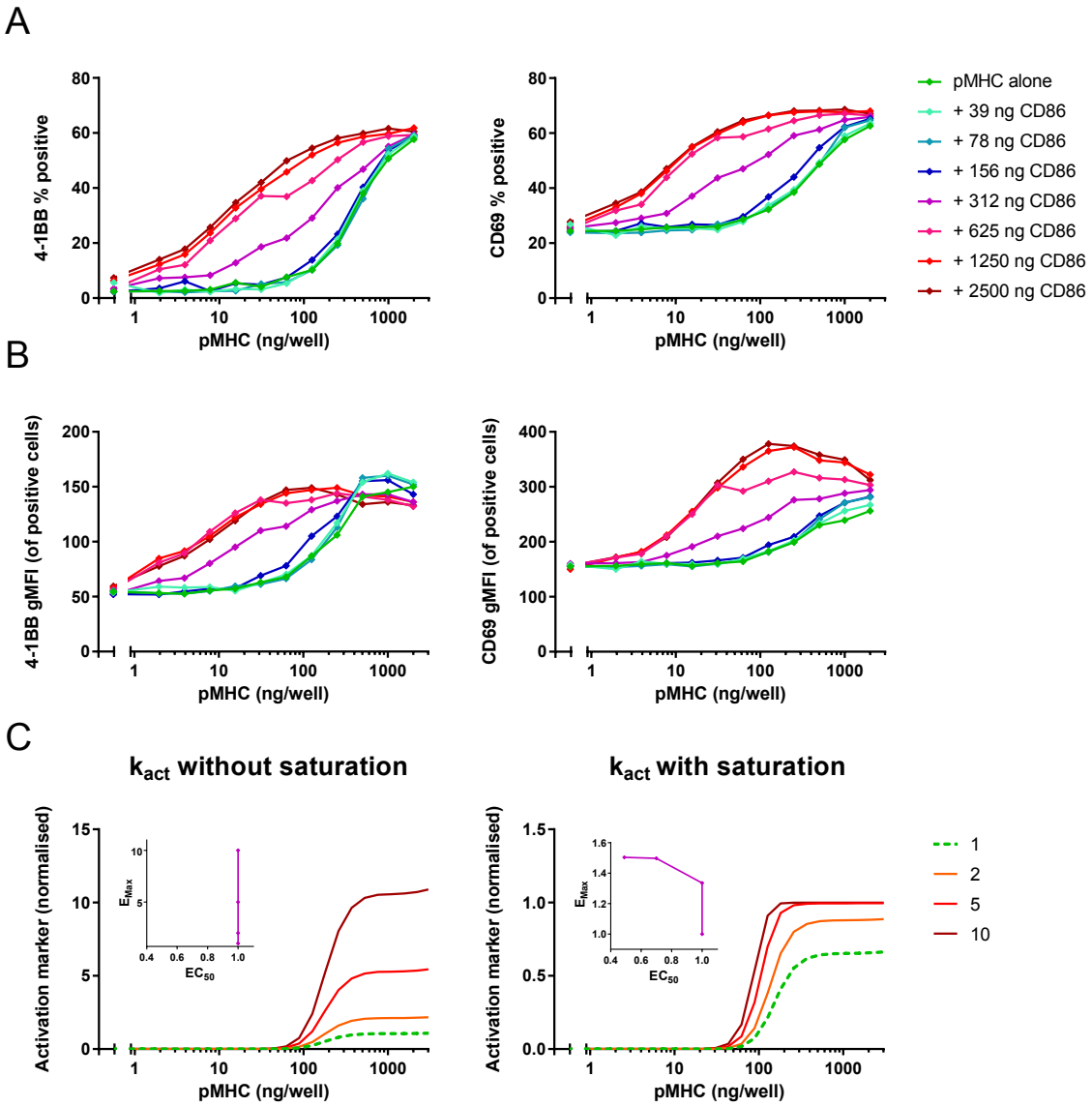


Fig. 3.8: Effect of CD28 costimulation on activation markers on the T cell surface. Primary human $CD8^+$ T cells carrying the $1G4^{Hi}$ TCR were stimulated for 8 h with the physiological-affinity pMHC variant 4A8K co-presented with a dose titration of recombinant CD86. The T cells were analysed for expression of the activation markers CD69 and 4-1BB by flow cytometry. A) fraction of the cells that express the respective marker. B) gMFI of the marker on the positive population. The data shown here is representative for four independent experiments with different donors. C) Simulated dose response curves for the fold-increases of k_{act} indicated in the legend with or without saturation of the activation marker. The insets show the curves' E_{max} over their EC_{50}.

3.2.6 Modelling CD28 Costimulation

We next compared the simulated costimulation phenotypes discussed in section 3.2.1 with the effects of CD28. Given that CD28 had no effect on TCR downregulation, we focussed on the intracellular signalling parameters k_{fy}, ny, sy and k_{act} which have been systematically modulated in Figure 3.2 where we showed that they do not affect the TCR itself. CD28 costimulation induced a 3-fold increase in maximal TNF-α production and a 4-fold decrease in TNF-α EC_{50}. We plotted these two parameters together in the same plot to be able to compare the data directly with our model output after modulating each parameter. The simulation results were normalised to the mean of the seven costimulation doses and E_{max} and EC_{50} were expressed as a fold-change compared to pMHC alone exactly as we did with the experimental data. Figure 3.9 shows that k_{act} only increases the E_{max} and has no effect on the EC_{50}. In contrast, the three switch parameters all have some effect on both the E_{max} and the EC_{50}. The switch amplifier k_{fy} strongly increases the E_{max} but has only a small effect on the EC_{50}. The switch steepness ny very strongly decreases the EC_{50}. The increase in E_{max}, however, saturated at less than 2-fold. Finally, modulation of the threshold sy resulted in an intermediate phenotype of the other two and led to a decrease in EC_{50} and an increase in E_{max} that were similar to what we observed in our data. Therefore, we concluded that a modulation of the activation threshold downstream of the TCR is sufficient to explain the effect of CD28 costimulation. We cannot exclude that a combination of two parameters, for example ny and k_{fy}, might produce an even better fit. However, any such combination would have to have in common that it lowers the T cell's activation threshold and amplifies overall cytokine production without affecting TCR downregulation.

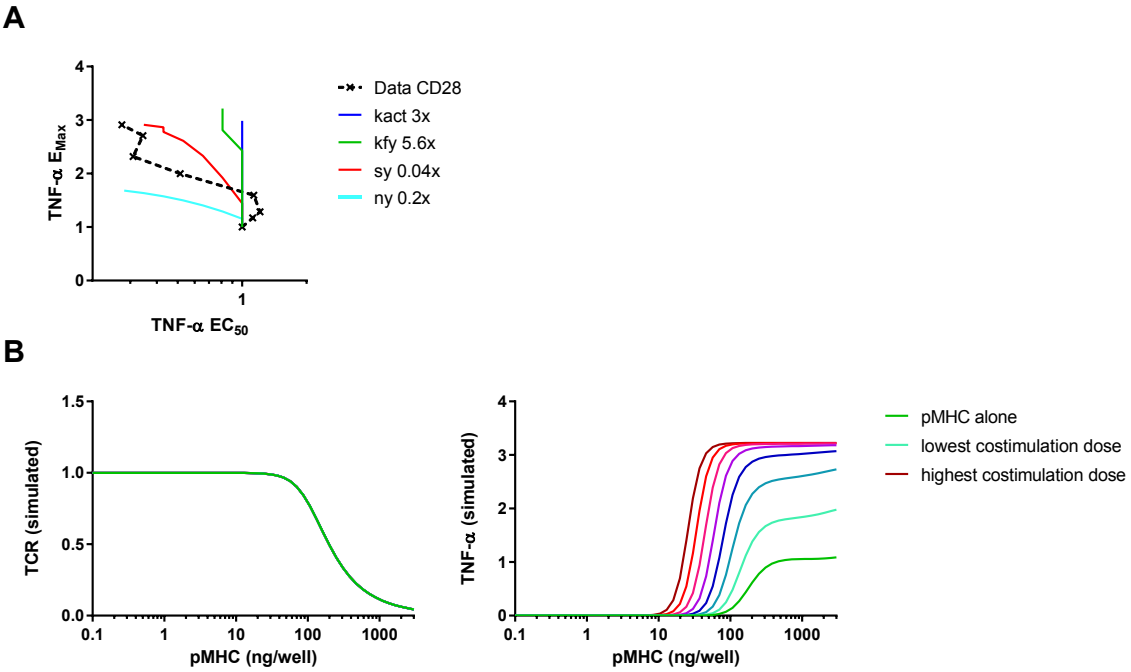


Fig. 3.9: Comparison of simulations with metrics extracted from CD28 data. The EC_{50} and E_{max} extracted from the experimental data (Figure 3.7) were re-plotted in a different format to enable a quantitative comparison with model simulations. The model output was normalised to the mean and E_{max} and EC_{50} were expressed as a fold-change exactly as we did with the experimental data. A) Each solid line represents the modulation of one parameter with 8 simulated costimulation doses that induced changes between 1-fold (pMHC alone) and the indicated maximum modulation. Only the downstream signalling parameters were modulated because all others would have an effect on the TCR IC_{50} which was not apparent in the experimental data (Figure 3.6).

3.2.7 Quantitative Effects of CD2 Costimulation on TCR Downregulation

We were interested in comparing the responses observed with CD28 ligands with costimulation through CD2. Figure 3.10 and Figure 3.11 show data from three donors with the same high- and low-affinity pMHC ligands as we used for CD28 costimulation. The T cells were stimulated with or without increasing concentrations of recombinant human CD58 which was co-immobilised on the plates alongside the pMHC titrations. TCR downregulation and cytokine production were measured after 8 h. The data fitting, normalisation and extraction of the metrics IC_{50}, EC_{50}, Hill coefficient and E_{max} were performed as described above for CD28. Representative dose response curves are shown in Figure 3.10 A and B.

CD58 had a much stronger effect on TCR downregulation than CD86, particularly on the IC_{50}. There was a strong (100-fold) CD58 dose-dependent decrease in IC_{50} with the low-affinity pMHC, and to a lesser degree with the high-affinity ligand (Figure 3.10 C). Of note, there seemed to be a sharp threshold between 100 and 200 ng of CD58 below which there was little effect on TCR downregulation. This explains the variability at 125 ng where one donor showed only a small decrease in IC_{50} whereas for the other two, the effect was already maximal. We also observed a corresponding decrease in the Hill numbers of both the low- and the high-affinity pMHC curves (Figure 3.10 D). It has been reported previously that CD2 increases TCR downregulation (Bachmann et al., 1999; Wild et al., 1999).

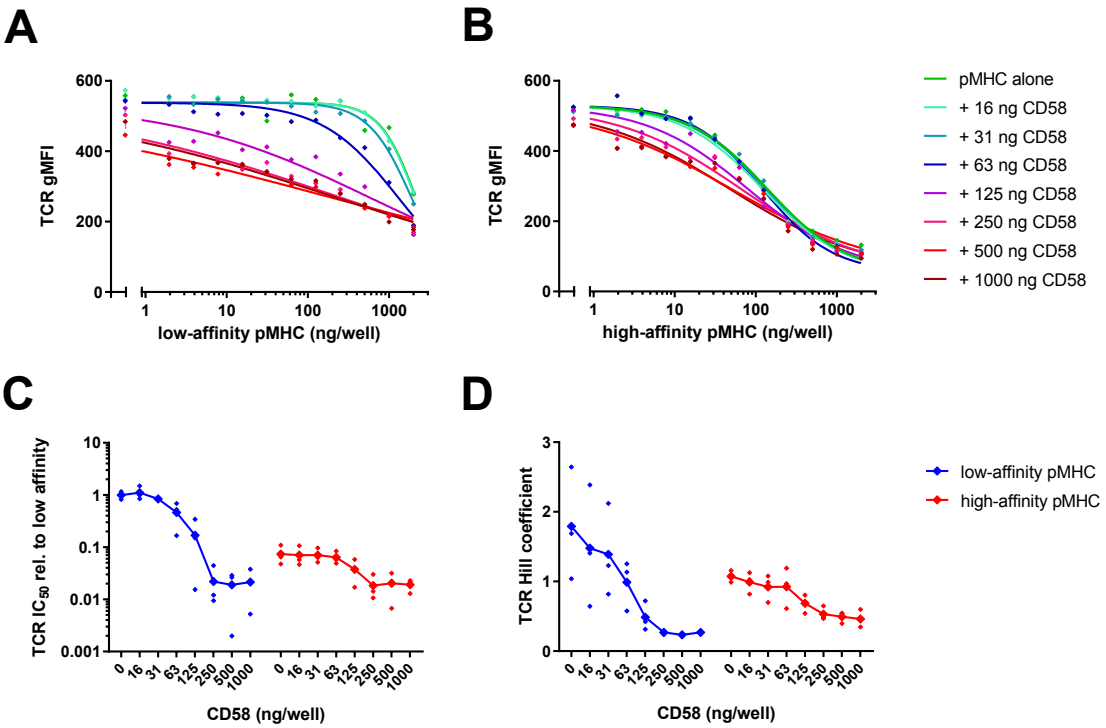


Fig. 3.10: Quantitative effects of CD2 costimulation on TCR downregulation. Primary human CD8$^+$ T cells carrying the 1G4^{Hi} TCR were stimulated for 8 h with the physiological-affinity pMHC variant 4A8K and the high-affinity variant 4A co-presented with a dose titration of recombinant CD58. TCR expression was measured by flow cytometry and curves were fitted using a four-parameter inhibitor dose response curve in Prism under the assumption that all curves start at the same baseline and would reach the same minimum given a high enough dose. A) Representative dose response curves for the low-affinity ligand. B) Representative dose response curves for the high-affinity ligand. C) Averaged IC_{50} values from three donors. The IC_{50} of the dose response curves were normalised to the mean of each dataset and are expressed as a fold-change to the low-affinity pMHC without CD58. D) Averaged Hill numbers from three donors. The data in this figure was generated by Johannes Pettmann and analysed by the author.

3.2.8 Quantitative Effects of CD2 Costimulation on Cytokine Production

In the same experiments, cytokine concentrations in the supernatant were measured by ELISA after 8 h of stimulation. Data from three donors was averaged as discussed in section 3.2.4 and the extracted EC_{50} and E_{max} were expressed as a fold-change to the low-affinity pMHC without CD58. Representative dose response curves are shown in Figure 3.11.

Perhaps surprisingly, CD58 led to stronger increases than CD86 in the production of all three cytokines tested. Again, IL-2 production was increased the most (32.6-fold), followed by IFN-γ (10.3-fold) and TNF-α (5.1-fold) on the low-affinity antigen and the effect was similar for the high-affinity pMHC. Cytokine production gradually increased with increasing CD58 dose and saturated at the highest doses.

The EC_{50}s of TNF-α, IL-2 and IFN-γ were all strongly decreased with increasing doses of CD58. This effect was stronger on the low-affinity pMHC with the interesting result that at low antigen doses, cytokine production from the low-affinity ligand with CD58 outperformed the high-affinity pMHC with CD58 (Figure 3.11 D). For the low-affinity pMHC, the response to CD58 somewhat mirrored the effect observed on TCR downregulation with a sharp threshold between 100 and 200 ng of CD58 at which the EC_{50} suddenly drops and quickly saturates. On the high-affinity antigen in contrast, the effect on the EC_{50} was more gradual. As for CD86, the Hill coefficients showed some outliers, but the overall trend was possibly a small reduction with CD58 dose on the low-affinity ligand for TNF-α and IL-2, but no effect on the high-affinity pMHC or on IFN-γ.

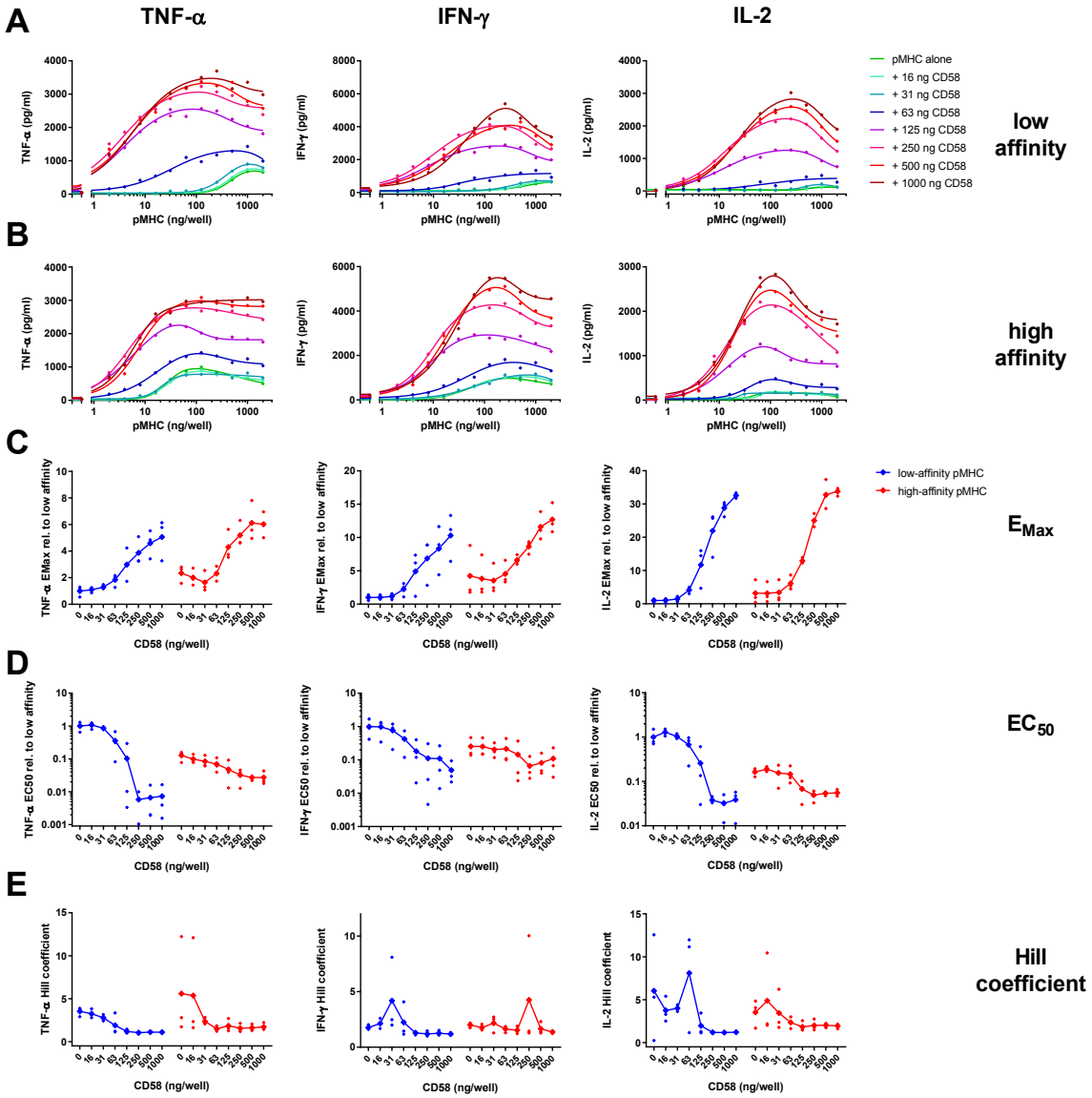


Fig. 3.11: Quantitative effects of CD2 costimulation on cytokine production. Primary human CD8$^+$ T cells carrying the 1G4^{Hi} TCR were stimulated for 8 h with the physiological-affinity pMHC variant 4A8K and the high-affinity variant 4A co-presented with a dose titration of recombinant CD58. Cytokine concentrations were measured by ELISA. A) Representative dose response curves for the low-affinity ligand for TNF-α, IFN-γ and IL-2. B) Representative dose response curves for the high-affinity ligand. C) Averaged E_{max} values from three donors. D) Averaged EC_{50} values from three donors. E) Averaged Hill numbers from three donors. The EC_{50} and E_{max} of the dose response curves were normalised to the mean of each dataset and are expressed as a fold-change to the low-affinity pMHC without CD58. The data in this figure was generated by Johannes Pettmann and analysed by the author.

3.2.9 Modelling CD2 Costimulation

As discussed for CD28, we next compared the effects of CD2 costimulation to model simulations by modulating each parameter. CD2 strongly decreased the IC_{50} of TCR downregulation (46-fold) and had an even stronger effect on the EC_{50} of TNF-α production (137-fold decrease). In addition, CD2 increased maximum TNF-α production 5-fold. Figure 3.12 shows the effects of CD2 costimulation on cytokine EC_{50} and E_{max} and TCR IC_{50} plotted together with variations in the model parameters. In contrast to CD28, this direct comparison reveals that modulation of one single parameter in our model is not sufficient to explain the CD2 effects. Effects on the binding parameters k_{on}, k_{off} and nb (i.e. adhesion effects) can reproduce a similar shift for both EC_{50}s (although CD2 seems to affect TNF-α slightly more than the TCR), but they fail to reproduce the increase in E_{max}. Conversely, the downstream signalling parameters k_{fy}, sy and ny have effects on the cytokine EC_{50} and E_{max} in the right direction, but they do not affect TCR downregulation at all and can therefore not explain the strong decrease in IC_{50} that we see with CD2 costimulation. Increasing the TCR downregulation rate k_{int} or the bystander downregulation rate k_{by} does decrease the TCR downregulation IC_{50}, but it also reduces overall cytokine production which is not consistent with the CD2 effect.

Given that no single parameter could explain the CD2 effects and we know from the literature that CD2 has adhesion as well as signalling functions (see section 3.1.2), we tested promising combinations of two, three or four parameters that were varied independently with costimulation dose. We used the modulations discussed above as the upper (or lower) limit. An algorithm was developed to systematically evaluate all possible combinations of adhesion effects (k_{off}, k_{on}, nb alone or in combinations of two) with signalling effects (k_{fy}, ny, sy, k_{act} alone or in combinations of two) with four different degrees of modulation for each parameter (i.e. four different simulated doses of costimulation). The results were ranked by their fit to the TNF-α EC_{50}, TCR IC_{50} and TNF-α $E_{max}$from the CD2 data. All the best fitting parameter sets included changes in k_{on} and k_{off} and at least one of the switch parameters. Given that CD2 is known to act as an adhesion molecule, it is not surprising to find changes in both k_{on} and k_{off}. Mechanistically, increases in the on-rate of TCR-pMHC interactions can be explained by CD2 bringing the T cell membrane

into close proximity to the antigen. A decreased off-rate can be explained by considering that a large number of CD2-CD58 bonds in the interface will likely reduce the pulling forces that act on the TCR-pMHC bond. This hypothesis is supported by the finding that elongated CD2 ligands reduce TCR-pMHC binding, whereas shortened ligands enhance its costimulatory effect (Wild et al., 1999; Milstein et al., 2008). Further, the results showed that the two parameters that determine the threshold of TNF-α production (sy and ny) were interchangeable (see fits in Figure 3.12 B). The same was true to a degree for k_{fy} and k_{act} although the fits with k_{fy} were consistently ranked higher than parameter sets with k_{act}. Although we have not found a unique parameter combination, we can conclude that overall, the highly ranked parameter sets that produced a good fit all consisted of changes in k_{on} and k_{off} in combination with one "threshold" parameter (ny or sy) and one "amplification" parameter (k_{fy} or k_{act}). This makes sense considering the effects these parameters have individually (Figure 3.12 A). Changes to the binding parameters k_{on} and k_{off} both decrease the TCR IC_{50}, but either one alone was not sufficient to explain the strong effect of CD2. A modulation of the cytokine production threshold is required to explain how the TNF-α EC_{50} is decreased even more than the TCR IC_{50}, because with effects on TCR binding alone, both TCR downregulation and TNF-α production would be affected to the same degree. Finally, a reduction in the cytokine production threshold alone is not sufficient to explain the increase in maximal TNF-α production, so a further amplification of the signal is required.

Note that none of the parameter modulations discussed above is able to explain the decrease in the Hill coefficient for TCR downregulation. Only changes in the cooperativity parameter on TCR-pMHC binding (nb) can produce shallower downregulation curves, but changes there also affect the EC_{50}/IC_{50} of all responses. We cannot exclude that there might be parameter combinations that can explain this phenotype, but it is also possible that a further modification of the model architecture is required to fully recapitulate this effect. Some ideas are discussed in section 5.2.2.

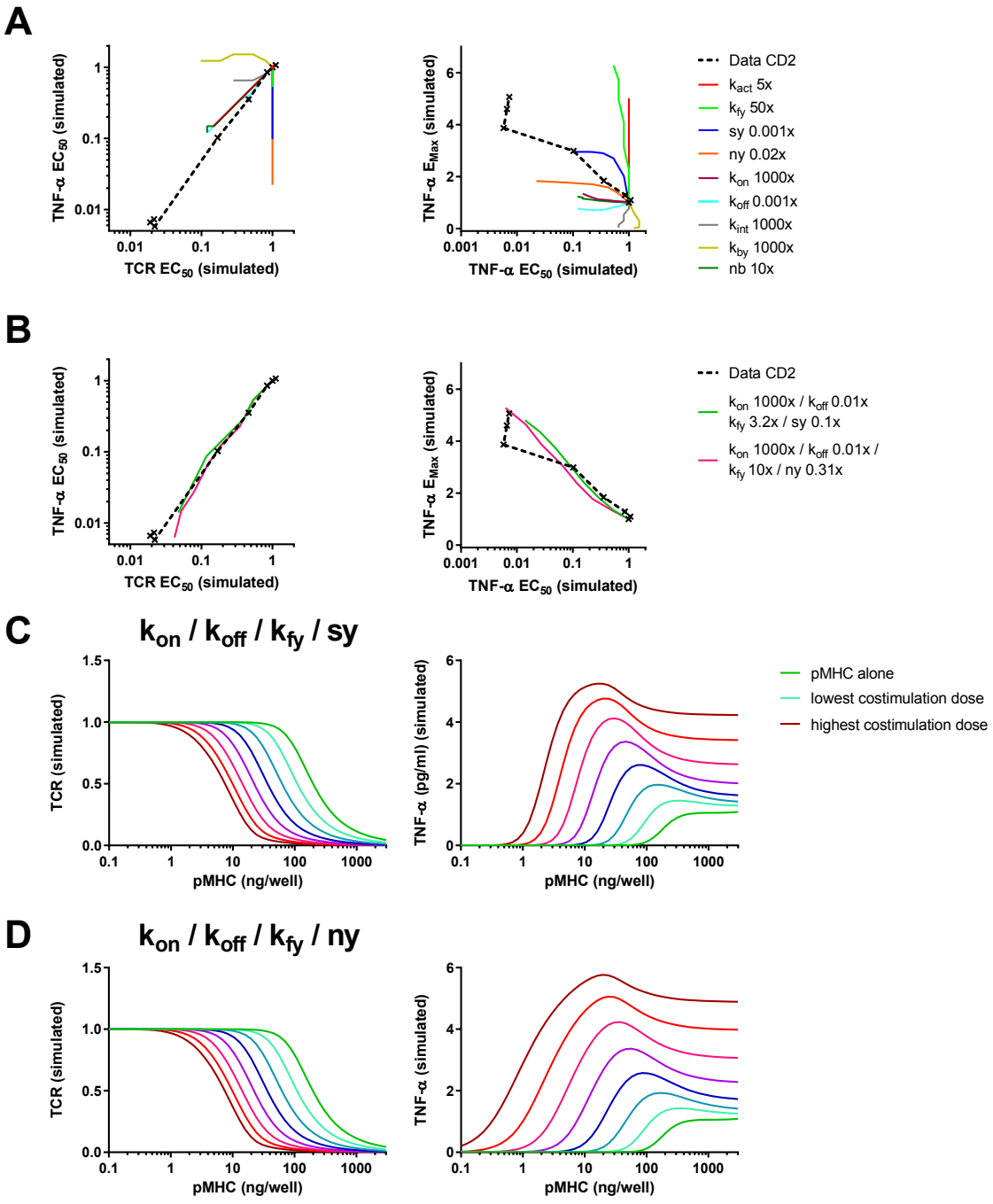


Fig. 3.12: Comparison of simulations with metrics extracted from CD2 data. The EC_{50}, IC_{50} and E_{max} extracted from the experimental data (Figure 3.10, Figure 3.11) were re-plotted in a different format to enable a quantitative comparison with model simulations. The model output was normalised to the mean and E_{max} and EC_{50} were expressed as a fold-change exactly as we did with the experimental data. A) Each solid line represents the modulation of one parameter in the model up or down (as in Figure 3.3 and Figure 3.2). The degree of modulation (fold-change) is indicated in the legend. k_p and k_t are not shown because they only had minor effects. B) The solid lines are the model results after modulating four parameters. These are the best fitting combinations after a systematic search of all combinations of adhesion effects (k_{off}, k_{on}, nb alone or in combinations of two) with signalling effects (k_{fy}, ny, sy, k_{act} alone or in combinations of two) with four different degrees of modulation for each parameter which were based on the values from A. C and D) Simulated cytokine production and TCR downregulation curves generated with the parameter modulations from B.

3.2.10 Costimulatory Receptor Up- and Downregulation

So far, we have assumed that the receptors CD2 and CD28 are stably expressed and do not change with T cell activation or upon engaging their ligands. To test this experimentally, we have performed pilot experiments as part of two short student projects supervised by the author.

The expression of CD28 was not overly modulated on T cells by stimulation with pMHC alone, although a slight increase was noted at higher pMHC concentrations (Figure 3.13 A). There was some degree of downregulation with increasing doses of CD86 (Figure 3.13 B), which is consistent with reports in the literature (Cefai et al., 1998; Badour et al., 2007), but CD28 was not lost completely from the cell surface.

Figure 3.13 C shows that CD2 was not affected by pMHC stimulation. By contrast, some previous studies found that CD2 is upregulated upon T cell stimulation, but this was observed after stimulation with anti-CD3 antibodies or PMA (Alberola-Ila et al., 1991; Zhu et al., 2006). We observed that CD2 is quickly downregulated upon engaging CD58 (Figure 3.13 D) which means that its effects on T cell activation will be self-limiting and mainly play a role during the early phase of stimulation. We would expect that the T cells costimulated through CD2 still show adaptation because the costimulatory receptor is downregulated on the same timescale as the TCR. There is some previous data that suggests that CD2 can be downregulated upon ligand engagement (Tibaldi and Reinherz, 2003; Singleton et al., 2006). These results are preliminary, but suggest that the receptor CD2 might exert its function mainly during the early phase of activation, whereas CD28 is more stable on the T cell surface and can modulate T cell signalling throughout the entire stimulation time. Once we have collected more data on the temporal dynamics of these receptors, we are planning to incorporate their up- and downregulation in our model and simulate their effects in time.

PMA = phorbol-12-myristate-13-acetate

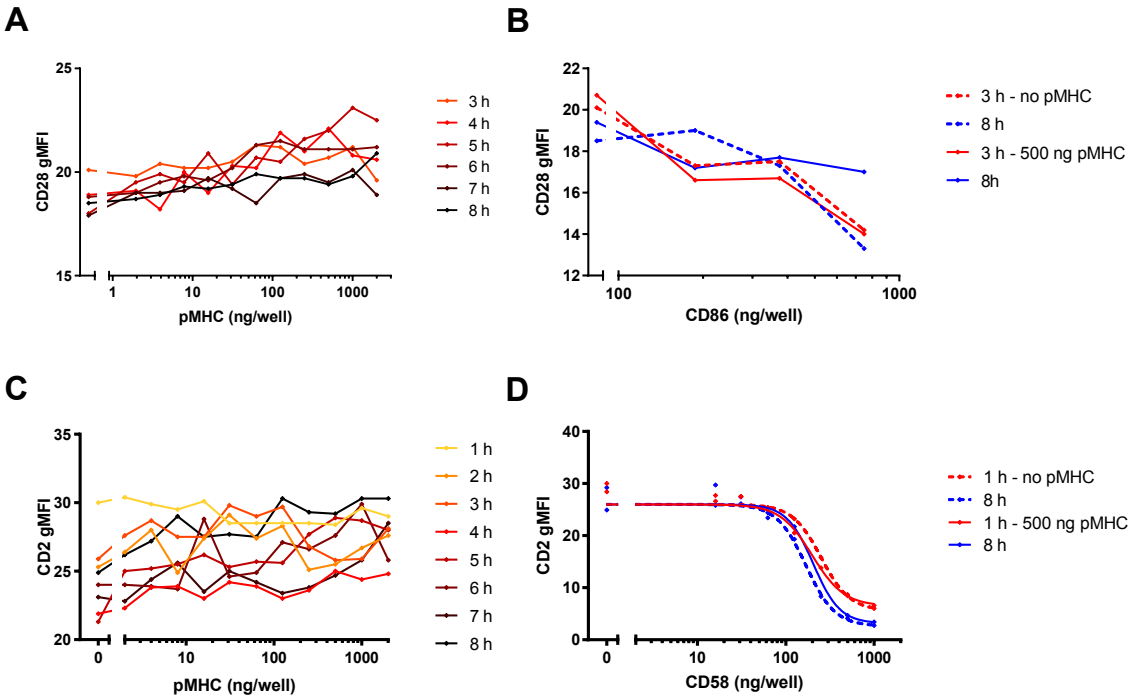


Fig. 3.13: CD2 and CD28 downregulation upon ligand engagement. Primary human CD8$^+$ T cells carrying the 1G4^{Hi} TCR were stimulated for 1-8 h with the physiological-affinity pMHC variant 4A8K co-presented with a dose titration of recombinant CD58. T cells from a different donor were stimulated for 3-8 h with the high-affinity pMHC variant 5Y co-presented with three doses of recombinant CD86. CD28 and CD2 expression was quantified by flow cytometry. A) CD28 expression at different times in response to pMHC stimulation only. B) CD28 expression at 3 or 8 h in response to CD86 with or without pMHC. C) CD2 expression at different times in response to pMHC stimulation only. D) CD28 expression at 1 or 8 h in response to CD58 with or without pMHC. The CD2 data was generated by Johannes Pettmann under the author's supervision. The CD28 data was generated by Jake Thomas under the author's supervision.

3.2.11 Quantitative Effects of CD6 Costimulation

Another receptor that is constitutively expressed on primary human $CD8^+$ T cells is CD6 (Figure 3.5). The functional role of CD6 is not very well understood, but it can have costimulatory properties (Zimmerman et al., 2006; Hassan et al., 2004). We stimulated our $1G4^{Hi}$ $CD8^+$ T cells with plate-immobilised pMHC with or without a dose titration of the ligand for CD6, recombinant human CD166, and measured TCR downregulation and cytokine production. The high-afinity variant used for this experiment was 5Y which has a comparable affinity to 4A ($K_D = 1.33 \times 10^{-3}$ μM).

The observed effects were as striking as they were difficult to interpret. The EC_{50} of all three cytokines increased dramatically with increasing doses of CD166 whereas maximal production decreased, particularly for the low-affinity pMHC, and the curves became less bell-shaped. A smaller increase in IC_{50} was also observed for TCR downregulation (Figure 3.14). Overall, this phenotype cannot be described as costimulation and looked more inhibitory. Similar results have been reproduced with another donor. We hypothesised that this result might be due to a passive steric hindrance effect on the plates, because the CD166 molecule is significantly larger than CD86 or CD58. It could be that CD166 blocked access to the pMHC ligands, effectively lowering the pMHC dose the T cells experience.

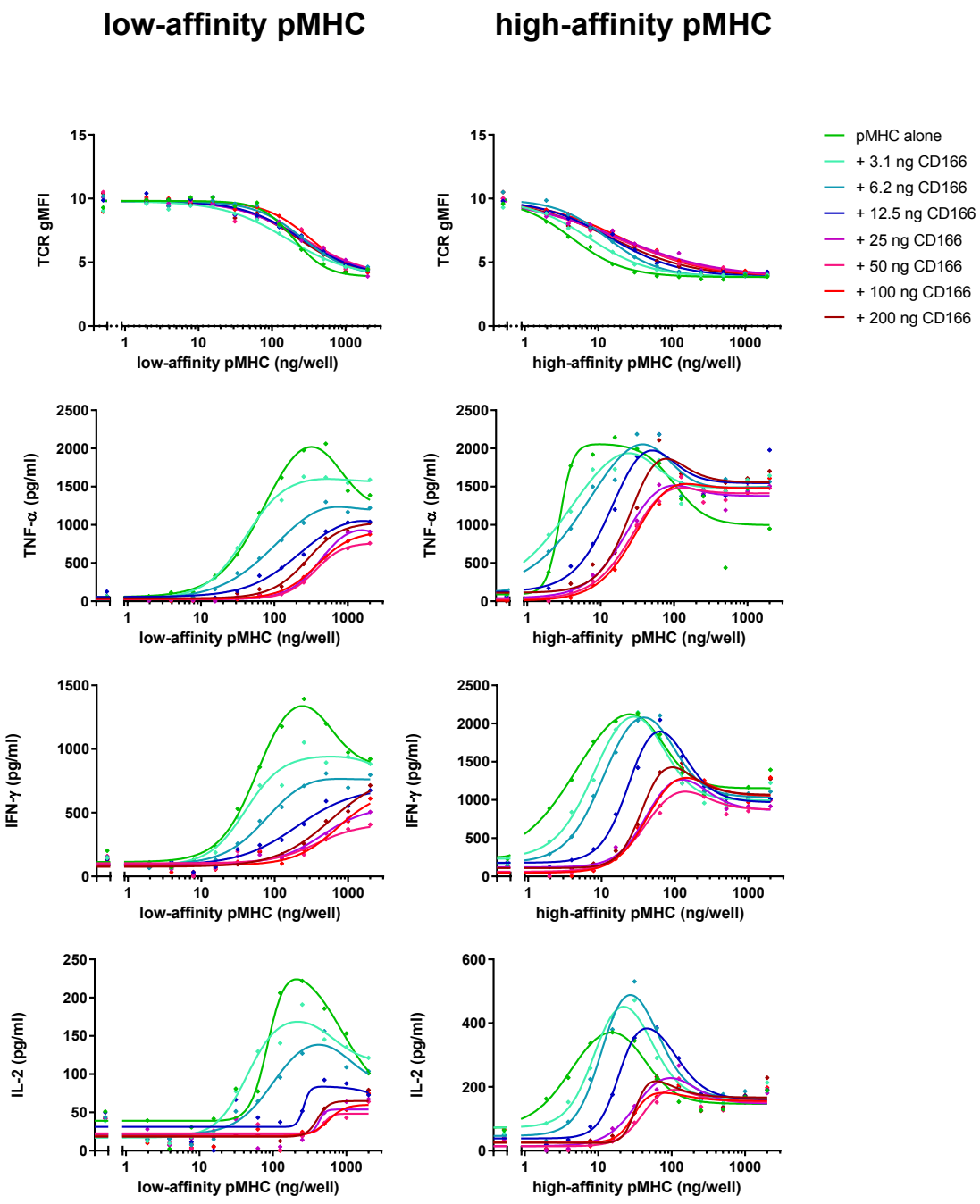


Fig. 3.14: Quantitative effects of CD6 costimulation. Primary human CD8+ T cells carrying the 1G4Hi TCR were stimulated for 8 h with the physiological-affinity pMHC variant 4A8K and the high-affinity variant 5Y co-presented with a dose titration of recombinant CD166. Cytokine concentrations were measured by ELISA, TCR downregulation was measured by flow cytometry. Similar results were observed for two donors.

We used our model to simulate a reduction of the effective pMHC dose or the pMHC-TCR on-rate with increasing CD166 concentration. The results show that both of these effects would cause an increase in the EC_{50} of cytokine production similar to what we see in the experiments, but they would also increase the IC_{50} of TCR downregulation to the same degree (Figure 3.15 A and B). In our experiments, the change in TCR IC_{50} was less pronounced and therefore, we conclude that a steric hindrance effect alone cannot explain the observed effect on cytokine production (Figure 3.15 C). It therefore appears that CD6 has an inhibitory effect on cytokine production in our system. Notably, the literature on CD6 is contradictory with some studies reporting it to be a costimulatory molecule (Zimmerman et al., 2006; Hassan et al., 2004) and others reporting an inhibitory function (Oliveira et al., 2012).

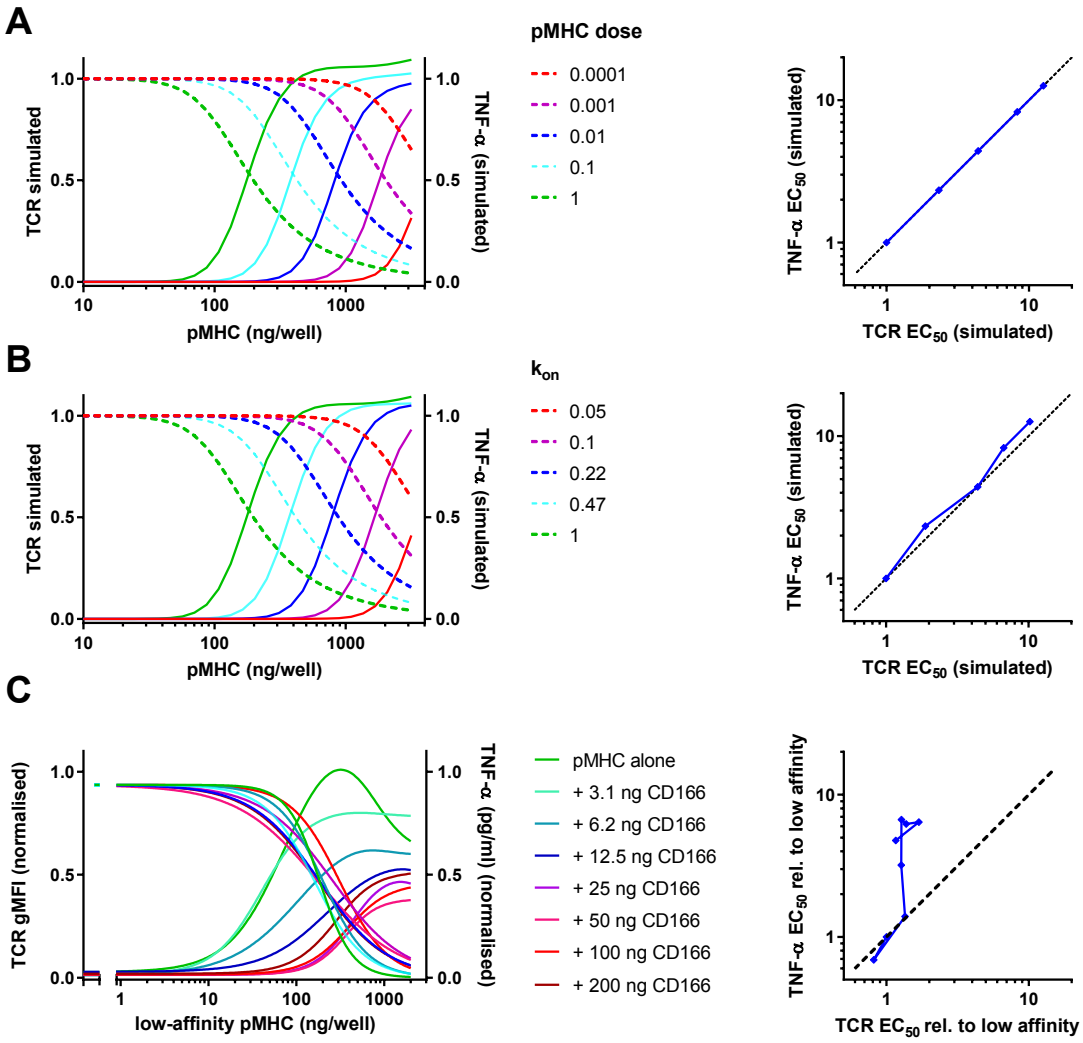


Fig. 3.15: Modelling of accessory ligand effects on effective pMHC concentration. The mathematical model was used to simulate a reduction of the effective pMHC dose (A) or the pMHC-TCR on-rate (B) with increasing CD166 concentration. The dashed lines show the simulated TCR downregulation curves, solid lines show the cytokine concentration at 8 h. The legend indicates the fold-change in ligand dose or k_{on}. The EC_{50}s of the cytokine and TCR curves are plotted together with a diagonal dashed line that indicates an equal effect on both EC_{50}s. C) TNF-α production and TCR downregulation curves for the low-affinity pMHC with different CD166 concentrations and the corresponding EC_{50}s.

3.2.12 Effect of CD86 Immobilisation on pMHC Detection

For the T cell stimulation assays with CD86, we have included controls to be able to measure whether CD86 immobilisation has an effect on pMHC concentrations on the plates. Importantly, CD86 and all other costimulatory ligands were always immobilised on the plates after the pMHC had been incubated. We stained plate-bound pMHC on the stimulation plates after the T cells were removed with the conformation-sensitive MHC class I antibody W6/32 and a fluorescently labelled goat-anti-mouse antibody. Fluorescence was quantified on the Odyssey® Sa Infrared Imaging System.

In five independent experiments, we always observed a CD86 dose-dependent decrease in pMHC detection on the stimulation plates. This data has been normalised to account for differences in absolute fluorescence and the X-values were adjusted to account for differences in pMHC immobilisation. After these transformations, the data from all five repeats was fitted with one curve per CD86 dose in Prism (Figure 3.16 A). This fit assumed that all the curves start at the same baseline, but they were allowed to fit different maxima.

EC_{50} values were extracted from the curves for each individual experiment. In order to compare between experiments, the EC_{50}s were normalised to the mean of the experiment and expressed as a fold-change to pMHC alone (low- and high-affinity pMHC datasets analysed separately). A clear dose-dependent increase in EC_{50} can be seen for both pMHCs although only two values were statistically significantly different from pMHC alone (Figure 3.16 B). Differences between the two antigens were not expected, because the one amino acid difference between the peptides should not affect the immobilisation of the pMHC complexes on the plates or the effect CD86 co-immobilisation has on them.

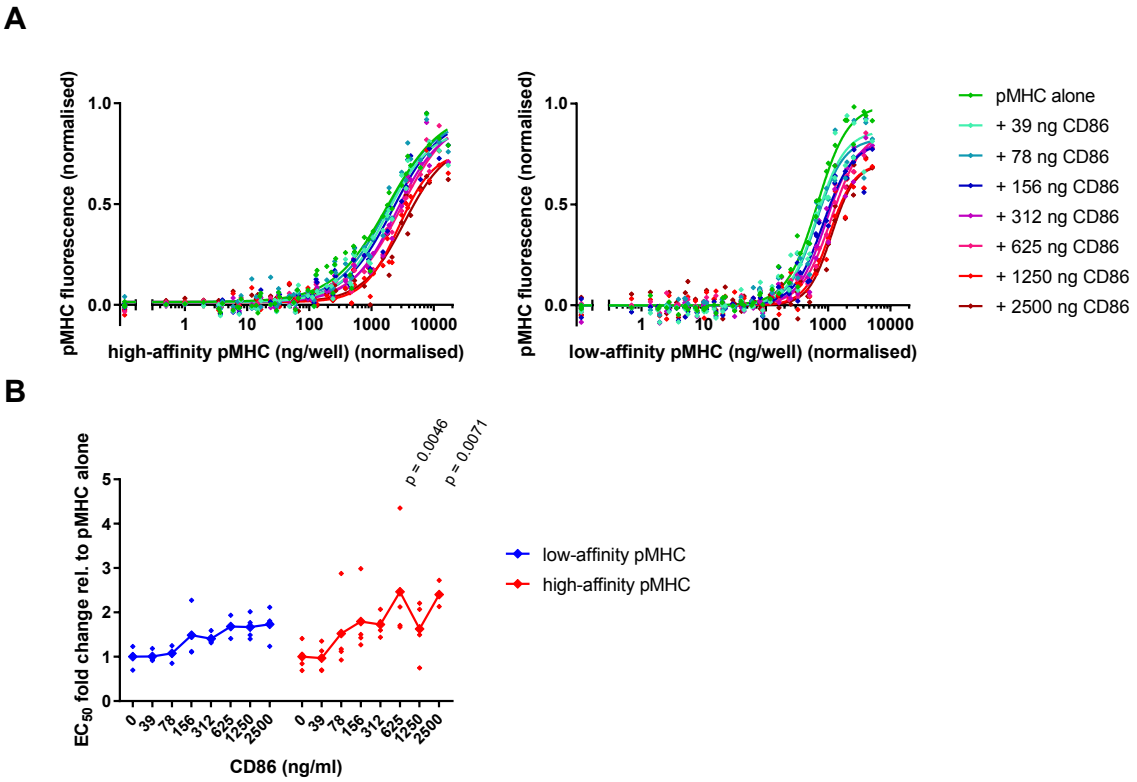


Fig. 3.16: Effect of CD86 immobilisation on pMHC detection. Recombinant *in vitro*-refolded biotinylated pMHC complexes were immobilised on streptavidin-coated plates. Recombinant biotinylated CD86 was immobilised on the same plate in a second step, after pMHC had been incubated for at least 45 min. After another incubation period, residual unbound protein was washed off and T cells were stimulated on the plates. After an 8 h stimulation, the cells were removed and plate-bound pMHC was detected with the W6/32 antibody and a secondary IRDye® 680RD-conjugated goat-anti-mouse antibody. Fluorescence was quantified using the Odyssey® Sa Infrared Imaging System. A) Dose response curves for low- and high-affinity pMHC ligand alone and with seven doses of CD86. B) EC_{50} values extracted from the dose response curves. Statistical analysis was performed using a two-way analysis of variance (ANOVA) in Prism and Dunnett's method was used to correct for multiple comparisons. All other comparisons to pMHC alone did not reach statistical significance.

The observed reduction in pMHC detection with increasing CD86 could have multiple reasons:

1) CD86 has displaced the pMHC because they compete for streptavidin binding sites.

2) CD86 has interacted directly with pMHC and changed the folding of the complex.

3) CD86 sterically hinders the antibody from binding (detecting) pMHC.

We believe that a displacement of pMHC from the streptavidin is highly unlikely given the strong interaction between streptavidin and biotin, but we have no way of knowing whether the pMHC complexes are disassembled or masked by CD86. In the latter case, this leaves us with the question whether the T cells would also experience a lower effective dose of pMHC with higher doses of CD86. We do not know how the streptavidin is immobilised on the plastic plates, but most likely (given the high binding capacity), there will be some kind of matrix which could make it more likely for CD86 to block access to the pMHC. In this case, we would expect equivalent CD86 dose-dependent increases in the IC_{50} for TCR downregulation and for all readouts of T cell activation, because the cells have experienced lower antigen doses with increasing CD86 concentration (see Figure 3.15 A). We have not observed such increases. The IC_{50} for TCR downregulation was not affected by CD86 and in fact, the EC_{50} for all cytokines slightly decreased with CD86 (Figure 3.7). This could mean that the T cells did not experience lower antigen doses with increasing CD86 and the pMHC detection assay results represent an artefact.

There is, however, an alternative explanation. CD86 could have two effects that cancel each other out. If CD86 does indeed reduce the pMHC available to the T cells during stimulation, it might counteract this through other effects which increase the T cells' sensitivity to pMHC dose and consequently shift the EC_{50} back. Given that TCR downregulation would have to be increased by such an effect as well as cytokine production, it is most likely that it would act on the level of TCR-pMHC binding. For example, an adhesion effect of CD86 leading to an increase in k_{on} could explain our results. However, it is worth noting that the decrease in EC_{50} of pMHC immobilisation was only 2-3-fold whereas the adhesion effect observed with CD58 led to a 100-fold decrease of the TCR downregulation IC_{50}. This means that a potential compensatory adhesion effect by CD86 would have to be on the order of 2-3-fold to result in no net effect on TCR downregulation. We

have decided to analyse the functional data without correcting for this potential effect because we do not have enough information at this point to factor it into the model, i.e. we cannot even tell with certainty if there is an effect.

The same considerations apply to the other costimulatory ligands, although we have not tested their effect on pMHC immobilisation systematically. In the future, we are aiming to develop a negative control for the effects observed here. We are currently developing reagents to be able to co-immobilise an inert ligand that is not bound by T cells to control for and quantify the passive effects of ligand immobilisation on the pMHC dose response curve.

3.3 Discussion

3.3.1 Costimulatory Effects in Context

We have developed a minimal plate-based stimulation system to systematically study and compare the effects of costimulatory receptors on T cell activation and TCR downregulation. The data presented here forms part of a larger project that aims to characterise the functional phenotypes of a large number of receptors that have so far only broadly been classified as either costimulatory or inhibitory. In this chapter, we show that CD28 and CD2 costimulation show distinct phenotypes that can be reproduced with specific modulations in our TCR downregulation model from chapter 2. Parsing out of these distinct aspects of the costimulatory effects allows us to draw quantitative conclusions. We found that CD28 costimulation has little effect on TCR downregulation and does not affect TCR-pMHC binding and proximal decision making (e.g. kinetic proofreading). Its main effect was an increase in cytokine production with a small decrease in the EC_{50}. Our model can reproduce these effects with a modification of one parameter downstream of the TCR, the threshold sy of the switch function which determines digital cytokine production. This means that less activated TCRs are required for the same cytokine output when CD28 is engaged. Our findings as to how CD28 affects primary human $CD8^+$ T cell activation confirm previous work in other experimental systems and T cell subsets. In direct comparisons with CD2 and LFA-1, it was shown that CD28 does not increase T cell adhesion and TCR-pMHC binding in cell-cell interactions and on lipid bilayers (Bromley et al., 2001; Bachmann et al., 1997a). Consequently, CD28 engagement has no effect on TCR downregulation (Cai et al., 1997; Bachmann et al., 1997a; Iezzi et al., 1998), yet it decreases the T cell activation threshold (Murtaza et al., 1999; Bachmann et al., 1996, 1997a). A reduced threshold also means that the remaining TCRs after downregulation are still sufficient for signalling together with CD28, which will prolong the overall signal duration. This is particularly important for the activation of naïve $CD4^+$ T cells where it has been shown that a longer TCR signalling duration is required for full activation (Iezzi et al., 1998) and that it influences the differentiation into helper cell subsets (Iezzi et al., 1999).

CD2 showed a markedly different phenotype to CD28. It also decreased the EC_{50} of cytokine production and increased the overall amount produced, but the effect on the EC_{50} was more than ten times stronger and CD2 also strongly increased TCR downregulation. This suggests that CD2 acts as an adhesion molecule which affects the binding kinetics between TCR and pMHC, i.e. it increases the number of engaged TCRs. This phenotype does not necessarily require signalling (although it could be affected by signalling). However, the adhesion effect was not sufficient to explain the strong amplification of cytokine production we observed, probably because more TCR engagement also means more TCR downregulation which sets a limit to downstream signalling and cytokine production. We were nevertheless able to reproduce the CD2 effect with our model by assuming that CD2 has three independent effects: an adhesion effect which increases TCR-pMHC binding, and two distinct downstream effects on cytokine production, a lowering of the threshold and an amplification. This phenotype is consistent with early work from different groups that tried to parse out the different effects of CD2 by mutating or truncating the intracellular tail. They concluded that CD2 independently increases adhesion and T cell signalling (Moingeon et al., 1989; Bierer et al., 1988; Hahn and Bierer, 1993; Hahn et al., 1992). However, there is also a body of work suggesting that T cell activation can increase the avidity of CD2 (Dustin et al., 1998; Hahn et al., 1992; Hahn and Bierer, 1993; Zhu et al., 2006) which could be mediated by an increase in expression or clustering or an increase in affinity, for example through a conformational change. In our study, we have not (yet) included the expression dynamics of the costimulatory receptors in the mathematical model, which means that we cannot definitely conclude whether our model is consistent with a positive feedback loop whereby TCR signalling increases CD2 avidity which in turn increases TCR signalling. We are planning to refine the model accordingly as soon as we have accumulated more data at different time points.

CD6 appeared to inhibit T cell activation in our experimental system, but it is also possible that the large CD166 molecule sterically hinders pMHC binding. We wanted to test this hypothesis by stimulating with a truncated version of the ligand that only contains the first two domains (including the CD6 binding site). However, due to complications with producing the protein in large enough quantities, we were not able to follow up on this and can therefore not draw definitive conclusions about the nature of the effect of CD6

on T cell activation.

3.3.2 Limitations

Some of the effects observed in the present study will most likely not accurately reflect what happens between a T cell and an antigen-presenting cell. One of the reasons is that many interactions between different receptor-ligand pairs will take place simultaneously between two cells, while we only co-present pMHC together with one ligand at a time. This minimal stimulation system has been intentionally designed aiming to allow observations of the costimulatory effects of individual receptors in isolation. This allows us to infer and model how they integrate with TCR signalling and contribute to a better understanding of their functional role in T cell activation. However, given the high complexity of the T cell signalling network, it is likely that costimulatory pathways do not only integrate with TCR signalling, but also with each other which our model would not be able to predict from the individual effects. Examples could include nonlinear synergistic effects where triggering of two costimulatory pathways enables a positive feedback loop which amplifies the combined signal beyond the sum of the two individual signals. For example, there is evidence from lipid bilayer studies that CD2 engagement can increase CD28 binding to its ligands (Bromley et al., 2001). In addition to synergies with other receptor-ligand pairs, CD28 costimulation is also affected by the inhibitory receptor CTLA-4 which is upregulated on T cells upon activation and binds the same ligands as CD28 (Collins et al., 2002). We have tried to minimise the effects of CTLA-4 by using CD86 as a ligand which has a less pronounced preference for CTLA-4 binding (Collins et al., 2002) and preferentially binds CD28 on lipid bilayers (Pentcheva-Hoang et al., 2004), but we cannot exclude the possibility that our results reflect a combination of CD28 and CTLA-4 ligation.

Many T cell activation studies have been performed with antibodies against the TCR and costimulatory receptors, either in solution or immobilised on beads or plates. We believe by using the endogenous ligands, our results are more relevant to the physiological context in which these receptors operate, but we recognise that our model system is not able to recapitulate important aspects of receptor biology, particularly lateral movements

in the membrane that lead to the formation of receptor clusters and eventually an immunological synapse. The size and dynamics of the contact area and the forces that act on the T cell membrane and consequently on receptor-ligand bonds will also be different in our system from a T cell-APC contact. CD28 is actively transported to the centre of the immunological synapse in microclusters distinct from those containing the TCR and this localisation has been shown to be of functional significance, particularly for the recruitment and activation of PKC-θ (Tseng et al., 2008; Liang et al., 2013; Sanchez-Lockhart et al., 2008; Bromley et al., 2001; Yokosuka et al., 2008). This process is dependent on TCR signalling (Tseng et al., 2008; Sanchez-Lockhart et al., 2008) and CD28 ligand engagement (Pentcheva-Hoang et al., 2004; Sanchez-Lockhart et al., 2008). CD2 has been observed to form clusters together with the TCR (Douglass and Vale, 2005; Faroudi et al., 2003; Milstein et al., 2008) either through binding its ligand or in response to TCR signalling (Douglass and Vale, 2005; Faroudi et al., 2003). CD2 and the TCR are both recruited to the centre of the immunological synapse (Grakoui et al., 1999; Leupin et al., 2000; Lee et al., 2003; Faroudi et al., 2003; Singleton et al., 2006; Zhu et al., 2006). None of these processes will take place in our system with immobilised ligands and this limitation is likely to affect the function of the costimulatory receptors. Eventually, we would therefore like to confirm our findings in a lipid bilayer system, either on glass beads or on plates, even though this would still not fully recapitulate the forces that influence the interaction of molecules on living cell membranes. However, so far, we did not have the technology to achieve reproducible immobilisation of multiple ligands on a large enough number of samples to be able to generate comparable dose response curves for the pMHC and costimulatory ligands.

4 CAR T Cells are Desensitised by Receptor Downregulation

4.1 Introduction to CAR T Cells

4.1.1 General CAR Design

CARs are engineered cell surface receptors that typically use a single-chain variable fragment of an antibody (scFv) for antigen recognition. The variable domains of the heavy and light chain are connected by a short linker sequence. This construct is connected to a flexible spacer domain, often derived from CD8 (Maude et al., 2018; Porter et al., 2015; Schuster et al., 2017; Beatty et al., 2018), CD28 (Lee et al., 2015; Kochenderfer et al., 2015), or immunoglobulin molecules (Savoldo et al., 2011; Turtle et al., 2016a,b). Some clinical studies used CARs without any extracellular spacer domain (Davila et al., 2014). A transmembrane domain, often from CD28 (Davila et al., 2014; Lee et al., 2015; Kochenderfer et al., 2015; Turtle et al., 2016a,b) or CD8 (Maude et al., 2018; Porter et al., 2015; Schuster et al., 2017; Beatty et al., 2018), occasionally also from other molecules (Savoldo et al., 2011; Lamers et al., 2013), connects the antigen-binding part to the intracellular signalling domains from CD3ζ alone (first-generation CARs) or in combination with signalling domains of one (second-generation CARs) or two (third-generation CARs) costimulatory receptors (Figure 4.1). Most receptors in clinical use are second-generation CARs with signalling domains from either 4-1BB or CD28.

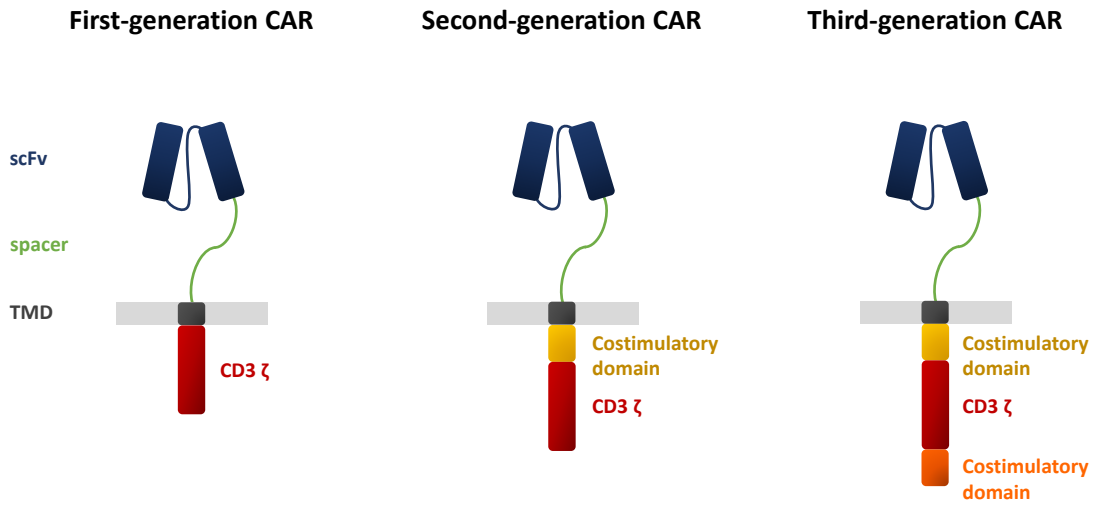


Fig. 4.1: Schematic overview of CAR design. First-generation CAR constructs usually consist of a single-chain variable fragment (scFv), an extracellular spacer domain, a transmembrane domain (TMD), and the intracellular signalling tail of CD3ζ. Second- or third-generation constructs include an additional one or two costimulatory signalling domains.

4.1.2 Clinical Trial Results

A new CAR T cell product is usually tested in *in vitro* T cell stimulation experiments in response to an antigen-expressing tumour cell line. However, due to the complexity of the *in vivo* environment, it remains unclear which *in vitro* readout of T cell activation is the best predictor of clinical efficacy. It has become apparent that the killing capacity *in vitro* does not always correlate with *in vivo* anti-tumour activity, probably because the threshold for cytotoxicity is much lower than those for other functions like cytokine production (James et al., 2010; Watanabe et al., 2015; Arcangeli et al., 2017) which are more important *in vivo*.

First-generation CAR T cell stimulation *in vitro* results in antigen-specific cytotoxicity and IFN-γ production, but limited IL-2 production (Hombach et al., 2001; Finney et al., 2004; Pulè et al., 2005; Shirasu et al., 2010; Lanitis et al., 2013) and consequently limited antigen-specific proliferation (Hombach et al., 2001; Finney et al., 2004; Pulè et al., 2005; Kowolik et al., 2006; Zhong et al., 2010). Consistent with the incomplete *in vitro* T cell activation, first-generation CAR T cells yielded disappointing anti-tumour responses in early clinical trials (Kershaw et al., 2006; Park et al., 2007; Till et al., 2008; Jensen et al., 2010; Lamers et al., 2013). In a direct comparison, a human *in vivo* study reported increased

expansion and persistence of CD28 second-generation CAR T cells compared to first-generation CAR T cells co-infused into the same patients (Savoldo et al., 2011).

Second-generation CAR T cells have achieved unprecedented complete response rates (70-90 %) and durable remissions in clinical trials with patients with relapsed or therapy-refractory acute B cell leukaemia (Davila et al., 2014; Maude et al., 2018; Lee et al., 2015; Turtle et al., 2016a). With the standard of care before CAR T cells, this patient group had a median survival of 24 weeks (Fielding et al., 2007). CAR T cells have also been used successfully in other B cell malignancies like chronic lymphocytic leukaemia (CLL) (Porter et al., 2015) and lymphomas (Kochenderfer et al., 2015; Turtle et al., 2016b; Schuster et al., 2017). These successes have led to the first two FDA approvals for CAR therapies with "Breakthrough Therapy" designations in 2017 (FDA News, 2017a,b). However, translating the clinical success from B cell malignancies into solid tumours has proven challenging and most trials to date have reported no or very limited clinical responses (Lamers et al., 2013; Ahmed et al., 2015; Heczey et al., 2017; Beatty et al., 2018).

On the other hand, all clinical trials with B cell malignancies have reported adverse events due to general immune activation ranging in severity from mild fevers to life-threatening cytokine release syndrome, in some cases involving neurotoxicity (Turtle et al., 2016a,b; Lee et al., 2015; Davila et al., 2014; Maude et al., 2018; Porter et al., 2015; Kochenderfer et al., 2015; Schuster et al., 2017). The severity has been reported to correlate with tumour burden at the time of infusion (Turtle et al., 2016a; Davila et al., 2014; Maude et al., 2018).

In addition to those adverse events, 10-20 % of the patients treated on clinical trials with anti-CD19 CAR T cells have later relapsed with CD19-negative leukaemia (Lim and June, 2017), suggesting that targeting one antigen alone might not be sufficient for tumour clearance. Indeed, multiple different strategies are under development to enable the targeting of combinations of antigens (Kloss et al., 2013; Zah et al., 2016; Hegde et al., 2016; Roybal et al., 2016; De Munter et al., 2018).

FDA = food and drug administration

4.1.3 The Optimal CAR Design

The design of optimal CARs for the desired T cell activation phenotype is essentially an engineering problem which has to take into account factors like affinity, CAR expression level, and CAR signalling. Those factors are inter-dependent, so that, for example, the optimal affinity of the CAR will depend on the CAR and antigen expression levels because all three contribute to the overall avidity. Surprisingly, it has been observed that a higher affinity does not necessarily initiate stronger T cell activation (Chmielewski et al., 2004; Haso et al., 2013; Liu et al., 2015). Instead, lower-affinity CARs were shown to elicit even stronger T cell responses than high-affinity CARs at high antigen doses (Chmielewski et al., 2004; Liu et al., 2015). In addition, higher affinities render CAR T cells more sensitive for low antigen doses (Chmielewski et al., 2004; Liu et al., 2015), which has proven detrimental upon clinical application, because it allowed high-affinity CAR T cells to target not only the tumour cells expressing the antigen at high levels, but also healthy tissues with a low expression level (Morgan et al., 2010; Lamers et al., 2013). This was seen in a patient who was treated for colon carcinoma with ErbB2-specific third-generation CAR T cells. They recognised ErbB2 expressed at low levels on lung epithelial cells and caused local inflammation and ultimately fatal systemic cytokine release syndrome (Morgan et al., 2010). This case illustrates the fundamental difference between CAR T cell and soluble antibody therapies, since the recognition domain of the CAR was the same as that of the routinely used therapeutic antibody Trastuzumab, which has a good safety profile (Morgan et al., 2010). The T cells most likely responded to the low antigen concentration because CARs are expressed at a high density on the 2D T cell surface, leading to avidity effects (Watanabe et al., 2015). In another report, CAR T cells directed against carbonic anhydrase IX, a tumour-associated antigen frequently overexpressed on renal cell carcinoma, caused cholangitis due to antigen expression on the bile duct epithelium, which could be prevented by blocking the antigen with the corresponding antibody (Lamers et al., 2013). These observations lead to the conclusion that in cases where the target antigen is also expressed on healthy tissue, CARs need to be fine-tuned to achieve optimal T cell activation in a narrow therapeutic window. There is some data that demonstrates that lowering CAR affinity can render the T cells inactive against cells with lower antigen expression but this might also not be the ideal solution as

it brings with it a reduction in their activity against high-expressing targets as well (Kloss et al., 2013; Caruso et al., 2015).

The per-cell expression level of the CAR also impacts T cell activation with lower CAR density leading to reduced sensitivity for low antigen doses (James et al., 2010; Caruso et al., 2015; Han et al., 2018). This parameter is more difficult to control than the affinity because it depends on multiple factors such as the strength of the promotor and the stability of the construct on the membrane (Eyquem et al., 2017). There is evidence from different systems showing that third-generation CARs are less well expressed than first- or second-generation constructs (Carpenito et al., 2009; Zhao et al., 2015) which might help to explain why they have not consistently shown greater T cell activation with the result that most clinical studies use second-generation constructs. However, CAR expression is often much higher than the expression of endogenous TCRs, because it is not limited by the availability of CD3 chains. This high density can lead to constitutive T cell signalling (Eyquem et al., 2017; Frigault et al., 2015; Long et al., 2015; Gomes-Silva et al., 2017) and consequently T cell exhaustion or activation-induced cell death in culture before they are transferred into the patient. To complicate things further, CARs form homodimers on the plasma membrane (Brentjens et al., 2003; Imai et al., 2004; Bridgeman et al., 2014) and can associate with endogenous molecules, for example CD3ζ (Bridgeman et al., 2014). This is most likely mediated by direct interactions in the transmembrane and spacer domains (i.e. it will be different for different CARs) but could also be explained with interactions with intracellular adaptors or accumulation in the same membrane domains.

4.1.4 CAR Downregulation

CARs are known to be downregulated upon antigen binding *in vitro* (James et al., 2010; Caruso et al., 2015; Arcangeli et al., 2017; Han et al., 2018) and *in vivo* (Eyquem et al., 2017) which is most likely followed by degradation (Eyquem et al., 2017). Several studies have indicated that this reduces the T cells' ability to respond to target cells (James et al., 2010; Caruso et al., 2015; Han et al., 2018). CAR downregulation has been shown to be a function of antigen dose (James et al., 2010; Caruso et al., 2015; Arcangeli et al., 2017)

and affinity (Caruso et al., 2015; Han et al., 2018), but the mechanisms or the functional consequences remain to be elucidated. The ligand-induced downregulation pathway is most likely similar to the endogenous TCR, i.e. it would be expected to rely on recruitment of E3 ubiquitin ligases upon CAR triggering (see section 2.1.1 for more details).

It is presently unclear whether the downregulation of non-engaged bystander receptors that has been described for TCRs (San Jose et al., 2000; Bonefeld et al., 2003; Monjas et al., 2004; von Essen et al., 2006; Fernández-Arenas et al., 2014) plays a role in CARs and whether this employs similar molecular mechanisms compared to the TCR. Investigators studying TCR downregulation have previously reported that a chimeric molecule with the CD3ζ signalling tail was subject to downregulation when triggered directly with an antibody, but it was also subject to bystander downregulation when the TCR was triggered instead (San Jose et al., 2000; Monjas et al., 2004). This suggests that CARs can be affected by TCR downregulation pathways that do not require the CD3γ di-Leucine motif. At least one signalling-induced mechanism of bystander downregulation has been reported to depend on non-phosphorylated ITAMs in the CD3 chains (Fernández-Arenas et al., 2014) and this could apply to CARs.

4.2 Results

4.2.1 A Novel CAR T Cell Stimulation System

We developed a novel *in vitro* stimulation system that allows us to study CAR T cell activation in response to large variations in antigen dose and affinity. We employ CARs that are based on an antibody which recognises the NY-ESO-$1_{157\text{-}165}$ HLA-A2 pMHC complex in a similar orientation to the $1G4^{Hi}$ TCR that was used for T cell stimulations throughout chapter 2 and chapter 3 (Stewart-Jones et al., 2009; Jakka et al., 2013; Maus et al., 2016). In the work presented in this chapter, we used the high-affinity T1 variant of the CAR which has been reported to bind to the 9V mutant of the wild type peptide (SLLMWITQV) with a 4 nM K_D (Stewart-Jones et al., 2009). As for the TCR, we used 9V as our index peptide for all experiments, because it is more stably bound to the MHC than the wild type 9C and has little effect on TCR or CAR binding (Chen et al., 2000; Stewart-Jones et al., 2009). Schematic representations of the three CAR constructs used in this chapter are shown in Figure 4.2 and the sequences are included in section 6.3.11.

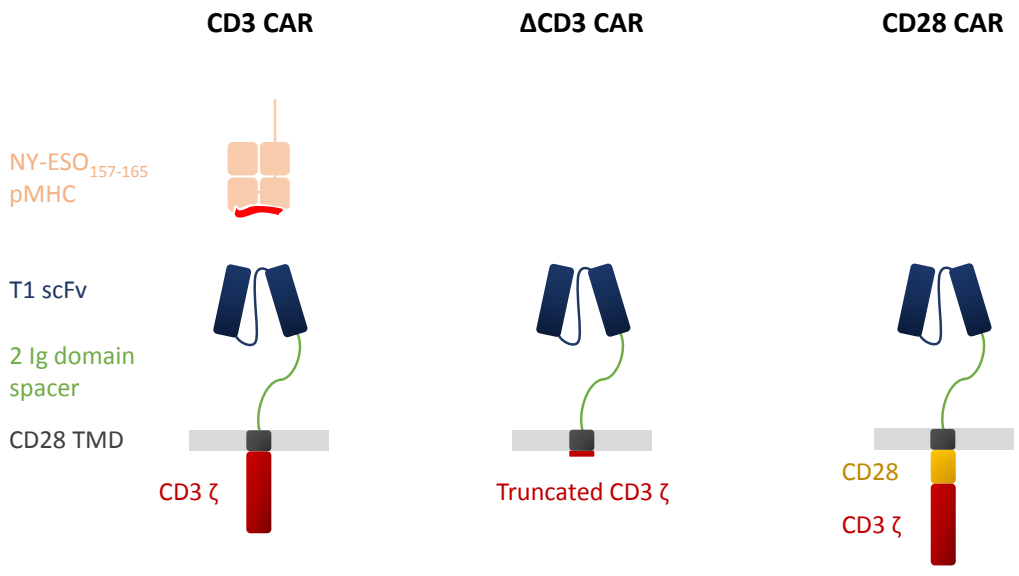


Fig. 4.2: Schematic of CAR contructs used in this project. All three constructs have the same extracellular domains, the T1 scFv binding to the NY-$ESO_{157\text{-}165}$ pMHC complex and a spacer domain consisting of 2 Ig domains from an IgG Fc part. All of the constructs have the CD28 transmembrane domain (TMD). The names CD3, ΔCD3 and CD28 CAR are used throughout the chapter to refer to these constructs.

Based on the crystal structure of the ligand-receptor complex (Stewart-Jones et al., 2009), we hypothesised that mutations to the peptide should affect the affinity of the interactions. In order to confirm that this system works, we have stimulated CAR T cells with titrations of different plate-immobilised pMHC mutants and measured their activation by flow cytometry and ELISA. The results shown in Figure 4.3 are from pilot experiments. One experiment was performed with $CD8^+$ T cells carrying a first-generation CAR and T cell activation was measured after 8 h of stimulation (Figure 4.3 A). The other experiment was performed with $CD4^+$ T cells from a different donor carrying a CD28 second-generation CAR and analysed after 24 h (Figure 4.3 C). They confirm that the stimulation assay works as expected. The fact that some of the pMHC mutants exhibit less potent activation compared to the 9V peptide suggests that those mutations have reduced the affinity, but the exact affinity measurements are currently ongoing. Importantly, this data shows that CAR downregulation is a function of antigen dose and (putative) affinity and correlates with other T cell activation markers (Figure 4.3 B). To the best of our knowledge, this is the first time CAR T cell responses to antigens of different affinity have been studied without modifying the receptor.

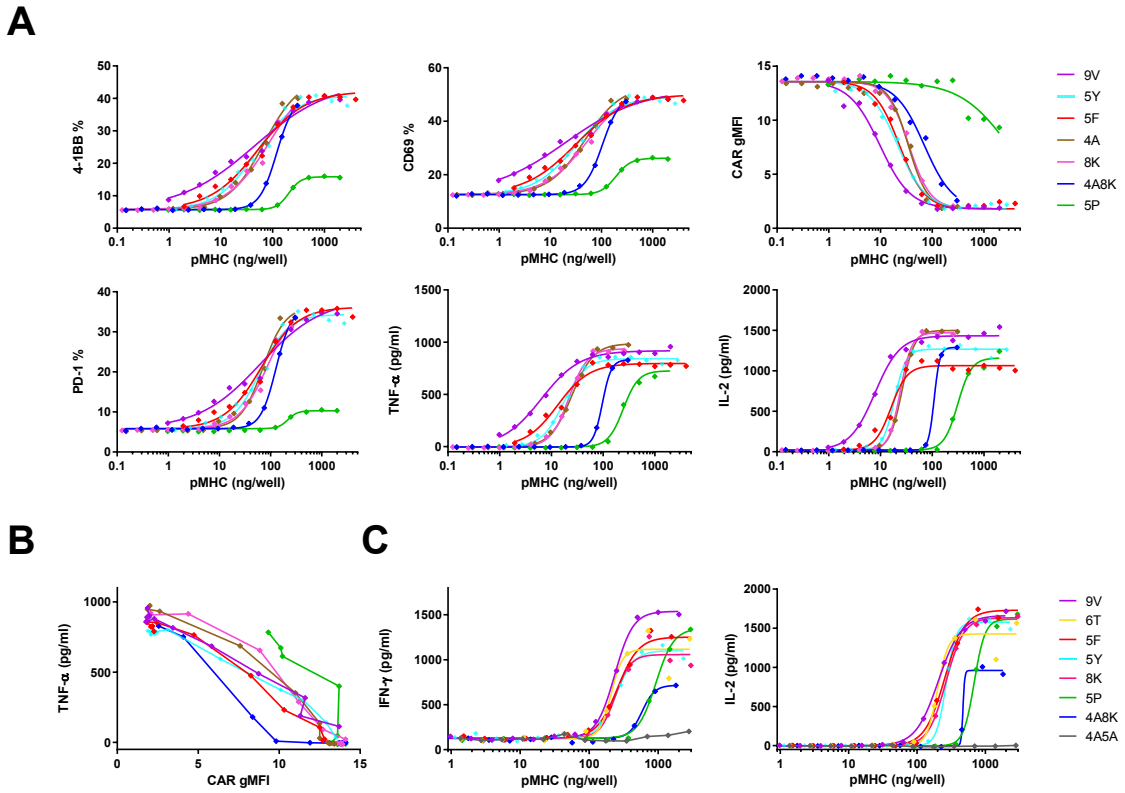


Fig. 4.3: CD8$^+$and CD4$^+$CAR T cell stimulation with different plate-bound pMHC mutants. A) Primary human CD8$^+$ T cells carrying the T1 first-generation CAR were stimulated for 8 h with titrations of seven different pMHC variants. B) Data from A showing TNF-α production plotted as a function of CAR gMFI. C) Primary human CD4$^+$ T cells carrying a CD28 second-generation CAR were stimulated for 24 h with titrations of eight different pMHC variants. The specific mutations are indicated in the legend and all are based on the 9V index peptide (SLLMWITQV). Surface marker expression was analysed by flow cytometry, cytokine concentrations in the supernatant were measured by ELISA. The X-values were corrected based on the measured immobilisation of each pMHC. Curves were fitted using the Prism algorithm for a four-parameter dose response curve (allowing variable slopes).

4.2.2 Effects of CAR Signalling on CAR Downregulation

We and others found a strong correlation between CAR downregulation and T cell activation in response to antigen dose and affinity (Figure 4.3) (James et al., 2010; Caruso et al., 2015; Arcangeli et al., 2017; Han et al., 2018). Similar observations have been reported in early studies on TCR downregulation (Valitutti et al., 1995; Viola and Lanzavecchia, 1996; Cai et al., 1997; Itoh et al., 1997; Martin and Bevan, 1998) and have let to some controversies and different interpretations with regard to the functional role of TCR downregulation in T cell activation (discussed in chapter 2). One important result was that TCR downregulation can proceed in the absence of TCR signalling, but only if the antigenic (or antibody) stimulus is strong enough (Figure 2.3) (San Jose et al., 2000; Monjas et al., 2004). This finding can be explained with the existence of two TCR downregulation pathways: The signalling-independent downregulation of engaged TCRs and the signalling-dependent downregulation of non-engaged bystander TCRs. Based on this data, we wanted to investigate in the same experimental system whether CAR downregulation is equally affected by Lck inhibition. We stimulated CAR T cells in the presence or absence of A-770041 or PP2 and measured CAR downregulation after 8 h. Surprisingly, both inhibitors appeared to increase CAR downregulation (A77: $p < 0.0001$, PP2: $p = 0.0032$), the opposite effect to what we have seen with the TCR (Figure 4.4 A). This would suggest that there is no bystander CAR downregulation induced by CAR signalling. However, the interpretation of those results is confounded by the fact that the CARs appear to be upregulated at intermediate antigen doses, before they are downregulated at the high doses. This has been observed with multiple donors and is illustrated by the green curve in Figure 4.4 B. In all cases, this effect was stronger with the CD28 second-generation CAR (Figure 4.4 B) and it was always signalling-dependent. Due to this unexpected finding, we cannot conclude whether CAR signalling leads to bystander downregulation as such an effect might be masked by signalling-induced upregulation. Notably, James et al. studied CAR downregulation and came to the conclusion that the number of CARs engaged by antigen and the number downregulated are almost identical (James et al., 2010) which would mean that there is no bystander downregulation. They then used a quantitative model to contrast their own CAR downregulation data with published TCR downregulation data which concluded that the number of TCRs down-

regulated is much higher than the number of antigens (Valitutti et al., 1995; Viola and Lanzavecchia, 1996) (discussed in section 2.3).

We can conclude from the above experiments that a signalling-independent CAR downregulation process does exist and we have confirmed this by using a previously reported truncated CAR with only the first 12 amino acids of the CD3ζ (RVKFSRSAEPPA) signalling tail which does not activate the cells (Figure 4.4 C) (Carpenito et al., 2009). This receptor was always expressed at lower levels compared to the first-generation CAR (representative donor shown in Figure 4.4 B), but importantly, it was downregulated similarly with increasing antigen doses (both receptors have the same binding domain, i.e. affinity). When both the first-generation CAR and the truncated CAR were normalised to their respective baseline expression level, the relative downregulation of the truncated CAR was stronger at low antigen doses (Figure 4.4 A). This further supports the notion that the upregulation observed with the first-generation CAR depends on CAR signalling. Downregulation was even stronger than with Lck inhibition which could suggest that other signalling mechanisms also play a role in CAR upregulation, but these findings have to be interpreted with caution due to the fact that two different receptors are compared. The results could also be explained with an intrinsic difference in the receptor stability on the membrane. It should also be noted that the truncated receptor still contains a 12 amino acid tail (including one lysine) and while this was sufficient to abrogate T cell activation (Figure 4.4 C) (Carpenito et al., 2009), those amino acids could potentially still induce the observed downregulation.

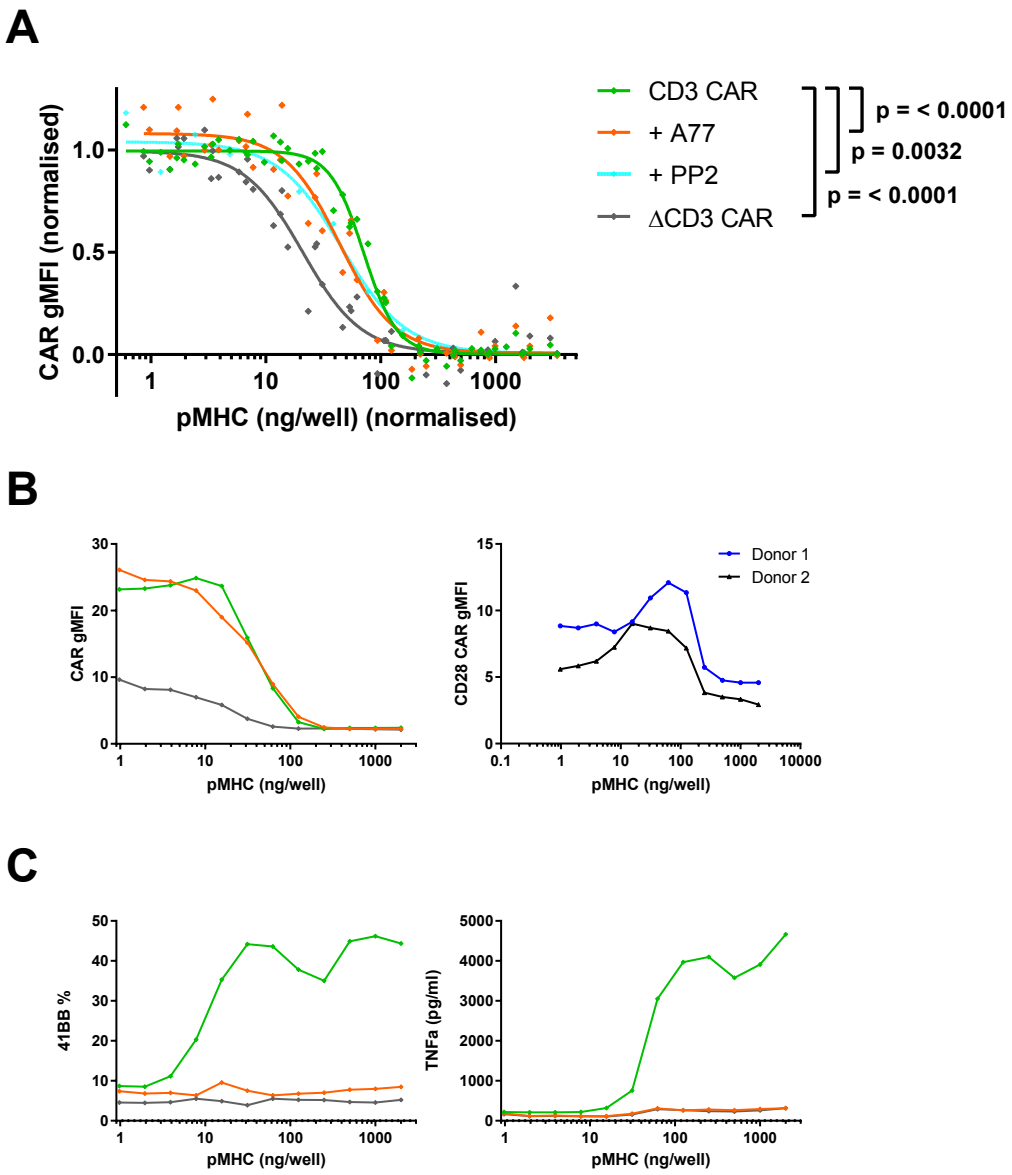


Fig. 4.4: Lck inhibition and CAR truncation affect CAR downregulation. Primary human $CD8^+$ T cells carrying different T1 CARs were stimulated for 8 h with 9V pMHC. A) Stimulation in the presence or absence of the Lck-specific inhibitor A-770041 (4 donors, 300-500 nM) or the Src family tyrosine kinase inhibitor PP2 (1 donor, 20 µM). To account for differences in CAR transduction efficiency, the background gMFI of the pMHC-only condition was set to 0 (the minimum of the fitted curve was subtracted) and the maximum of the pMHC-only curve was set to 1. The truncated CAR was normalised to its own baseline expression. To account for differences in pMHC immobilisation, the X-values for each donor were corrected depending on the IC_{50} of the pMHC-only curve ($X = [pMHC] \,/\, (IC_{50}/meanIC_{50})$). That means relative differences between the the curves with and without inhibitors are preserved. B) Representative raw gMFI values showing signalling-dependent upregulation of first- and second-generation CARs. C) T cell activation markers from one representative experiment with the first-generation CAR with and without Lck inhibition and with the truncated CAR. Surface marker expression was analysed by flow cytometry, cytokine concentrations in the supernatant were measured by ELISA. An F-test was used for statistical analysis in Prism comparing the IC_{50}s of the curves. We note that we did not correct the p-values reported here for multiple comparisons and this might have rendered the difference in IC_{50} with PP2 non-significant.

4.2.3 CAR T Cells Get Desensitised by Antigen

We tested whether CAR T cells show a similar desensitisation phenotype to TCR T cells using a similar transfer assay format as described above for the $1G4^{Hi}$ TCR (Figure 2.7). CAR T cells were stimulated with 9V pMHC for 4 h, rested for 4 h, and then transferred to the same dose response curve of pMHC again for another 16 h. We then compared their cytokine production during this second stimulation with the production from fresh cells. Indeed, we found the same desensitisation of cytokine production with a first-generation CAR when transferred to the same antigen. The pre-stimulated cells produced much less cytokines than the fresh cells. Representative dose-response curves from one donor are shown in Figure 4.5 A. The quantification of the maximal cytokine production from multiple donors revealed that pre-stimulated cells produced only 26.9 % of the maximal TNF-α (p = 0.0183) and 26.3 % of the maximal IFN-γ (p = 0.0411) produced by fresh cells (Figure 4.5 B). Desensitisation was even stronger (2.1 %) with regard to IL-2 production (Figure 4.5 B). However, there was also more variability in the IL-2 production of the unstimulated cells which resulted in the difference becoming non-significant (p = 0.1103).

Intriguingly, we found that T cells with a second-generation CAR containing the CD28 and CD3ζ signalling domains exhibited much less desensitisation (Figure 4.5) and still produced 48.3 % of the maximal TNF-α, 79.5 % of the maximal IL-2 and 50 % of the maximal IFN-γ produced by their fresh counterparts. None of these differences reached statistical significance.

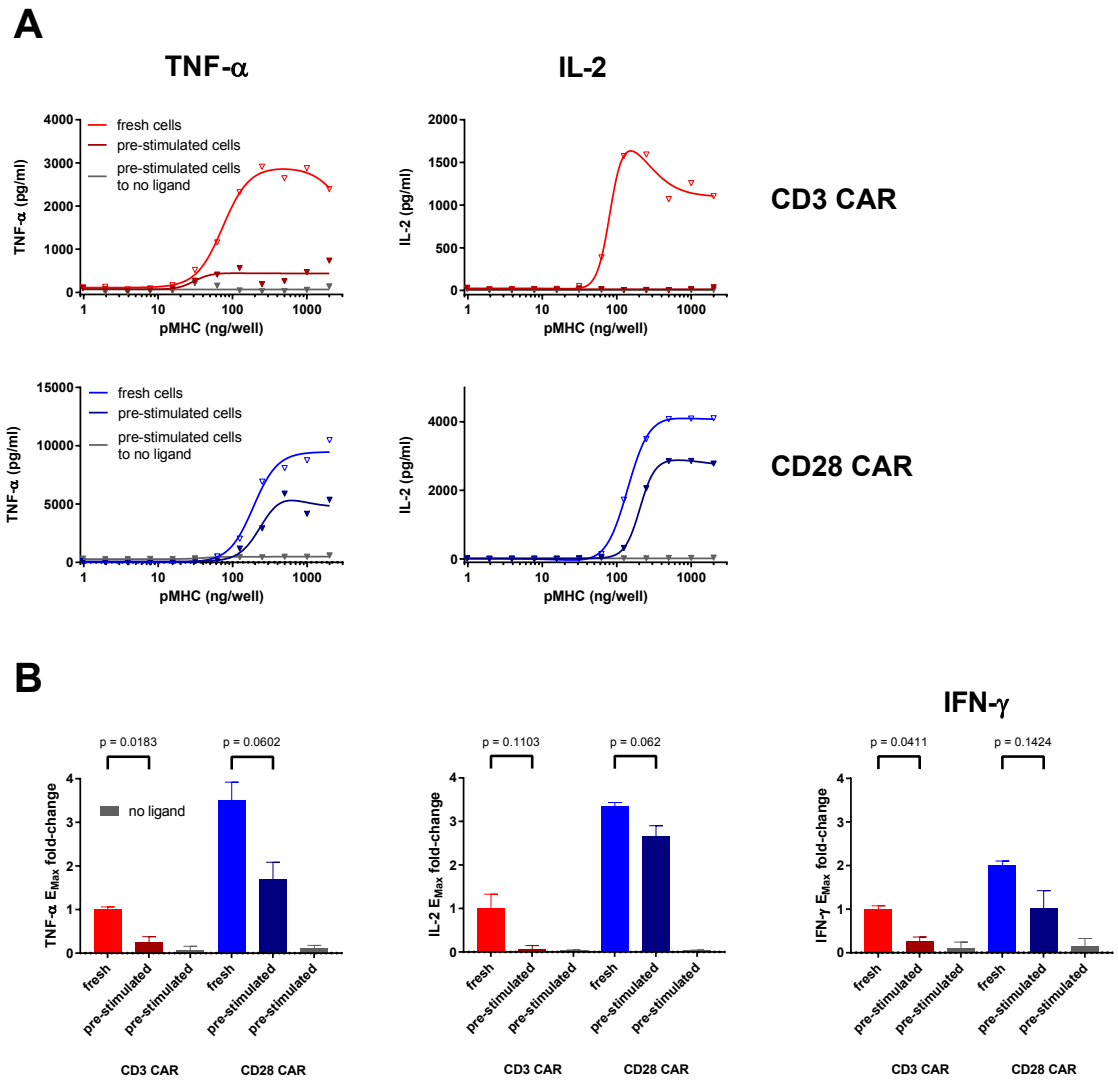


Fig. 4.5: CAR T cells get desensitised by antigen. Primary human CD8$^+$ T cells with a first-generation CAR or CD28 second-generation CAR were stimulated with 9V pMHC for 4 h, rested for 4 h, and then transferred to the same dose response curve of pMHC again for another 16 h. Cytokine production during this second stimulation was compared to the production from fresh cells. A) Representative dose response curves from one donor. B) Quantification of the maximum of the fitted curve for each dose response. In order to be able to compare between donors, the data was normalised to the mean of each dataset and a fold-change relative to the production of fresh cells was calculated. The TNF-α and IL-2 data is based on three donors and was included in (Trendel et al., 2019). IFN-γ data is based on two donors. Statistical analysis was performed in Prism using a one-way ANOVA corrected for multiple comparisons with the Holm-Šidák method.

We noted that overall cytokine production was higher from second-generation CAR T cells for all donors (Figure 4.5) even though the receptor was always expressed at lower levels per cell (Figure 4.6). The difference between the two CARs was statistically significant for IL-2 (3.34-fold, p = 0.023) and for TNF-α (3.51-fold, p = 0.0238), but not for IFN-γ (2.02-fold, p = 0.1405).

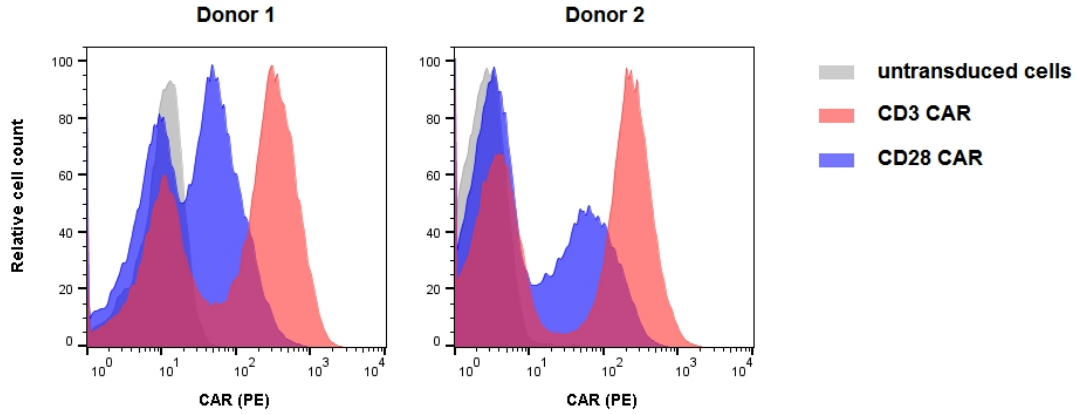


Fig. 4.6: Expression of first- and second-generation CARs. Primary human CD8$^+$ T cells expressing first-generation CD3 or second-generation CD28 CARs were stained with fluorescently labelled pMHC tetramers and CAR expression was analysed by flow cytometry. Data from two independent donors. This data was included in (Trendel et al., 2019).

4.2.4 Extrinsic Costimulation Overrides CAR T Cell Desensitisation

Since CAR T cells have been shown to be responsive to extrinsic costimulation (Zhao et al., 2015; Brentjens et al., 2007), we tested whether desensitised CAR T cells can be re-activated by extrinsic CAR-independent CD28 costimulation by adding CD86 to the stimulation plate as we did with the 1G4^{Hi} TCR (Figure 2.8). The results are preliminary, but support the conclusion that costimulatory signalling can override the desensitisation of first-generation CAR T cells as it did with the TCR. Interestingly, CD28 second-generation CAR T cells did not respond very strongly to costimulation whereas the response of first-generation CAR T cells was amplified considerably and both the pre-stimulated cells and the fresh cells produced more cytokines than the fresh cells without CD86 (Figure 4.7).

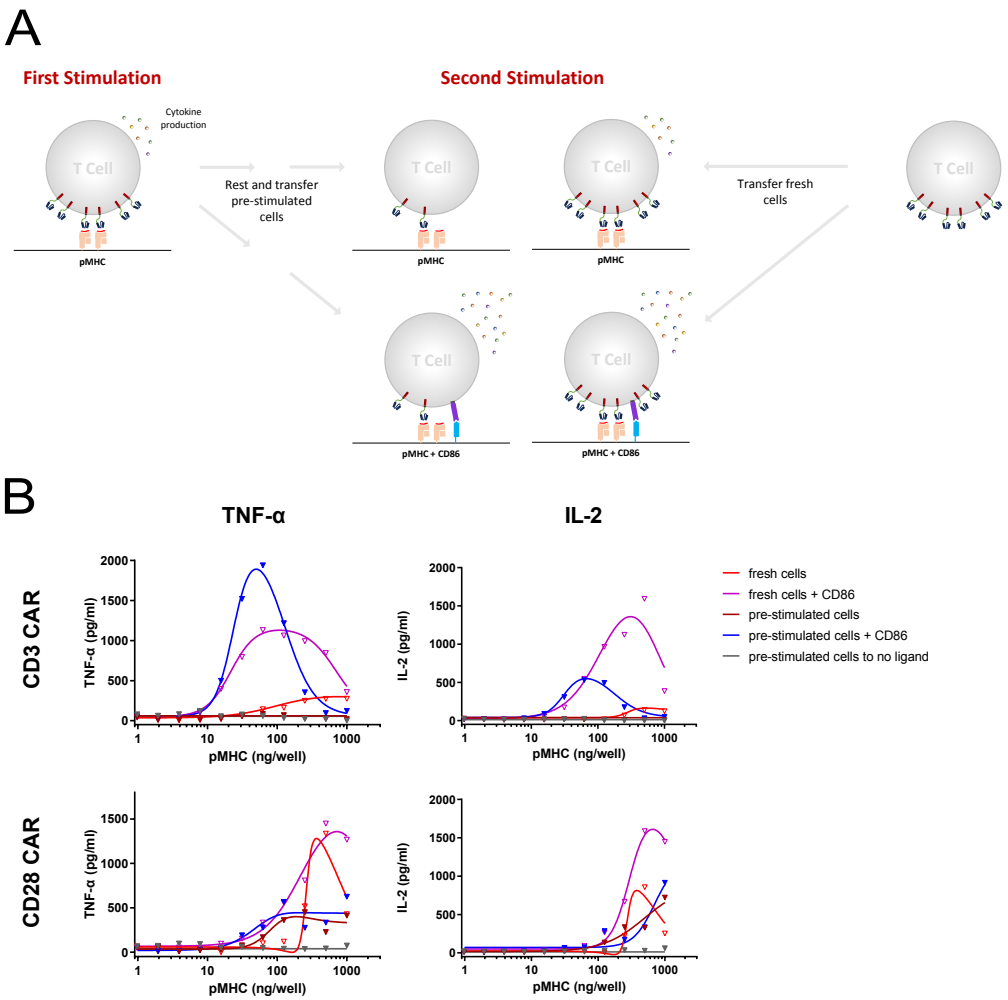


Fig. 4.7: Desensitised CAR T cells can be re-activated by costimulation. Primary human CD8$^+$ T cells with a first-generation CAR or CD28 second-generation CAR were stimulated with 9V pMHC for 8 h and then transferred to the same dose response curve of pMHC with or without 1000 ng CD86 for another 16 h. Cytokine production during this second stimulation was compared to the production from fresh cells. A) Schematic of the experiment. B) Dose response curves from one donor. This data was included in (Trendel et al., 2019).

4.3 Discussion

We have developed a novel CAR T cell stimulation platform that can be used to study the quantitative effects of CAR-antigen binding affinity and antigen dose without changing the receptor. Previous attempts at elucidating the effects of CAR affinity always used different CAR constructs with mutations in the binding domain or entirely different scFvs (Chmielewski et al., 2004; Kloss et al., 2013; Arcangeli et al., 2017; Hudecek et al., 2013; Caruso et al., 2015) which can lead to differences in stability, aggregation and expression level (Martin Pulè, personal communication). We have further shown that, as for the TCR, CAR downregulation correlates with other T cell activation markers, but it is independent of CAR signalling. First-generation CAR T cells show a similar desensitisation by antigen as TCR T cells, but this is much reduced in CD28 second-generation CAR T cells. Furthermore, preliminary data suggests that extrinsic costimulation can re-activate desensitised CAR T cells. Our data therefore suggests that our model of TCR downregulation (chapter 2) can also be applied to CARs with a similar phenotypic outcome: Receptor levels are adjusted to antigen dose and affinity so that the cells become unresponsive until they receive a stronger stimulus, either from a higher antigen dose or affinity, or through costimulatory signalling.
However, given that we found CAR downregulation in response to antigen to be even more complex than TCR downregulation due to the signalling-dependent upregulation at intermediate doses, more data will be required to support this conclusion.

4.3.1 Implications of CAR T Cell Adaptation

There are different theories about the purpose of the downregulation of the TCR in response to antigen. By contrast, CARs are synthetic molecules that have not evolved to serve a cellular function. Instead, their capacity to downregulate upon ligand engagement must have been transferred upon CARs together with the capacity of T cell activation. This is most likely a consequence of using the whole CD3ζ chain. Receptor downregulation will nevertheless have important implications for CAR T cell activity and eventually, clinical efficacy. As for the TCR, it is well established that lower CAR expression levels render the T cells less responsive to antigen (James et al., 2010; Caruso et al., 2015;

Han et al., 2018; Arcangeli et al., 2017). On the other hand, high CAR expression can lead to constitutive signalling and T cell exhaustion (Eyquem et al., 2017; Frigault et al., 2015; Long et al., 2015; Gomes-Silva et al., 2017). While other characteristics like CAR affinity have been widely studied to determine their effect on CAR T cell activation, the engineering of CARs for optimal downregulation dynamics has not been explored. Our results suggest that T cell activity might be improved by specifically modulating CAR downregulation upon antigen encounter, for example to reduce downregulation and prevent CAR T cell adaptation *in vivo*. However, at the present time, the ligand-induced downregulation pathway is not very well understood, although specific ubiquitination sites in CD3ζ have been identified (Hou et al., 1994).

It is likely that receptor downregulation will limit the activity of CAR T cells particularly in response to solid malignancies because there, cytokine production is critical for their ability to overcome the immunosuppressive microenvironment. The CAR T cells' ability to kill tumour cells would be expected to be less affected by receptor downregulation, because the killing of a target cell requires a lower activation threshold than cytokine production (James et al., 2010; Watanabe et al., 2015; Arcangeli et al., 2017) and is less affected by changes in CAR affinity (Hudecek et al., 2013; Chmielewski et al., 2004; Caruso et al., 2015) or expression level (James et al., 2010; Arcangeli et al., 2017). This interpretation is in line with the finding that improved clinical outcomes with second-generation CARs cannot be explained with improvements in direct cytotoxicity, since many investigators have demonstrated that their *in vitro* killing capacity is no different from first-generation receptors (Brentjens et al., 2007; Pulè et al., 2005; Carpenito et al., 2009; Zhao et al., 2015). The differences in the *in vivo* activity most likely result from stronger inflammatory cytokine production and longer persistence of the second-generation CAR T cells (Savoldo et al., 2011; Brentjens et al., 2007; Carpenito et al., 2009; Zhao et al., 2015; Kloss et al., 2013). Consequently, new CAR T cell products are under development which are engineered to secrete cytokines like IL-12 (Chmielewski et al., 2011; Pegram et al., 2012), IL-15 (Hurton et al., 2016) or IL-18 (Hu et al., 2017; Chmielewski and Abken, 2017; Avanzi et al., 2018), either constitutively or upon CAR signalling.

We observed reduced desensitisation with a CD28 second-generation CAR which could help to explain why second-generation CARs generate much more potent and persistent

anti-tumour responses *in vivo* (Savoldo et al., 2011; Brentjens et al., 2007; Carpenito et al., 2009; Zhao et al., 2015). Our model would predict that second-generation CAR T cells do not only produce cytokines at a higher initial rate, but will also produce them for longer, i.e. show delayed or completely absent adaptation. Our findings have further implications for the optimal design of the costimulatory signal. Our model would predict that costimulation through a separate receptor should be more efficient because ligand-induced downregulation of the CAR which includes the costimulatory domains would limit their signalling. The co-expression of CARs together with separate costimulatory molecules has been demonstrated by different groups (Zhao et al., 2015; Curran et al., 2015; Kloss et al., 2013). Zhao et al. performed a direct comparison of T cells expressing a third-generation CAR that included CD28 and 4-1BB signalling domains with a second-generation CD28 CAR plus separate 4-1BB ligand. Notably, the separate 4-1BB signal resulted in much better *in vivo* activity and tumour control (Zhao et al., 2015). Downregulation upon CAR engagement might be particularly limiting for the 4-1BB signal, because endogenous 4-1BB is only upregulated on T cells upon activation and probably plays a role later during the response.

5 Conclusion

5.1 Summary

We have developed a minimal experimental platform for high-throughput human T cell stimulation by immobilising recombinant pMHC complexes and costimulatory ligands on plastic plates. This system allows us to systematically study the effects of parameters like antigen dose, antigen affinity and stimulation time on different T cell activation markers. A range of pMHC variants have been developed in the past that exhibit different binding affinities for the $1G4^{Hi}$ TCR (Lever et al., 2016). In addition, we now have a CAR that binds to the same pMHC antigens and we can therefore study CAR T cell activation with the same experimental platform. We have then developed the system further to be able to include ligands to accessory receptors on T cells which are known or believed to modulate T cell responses. By using the recombinant endogenous ligands immobilised on plates, we can study their effects on T cell activation in isolation, i.e. without potential compensatory or competing effects from other receptor ligand interactions.

By studying T cell cytokine production over time, we described an adaptation phenotype, i.e. cytokine production stops after a few hours even though the antigen is still present (Figure 2.2). This phenotype was observed in response to all doses of a high- and a low-affinity pMHC. We have also found that the stimulated cells rapidly downregulate their TCRs (Figure 2.2). Based on this data, we generated a mathematical model that was able to reproduce the temporal dynamics of TCR downregulation (Figure 2.5) and showed that TCR downregulation is sufficient to explain why cytokine production stops (Figure 2.6). Importantly, TCR downregulation at low and intermediate antigen doses was incomplete, but the slight reduction in TCR expression was enough to fall below the threshold for cytokine production. We showed that the remaining TCRs were fully functional by re-activating the adapted T cells with a higher-affinity pMHC ligand (Figure 2.7). The adaptation phenotype has potential implications for peripheral tolerance, because it suggests a mechanism by which T cells can adjust their TCR levels to low-affinity self-antigens so that they become unresponsive to them, but are not completely inactivated, so that they can still respond to a higher-affinity foreign antigen in the case of an infection.

We studied CAR T cell activation and receptor downregulation in the same experimental system as we did for the TCR which allowed us to use ligands with different affinities while keeping the receptor constant. We found that CARs were also downregulated upon antigen engagement (Figure 4.4). T cells carrying a first-generation CAR with CD3ζ signalling also became unresponsive after a few hours of stimulation, but this phenotype was much less pronounced when the CAR also contained a CD28 signalling domain (Figure 4.5). This downregulation-induced adaptation could help to explain why first-generation CAR T cells did not show clinical anti-tumour activity (Kershaw et al., 2006; Park et al., 2007; Till et al., 2008; Jensen et al., 2010; Lamers et al., 2013; Savoldo et al., 2011) whereas second-generation CARs containing costimulatory signalling domains were much more potent, particularly with regard to cytokine release and persistence *in vivo* (Savoldo et al., 2011; Davila et al., 2014; Maude et al., 2018; Lee et al., 2015; Turtle et al., 2016a).

We then used our experimental system to quantitatively compare the effects of two costimulatory receptors, CD2 and CD28. CD28 increased cytokine production (Figure 3.7), but did not affect TCR downregulation (Figure 3.6). The fact that we observed no changes in TCR downregulation means that CD28 did not significantly affect TCR-pMHC binding dynamics, i.e. it had no adhesion effect in our system. To reproduce this phenotype with the mathematical model, we systematically modulated each parameter up or down and found that a decrease in the threshold of T cell activation downstream of the TCR was sufficient to explain the effect of CD28 (Figure 3.9). As a consequence of the lowered threshold, CD28 costimulation (together with pMHC) was also able to re-activate T cells that had adapted to pMHC stimulation by downregulating their TCRs and did no longer respond to that pMHC alone (Figure 2.8). Preliminary data suggests that adapted first-generation CAR T cells can also be re-activated through CD28 costimulation (Figure 4.7).

The effects of CD2 costimulation were overall stronger than what we observed for CD28 and they were more difficult to explain. CD2 increased cytokine production, too, particularly at lower antigen doses (Figure 3.11), but it also dramatically increased TCR downregulation (Figure 3.10). We were not able to explain this phenotype by modulating only one parameter in the model. Instead, we found combinations of parameter modula-

tions that could reproduce the observed effects. These combinations generally consisted of an adhesion effect that increased TCR-pMHC binding and of downstream signalling effects that affected the threshold for cytokine production and the production rate (Figure 3.12). This shows that CD28 and CD2 both play important roles in the activation of human $CD8^+$ T cells, but their mechanisms of action are clearly distinct.

5.2 Future Directions

5.2.1 The Role of Adaptation

We have investigated TCR downregulation-induced T cell adaptation in human $CD8^+$ effector T cell blasts stimulated on plastic plates. While TCR downregulation has been observed by others in many experimental systems that used APCs for stimulation, we would like to reproduce the phenotype we observed in a more physiological cell-cell system and investigate whether TCR downregulation and cytokine production follow similar or very different temporal dynamics. In addition, it would be interesting to study if there are differences in TCR downregulation and T cell adaptation between T cell subsets, particularly between naïve and memory T cells and between $CD8^+$ and $CD4^+$ T cells.

5.2.2 Model Refinement

Our current model reproduces the phenotypes we see in our data, but we have not attempted to systematically rule out other possible models. An exhaustive search of all possible models of similar complexity with a comprehensive parameter search is not computationally feasible. However, there are some alternative designs that could result in a similar or better fit which we would like to investigate further. First, the Hill coefficient of the intracellular switch is currently set at 1.67 which means that cytokine production is not truly digital (a shallower dose response means there is no sharp threshold). As a consequence, the simulated T cell never completely stops to produce cytokines, it only dramatically slows down production. This parameter value was determined by Nicola Trendel's ABC-SMC fitting algorithm and is probably a result of the relatively shallow dose response curves of TNF-α production that we used as an input. If we set this parameter

considerably higher to generate a steeper switch function, the fit gets worse, because the real dose response curves are not very steep. However, as we have discussed in section 2.3.3, the dose response of a population of cells will always be shallower than a single-cell response, so we could amend the model to include population heterogeneity and fit the data while retaining a sharp threshold for cytokine production.

Secondly, there are several modifications to the TCR downregulation functions that could affect the mechanistic interpretation or the integration points for costimulatory molecules. Currently, the ultrasensitivity in pMHC-TCR binding is implemented as $TCR_{bound} = (TCR_{free} * pMHC)^{nb}$ which establishes a sharp threshold for downregulation and ensures that TCR downregulation stops after the expression level drops below this threshold. The same could be achieved with a switch function as we have used for cytokine production and it might be worth exploring whether this implementation would also fit our data. Moreover, the downregulation of non-engaged bystander TCRs does not currently exhibit ultrasensitivity which explains why TCR downregulation overall does indeed not stop completely in our model simulations (Figure 2.5). The simulated differences between 1 and 8 h were so small that they were within the error in our downregulation data, but given that this parameter is affected by signalling and could therefore be a target of costimulation, it will be important to consider other possible model designs. Bystander downregulation could be endowed with an ultrasensitive response by using either of the two functions discussed above. However, another alternative could be that bystander downregulation is induced by a signalling pathway that acts after the same intracellular switch that regulates cytokine production. This would have implications for the integration of costimulatory signals, because an effect of the activation threshold would now also modulate bystander TCR downregulation. Importantly, some of those model modifications might help to better explain the costimulatory effects we see on the Hill coefficient of TCR downregulation.

5.2.3 Extended Costimulation Project

The systematic analysis of T cell responses to CD2 and CD28 ligands has shown qualitatively and quantitatively different phenotypes. Building on this data, we were able to

use mathematical modelling to generate hypotheses for the molecular mechanisms underlying their costimulation potential. The impact of this analysis can be further increased by comparing the CD2 and CD28 phenotypes to other accessory receptors (for example ICAM-1, 4-1BB, CD27, etc.). In order to be able to identify the integration points of the accessory receptors based on input-output T cell stimulation data, it has become apparent in the present study that more detailed datasets will be required, particularly with regard to temporal resolution. For example, it will be informative to be able to distinguish more clearly between effects that increase the cytokine production rate and those that increase the production time by preventing or delaying adaptation. Most importantly, however, our preliminary data suggests that detailed time courses of the expression levels for each accessory receptor will be critical to generate a model that accurately reproduces their effects over the course of the stimulation (Figure 3.13). Furthermore, by modelling the receptor ligand interaction explicitly, we will also be able to simulate saturation effects of the costimulatory pathway which may be important depending on the ligand dose range that is chosen for stimulation.

Our experimental system can also be used to study accessory receptors that inhibit T cell activation. However, such an analysis might be complicated by the finding that some inhibitory receptors exert their effects mainly on other costimulatory signalling pathways and not directly on TCR signalling. One such example that has recently been reported is PD-1. This receptor plays an important role in inhibiting T cell function in tumours and is the target of checkpoint inhibitor antibodies that aim to re-activate those tumour-specific T cells by blocking PD-1 interaction with its ligands. Based on the clinical observation that expression of the ligand PD-L1 on tumour cells was not a good biomarker for anti-PD-L1 checkpoint inhibitor therapy, Hui et al. carried out a detailed study of the effects of PD-1 signalling and discovered that it only had a comparatively weak inhibitory effect on TCR signalling, while it strongly inhibited CD28 (Hui et al., 2017). This will make the study of PD-1 and potentially other inhibitory receptors in our system difficult, because we would have to test them with all combinations of costimulatory receptors to determine where they exert their effect. Given the potential confounding effect of accessory ligands on the pMHC immobilisation or accessibility (Figure 3.16), the study of inhibitory receptors will also require more stringent controls to exclude (or at least quantify) any such passive

effects of ligand immobilisation. We are currently developing an inert ligand that can be co-immobilised with pMHC to study those effects. The same considerations of course apply to all ligands, particularly those that are expected to mainly have adhesion effects and not induce signal amplification, like ICAM-1. However, with regard to inhibitory effects, it would be particularly difficult to infer how much of the observed inhibition is due to inhibitory signalling and how much to the obstruction of pMHC on the plate.

5.2.4 Optimising CAR T Cells

The CAR T cell stimulation system described in chapter 4 allows for a detailed investigation of T cell activation in response to finely controlled antigen dose and affinity. It has the potential to be of use for the systematic and quantitative study of new CAR designs, particularly in combination with phenotypic modelling. One application could be the direct comparison of combinations of signalling domains within the CAR which has so far often been limited to few datapoints in the vast space of experimental conditions such as antigen dose, antigen affinity, time, and signalling domains. For example, our finding that a CD28 second-generation CAR showed reduced adaptation raises the question how other signalling domains might affect this phenotype. This could be tested with our CAR T cell stimulation system in the future by comparing cytokine production from T cells with different CARs over time, ideally with antigens of different affinities. However, this might require more complex modelling that takes into account potential differences in expression level between the constructs. The finding that CARs are downregulated upon antigen engagement also implies that there might be unexplored design modifications that could modulate downregulation and thereby control the duration of CAR T cell cytokine production. This could be supplemented with a more detailed investigation of the effects of CAR expression levels on T cell responses.

6 Materials and Methods

6.1 Reagent Suppliers and Brands

Supplier	Brand	Headquarters
Agilent Technologies Inc		Santa Clara, USA
Andreas Hettich GmbH		Tuttlingen, Germany
American Type Culture Collection (ATCC®)		Manassas, USA
Avantor Performance Materials, LLC	VWR Chemicals	Center Valley, USA
Avidity LLC	AviTag™	Aurora, USA
Beckman Coulter Inc		Brea, USA
Becton, Dickinson and Company	BD Biosciences, Flowjo®	Franklin Lakes, USA
Biolegend Inc		San Diego, USA
Bioline Reagents Ltd		London, UK
Biometra GmbH		Göttingen, Germany
BioTek Instruments Inc		Winooski, USA
Bio-Rad Laboratories Inc		Hercules, USA
Bio-Techne	R&D Systems	Minneapolis, USA
Chemometec A/S		Allerod, Denmark
Corning Inc	Costar®	Corning, USA
Cytek Biosciences Inc		Fremont, USA
Eppendorf AG		Hamburg, Germany
Eurofins Genomics GmbH		Ebersberg, Germany
GE Healthcare	Amersham Biosciences	Piscataway, USA
Geneflow Ltd		Elmhurst, UK
Genscript Inc		Picataway, USA
GraphPad Software Inc	Prism	La Jolla, USA

Supplier	Brand	Headquarters
Jackson ImmunoResearch Laboratories Inc		West Grove, USA
LI-COR Inc	Odyssey®	Lincoln, USA
Mathworks Inc	Matlab	Natick, USA
Medicell Membranes Ltd		London, UK
Merck Millipore	Sigma-Aldrich, Millipore	Burlington, USA
MP Biomedical Inc		Santa Ana, USA
Molecular Devices LLC		San Jose, USA
New England Biolabs		Ipswich, USA
Oxoid Ltd		Basingstoke, UK
Peprotech Inc		Rocky Hill, USA
Perkin Elmer Inc		Waltham, USA
Qiagen GmbH		Hilden, Germany
Sartorius Stedim	Minisart®	Göttingen, Germany
Scientific Laboratory Supplies Ltd		Nottingham, UK
Source BioScience Inc		Nottingham, UK
Stemcell Technologies Canada Inc		Vancouver, Canada
Stratagene Corporation		San Diego, USA
Synoptics Ltd	Syngene	Cambridge, UK
Takara Bio Inc		Kusatsu, Japan
Thermo Fisher Scientific	Invitrogen™, Gibco™	Waltham, USA
Veolia Environnement SA	Elga LabWater	Paris, France

Tab. 6.1: List of Suppliers and Brands. Listed are the suppliers of reagents, equipment, services, and materials, their associated brands and headquarters.

6.2 List of Reagents

Reagent	Supplier	Catalogue number
Agarose	Geneflow	A4-0700
Ampicillin	Sigma-Aldrich	A5354
Ampicillin agar plates	made in house	
BirA biotin-protein ligase bulk reaction kit	Avidity	bulk BirA
CutSmart® Buffer	New England Biolabs	B7204S
dH_2O	made in house with Purelab® flex 2 (Elga Labwater)	
DMSO, for PCR	Agilent Technologies	600675
dNTPs (1:1 mix of dATP, dTTP, dGTP, and dCTP)	Bioline Reagents	BIO-39049
Ethanol	VWR Chemicals	20821.310
Ethidium Bromide	Sigma-Aldrich	E1510
Gel loading dye	Bioline Reagents	BIO-33026
Guanidine-hydrochloride	Sigma-Aldrich	G3272
Herculase II Fusion DNA Polymerase	Agilent Technologies	600675
Herculase II reaction buffer	Agilent Technologies	600675
HiSpeed® Plasmid Maxi Kit	Qiagen	12662
Hyperladder™ 1kb	Bioline Reagents	BIO-33026
In-Fusion® Kit	Takara Bio	638911
Isopropanol	Sigma-Aldrich	278475
LB medium	made in house	

DMSO = dimethyl sulfoxide, PCR = polymerase chain reaction, dNTP = desoxynucleoside triphosphate, LB = lysogeny broth

Reagent	Supplier	Catalogue number
NEBuffer™ 2.1	New England Biolabs	B7202
NEBuffer™ 3.1	New England Biolabs	B7203
NheI	New England Biolabs	R0131
Nickle-NTA Agarose	Qiagen	30210
other Oligos	Eurofins Genomics	custom
PCR primers	Sigma-Aldrich	custom
peptides (see Table 6.8)	Genscript	custom
PMSF	Sigma-Aldrich	P7626
QIAprep Spin® Miniprep Kit	Qiagen	27106
QIAquick® Gel Extraction Kit	Qiagen	28704
SalI	New England Biolabs	R0138
Streptavidin-PE	Bio-Rad	STAR4B
SOC medium	Takara Bio	38911

Tab. 6.2: List of Reagents. Listed are the general reagents used for the experiments in this thesis with their manufacturers and catalogue numbers. Buffers, cell culture reagents and antibodies can be found in Table 6.3, Table 6.5, and Table 6.4, respectively.

Buffer	Supplier	Catalogue number
Dialysis solution pH 8		
10 mM Trizma® base	Sigma-Aldrich	77-86-1
150 mM NaCl	VWR Chemicals	27810.364
Flow cytometry staining buffer		
sterile PBS	Sigma-Aldrich	D8662
1 % Bovine Serum Albumin	Fluka Biochemika	05473

NTA = nitrilotriacetic acid, PMSF = phenylmethanesulfonyl fluoride, PE = phycoerythrin, SOC = super optimal broth with catabolite repression, PBS = phosphate-buffered saline

Buffer	Supplier	Catalogue number
Hepes-buffered saline (HBS)-EP		
10 mM Hepes	Sigma-Aldrich	H3375
150 mM NaCl		
3 mM EDTA	Sigma-Aldrich	E6758
0.005 % Tween® 20	Sigma-Aldrich	P9416
NTA column elution buffer		
20 mM Trizma® base		
300 mM NaCl		
50 mM Immidazole	Sigma-Aldrich	68268
10 % Glycerol	Thermo Fisher Scientific	G/0650/08
Ni-NTA column wash buffer 1 pH 8		
20 mM Trizma® base		
300 mM NaCl		
Ni-NTA column wash buffer 2 pH 8		
20 mM Trizma® base		
300 mM NaCl		
5 mM Immidazole		
PBS		
10 PBS tablets l^{-1}	Oxoid	BR0014G
OR sterile PBS		
PBS-Tween		
PBS		
0.05 % Tween® 20		
OR 0.05 % Polysorbate 20	MP Biomedical	0210316880
pMHC refolding buffer		
100 mM Trizma® pH 8		

EDTA = Ethylenediaminetetraacetic acid

Buffer	Supplier	Catalogue number
400 mM L-Arginine monohydrochloride	Sigma-Aldrich	1042601
2 mM EDTA		
5 mM reduced glutathione	Sigma-Aldrich	G4251
0.5 mM oxidised glutathione	Sigma-Aldrich	G4376
0.1 mM PMSF		
TAE (Tris, Acetic acid, EDTA) buffer pH 8.0		
40 mM Trizma® base		
20 mM Acetic acid	Thermo Fisher Scientific	A38-212
1 mM EDTA		
Tris-buffered saline (TBS) pH 7.5		
10 mM Trizma® base		
150 mM NaCl		

Tab. 6.3: Buffer compositions. Listed are the buffers used in this thesis with their composition and manufacturers and catalogue numbers of the components.

Antibody target	Species	Clone	Conjugate	Supplier	Catalogue number
Flow cytometry					
human BTLA	mouse	MIH26	PE	Biolegend	344505
human CD127	mouse	HIL-7R-M21	Brilliant Violet™ 421	BD Biosciences	562436
human CD2	mouse	299812	APC	R&D Systems	FAB18561A
human CD25	mouse	BC96	PE	Biolegend	302606

APC = allophycocyanin

Antibody target	Species	Clone	Conjugate	Supplier	Catalogue number
human CD28	mouse	CD28.2	Alexa Fluor® 488	Biolegend	302916
human CD6	mouse	BL-CD6	FITC	Biolegend	313904
human CD69	mouse	FN50	Alexa Fluor® 647	Biolegend	310918
human CD69	mouse	FN50	PE	Biolegend	310906
human CD69	mouse	FN50	PerCP	Biolegend	310928
human HLA-A2	mouse	BB7.2	-	BD Biosciences	551230
human IgG Fc	goat	polyclonal	PE	Invitrogen™	12-4998-82
human PD-1	mouse	EH12.2H7	Alexa Fluor® 488	Biolegend	329936
human TCR Vβ 13.1	mouse	H131	FITC	Invitrogen™	11-5792-41
human 4-1BB	mouse	4B4-1	PerCP/Cy5.5	Biolegend	309814
human 4-1BB	mouse	4B4-1	Alexa Fluor® 647	Biolegend	309824
Ligand immobilisation					
human CD166	mouse	105901	-	R&D Systems	MAB656
human CD58	mouse	TS2/9	-	Biolegend	330902

PerCP = peridinin-chlorophyll-protein, IgG = immunoglobulin G

Antibody target	Species	Clone	Conjugate	Supplier	Catalogue number
human CD80	mouse	2D10	-	Biolegend	305202
human CD86	mouse	IT2.2	-	Biolegend	305402
human HLA-A/B/C	mouse	W6/32	-	Bio-Rad	MCA81
human PD-L1	mouse	29E.2A3	-	Biolegend	329702
Secondary Antibodies					
anti-mouse	goat	polyclonal $F(ab')_2$	FITC	Jackson	115-096-072
anti-mouse	goat	polyclonal	IRDye® 680RD	LI-COR	926-68070
ELISA kits					
human CCL4/MIP-1β	Uncoated ELISA Kit (former eBioscience Ready-SET-Go!)			Invitrogen™	88-7034-88
human GM-CSF	Uncoated ELISA Kit			Invitrogen™	88-8337-88
human IFN-γ	Uncoated ELISA Kit			Invitrogen™	88-7316-77
human IL-2	Uncoated ELISA Kit			Invitrogen™	88-7025-77
human IL-8	Uncoated ELISA Kit			Invitrogen™	88-8086-77
human TNF-α	Uncoated ELISA Kit			Invitrogen™	88-7346-77

Tab. 6.4: Antibodies. Listed are the antibodies and ELISA kits used in this thesis.

CCL = CC chemokine ligand

Reagent	Supplier	Catalogue number
CellTrace™ Far Red	Invitrogen™	C34564
DMSO, Hybri-Mat™	Sigma-Aldrich	D2650
Dynabeads Human T-Activator CD3/CD28	Gibco™	111.32D
Ficoll®-Paque	Amersham Biosciences	17-1440-02
polyethylenimine (PEI)	Sigma-Aldrich	03880
Recombinant human IL-2	Peprotech	200-02
Red Blood Cell Lysis Buffer	Sigma-Aldrich	000000011814389001
RosetteSep™ Human $CD4^+$ T Cell Enrichment Cocktail	Stemcell Technologies	15062
RosetteSep™ Human $CD8^+$ T Cell Enrichment Cocktail	Stemcell Technologies	15063
Solution 13	Chemometec	910-3013
TrypLE Express	Gibco™	12604013
X-tremeGENE™ HP Transfection Reagent	Sigma-Aldrich	06366546001
CHO production medium		
L-glutamine free DMEM	Sigma-Aldrich	D6546
2.5 % FBS	Gibco™	10500064
100 U/ml Penicillin, 100 µg Streptomycin	Gibco™	15140122
2 % GSEM Supplement	Sigma-Aldrich	G9785
1 mM Sodium Pyruvate	Sigma-Aldrich	S8636
CHO selection medium		

CHO = Chinese hamster ovary, DMEM = Dulbecco's modified Eagle's medium, FBS = Fetal Bovine Serum, GSEM = glutamine synthetase expression medium

Reagent	Supplier	Catalogue number
L-glutamine free DMEM		
10 % dialysed FBS	Gibco FBS dialysed in house	
100 U/ml Penicillin, 100 µg Streptomycin		
2 % GSEM Supplement		
D10 medium		
DMEM	Sigma-Aldrich	D5429
10 % FBS		
100 U/ml Penicillin, 100 µg Streptomycin		
R10 medium		
RPMI1640	Sigma-Aldrich	R8750
10 % FBS		
100 U/ml Penicillin, 100 µg Streptomycin		

Tab. 6.5: Cell culture reagents and media. Listed are media, reagents and buffers used in cell culture.

6.3 Molecular Biology

6.3.1 Polymerase Chain Reaction

DMSO, dH_2O, dNTPs, Herculase II, and Herculase II Buffer were added together in a master mix and then added to the template DNA and primers. Concentrations and reaction conditions were adjusted depending on primer melting temperatures and template size according to Table 6.6. PCRs were carried out in a T3 Thermocycler (Biometra). The size of PCR products was confirmed by agarose gel electrophoresis (section 6.3.2).

RPMI = Roswell Park Memorial Institute

Reagent	**Concentration**
DMSO	1-4 %
dNTPs	25 mM each
Herculase II Buffer	10 %
Herculase II	1.6 %
primers	0.7 µM
template	10-100 ng
dH_2O	to 50 µl
Temperature	**Time**
95°C	2 min
start cycle	
95°C	10 s
primer melting temp -1°C	30 s
72°C	30 s per 1000 template base pairs
end after 35/39 cycles (colony PCR/other PCRs)	
72°C	10 min

Tab. 6.6: PCR composition and reaction conditions. Listed are the concentrations for all reagents used in PCRs and the cycling conditions used for the reactions.

6.3.2 Agarose Gel Electrophoresis

All PCR products, restriction digests and purified plasmids were validated by gel electrophoresis. 0.5-1 % agarose was boiled in TAE buffer until all particles were dissolved. The solution was then cooled down before ethidium bromide was added at a 1:10.000 dilution, and the mix poured into a gel casting chamber (Geneflow). After the gel had solidified, the chamber was filled with TAE buffer. Gel loading dye was added to the DNA at a 1:5 ratio and the mix was pipetted into a gel pocket. For colony PCRs, one fifth of the reaction volume was used, for purified plasmids, 300 ng were used, for other PCRs and restriction digests, all DNA was added and later extracted from the gel (section 6.3.3).

The gel was run at 90 V for 18 min. A photograph was taken with a Gene Genius Bioimaging System and GeneTools software (Syngene) and relevant bands were cut out with a razor blade on a Transilluminator 2040 EV (Stratagene) and stored at 4 °C or immediately used for DNA extraction (section 6.3.3).

6.3.3 DNA Extraction

Agarose gel bands were weighed and DNA was purified using QIAquick® Gel Extraction Kit according to the manufacturer's instructions. PCR products and restriction digest fragments were stored at 4 °C in dH_2O for further cloning steps. DNA concentrations were measured as described in section 6.3.9.

6.3.4 Restriction Enzyme Digest

Restriction digest was used to cut the backbone of lentiviral plasmids. 1-5 µg of plasmid DNA were incubated with 1 µl NheI in 1x NEBuffer™ 2.1 (topped up to 50 µl total with dH_2O) for 30 min at 37 °C. Then SalI was added and the salt concentrations adjusted to match NEBuffer™ 3.1 by adding 0.6 µl 5 M NaCl and 2.2 µl 1 M Tris-HCL. The reaction was incubated for another 30 min at 37 °C. The size of the cleaved products was confirmed by agarose gel electrophoresis (section 6.3.2).

6.3.5 In-Fusion® Reaction

In-Fusion® cloning was performed to generate CAR constructs according to the manufacturers protocol. CAR fragments were generated by PCR with primers with 15 base pair overhangs for the adjacent fragment (Table 6.7) so that the In-Fusion® reaction could be used to ligate them together. The CD28 second-generation CAR was used as the template (see section 6.3.11).

Primer name	Sequence	Melting temperature (without overhang)
CD3ζ 5' (TM overhang)	ATTATTTTCTGGGTG_CTGAGAGTG AAGTTCAGCAGGAG	64.6 °C
CD3ζ 3'	AGGTTGATTGTCGAC_TTAGCGAGG GGGCAGGG	59.8 °C
ΔCD3 3' (vector overhang)	AGGTTGATTGTCGAC_TTACGCGGG GGGCTCTGCG	66.1 °C
TM 3'	CACCCAGAAAATAATAAAGGCCACT G	64.6 °C
CAR 5' (vector overhang)	GTGTCGTGAGCTAGC_ATGGATTTT CAGGTGCAGATTTTC	60.3 °C

Tab. 6.7: DNA primers for In-Fusion® cloning and their sequences. Listed are the names and sequences of all primers used for PCRs and sequencing. The _ indicates where the overhang ends.

6.3.6 Bacterial Cell Transformation

50 µl chemically competent Escherichia coli DH5α cells (prepared by Marcus Bridge, stored at -80 °C) were thawed on ice. The whole volume of an In-Fusion® reaction or 100-300 ng of plasmid DNA were added and incubated for 30 min on ice. The bacteria were then heat-shocked at 42 °C for 40 s and rested on ice for 5 min. 200 µl SOC medium were added and the bacteria were placed in a shaking incubator for 1 h. For purified plasmids, 20 µl of the culture were streaked onto agar plates containing 100 mg ml^{-1} Ampicillin; for In-Fusion® reactions, the whole culture was streaked. Plates were incubated at 37 °C for 20 h (30 °C for lentiviral plasmids).

6.3.7 Colony PCR

A single bacterial colony was picked from a transformation plate and transferred to a PCR tube. The same tip was then used to inoculate a culture with 1 ml LB medium which was incubated in a shaking incubator for 3-5 h. The PCR was set up as described in

TM = transmembrane domain DNA fragment

section 6.3.1 with primers spanning the backbone and the insert, but without template DNA. If bands of the expected size were detected, the corresponding cultures were used to start an overnight culture in 7-10 ml LB medium at 37 °C in a shaking incubator.

6.3.8 DNA Extraction from Bacterial Cultures

DNA from 7-10 ml or 200-500 ml overnight bacterial cultures was extracted using QIAprep Spin® Miniprep Kit or HiSpeed® Plasmid Maxi Kit, respectively, according to the manufacturer's instructions. The resulting plasmid solutions were stored in buffer TE at 4 °C.

6.3.9 DNA Quantification

DNA concentrations were determined via spectrophotometric quantitation on a Nanodrop 1000 (Thermo Fisher Scientific). The instrument was initialised with 1 µl dH_2O, a blank was measured with 1 µl buffer TE or dH_2O (depending on what the DNA was resolved in), and then 1 µl of the sample was added. Absorbance at 260 nm was measured and converted to a $ng\,\mu l^{-1}$ concentration in Nanodrop 1000 software version 3.1.

6.3.10 DNA Sequencing

Plasmids or PCR products were sent either to Source BioScience or to Eurofins Genomics for sequencing.

6.3.11 Receptor Constructs

The TCR used throughout chapter 2 and chapter 3 is a high-affinity variant of the 1G4 TCR isolated from a melanoma patient (Chen et al., 2000). The affinity maturation to the c58/c61 variant used herein (referred to as $1G4^{Hi}$) was carried out by Adaptimmune Ltd. The TCR and all CARs in this study have been used in a third-generation lentiviral vector with the EIFα promoter that was also provided by Adaptimmune Ltd. Three CAR

EIF = eukaryotic initiation factor

constructs that bind the NY-ESO-$1_{157\text{-}165}$ HLA-A2 pMHC complex (Jakka et al., 2013) were a kind gift from Christoph Renner (Zurich). The three different CARs bind the antigen with different affinities (Stewart-Jones et al., 2009; Maus et al., 2016), but only the high-affinity version T1 was used for this project. All CAR constructs contained the scFv binding domain, a 2 Ig domain spacer derived from an IgG antibody Fc part and the CD28 transmembrane domain. We modified the different CARs to contain the following signalling domains (shown schematically in Figure 4.2):

A first-generation CAR with the CD3ζ signalling tail (CTGAGAGTGAAGTTCAGCAGGAGCGCAGACGC CCCCGCGTACCAGCAGGGCCAGAACCAGCTCTATAACGAGCTCAATCTAGGACGAAGAGAGGAGTACGATGTTTTGGACAAG AGACGTGGCCGGGACCCTGAGATGGGGGGAAAGCCGAGAAGGAAGAACCCTCAGGAAGGCCTGTACAATGAACTGCAGAAA GATAAGATGGCGGAGGCCTACAGTGAGATTGGGATGAAAGGCGAGCGCCGGAGGGGCAAGGGGCACGATGGCCTTTACCAG GGTCTCAGTACAGCCACCAAGGACACCTACGACGCCCTTCCTGCCCCCTCGCTAA) (referred to as CD3 CAR).
A second-generation CAR with the CD28 signalling domain (AGGAGTAAGAGGAGCAGGCTCCTGC ACAGTGACTACATGAACATGACTCCCCGCCGCCCCGGGCCCACCCGCAAGCATTACCAGCCCTATGCCCCCCCACGCGACTT CGCAGCCTATCGCTCC) in addition to CD3ζ (referred to as CD28 CAR).
A truncated CAR with only the first 12 intracellular amino acids of CD3ζ (CTGAGAGTGAAGTT CAGCAGGAGCGCAGACGCCCCCGCG) (referred to as ΔCD3).

6.4 Protein Production

6.4.1 pMHC Refolding

pMHCs were refolded *in vitro* from the extracellular residues 1-287 of the HLA-A*02:01 α-chain, β2-microglobulin (both produced in Escherichia Coli by Marcus Bridge and Mikhail Kutuzov and stored in 8 M urea at -20 °C) and NY-ESO-$1_{157\text{-}165}$ peptide variants (Table 6.8). 1 mg (10 µM) peptide, 26 mg (2 µM) β2-microglobulin and 32 mg (1 µM) A2 α-chain were added dropwise and in this order to 100 ml refolding buffer while stirring gently at 4 °C. The mix was incubated for 40-72 h while stirring at 4 °C. The refold was then filtered (5 µm cutoff) to remove aggregates and concentrated by spinning multiple times for around 30 min at 3273 x g in a Centricon Plus-70 concentrator (Millipore) to a final volume of around 700 µl. The pMHC was then biotinylated (see section 6.4.4).

Peptide name	Amino Acid Sequence	K_D [M] for 1G4^{Hi} TCR
9V	SLLMWITQV	7.07×10^{-12}
4A	SLL**A**WITQV	1.09×10^{-9}
5Y	SLLM**Y**ITQV	1.33×10^{-9}
5F	SLLM**F**ITQV	9.31×10^{-8}
8K	SLLMWIT**K**V	2.03×10^{-7}
5P	SLLM**P**ITQV	4.85×10^{-7}
4A8K	SLL**A**WIT**K**V	1.78×10^{-6}
4A5A	SLL**AA**ITQV	2.24×10^{-5}
4A5P8K	SLL**AP**IT**K**V	$>1.0 \times 10^{-4}$

Tab. 6.8: Peptides and their sequences. Listed are the peptides used for pMHC refolding. All peptides were ordered from Genscript (see Table 6.2) and stored at 10 mg ml^{-1} in DMSO at -20 °C. K_D values were obtained by surface plasmon resonance measurements with a soluble recombinant version of the c58/c61 1G4^{Hi} TCR by Melissa Lever, Hong-Sheng Lim, Marcus Bridge and Mikhail Kutuzov. They have been reported in (Lever et al., 2016).

6.4.2 Fluorescent pMHC Tetramers

Fluorescent pMHC tetramers for use as a staining reagent in flow cytometry were produced from refolded 9V pMHC complexes and Streptavidin-PE. 66.6 µg pMHC were placed in a shaker at room temperature and 10 µl Streptavidin-PE were added 10 times every 10 min. The solution was then stored at 4 °C. A working dilution (1:50 - 1:500) was determined by titration on cells expressing the 1G4^{Hi} TCR and/or 3m4e5, D53N, or T1 CARs.

6.4.3 Nickle/NTA Column Protein Purification

Supernatants from transiently transfected HEK293T cells (see section 6.7.1) or from stable CHO cell lines (see section 6.5.4) were sterile-filtered through a 0.22 µm bottle top filter (SCGPU05RE, Millipore) and 100 µM PMSF was added. Supernatants were stored at -20 °C if not immediately used for protein purification. Supernatants were dialysed to

HEK293T = human embryonic kidney 293 cells that express the simian virus 40 large T antigen

remove potential contaminants that would interfere with protein purification. The supernatant was poured into a 12-14 kDa cutoff visking tube (DTV12000.13.000, Medicell). This was then placed in a 10 l bucket of dialysis solution which was stirred at 4 °C over night.

After washing the Nickle-NTA Agarose resin with dH_2O, 1 ml was added to 100 ml supernatant and incubated at 4 °C for 1 h under gentle agitation. The mixture was then transferred into a column. After everything had run through, the gel was washed once with 10 ml wash buffer 1 and once with 10 ml wash buffer 2 before the His-tagged proteins were eluted with 10 ml elution buffer into an Amicon Ultra-15 centrifugal filter unit with a 10 kDa mass weight cutoff (UFC901008, Millipore). This column was spun at full speed (3273 x g) for 30 min at 4 °C. If more than 2 ml of volume remained above the filter, the centrifugation was repeated for another 10 min. Once the volume was less than 2 ml, it was topped up with 10 ml wash buffer 1 and spun again as before to wash out the immidazole. The final volume was adjusted with wash buffer 1 to 700 µl for biotinylation.

6.4.4 Biotinylation

BirA biotin-protein ligase bulk reaction kit was used for *in vitro*-biotinylation at the C-terminal AviTag™ biotinylation site (SGLNDIFEAQKIEW) of refolded pMHC complexes and of purified costimulatory ligands according to the manufacturer's instructions. The reaction was incubated at 4 °C over night.

6.4.5 Fast Protein Liquid Chromatography

After biotinylation, the proteins were purified by size-exclusion chromatography and stored in aliquots at -80 °C. Chromatography was performed using a Superdex™ 200 column (GE Healthcare) on an ÄKTA™ pure chromatography system (GE Healthcare) with HBS-EP as the flow buffer.

6.5 Culture of Cell Lines

6.5.1 Incubation

All cells cultured in DMEM were incubated at 37 °C with 10 % CO_2; all cells cultured in RPMI were incubated at 37 °C with 5 % CO_2 (Galaxy 170R incubator, Eppendorf). Cell culture dishes (Corning® T25, T75, T175 flasks and Costar® 6-well, 24-well, 96-well plates) were purchased from Scientific Laboratory Supplies. All centrifugation steps were carried out for 5 min in a Megafuge 8R (Thermo Fisher Scientific) at 1700 rpm (533 x g) or in an Allegra X-15R (Beckman Coulter) at 1500 rpm (523 x g) unless otherwise stated.

6.5.2 Jurkat

The acute T cell leukaemia cell line Jurkat (clone E6.1, ATCC® TIB-152™) was cultured in R10 medium (see Table 6.5) and passaged every 2-3 days. The suspension culture was pelleted by centrifugation, resuspended in fresh pre-warmed medium, and $\frac{1}{8}$-$\frac{1}{10}$ of the volume was transferred into a new flask and topped up with fresh medium.

6.5.3 HEK293T

HEK293T cells (ATCC® CRL-3216™) were cultured in D10 medium (see Table 6.5) and passaged every 2-3 days. The old medium was removed and the cells were gently flushed off the flask with fresh pre-warmed medium. $\frac{1}{8}$ of the volume was then transferred into a new flask and topped up with fresh medium.

6.5.4 CHO

CHO cell lines (ATCC® CCL-61™) permanently expressing the extracellular part of human PD-L1 (amino acids 1-231), CD86 (amino acids 6-247), CD80 (amino acids 1-235) or CD58 (amino acids 29-213) were kindly provided by Simon Davis (Weatherall Institute of Molecular Medicine, University of Oxford, UK). The constructs further included

an N-terminal signal peptide for secretion (MGILPSPGMPALLSLVSLLSVLLMGCVAE), a C-terminal 6-Histidine tag, and a BirA biotinylation site (SGLNDIFEAQKIEW).

Cells were cultured in selection medium (see Table 6.5) and passaged every 3-4 days. Old medium was removed and the cells washed with pre-warmed PBS, before they were incubated with 3 ml TrypLE Express for 5 min at 37 °C. The enzymatic reaction was stopped with 10 ml fresh medium and the cells were pelleted by centrifugation. The supernatant was then discarded and the cells were resuspended in fresh medium and $\frac{1}{4}$ transferred to a new flask.

After 4-5 passages from thawing a new vial, cells from 2 confluent T175 flasks were transferred into a cell factory with 600 ml selection medium and incubated for 5-7 days after which the medium was replaced with 600 ml production medium. The supernatant was harvested for protein purification after another three weeks (see section 6.4.3).

6.5.5 Freezing and Thawing

5-20 $\times 10^6$ cells were pelleted from culture and resuspended in 1.5 ml FBS with 10 % DMSO. The suspension was transferred into a cryo-vial and placed inside an isopropanol container for freezing at -80 °C. Frozen vials were transferred to liquid nitrogen for long-term storage (more than 6 months).

Cells were thawed at room temperature and transferred into 10 ml of their respective culture medium, then pelleted and resuspended in medium again to wash out the DMSO before they were incubated as described in section 6.5.

6.5.6 Cell Counting

Cell suspensions were mixed well by pipetting before a sample of 19 µl was taken out and mixed with 1 µl Solution 13. The mix was then pipetted into a NC-Slide A8™ and the live cell concentration and viability were measured on a Nucleocounter® NC-3000™ (Chemometec).

6.6 Isolation and Culture of Primary T Cells

6.6.1 Blood Collection

Up to 50 ml peripheral blood were collected by a trained phlebotomist from healthy volunteer donors after informed consent had been taken. This project has been approved by the Medical Sciences Inter-Divisional Research Ethics Committee of the University of Oxford (R51997/RE001) and all samples were anonymised in compliance with the Data Protection Act. Blood was collected using BD Vacutainer® Push Button Blood Collection Set (BD, 367355) and BD Vacutainer® Sodium Heparin Plasma Tubes (BD, 368480) and immediately processed. Leukocyte cones were purchased from National Health Services Blood and Transplant under the project number T573.

6.6.2 HLA Typing

400 µl of peripheral blood from previously untested donors were pelleted at 5470 x g (Mikro 22 R, Hettich) for 5 min and resuspended in 800 µl Red Blood Cell Lysis Buffer. From a leukocyte cone, 40 µl were topped up with 800 µl Red Blood Cell Lysis Buffer and both were then processed following the same protocol. They were incubated for 10 min and then pelleted at 5470 x g for 7 min. The supernatant including the remains of red blood cells was carefully pipetted out and the cell pellet was washed once with PBS without resuspending it, before it was resuspended in 200 µl PBS containing the anti-HLA-A2 antibody or an isotype control at a 1:200 dilution. The cells were incubated with the primary antibody for 30 min before they were pelleted again and resuspended in 200 µl PBS containing the goat-anti-mouse FITC secondary antibody. After another 30 min incubation, the cells were pelleted again, resuspended in 300 µl PBS and analysed on a Cytek flow cytometer. Three examples are shown in Figure 6.1.

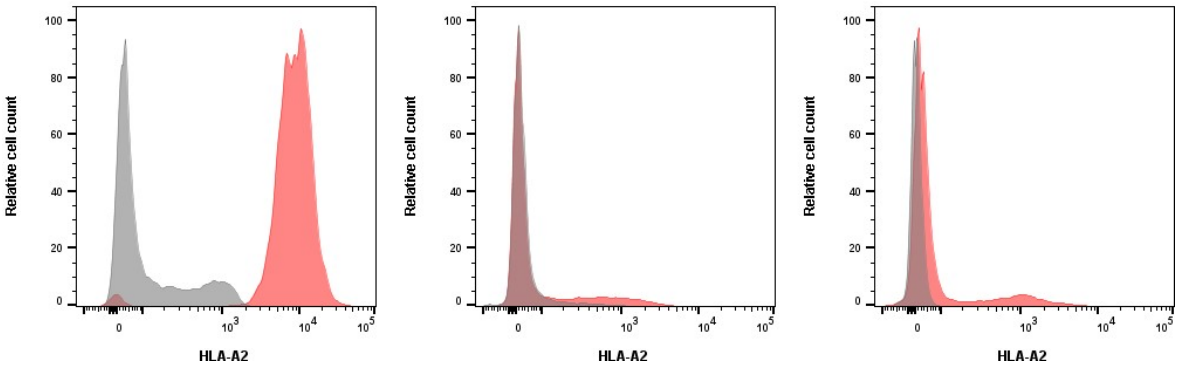


Fig. 6.1: Results of HLA-A2 staining for three donors. Shown are the flow cytometry histograms for the lymphocyte population (based on their FSC/SSC phenotype). Isotype controls are shown in grey, HLA-A2 staining is shown in red. Note that there is some background staining of a subset of cells most likely due to non-specific Fc receptor binding. A true HLA-A2$^+$ donor always showed much stronger staining of all lymphocytes as seen in the first panel.

6.6.3 T Cell Isolation

CD8$^+$ or CD4$^+$ T cells were isolated only from HLA-A2$^-$ peripheral blood or leukocyte cones due to the cross-reactivity of the high-affinity receptors used in this project which leads to fratricide of HLA-A2$^+$ T cells (Tan et al., 2015; Stewart-Jones et al., 2009; Maus et al., 2016). The blood was first treated with the CD8$^+$ or CD4$^+$ T Cell Enrichment Cocktail at a dilution of 150 µl per ml leukocyte cone or 6 µl per ml whole blood for 20 min. It was then diluted 1:5 for a leukocyte cone and 1:2 for whole blood with PBS and carefully layered over 15 ml Ficoll. Density gradient centrifugation was performed at 1000 x g for 30 min with the break disabled. The CD8$^+$ or CD4$^+$ T cell layer above the Ficoll was carefully pipetted off without disturbing the erythrocyte pellet, topped up with PBS to 40 ml and pelleted. The pellet was then resuspended in 5 ml R10 and the T cells were counted.

6.6.4 T Cell Expansion

1×10^6 freshly isolated T cells were seeded into one well of a 24-well plate in 500 µl R10 supplemented with 50 U/ml IL-2. The cells were stimulated with anti-CD3/anti-CD28 beads at a concentration of 0.8 beads per T cell for 24 h before they were transduced with lentiviruses for the expression of the TCR or CAR (see section 6.8), or left as untransduced controls. 2 ml of medium were pipetted off on day 3 after transduction and replaced

FSC = forward scatter, SSC = side scatter

with 1 ml fresh R10 with 75 U/ml IL-2 (for a final concentration of 50 U/ml IL-2). The cells were also resuspended at this stage. On day 5 after transduction, the cells were resuspended and the suspension placed in a Dynal MPC-1 magnet (Thermo Fisher, 12001D). After 2 min, the cell suspension was pipetted out leaving the stimulation beads behind. The cells were then counted, pelleted and resuspended in fresh R10 supplemented with 50 U/ml IL-2. At this point, the cells usually started to recover from the viral transduction with viabilities around 70-85 % and absolute numbers back to around 1×10^6 cells. This procedure was repeated every other day and the T cells were always resuspended to 1×10^6 cells ml^{-1}. The suspensions were transferred to 6-well plates when they reached 1×10^6 cells, to T25 flasks when they reached 3×10^6 cells, to T75 flasks when they reached 8×10^6, and to T175 flasks when they reached 30×10^6, keeping the cell density between 1×10^5 and 5×10^5 cells per cm^2.

6.6.5 Measuring Receptor Expression

The TCR or CAR expression of expanded and transduced primary T cells was confirmed by flow cytometry between day 5 and day 7 after transduction. We routinely observed expression levels greater than 50 %, but we also noted a negative correlation between higher expression levels and the growth of the cells, suggesting that higher viral titers achieved better transduction efficiency, but also inhibited the expansion of the T cell culture. An example growth curve comparing untransduced cells to cells transduced with 1 ml or 2 ml of supernatant containing $1G4^{Hi}$ lentiviral particles, and to cells transduced with the D53N first generation CAR is shown in Figure 6.2. It shows that untransduced cells have expanded 483-fold by day 11, while the transduced cells have expanded 127-fold, 26-fold, and 10-fold correlating negatively with their receptor expression level of 55 %, 75 %, and 85 %, respectively.

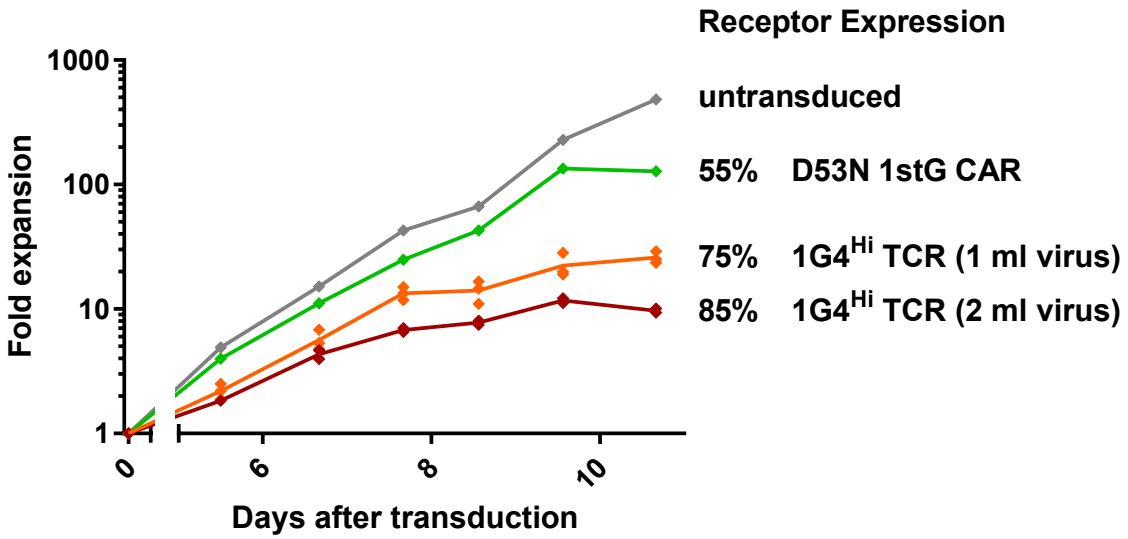


Fig. 6.2: Growth curve of transduced CD8$^+$ T cells shows that higher receptor expression levels correlate with reduced expansion. Human CD8$^+$ T cells isolated from peripheral blood were stimulated with anti-CD3/anti-CD28 beads and transduced with 1 ml or 2 ml of supernatant containing 1G4^{Hi} TCR lentiviral particles, or with the D53N first generation CAR. Cell numbers were monitored from day 5 to day 11 after transduction. Cells were stained with pMHC tetramers and receptor expression was measured by flow cytometry on day 6. The 1 ml or 2 ml curves represent the arithmetic mean of three and two replicates, respectively.

6.7 HEK293T Transfection

6.7.1 Polyethylenimine Transfection

PEI was used for transient transfection of HEK293T cells for CD166 protein production. CD166 pHL-sec constructs were kindly provided by Marion H. Brown (Sir William Dunn School of Pathology, University of Oxford, UK). As with the CHO cells, the ligands were expressed as the full-length extracellular domains with a BirA biotinylation site and a 6 His-tag for purification.

9×10^6 cells were seeded into each of 10 T175 flasks a day before the transfection. The medium was changed to 15 ml plain DMEM 2 h before the transfection. PEI was diluted in 1 ml plain DMEM at a concentration of 112 µg ml^{-1} per flask. The expression plasmid was diluted in 1 ml plain DMEM at a concentration of 56 µg ml^{-1} per flask. Both solutions were then mixed and incubated at room temperature for 30 min before 2 ml were added dropwise to each flask. The medium was replaced with D10 or D5 after 4-5 h. Supernatant was harvested after 2 days and the medium replaced with fresh D10 or D5 for another 2 days. Supernatants were stored at -20 °C.

6.7.2 X-tremeGENE™ HP Transfection for Lentivirus Production

6×10^5 HEK293T cells were seeded into one well of a 6-well plate in 3 ml D10 on the day before transfection. 9 µl X-tremeGENE™ HP transfection reagent were pipetted directly into 91 µl plain DMEM. 0.8 µg of the expression plasmid were diluted with plain DMEM up to a final volume of 100 µl. The lentiviral packaging plasmids (0.95 µg pRSV, 0.37 µg pVSV-G, 0.95 µg pGAG) were diluted with plain DMEM up to a final volume of 10 µl and then added to the diluted expression vector. The DNA solution was then combined with the diluted X-tremeGENE™ and mixed by pipetting. After a 30 min incubation, 1 ml of medium was removed from the cells, and the transfection mix was added dropwise.

6.8 Lentiviral Transduction

Supernatants from HEK293T cells transfected with plasmids for lentivirus production were harvested 24 h after the transfection. 2 ml supernatant were filtered through a 0.45 µm Minisart® cellulose acetate syringe end filter, supplemented with 50 U/ml IL-2 and added to 1 million primary T cells in 0.5 ml R10 medium 24 h after isolation and stimulation (see section 6.6.3). The cells were then resuspended.

6.9 T Cell Stimulation

6.9.1 Ligand Immobilisation on Streptavidin-coated Plates

T cells were stimulated with titrations of plate-immobilised pMHC ligands with or without co-immobilised ligands for accessory receptors. All ligands were purified and biotinylated as described above. They were thawed at room temperature and diluted to the working concentrations in sterile PBS. 50 µl serially two-fold diluted pMHC were added to each well of 96-well plates pre-coated with streptavidin for a high binding capacity (15500, Thermo Fisher). After a minimum 45 min (up to over night) incubation, the plates were washed once with sterile PBS. Where accessory receptor ligands were used, those were similarly diluted and added to the plate for a second incubation of 45-90 min.

6.9.2 Quantification of Ligand Immobilisation

In order to compare T cell activation by different pMHC ligands (i.e. affinities), we had to ensure equal immobilisation of correctly folded pMHC complexes from the different refolds. We quantified the level of active immobilised pMHC in each well by staining with the conformation-sensitive HLA class I antibody clone W6/32 and a fluorescent goat-anti-mouse IRDye® 680RD secondary antibody (Table 6.4). After pMHC immobilisation, the plate was washed once with PBS. The primary antibody was diluted 1:500 in PBS and 50 µl were added to each well. After a 45 min incubation at room temperature, the plate was washed again and 100 µl of the 1:5000 secondary antibody dilution were added and incubated in the dark at room temperature for another 45 min. The plate was then washed again, emptied and fluorescence was quantified with the Odyssey® Sa Infrared Imaging System. In experiments comparing multiple different pMHC ligands, a Hill function was fitted to each pMHC's fluorescence over the pMHC concentration in ng ml^{-1} in Prism. The pMHC concentrations of the corresponding T cell dose response datasets were adjusted to account for differences in pMHC immobilisation between the different refolds (corresponding to different affinities) as follows:

$$log([pMHC])^{corrected} = log([pMHC]) + log(EC_{50}^{highest\ affinity}) - log(EC_{50})$$

The same assay was employed to quantify pMHC levels with and without the subsequent addition of different accessory receptor ligands.

Alternatively, the detection could also be performed after removal of the T cells from a stimulation assay. The stimulation plate was then treated as described above. Figure 6.3 shows that the amount of pMHC detected on the plate after an 8 h T cell stimulation in R10 medium at 37 °C is equal to that detected on a plate prepared in parallel but incubated in PBS at 4 °C.

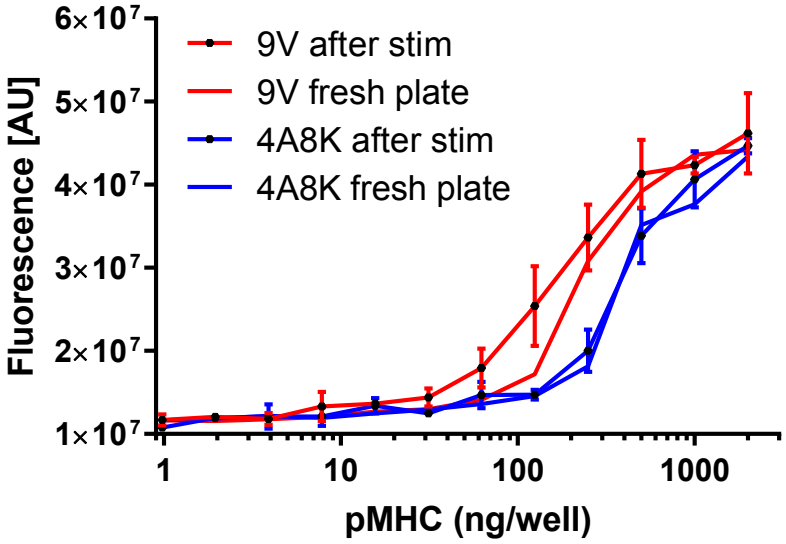


Fig. 6.3: Detection of pMHC on plates after T cell stimulation. Immobilised levels of correctly folded pMHC were measured on a plate stored at 4 °C in PBS (fresh plate) and compared to levels on a plate after T cell stimulation at 37 °C. Both plates were prepared in parallel from the same serial dilutions of pMHCs. There were three replicates of each pMHC titration (9V or 4A8K) immobilised on the stimulation plate. The curve represents the arithmetic mean, error bars show the standard deviation.

6.9.3 T Cell Incubation with Small Molecule Inhibitors

In experiments with small molecule inhibitors, the T cells were always incubated with the inhibitor at 37 °C for 20-30 min prior to the start of the stimulation. The inhibitors were left in the medium for the whole duration of the stimulation. All control conditions were incubated with DMSO at a 1:1000 dilution so that the DMSO concentration was the same for inhibitor and non-inhibitor samples. The Lck inhibitor A-770041 (Stachlewitz et al., 2005) was titrated from 1 nM to 1000 nM (Figure 6.4) and a concentration of 300-500 nM was subsequently used for experiments that required full inhibition of $CD8^+$ T cell activation. PP2 was used at a 20 µM concentration based on the literature (Campi et al., 2005).

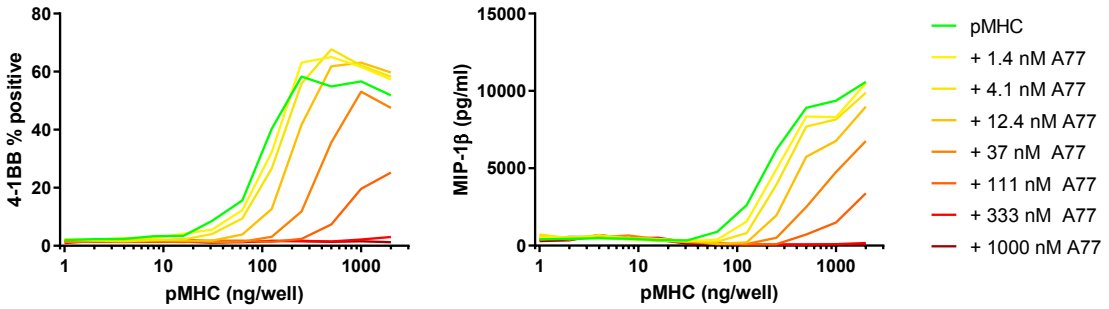


Fig. 6.4: Titration of Lck inhibitor A-770041. Primary human $CD8^+$ T cells carrying the $1G4^{Hi}$ TCR were stimulated for 24 h with plate-immobilised pMHC (variant 5Y) and activation was measured by flow cytometry (upregulation of 4-1BB) and ELISA (production of MIP-1β). Cells were incubated with the indicated concentration of A-770041 20 min prior to and during the stimulation.

6.9.4 T Cell Stimulation

T cells were stimulated on plates with dose titrations of pMHC ligands of various affinities in the presence or absence of ligands for accessory receptors and small molecule inhibitors. The preparation of the plates is described in section 6.9.1. After washing the plate with PBS, T cells were counted, pelleted and resuspended in fresh warm R10 (without IL-2) at a concentration of 3.75×10^5 cells per ml. 200 µl were added to each well for a final number of 7.5×10^4 T cells for each stimulation condition. The plates were spun at 9 x g for 2 min to settle down the cells and then incubated at 37 °C with 5 % CO_2.

6.9.5 Transfer Experiments

Transfer experiments are T cell stimulation experiments that involved stimulation in two phases. After stimulation under one set of conditions (for example a specific pMHC ligand with and without an Lck inhibitor), the T cells were pipetted into a V-bottom plate and pelleted. The supernatant was stored at -20 °C for later cytokine ELISAs, the cells were resuspended in 200 µl fresh R10 medium and – depending on the experiment – either rested for some time or transferred to another stimulation plate with a new set of conditions (for example the same pMHC ligand versus a higher affinity). The cells were then again settled down by centrifuging at 9 x g and incubated. The first stimulation phase was mostly 4 or 8 h, the second phase 16 h.

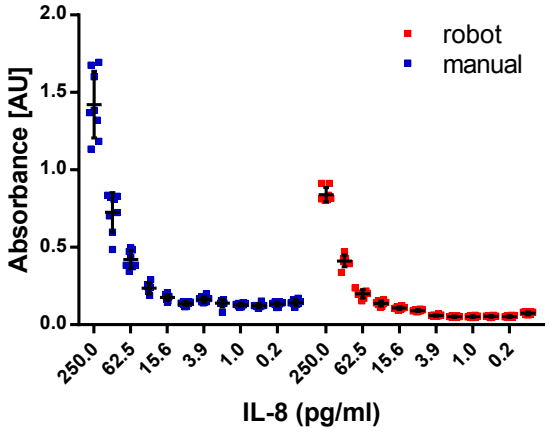
6.9.6 Flow Cytometry

Flow cytometry was used for HLA-typing, to assess receptor expression after TCR and CAR transductions, and to quantify T cell activation and receptor downregulation at the end of stimulation experiments. In order to measure receptor expression, 1×10^5 cells were taken from culture, pelleted and resuspended in 40 µl staining buffer with PE-conjugated 9V pMHC tetramers at a previously determined dilution (ranging from 1:50 to 1:500 for different batches of tetramers). The staining was incubated for 20-60 min after which the cells were pelleted, resuspended in 100 µl PBS and analysed on a Cytek or FACSCalibur™ (BD) flow cytometer.

After stimulation, the 7.5×10^4 cells from each well were transferred to a V-bottom plate and pelleted. The cells were then stained as described above with PE-conjugated 9V pMHC tetramers and the following antibodies at a 1:250 dilution: 4-1BB-Alexa Fluor® 647, CD69-PerCP, PD-1-Alexa Fluor® 488. They were then resuspended in 70 µl PBS and analysed on the FACSCalibur™ making use of the High Troughput Sampler for automated sample acquisition (BD Biosciences). Flow cytometry data was analysed with Flowjo V10.0.

6.9.7 ELISA

When the cells were pelleted and stained for flow cytometry after a stimulation assay, the supernatant was transferred to another plate and stored at -20 °C. The cytokine concentrations in those supernatants were measured by ELISAs (see Table 6.4) according to the manufacturer's instructions in Nunc MaxiSorp™ flat-bottom plates (Invitrogen, 44-2404-21). Antibodies and horseradish peroxidase were added by a Janus 8-tip liquid handling robot (Perkin Elmer). The precision of the robot was assessed in different assay formats and was found to be consistently equal to or superior to manual pipetting. Figure 6.5 shows such a comparison for a serial dilution of IL-8 ELISA standard where the coefficient of variation is lower for the robot at almost all concentrations. Plates were washed on a ELx405 plate washer (BioTek). Absorbance was measured with a SpectraMax Gemini plate reader (Molecular Devices) and cytokine concentrations were calculated according to a standard curve (in duplicates) on each plate.



Coefficient of variation

IL8 (pg/ml)	250	125	62.5	31.2	15.6	7.8	3.9	2	1	0.5	0.2	0.1
robot	5.47%	9.08%	13.05%	12.06%	7.84%	6.45%	9.29%	8.09%	10.40%	9.12%	10.81%	12.51%
manual	15.15%	17.56%	13.63%	15.27%	11.34%	9.13%	12.64%	17.67%	8.48%	10.78%	10.45%	12.61%

Fig. 6.5: Comparison of manual pipetting to liquid handling robot. A stock solution of 250 pg/ml IL-8 was prepared according to the manufacturer's instructions. This was diluted in two-fold serial dilutions and added to antibody-coated ELISA plates by manual pipetting or with the Janus 8-tip liquid handling robot. Plate preparation and all subsequent ELISA steps were carried out by the robot. The coefficient of variation was calculated as follows: $CV = \sigma / \mu * 100\%$.

6.10 Analysis

6.10.1 Data fitting

We used the data fitting function *inhibitor dose response curve with variable slope* in Prism for all TCR, CAR and CD2 downregulation curves. In some cases that are indicated in the text or figure legends, we constrained the fit by assuming that all curves start at the same value, i.e. T cells in all conditions start the experiment expressing the same average number of receptors. The pMHC immobilisation curves were fitted using the *activator dose response curve* and the resulting EC_{50} values were used to correct functional data for the amount of pMHC immobilised (see section 6.9.2).

Fitting the dose response curves of cytokine production proved problematic with standard algorithms, because they showed a more or less pronounced bell shape, i.e. an optimum at intermediate doses and a clear downward trend at the higher doses. In order to be able to extract EC_{50}, Hill coefficient and E_{Max} values from such dose response curves,

a custom Matlab data-fitting algorithm was used. This algorithm was initially developed by John Nguyen and Omer Dushek and modified for the purposes of this project by the author. It uses the Matlab function *lsqcurvefit* to optimise the parameters for the fitting function which is the difference between two Hill curves:

$$y = background + \left(\alpha_1 * 1/(1+\beta_1/x)^{\gamma_1})\right) - \left(\alpha_1 * \alpha_2 * 1/(1+\beta_2/x)^{\gamma_2})\right)$$

In a few cases, individual outlier values were excluded from the data before fitting, but they are still shown as dots in the respective figures.

6.10.2 Data Normalisation

In order to be able to average data from different donors that showed differences, for example, in the transduction efficiency of the TCR or in the absolute amount of cytokines produced, we fitted curves to the dose response data as described above and extracted IC_{50}/EC_{50}, E_{max} and Hill coefficient from each curve. The resulting values were still absolute values that reflected the variability between donors, so we normalised each value to the mean of the data from that donor. This transformation allowed us to dramatically reduce the variability and directly average the data from multiple donors. We applied one further transformation to express the values as a fold-change compared to pMHC alone (in the case of costimulation datasets in chapter 3) or compared to the dose response curve from fresh or unstimulated cells (in the case of transfer experiments). This only re-scales the Y-axis to make the reported values more intuitive.

For receptor expression data, we used the gMFI of the entire population of cells (positive and negative). To account for differences in transduction efficiency, we normalised each dataset by setting the fitted maximum gMFI to 1. This normalises potential differences in expression level between donors. We also subtracted the gMFI of the receptor-negative cell population which set the minimum of the curves to 0. This means we assumed complete downregulation at the highest antigen doses and we based this assumption on the TCR flow cytometry histograms an example of which is shown in Figure 2.2.

6.10.3 Statistical Analysis

The statistical tests used throughout this thesis are listed in Table 6.9. Statistical significance was defined as $\alpha <= 0.05$.

Figure	Statistical Test	Correction method
Figure 2.3	F-test	N/A
Figure 2.7	Two-tailed t-test	N/A
Figure 2.8	Two-tailed t-test	N/A
Figure 3.16	Two-way ANOVA	Dunnett
Figure 4.4	F-test	N/A
Figure 4.5	One-way ANOVA	Holm-Šidák

Tab. 6.9: Statistical tests. Listed are the statistical tests used in this thesis and the respective correction for multiple comparisons. All statistical testing was performed with Prism.

6.11 Mathematical Modelling

The mathematical model for T cell activation used in this project is the result of a team effort that represents an iterative process of testing different model architectures based on information from the literature and data generated by multiple members of the group. The rationale behind the inclusion of certain motifs and reactions is described in detail in chapter 2. The parameter values (Table 6.10) represent the best-fitting particle determined by an ABC-SMC fitting algorithm developed by Nicola Trendel. Reaction rates in the model are described by mass-action kinetics with the exception of TCR-pMHC binding and the digital activation of the signalling node Y. The model was numerically integrated using the solver *ode23s* in Matlab. The following set of ordinary differential equations describes the model:

$$\frac{dpMHC}{dt} = -k_{on} * (pMHC * TCR)^{nb} + (k_{off} + k_{basal}) * (C_0 + C_{act} + C_{tag} + C_{act+tag}) + k_{int} * (C_{tag} + C_{act+tag})$$

$$\frac{dTCR}{dt} = k_{syn} + k_{off} * (C_0 + C_{act} + C_{tag} + C_{act+tag}) - k_{on} * (pMHC * TCR)^{nb} - k_{basal} * TCR - k_{by} * TCR * (C_{act} + C_{act+tag})$$

$$\frac{dC_0}{dt} = k_{on} * (pMHC * TCR)^{nb} - (k_{off} + k_p + k_t) * C_0 - k_{basal} * C_0$$

$$\frac{dC_{act}}{dt} = k_p * C_0 - (k_{off} + k_t) * C_{act} - k_{basal} * C_{act}$$

$$\frac{dC_{tag}}{dt} = k_t * C_0 - (k_{off} + k_p + k_{int}) * C_{tag} - k_{basal} * C_{tag}$$

$$\frac{dC_{act+tag}}{dt} = k_t * C_{act} + k_p * C_{tag} - (k_{off} + k_{int}) * C_{act+tag} - k_{basal} * C_{act+tag}$$

$$\frac{dY}{dt} = k_{fy} * \frac{(C_{act} + C_{act+tag})^{ny}}{sy^{ny} + (C_{act} + C_{act+tag})^{ny}} * (1 - Y) - k_{ry} * Y$$

$$\frac{dZ}{dt} = k_{act} * Y$$

Parameter / Species	**Description**	**Initial Conditions**
pMHC	free pMHC	variable input signal
TCR	free TCR	100 molecules μm^{-2}
C_0	TCR-pMHC complex	0
C_{act}	activated TCR-pMHC complex	0
C_{tag}	TCR-pMHC complex tagged for downregulation	0
$C_{act+tag}$	activated and tagged TCR-pMHC complex	0
Y	signalling node activated digitally	0
Cyt	cumulative cytokine	0
k_{basal}	basal TCR downregulation rate	3.1178×10^{-6} molecules s^{-1}
k_{syn}	TCR de novo synthesis rate	3.1178×10^{-4} molecules μm^{-2}
k_{on}	TCR-pMHC binding on-rate	3.2020×10^{-4} μm^2 / molecules s^{-1}
k_{off}	TCR-pMHC binding off-rate	139.9238 s^{-1}
nb	TCR-pMHC binding cooperativity	2.9294
k_{int}	TCR internalisation rate	0.1090
k_{by}	bystander TCR internalisation rate	0.0027
k_p	kinetic proofreading rate	835.3769
k_t	tagging rate	25.0469
k_{fy}	activation rate of Y	181.4416
k_{ry}	inactivation rate of Y	263.3882
ny	steepness of Y activation	1.6748
sy	threshold of Y activation	0.0285
k_{act}	cytokine production rate	2.7464×10^{-4}

Tab. 6.10: Mathematical model species and parameters. Listed are the species or nodes that make up the model and the parameters that determine their interactions.

Appendix

List of Abbreviations

$1G4^{Hi}$	affinity-matured 1G4 TCR (c58/c61)
ABC-SMC	Approximate Bayesian Computation - Sequential Monte Carlo
ANOVA	Analysis of variance
AP	Activator protein
APC	Antigen-presenting cell
APC	Allophycocyanin
ATCC	American Type Culture Collection
BTLA	B and T lymphocyte attenuator
CAR	Chimeric antigen receptor
CCL	CC chemokine ligand
CD	Cluster of differentiation
CDR	Complementarity-determining region
CHO	Chinese hamster ovary
CIN85	Cbl-interacting protein of 85 kDa
CMS	Cas ligand with multiple Src homology 3 domains
Csk	C-terminal Src kinase
cSMAC	Central supermolecular activation cluster
CTLA	Cytotoxic T lymphocyte-associated protein
DH5α	Douglas Hanahan 5α
DMEM	Dulbecco's modified Eagle's medium
DMSO	Dimethyl Sulfoxide
DNA	Desoxyribonucleic acid
dNTPs	Desoxynucleoside triphosphate
EC_{50}	Half-maximal effective concentration
EDTA	Ethylenediaminetetraacetic acid
e.g.	exempli gratia (for example)
EIF	Eukaryotic initiation factor

ELISA	Enzyme-linked immunosorbent assay
ERK	Extracellular-signal regulated kinase
Fas	First apoptosis signal
FBS	Fetal bovine serum
FDA	Food and Drug Administration
FITC	Fluorescein isothiocyanate
FPLC	Fast protein liquid chromatography
FoxP3	Forkhead box P3
GM-CSF	Granulocyte-macrophage colony-stimulating factor
gMFI	Geometric mean fluorescence intensity
Grb2	Growth factor receptor-bound protein 2
GSEM	Glutamine synthetase expression medium
HBS	Hepes-buffered saline
HEK293T cells	Human embryonic kidney 293 cells expressing the simian virus 40 large T antigen
HLA	Human leukocyte antigen
IC_{50}	Half-maximal inhibitory concentration
ICAM-1	Intercellular adhesion molecule 1
ICOS	Inducible T cell costimulator
i.e.	id est (that is)
IFN	Interferon
IgG	Immunoglobulin G
IL	Interleukin
ImmTAC	Immune mobilising monoclonal T cell receptors against cancer
ITAM	Immunoreceptor tyrosine-based activation motif
ITK	Interleukin-2-inducible T-cell kinase
K_D	Dissociation constant
LAT	Linker for activation of T cells
LB medium	Lysogeny broth

LFA-1	Lymphocyte function-associated antigen
Lck	Lymphocyte-specific protein tyrosine kinase
MAGE	Melanoma-associated antigen
MAPK	Mitogen-activated protein kinase
MIP	Macrophage inflammatory protein
mRNA	Messenger ribonucleic acid
NFAT	Nuclear factor of activated T cells
NFκB	Nuclear factor kappa-light-chain enhancer of activated B cells
NK cell	Natural killer cell
NTA	Nitrilotriacetic acid
NY-ESO	New York esophageal squamous cell carcinoma
PAMP	Pathogen-associated Molecular Pattern
PBS	Phosphate-buffered saline
PCR	Polymerase chain reaction
PD-1	Programmed cell death protein 1
PE	Phycoerythrin
PEI	Polyethylenimine
PerCP	Peridinin-chlorophyll-protein
PI3K	Phosphoinositide 3-kinase
PKC	Protein kinase C
PLC	Phospholipase C
PMA	Phorbol-12-myristate-13-acetate
pMHC	Peptide major histocompatibility complex
PMSF	Phenylmethanesulfonyl fluoride
PP2	Pyrazolopyrimidine 2
PRR	Pattern Recognition Receptor
pSMAC	Peripheral supermolecular activation cluster
RANTES	Regulated on activation, normal T cell expressed and secreted

RPMI	Roswell Park Memorial Institute
scFv	Single-chain variable fragment of an antibody
SH	Src homology region
SHP-1	Src homology region 2 domain-containing phosphatase 1
SLAM	Signaling lymphocytic activation molecule
SLP76	SH2 domain-containing leukocyte protein of 76 KDa
SOC medium	Super optimal broth with catabolite repression
SYK	Spleen tyrosine kinase
TAE	Tris, Acetic acid, EDTA
TBS	Tris-buffered saline
TCR	T cell receptor
TILs	Tumour-infiltrating lymphocytes
TLR	Toll-lie Receptor
TMD	Transmembrane domain
TNF	Tumour necrosis factor
WASp	Wiskott-Aldrich Syndrome protein
ZAP70	Zeta chain-associated protein of 70 kDa

List of Figures

2.1 Schematic of TCR downregulation pathways 25
2.2 T cell adaptation and TCR downregulation kinetics 30
2.3 Lck inhibition affects TCR downregulation 33
2.4 TCR downregulation model schematic 35
2.5 Mathematical model reproduces TCR downregulation dynamics 36
2.6 Mathematical model reproduces cytokine production dynamics 38
2.7 T cells desensitised to a low-affinity antigen can be re-activated with a high-affinity ligand 40
2.8 Re-activation of adapted T cells with CD28 costimulation 43
2.9 Modelling population heterogeneity 48
2.10 Comparison of incoherent feed-forward model architecture with TCR downregulation model 50

3.1 TCR downregulation model schematic 61
3.2 Simulation of modulating effects on downstream signalling parameters . 63
3.3 Simulation of modulating effects on TCR-pMHC binding parameters . . . 65
3.4 Simulation of modulating effects on TCR downregulation rates 67
3.5 Expression of costimulatory receptors on primary human $CD8^+$ T cells . 68
3.6 Quantitative effects of CD28 costimulation on TCR downregulation 70
3.7 Quantitative effects of CD28 costimulation on cytokine production 72
3.8 Effect of CD28 costimulation on activation markers on the T cell surface 74
3.9 Comparison of simulations with metrics extracted from CD28 data 76
3.10 Quantitative effects of CD2 costimulation on TCR downregulation 78
3.11 Quantitative effects of CD2 costimulation on cytokine production 80
3.12 Comparison of simulations with metrics extracted from CD2 data 83
3.13 CD2 and CD28 downregulation upon ligand engagement 85
3.14 Quantitative effects of CD6 costimulation 87
3.15 Modelling of accessory ligand effects on effective pMHC concentration . 89
3.16 Effect of CD86 immobilisation on pMHC detection 91

4.1 Schematic overview of CAR design 101
4.2 Schematic of CAR contructs used in this project 106
4.3 $CD8^+$and $CD4^+$CAR T cell stimulation with different plate-bound pMHC mutants 108
4.4 CAR signalling affects CAR downregulation 111
4.5 CAR T cells get desensitised by antigen 113
4.6 Expression of first- and second-generation CARs 114
4.7 Desensitised CAR T cells can be re-activated by costimulation 115

6.1 Flow cytometry results for HLA-A2 staining 148
6.2 Growth curve of transduced $CD8^+$ T cells 150
6.3 Detection of pMHC on plates after T cell stimulation 153
6.4 Titration of Lck inhibitor A-770041 154
6.5 Liquid handling robot performance 156

List of Tables

0.1 Contributions from other lab members to figures in this thesis III

6.1 Suppliers and Brands 129
6.2 General Reagents 131
6.3 Buffer Compositions 133
6.4 Antibodies 135
6.5 Cell Culture Reagents and Media 137
6.6 PCR Composition and Reaction Conditions 138
6.7 DNA primers for In-Fusion® cloning and their sequences 140
6.8 NY-ESO-1 Peptides and Their Sequences 143
6.9 Statistical tests 158
6.10 Mathematical model species and parameters 160

References

Ahmed, N., Brawley, V. S., Hegde, M., Robertson, C., Ghazi, A., Gerken, C., Liu, E., Dakhova, O., Ashoori, A., Corder, A., Gray, T., Wu, M.-F., Liu, H., Hicks, J., Rainusso, N., Dotti, G., Mei, Z., Grilley, B., Gee, A., Rooney, C. M., Brenner, M. K., Heslop, H. E., Wels, W. S., Wang, L. L., Anderson, P., and Gottschalk, S. (2015). Human Epidermal Growth Factor Receptor 2 (HER2) –Specific Chimeric Antigen Receptor–Modified T Cells for the Immunotherapy of HER2-Positive Sarcoma. *J. Clin. Oncol.*

Ahrends, T., Spanjaard, A., Pilzecker, B., Bąbała, N., Bovens, A., Xiao, Y., Jacobs, H., and Borst, J. (2017). CD4+T Cell Help Confers a Cytotoxic T Cell Effector Program Including Coinhibitory Receptor Downregulation and Increased Tissue Invasiveness. *Immunity*, 47(5):848—-861.e5.

Alberola-Ila, J., Places, L., de la Calle, O., Romero, M., Yagüe, J., Gallart, T., Vives, J., and Lozano, F. (1991). Stimulation through the TCR/CD3 complex up-regulates the CD2 surface expression on human T lymphocytes. *J. Immunol.*

Alcover, A., Alar, B., and Bartolo, V. D. (2018). Cell Biology of T Cell Receptor Expression and Regulation. *Annu. Rev. Immunol*, 36(December 2017):85–107.

Alcover, A., Alberini, C., Acuto, O., Clayton, L., Transy, C., Spagnoli, G., Moingeon, P., Lopez, P., and Reinherz, E. (1988). Interdependence of CD3-Ti and CD2 activation pathways in human T lymphocytes. *EMBO J.*

Aleksic, M., Liddy, N., Molloy, P. E., Pumphrey, N., Vuidepot, A., Chang, K. M., and Jakobsen, B. K. (2012). Different affinity windows for virus and cancer-specific T-cell receptors: Implications for therapeutic strategies. *Eur. J. Immunol.*, 42(12):3174–3179.

Allie, N., Grivennikov, S. I., Keeton, R., Hsu, N.-J., Bourigault, M.-L., Court, N., Fremond, C., Yeremeev, V., Shebzukhov, Y., Ryffel, B., Nedospasov, S. A., Quesniaux, V. F. J.,

and Jacobs, M. (2013). Prominent role for T cell-derived Tumour Necrosis Factor for sustained control of Mycobacterium tuberculosis infection. *Sci. Rep.*, 3:1809.

Altan-Bonnet, G. and Germain, R. N. (2005). Modeling T Cell Antigen Discrimination Based on Feedback Control of Digital Erk Responses. *PLoS Biol*, 3(11):e356.

Apostolou, I. and von Boehmer, H. (2004). In Vivo Instruction of Suppressor Commitment in Naive T Cells. *J. Exp. Med.*, 199(10):1401 LP – 1408.

Arcangeli, S., Rotiroti, M. C., Bardelli, M., Simonelli, L., Magnani, C. F., Biondi, A., Biagi, E., Tettamanti, S., and Varani, L. (2017). Balance of Anti-CD123 Chimeric Antigen Receptor Binding Affinity and Density for the Targeting of Acute Myeloid Leukemia. *Mol. Ther.*, 25(8):1933–1945.

Artyomov, M. N., Lis, M., Devadas, S., Davis, M. M., and Chakraborty, A. K. (2010). CD4 and CD8 Binding to MHC Molecules Primarily Acts to Enhance Lck Delivery. *Proc. Natl. Acad. Sci.*, 107(39):16916–16921.

Avanzi, M. P., Yeku, O., Li, X., Wijewarnasuriya, D. P., van Leeuwen, D. G., Cheung, K., Park, H., Purdon, T. J., Daniyan, A. F., Spitzer, M. H., and Brentjens, R. J. (2018). Engineered Tumor-Targeted T Cells Mediate Enhanced Anti-Tumor Efficacy Both Directly and through Activation of the Endogenous Immune System. *Cell Rep.*

Azzam, H. S., DeJarnette, J. B., Huang, K., Emmons, R., Park, C.-S., Sommers, C. L., El-Khoury, D., Shores, E. W., and Love, P. E. (2001). Fine Tuning of TCR Signaling by CD5. *J. Immunol.*

Bacchetta, R., Barzaghi, F., and Roncarolo, M.-G. (2016). From IPEX syndrome to FOXP3 mutation: a lesson on immune dysregulation. *Ann. N. Y. Acad. Sci.*, 1417(1):5–22.

Bachmaier, K., Krawczyk, C., Kozieradzki, I., Kong, Y. Y., Sasaki, T., Oliveira-Dos-Santos, A., Mariathasan, S., Bouchard, D., Wakeham, A., Itie, A., Le, J., Ohashi, P. S., Sarosi, I., Nishina, H., Lipkowitz, S., and Penninger, J. M. (2000). Negative regulation of lymphocyte activation and autoimmunity by the molecular adaptor Cbl-b. *Nature*.

Bachmann, M. F., Barner, M., and Kopf, M. (1999). CD2 sets quantitative thresholds in T cell activation. *J. Exp. Med.*, 190(10):1383–1392.

Bachmann, M. F., Mckall-faienza, K., Schmits, R., Bouchard, D., Beach, J., Speiser, D. E., Mak, T. W., and Ohashi, P. S. (1997a). Distinct Roles for LFA-1 and CD28 during Activation of Naive T Cells : Adhesion versus Costimulation. *Immunity*, 7:549–557.

Bachmann, M. F., Oxenius, A., Speiser, D. E., Mariathasan, S., Hengartner, H., Zinkernagel, R. M., and Ohashi, P. S. (1997b). Peptide-induced T cell receptor down-regulation on naive T cells predicts agonist/partial agonist properties and strictly correlates with T cell activation. *Eur. J. Immunol.*, 27(9):2195–2203.

Bachmann, M. F., Sebzda, E., Kündig, T. M., Shahinian, A., Speiser, D. E., Mak, T. W., and Ohashi, P. S. (1996). T cell responses are governed by avidity and co-stimulatory thresholds. *Eur. J. Immunol.*

Badour, K., McGavin, M. K. H., Zhang, J., Freeman, S., Vieira, C., Filipp, D., Julius, M., Mills, G. B., and Siminovitch, K. A. (2007). Interaction of the Wiskott–Aldrich syndrome protein with sorting nexin 9 is required for CD28 endocytosis and cosignaling in T cells. *Proc. Natl. Acad. Sci. U. S. A.*, 104(5):1593–1598.

Badour, K., Zhang, J., Shi, F., McGavin, M. K. H., Rampersad, V., Hardy, L. A., Field, D., and Siminovitch, K. A. (2003). The Wiskott-Aldrich Syndrome Protein Acts Downstream of CD2 and the CD2AP and PSTPIP1 Adaptors to Promote Formation of the Immunological Synapse. *Immunity*, 18(1):141–154.

Beatty, G. L., O'Hara, M. H., Lacey, S. F., Torigian, D. A., Nazimuddin, F., Chen, F., Kulikovskaya, I. M., Soulen, M. C., McGarvey, M., Nelson, A. M., Gladney, W. L., Levine, B. L., Melenhorst, J. J., Plesa, G., and June, C. H. (2018). Activity of Mesothelin-specific Chimeric Antigen Receptor T cells Against Pancreatic Carcinoma Metastases in a Phase 1 Trial. *Gastroenterology*.

Beddoe, T., Chen, Z., Clements, C. S., Ely, L. K., Bushell, S. R., Vivian, J. P., Kjer-Nielsen, L., Pang, S. S., Dunstone, M. A., Liu, Y. C., Macdonald, W. A., Perugini, M. A., Wilce, M. C. J., Burrows, S. R., Purcell, A. W., Tiganis, T., Bottomley, S. P., McCluskey,

J., and Rossjohn, J. (2009). Antigen Ligation Triggers a Conformational Change within the Constant Domain of the $\alpha\beta$ T Cell Receptor. *Immunity*, 30(6):777–788.

Bell, G. M., Fargnoli, J., Bolen, J. B., Kish, L., and Imboden, J. B. (1996). The SH3 Domain of P56Lck Binds to Proline-Rich Sequences in the Cytoplasmic Domain of CD2. *J Exp Med*, 183(1):169–178.

Berman, D., Korman, A., Peck, R., Feltquate, D., Lonberg, N., and Canetta, R. (2015). The development of immunomodulatory monoclonal antibodies as a new therapeutic modality for cancer: The Bristol-Myers Squibb experience. *Pharmacol. Ther.*, 148:132–153.

Bierer, B. E., Peterson, A., Gorga, J. C., Herrmann, S. H., and Burakoff, S. J. (1988). Synergistic T Cell Activation Via the Physiological Ligands for Cd2 and the T Cell Receptor. *J. Exp. Med.*, 168(3):1145–1156.

Bockenstedt, L. K., Goldsmith, M. a., Dustin, M., Olive, D., Springer, T. a., and Weiss, a. (1988). The CD2 ligand LFA-3 activates T cells but depends on the expression and function of the antigen receptor. *J. Immunol.*

Bohineust, A., Garcia, Z., Beuneu, H., Lemaître, F., and Bousso, P. (2018). Termination of T cell priming relies on a phase of unresponsiveness promoting disengagement from APCs and T cell division. *J. Exp. Med.*

Boise, L. H., Minn, A. J., Noel, P. J., June, C. H., Accavitti, M. A., Lindsten, T., and Thompson, C. B. (1995). CD28 costimulation can promote T cell survival by enhancing the expression of Bcl-xL. *Immunity*, 3(1):87–98.

Bonefeld, C. M., Haks, M., Nielsen, B., von Essen, M., Boding, L., Hansen, A. K., Larsen, J. M., Odum, N., Krimpenfort, P., Kruisbeek, A., Christensen, J. P., Thomsen, A. R., and Geisler, C. (2008). TCR down-regulation controls virus-specific CD8+ T cell responses. *J. Immunol.*

Bonefeld, C. M., Rasmussen, A. B., Lauritsen, J. P. H., von Essen, M., Ødum, N., Andersen, P. S., and Geisler, C. (2003). TCR comodulation of nonengaged TCR takes place by a protein kinase C and CD3 gamma di-leucine-based motif-dependent mechanism. *J. Immunol.*

Boomer, J. S. and Green, J. M. (2010). An Enigmatic Tail of CD28 Signaling. *Cold Spring Harb. Perspect. Biol.*, 2(8).

Brameshuber, M., Kellner, F., Rossboth, B. K., Ta, H., Alge, K., Sevcsik, E., Göhring, J., Axmann, M., Baumgart, F., Gascoigne, N. R. J., Davis, S. J., Stockinger, H., Schütz, G. J., and Huppa, J. B. (2018). Monomeric TCRs drive T cell antigen recognition. *Nat. Immunol.*, 19(May).

Brentjens, R. J., Latouche, J.-B., Santos, E., Marti, F., Gong, M. C., Lyddane, C., King, P. D., Larson, S., Weiss, M., Riviere, I., and Sadelain, M. (2003). Eradication of Systemic B-Cell Tumors by Genetically Targeted Human T Lymphocytes Co-Stimulated by CD80 and Interleukin-15. *Nat Med*, 9(3):279–286.

Brentjens, R. J., Santos, E., Nikhamin, Y., Yeh, R., Matsushita, M., La Perle, K., Quintás-Cardama, A., Larson, S. M., and Sadelain, M. (2007). Genetically Targeted T Cells Eradicate Systemic Acute Lymphoblastic Leukemia Xenografts. *Clin. Cancer Res.*, 13(18):5426–5435.

Bretscher, P. and Cohn, M. (1970). A Theory of Self-Nonself Discrimination. *Science (80-.).*, 169(3950):1042 LP – 1049.

Bridgeman, J. S., Ladell, K., Sheard, V. E., Miners, K., Hawkins, R. E., Price, D. A., and Gilham, D. E. (2014). CD3zeta-Based Chimeric Antigen Receptors Mediate T Cell Activation Via Cis- and Trans-Signalling Mechanisms: Implications for Optimization of Receptor Structure for Adoptive Cell Therapy. *Clin Exp Immunol*, 175(2):258–267.

Bromley, S. K., Iaboni, A., Davis, S. J., Whitty, A., Green, J. M., Shaw, A. S., Weiss, A., and Dustin, M. L. (2001). The immunological synapse and CD28-CD80 interactions. *Nat. Immunol.*, 2(12):1159–1166.

Brown, M. H., Cantrell, D. A., Brattsand, G., Crumpton, M. J., and Gullberg, M. (1989). The CD2 antigen associates with the T-cell antigen receptor CD3 antigen complex on the surface of human T lymphocytes. *Nature*.

Cai, Z., Kishimoto, H., Brunmark, A., Jackson, M. R., Peterson, P. A., and Sprent, J. (1997). Requirements for Peptide-Induced T Cell Receptor Downregulation on Naive CD8 T Cells. *J. Exp. Med.*, 185(4):641–652.

Call, M. E., Pyrdol, J., and Wucherpfennig, K. W. (2004). Stoichiometry of the T-cell receptor–CD3 complex and key intermediates assembled in the endoplasmic reticulum. *EMBO J.*, 23(12):2348–2357.

Campi, G., Varma, R., and Dustin, M. L. (2005). Actin and agonist MHC-peptide complex-dependent T cell receptor microclusters as scaffolds for signaling. *J. Cell Biol.*, 171(2):1031–1036.

Carmo, A. M., Mason, D. W., and Beyers, A. D. (1993). Physical association of the cytoplasmic domain of CD2 with the tyrosine kinases p56lck and p59fyn. *Eur. J. Immunol.*

Carpenito, C., Milone, M. C., Hassan, R., Simonet, J. C., Lakhal, M., Suhoski, M. M., Varela-Rohena, A., Haines, K. M., Heitjan, D. F., Albelda, S. M., Carroll, R. G., Riley, J. L., Pastan, I., and June, C. H. (2009). Control of Large, Established Tumor Xenografts with Genetically Retargeted Human T Cells Containing Cd28 and Cd137 Domains. *Proc. Natl. Acad. Sci.*, 106(9):3360–3365.

Caruso, H. G., Hurton, L. V., Najjar, A., Rushworth, D., Ang, S., Olivares, S., Mi, T., Switzer, K., Singh, H., Huls, H., Lee, D. A., Heimberger, A. B., Champlin, R. E., and Cooper, L. J. (2015). Tuning sensitivity of CAR to EGFR density limits recognition of normal tissue while maintaining potent antitumor activity. *Cancer Res.*, 75(17):3505–3518.

Cefai, D., Schneider, H., Matangkasombut, O., Kang, H., Brody, J., and Rudd, C. E. (1998). CD28 Receptor Endocytosis Is Targeted by Mutations That Disrupt Phosphatidylinositol 3-Kinase Binding and Costimulation. *J. Immunol.*, 160(5):2223 LP – 2230.

Chan, A. C., Iwashima, M., Turck, C. W., and Weiss, A. (1992). ZAP-70: A 70 kd protein-tyrosine kinase that associates with the TCR zeta chain. *Cell*, 71(4):649–662.

Chang, H.-C., Moingeon, P., Lopez, P., Krasnow, H., Stebbins, C., and Reinherz, E. L. (1989). Dissection of the human CD2 intracellular domain. Identification of a segment required for signal transduction and interleukin 2 production. *J. Exp. Med.*

Chang, V. T., Fernandes, R. A., Ganzinger, K. A., Lee, S. F., Siebold, C., McColl, J., Jönsson, P., Palayret, M., Harlos, K., Coles, C. H., Jones, E. Y., Lui, Y., Huang, E.,

Gilbert, R. J. C., Klenerman, D., Aricescu, A. R., and Davis, S. J. (2016). Initiation of T cell signaling by CD45 segregation at 'close contacts'. *Nat. Immunol.*, 17(5):574–582.

Chen, J.-L., Stewart-Jones, G., Bossi, G., Lissin, N. M., Wooldridge, L., Choi, E. M. L., Held, G., Dunbar, P. R., Esnouf, R. M., Sami, M., Boulter, J. M., Rizkallah, P., Renner, C., Sewell, A., Van der Merwe, P. A., Jakobsen, B. K., Griffiths, G., Jones, E. Y., and Cerundolo, V. (2005). Structural and Kinetic Basis for Heightened Immunogenicity of T Cell Vaccines. *J. Exp. Med.*, 201(8):1243–1255.

Chen, J.-L. L., Dunbar, P. R., Gileadi, U., Jäger, E., Gnjatic, S., Nagata, Y., Stockert, E., Panicali, D. L., Chen, Y.-T. T., Knuth, A., Old, L. J., Cerundolo, V., Jager, E., Gnjatic, S., Nagata, Y., Stockert, E., Panicali, D. L., Chen, Y.-T. T., Knuth, A., Old, L. J., Cerundolo, V., Jäger, E., Gnjatic, S., Nagata, Y., Stockert, E., Panicali, D. L., Chen, Y.-T. T., Knuth, A., Old, L. J., and Cerundolo, V. (2000). Identification of NY-ESO-1 peptide analogues capable of improved stimulation of tumor-reactive CTL. *J. Immunol.*, 165(2):948–955.

Chen, L. and Flies, D. B. (2013). Molecular Mechanisms of T Cell Co-Stimulation and Co-Inhibition. *Nat Rev Immunol*, 13(4):227–242.

Chen, Y.-T., Scanlan, M. J., Sahin, U., Türeci, Ö., Gure, A. O., Tsang, S., Williamson, B., Stockert, E., Pfreundschuh, M., and Old, L. J. (1997). A testicular antigen aberrantly expressed in human cancers detected by autologous antibody screening. *Proc. Natl. Acad. Sci.*, 94(5):1914 LP – 1918.

Chiodetti, L., Choi, S., Barber, D. L., and Schwartz, R. H. (2006). Adaptive Tolerance and Clonal Anergy Are Distinct Biochemical States. *J. Immunol.*, 176(4):2279–2291.

Chmielewski, M. and Abken, H. (2017). CAR T Cells Releasing IL-18 Convert to T-Bet high FoxO1 low Effectors that Exhibit Augmented Activity against Advanced Solid Tumors. *Cell Rep.*

Chmielewski, M., Hombach, A., Heuser, C., Adams, G. P., and Abken, H. (2004). T Cell Activation by Antibody-Like Immunoreceptors: Increase in Affinity of the Single-Chain Fragment Domain above Threshold Does Not Increase T Cell Activation against Antigen-Positive Target Cells but Decreases Selectivity. *J. Immunol.*, 173(12):7647–7653.

Chmielewski, M., Hombach, A. A., and Abken, H. (2011). CD28 Cosignalling Does Not Affect the Activation Threshold in a Chimeric Antigen Receptor-Redirected T-Cell Attack. *Gene Ther*, 18(1):62–72.

Choudhuri, K., Wiseman, D., Brown, M. H., Gould, K., and Van der Merwe, P. A. (2005). T-cell receptor triggering is critically dependent on the dimensions of its peptide-MHC ligand. *Nature*, 436(7050):578–582.

Clarkson, N. G. and Brown, M. H. (2009). INHIBITION AND ACTIVATION BY CD244 DEPENDS ON CD2 AND PLC-γ1. *J. Biol. Chem.*, 284(37):24725–24734.

Collins, A. V., Brodie, D. W., Gilbert, R. J., Iaboni, A., Manso-Sancho, R., Walse, B., Stuart, D. I., Van der Merwe, P. A., and Davis, S. J. (2002). The Interaction Properties of Costimulatory Molecules Revisited. *Immunity*, 17(2):201–210.

Coombs, D., Kalergis, A. M., Nathenson, S. G., Wofsy, C., and Goldstein, B. (2002). Activated TCRs remain marked for internalization after dissociation from pMHC. *Nat. Immunol.*, 3(10):926–931.

Coulie, P. G., Lehmann, F., Lethé, B., Herman, J., Lurquin, C., Andrawiss, M., and Boon, T. (1995). A mutated intron sequence codes for an antigenic peptide recognized by cytolytic T lymphocytes on a human melanoma. *Proc. Natl. Acad. Sci.*, 92(17):7976 LP – 7980.

Courtney, A. H., Lo, W.-L., and Weiss, A. (2018). TCR Signaling: Mechanisms of Initiation and Propagation. *Trends Biochem. Sci.*, 43(2):108–123.

Curran, K. J., Seinstra, B. A., Nikhamin, Y., Yeh, R., Usachenko, Y., Van Leeuwen, D. G., Purdon, T., Pegram, H. J., and Brentjens, R. J. (2015). Enhancing Anti-Tumor Efficacy of Chimeric Antigen Receptor T Cells through Constitutive CD40L Expression. *Mol Ther*.

Danielian, S., Alcover, A., Polissard, L., Stefanescu, M., Acuto, O., Fischer, S., and Fagard, R. (1992). Both T cell receptor (TCR)-CD3 complex and CD2 increase the tyrosine kinase activity of p56Lck. CD2 can mediate TCR-CD3-independent and CD45-dependent activation of p56Lck. *Eur. J. Immunol.*

Das, V., Nal, B., Dujeancourt, A., Thoulouze, M.-I., Galli, T., Roux, P., Dautry-Varsat, A., and Alcover, A. (2004). Activation-induced polarized recycling targets T cell antigen receptors to the immunological synapse; involvement of SNARE complexes. *Immunity*, 20(5):577–588.

Davila, M. L., Riviere, I., Wang, X., Bartido, S., Park, J., Curran, K., Chung, S. S., Stefanski, J., Borquez-Ojeda, O., Olszewska, M., Qu, J., Wasielewska, T., He, Q., Fink, M., Shinglot, H., Youssif, M., Satter, M., Wang, Y., Hosey, J., Quintanilla, H., Halton, E., Bernal, Y., Bouhassira, D. C. G., Arcila, M. E., Gonen, M., Roboz, G. J., Maslak, P., Douer, D., Frattini, M. G., Giralt, S., Sadelain, M., and Brentjens, R. (2014). Efficacy and Toxicity Management of 19-28z CAR T Cell Therapy in B Cell Acute Lymphoblastic Leukemia. *Sci. Transl. Med.*, 6(224):224ra25.

Davis, M. M. and Bjorkman, P. J. (1988). T-cell antigen receptor genes and T-cell recognition. *Nature*, 334:395.

Davis, S. J. and Van Der Merwe, P. A. (1996). The structure and ligand interactions of CD2: implications for T-cell function. *Immunol. Today*, 17(4):177–187.

Davis, S. J. and Van Der Merwe, P. A. (2006). The kinetic-segregation model: TCR triggering and beyond. *Nat. Immunol.*, 7(8):803–809.

De Munter, S., Ingels, J., Goetgeluk, G., Bonte, S., Pille, M., Weening, K., Kerre, T., Abken, H., and Vandekerckhove, B. (2018). Nanobody Based Dual Specific CARs.

Deenick, E. K., Gett, A. V., and Hodgkin, P. D. (2003). Stochastic Model of T Cell Proliferation: A Calculus Revealing IL-2 Regulation of Precursor Frequencies, Cell Cycle Time, and Survival. *J. Immunol.*, 170(10):4963 LP – 4972.

Derbinski, J., Gäbler, J., Brors, B., Tierling, S., Jonnakuty, S., Hergenhahn, M., Peltonen, L., Walter, J., and Kyewski, B. (2005). Promiscuous gene expression in thymic epithelial cells is regulated at multiple levels. *J. Exp. Med.*, 202(1):33 LP – 45.

Dietrich, J. (1997). Molecular characterization of the Di-leucine based internalization motif of the T cell receptor. *Immunol. Lett.*, 56(1-3):58.

Dietrich, J., Hou, X., Wegener, A. M., and Geisler, C. (1994). CD3 gamma contains a phosphoserine-dependent di-leucine motif involved in down-regulation of the T cell receptor. *EMBO J.*

Dietrich, J., Menne, C., Lauritsen, J. P. H., von Essen, M., Rasmussen, A. B., Odum, N., and Geisler, C. (2002). Ligand-Induced TCR Down-Regulation Is Not Dependent on Constitutive TCR Cycling. *J. Immunol.*, 168(11):5434–5440.

D'Oro, U., Vacchio, M. S., Weissman, A. M., and Ashwell, J. D. (1997). Activation of the Lck tyrosine kinase targets cell surface T cell antigen receptors for lysosomal degradation. *Immunity*, 7(5):619–628.

Dorothee, G., Vergnon, I., El Hage, F., Chansac, B. L. M., Ferrand, V., Lecluse, Y., Opolon, P., Chouaib, S., Bismuth, G., and Mami-Chouaib, F. (2005). In Situ Sensory Adaptation of Tumor-Infiltrating T Lymphocytes to Peptide-MHC Levels Elicits Strong Antitumor Reactivity. *J. Immunol.*

Douglass, A. D. and Vale, R. D. (2005). Single-molecule microscopy reveals plasma membrane microdomains created by protein-protein networks that exclude or trap signaling molecules in T cells. *Cell*, 121(6):937–950.

Dushek, O., Aleksic, M., Wheeler, R. J., Zhang, H., Cordoba, S. P., Peng, Y. C., Chen, J. L., Cerundolo, V., Dong, T., Coombs, D., and Others (2011). Antigen potency and maximal efficacy reveal a mechanism of efficient T cell activation. *Sci. Signal.*, 4(176):ra39.

Dustin, M. L., Golan, D. E., Zhu, D. M., Miller, J. M., Meier, W., Davies, E. A., and Van der Merwe, P. A. (1997). Low affinity interaction of human or rat T cell adhesion molecule CD2 with its ligand aligns adhering membranes to achieve high physiological affinity. *J. Biol. Chem.*, 272(49):30889–30898.

Dustin, M. L., Olszowy, M. W., Holdorf, A. D., Li, J., Bromley, S., Desai, N., Widder, P., Rosenberger, F., Van der Merwe, P. A., Allen, P. M., and Shaw, A. S. (1998). A novel adaptor protein orchestrates receptor patterning and cytoskeletal polarity in T-cell contacts. *Cell*, 94(5):667–677.

Dustin, M. L., Sanders, M. E., Shaw, S., and Springer, T. A. (1987). Purified lymphocyte function-associated antigen 3 binds to CD2 and mediates T lymphocyte adhesion. *J. Exp. Med.*

Ehrlich, P. (1909). Ueber Den Jetzigen Stand Der Karzinomforschung. *Ned. Tijdschr. voor Geneeskd.*

Esensten, J. H., Helou, Y. A., Chopra, G., Weiss, A., and Bluestone, J. A. (2016). CD28 Costimulation: From Mechanism to Therapy.

Espagnolle, N., Depoil, D., Zaru, R., Demeur, C., Champagne, E., Guiraud, M., and Valitutti, S. (2007). CD2 and TCR synergize for the activation of phospholipase Cγ1/calcium pathway at the immunological synapse. *Int. Immunol.*

Eyquem, J., Mansilla-Soto, J., Giavridis, T., Van Der Stegen, S. J. C., Hamieh, M., Cunanan, K. M., Odak, A., Gönen, M., and Sadelain, M. (2017). Targeting a CAR to the TRAC locus with CRISPR/Cas9 enhances tumour rejection. *Nature*, 543(7643):113–117.

Faroudi, M., Zaru, R., Paulet, P., Müller, S., and Valitutti, S. (2003). Cutting Edge: T Lymphocyte Activation by Repeated Immunological Synapse Formation and Intermittent Signaling. *J. Immunol.*, 171(3):1128 LP – 1132.

FDA News (2017a). Press Announcements - FDA approval brings first gene therapy to the United States.

FDA News (2017b). Press Announcements - FDA approves CAR-T cell therapy to treat adults with certain types of large B-cell lymphoma.

Ferber, I., Schönrich, G., Schenkel, J., Mellor, A. L., Hämmerling, G. J., and Arnold, B. (1994). Levels of peripheral T cell tolerance induced by different doses of tolerogen. *Science*, 263(February):674–676.

Fernández-Arenas, E., Calleja, E., Martínez-Martín, N., Gharbi, S. I., Navajas, R., García-Medel, N., Penela, P., Alcamí, A., Mayor, F., Albar, J. P., and Alarcõn, B. (2014). β-arrestin-1 mediates the TCR-triggered re-routing of distal receptors to the immunological synapse by a PKC-mediated mechanism. *EMBO J.*

Fielding, A. K., Richards, S. M., Chopra, R., Lazarus, H. M., Litzow, M. R., Buck, G., Durrant, I. J., Luger, S. M., Marks, D. I., Franklin, I. M., McMillan, A. K., Tallman, M. S., Rowe, J. M., and Goldstone, A. H. (2007). Outcome of 609 adults after relapse of acute lymphoblastic leukemia (ALL); an MRC UKALL12/ECOG 2993 study. *Blood*, 109(3):944–950.

Finetti, F., Paccani, S. R., Riparbelli, M. G., Giacomello, E., Perinetti, G., Pazour, G. J., Rosenbaum, J. L., and Baldari, C. T. (2009). Intraflagellar transport is required for polarized recycling of the TCR/ CD3 complex to the immune synapse. *Nat. Cell Biol.*

Finney, H. M., Akbar, A. N., and Lawson, A. D. G. (2004). Activation of Resting Human Primary T Cells with Chimeric Receptors: Costimulation from Cd28, Inducible Costimulator, Cd134, and Cd137 in Series with Signals from the TCR Zeta Chain. *J Immunol*, 172(1):104–113.

Frank, S. J. and Fuchs, S. Y. (2008). Modulation of growth hormone receptor abundance and function: roles for the ubiquitin-proteasome system.

Fraser, J. D., Irving, B. A., Crabtree, G. R., and Weiss, A. (1991). Regulation of interleukin-2 gene enhancer activity by the T cell accessory molecule CD28. *Science (80-.).*

Freund, C., Kühne, R., Yang, H., Park, S., Reinherz, E. L., and Wagner, G. (2002). Dynamic interaction of CD2 with the GYF and the SH3 domain of compartmentalized effector molecules. *EMBO J.*

Frigault, M. J., Lee, J., Basil, M., Carpenito, C., Motohashi, S., Scholler, J., Kawalekar, O. U., Guedan, S., Mcgettigan, S., Posey A., J., Ang, S., Cooper, L. J., Platt, J., Johnson, F. B., Paulos, C. M., Zhao, Y., Kalos, M., Milone, M., and June, C. H. (2015). Identification of Chimeric Antigen Receptors That Mediate Constitutive or Inducible Proliferation of T Cells. *Cancer Immunol Res*.

Galizia, C. G. and Lledo, P.-M. (2013). *Neurosciences - From Molecule to Behavior: A University Textbook*.

Gassmann, M., Amrein, K. E., Flint, N. A., Schraven, B., and Burn, P. (1994). Identification of a signaling complex involving CD2, zeta chain and p59 (fyn) in T lymphocytes. *Eur.J.Immunol.*, 24(1):139–144.

Gett, a. V. and Hodgkin, P. D. (2000). A cellular calculus for signal integration by T cells. *Nat. Immunol.*, 1(3):239–244.

Gewurz, B. E., Gaudet, R., Tortorella, D., Wang, E. W., Ploegh, H. L., and Wiley, D. C. (2001). Antigen presentation subverted: Structure of the human cytomegalovirus protein US2 bound to the class I molecule HLA-A2. *Proc. Natl. Acad. Sci.*

Gomes-Silva, D., Mukherjee, M., Srinivasan, M., Krenciute, G., Dakhova, O., Zheng, Y., Cabral, J. M., Rooney, C. M., Orange, J. S., Brenner, M. K., and Mamonkin, M. (2017). Tonic 4-1BB Costimulation in Chimeric Antigen Receptors Impedes T Cell Survival and Is Vector-Dependent. *Cell Rep.*

Grakoui, A., Bromley, S., Sumen, C., Davis, M., Shaw, A., Allen, P., and Dustin, M. (1999). The Immunological Synapse: A Molecular Machine Controlling T Cell Activation. *Science (80-.).*, 285(5425):221–227.

Green, J. M., Karpitskiy, V., Kimzey, S. L., and Shaw, A. S. (2000). Coordinate Regulation of T Cell Activation by CD2 and CD28. *J. Immunol.*

Grossman, Z. and Paul, W. E. (1992). Adaptive cellular interactions in the immune system: the tunable activation threshold and the significance of subthreshold responses. *Proc. Natl. Acad. Sci. U. S. A.*, 89(21):10365–10369.

Gubin, M. M., Zhang, X., Schuster, H., Caron, E., Ward, J. P., Noguchi, T., Ivanova, Y., Hundal, J., Arthur, C. D., Krebber, W.-J., Mulder, G. E., Toebes, M., Vesely, M. D., Lam, S. S. K., Korman, A. J., Allison, J. P., Freeman, G. J., Sharpe, A. H., Pearce, E. L., Schumacher, T. N., Aebersold, R., Rammensee, H.-G., Melief, C. J. M., Mardis, E. R., Gillanders, W. E., Artyomov, M. N., and Schreiber, R. D. (2014). Checkpoint blockade cancer immunotherapy targets tumour-specific mutant antigens. *Nature*, 515:577.

Hahn, W. C. and Bierer, B. E. (1993). Separable portions of the CD2 cytoplasmic domain involved in signaling and ligand avidity regulation. *J Exp Med*, 178(5):1831–1836.

Hahn, W. C., Rosenstein, Y., Calvo, V., Burakoff, S. J., and Bierer, B. E. (1992). A distinct cytoplasmic domain of CD2 regulates ligand avidity and T-cell responsiveness to antigen. *Proc. Natl. Acad. Sci. U. S. A.*, 89(15):7179–7183.

Han, C., Sim, S. J., Kim, S. H., Singh, R., Hwang, S., Kim, Y. H. I. H. I. H. I., Park, S. H., Kim, K. H., Lee, D. G., Oh, H. S., Lee, S., Kim, Y. H. I. H. I. H. I., Choi, B. K., and Kwon, B. S. (2018). Desensitized Chimeric Antigen Receptor T Cells Selectively Recognize Target Cells with Enhanced Antigen Expression. *Nat Commun*, 9(1):468.

Han, S., Asoyan, A., Rabenstein, H., Nakano, N., and Obst, R. (2010). Role of antigen persistence and dose for CD4+ T-cell exhaustion and recovery. *Proc. Natl. Acad. Sci.*

Harding, F. A., Mcarthur, J. G., Gross, J. A., Raulet, D. H., and Allison, J. P. (1992). CD28-Mediated Signalling Co-Stimulates Murine T Cells and Prevents Induction of Anergy in T-Cell Clones. *Nature*, 356(6370):607–609.

Haso, W., Lee, D. W., Shah, N. N., Stetler-Stevenson, M., Yuan, C. M., Pastan, I. H., Dimitrov, D. S., Morgan, R. A., Fitzgerald, D. J., Barrett, D. M., Wayne, A. S., Mackall, C. L., and Orentas, R. J. (2013). Anti-Cd22–Chimeric Antigen Receptors Targeting B-Cell Precursor Acute Lymphoblastic Leukemia. *Blood*, 121(7):1165–1174.

Hassan, N. J., Barclay, A. N., and Brown, M. H. (2004). Frontline: Optimal T cell activation requires the engagement of CD6 and CD166. *Eur. J. Immunol.*, 34(4):930–940.

Hausmann, J., Pagenstecher, A., Baur, K., Richter, K., Rziha, H.-J., and Staeheli, P. (2005). CD8 T Cells Require Gamma Interferon To Clear Borna Disease Virus from the Brain and Prevent Immune System-Mediated Neuronal Damage. *J. Virol.*, 79(21):13509 LP – 13518.

Hawiger, D., Masilamani, R. F., Bettelli, E., Kuchroo, V. K., and Nussenzweig, M. C. (2004). Immunological unresponsiveness characterized by increased expression of CD5 on peripheral T cells induced by dendritic cells in vivo. *Immunity*.

Heczey, A., Louis, C. U., Savoldo, B., Dakhova, O., Durett, A., Grilley, B., Liu, H., Wu, M. F., Mei, Z., Gee, A., Mehta, B., Zhang, H., Mahmood, N., Tashiro, H., Heslop, H. E., Dotti, G., Rooney, C. M., and Brenner, M. K. (2017). CAR T Cells Administered

in Combination with Lymphodepletion and PD-1 Inhibition to Patients with Neuroblastoma. *Mol. Ther.*, 25(9):2214–2224.

Hegde, M., Mukherjee, M., Grada, Z., Pignata, A., Landi, D., Navai, S. A., Wakefield, A., Fousek, K., Bielamowicz, K., Chow, K. K., Brawley, V. S., Byrd, T. T., Krebs, S., Gottschalk, S., Wels, W. S., Baker, M. L., Dotti, G., Mamonkin, M., Brenner, M. K., Orange, J. S., and Ahmed, N. (2016). Tandem CAR T cells targeting HER2 and IL13Rα2 mitigate tumor antigen escape. *J. Clin. Invest.*

Hernandez, J., Aung, S., Redmond, W. L., and Sherman, L. A. (2001). Phenotypic and Functional Analysis of CD8 T Cells Undergoing Peripheral Deletion in Response to Cross-Presentation of Self-Antigen. *J. Exp. Med.*, 194(6):707 LP – 718.

Hombach, A., Sent, D., Schneider, C., Heuser, C., Koch, D., Pohl, C., Seliger, B., and Abken, H. (2001). T-Cell Activation by Recombinant Receptors: Cd28 Costimulation Is Required for Interleukin 2 Secretion and Receptor-Mediated T-Cell Proliferation but Does Not Affect Receptor-Mediated Target Cell Lysis. *Cancer Res*, 61(5):1976–1982.

Honda, T., Egen, J. G., Lammermann, T., Kastenmuller, W., Torabi-Parizi, P., and Germain, R. N. (2014). Tuning of Antigen Sensitivity by T Cell Receptor-Dependent Negative Feedback Controls T Cell Effector Function in Inflamed Tissues. *Immunity*, 40(2):235–247.

Hou, D., Cenciarelli, C., Jensen, J. P., Nguyen, H. B., and Weissman, A. M. (1994). Activation-dependent ubiquitination of a T cell antigen receptor subunit on multiple intracellular lysines. *J. Biol. Chem.*

Hu, B., Ren, J., Luo, Y., Keith, B., Young, R. M., Scholler, J., Zhao, Y., and June, C. H. (2017). Augmentation of Antitumor Immunity by Human and Mouse CAR T Cells Secreting IL-18. *Cell Rep.*

Huang, J., Brameshuber, M., Zeng, X., Xie, J., jing Li, Q., hsiu Chien, Y., Valitutti, S., Davis, M. M., jing Li, Q., hsiu Chien, Y., Valitutti, S., Davis, M. M., jing Li, Q., hsiu Chien, Y., Valitutti, S., and Davis, M. M. (2013). A Single peptide-major histocompatibility complex ligand triggers digital cytokine secretion in CD4+ T Cells. *Immunity*, 39(5):846–857.

Huber, M. L., Haynes, L., Parker, C., and Iversen, P. (2012). Interdisciplinary Critique of Sipuleucel-T as immunotherapy in castration-resistant prostate cancer.

Hudecek, M., Lupo-Stanghellini, M. T., Kosasih, P. L., Sommermeyer, D., Jensen, M. C., Rader, C., and Riddell, S. R. (2013). Receptor Affinity and Extracellular Domain Modifications Affect Tumor Recognition by Ror1-Specific Chimeric Antigen Receptor T Cells. *Clin Cancer Res*, 19(12):3153–3164.

Hui, E., Cheung, J., Zhu, J., Su, X., Taylor, M. J., Wallweber, H. A., Sasmal, D. K., Huang, J., Kim, J. M., Mellman, I., and Vale, R. D. (2017). T cell costimulatory receptor CD28 is a primary target for PD-1–mediated inhibition. *Science (80-.).*, 355(6332):1428–1433.

Huppa, J. B., Gleimer, M., Sumen, C., and Davis, M. M. (2003). Continuous T cell receptor signaling required for synapse maintenance and full effector potential. *Nat. Immunol.*, 4(8):749–755.

Hurton, L. V., Singh, H., Najjar, A. M., Switzer, K. C., Mi, T., Maiti, S., Olivares, S., Rabinovich, B., Huls, H., Forget, M.-A., Datar, V., Kebriaei, P., Lee, D. A., Champlin, R. E., and Cooper, L. J. N. (2016). Tethered IL-15 augments antitumor activity and promotes a stem-cell memory subset in tumor-specific T cells. *Proc. Natl. Acad. Sci.*

Hutchingst, N. J., Clarkson, N., Chalkley, R., Barclay, A. N., and Brown, M. H. (2003). Linking the T cell surface protein CD2 to the actin-capping protein CAPZ via CMS and CIN85. *J. Biol. Chem.*

Iezzi, G., Karjalainen, K., and Lanzavecchia, A. (1998). The duration of antigenic stimulation determines the fate of naive and effector T cells. *Immunity*, 8(1):89–95.

Iezzi, G., Scotet, E., Scheidegger, D., and Lanzavecchia, A. (1999). The interplay between the duration of TCR and cytokine signaling determines T cell polarization. *Eur. J. Immunol.*

Imai, C., Mihara, K., Andreansky, M., Nicholson, I. C., Pui, C. H., Geiger, T. L., and Campana, D. (2004). Chimeric Receptors with 4-1bb Signaling Capacity Provoke Potent Cytotoxicity against Acute Lymphoblastic Leukemia. *Leukemia*, 18(4):676–684.

Irles, C., Symons, A., Michel, F., Bakker, T. R., Van der Merwe, P. A., and Acuto, O. (2003). CD45 ectodomain controls interaction with GEMs and Lck activity for optimal TCR signaling. *Nat. Immunol.*, 4(2):189–197.

Irvine, D. J., Purbhoo, M. A., Krogsgaard, M., and Davis, M. M. (2002). Direct Observation of Ligand Recognition by T Cells. *Nature*, 419(6909):845–849.

Itoh, M., Takahashi, T., Sakaguchi, N., Kuniyasu, Y., Shimizu, J., Otsuka, F., and Sakaguchi, S. (1999). Thymus and Autoimmunity: Production of CD25⁺CD4⁺ Naturally Anergic and Suppressive T Cells as a Key Function of the Thymus in Maintaining Immunologic Self-Tolerance. *J. Immunol.*, 162(9):5317 LP – 5326.

Itoh, Y., Germain, R., and Itoh, Y; Germain, R. (1997). Single cell analysis reveals regulated hierarchical T cell antigen receptor signaling thresholds and intraclonal heterogeneity. *J. Exp. Med.*, 186(5).

Iwasaki, A. and Medzhitov, R. (2015). Control of adaptive immunity by the innate immune system. *Nat. Immunol.*, 16:343.

Jakka, G., Schuberth, P. C., Thiel, M., Held, G., Stenner, F., Van Den Broek, M., Renner, C., Mischo, A., and Petrausch, U. (2013). Antigen-Specific in Vitro Expansion of Functional Redirected Ny-Eso-1-Specific Human Cd8+ T-Cells in a Cell-Free System. *Anticancer Res*, 33(10):4189–4201.

James, J. R. and Vale, R. D. (2012). Biophysical Mechanism of T-Cell Receptor Triggering in a Reconstituted System. *Nature*, 487(7405):64–69.

James, J. R., White, S. S., Clarke, R. W., Johansen, A. M., Dunne, P. D., Sleep, D. L., Fitzgerald, W. J., Davis, S. J., and Klenerman, D. (2007). Single-molecule level analysis of the subunit composition of the T cell receptor on live T cells. *Proc. Natl. Acad. Sci. U. S. A.*, 104(45):17662–17667.

James, S. E., Greenberg, P. D., Jensen, M. C., Lin, Y., Wang, J., Budde, L. E., Till, B. G., Raubitschek, A. A., Forman, S. J., and Press, O. W. (2010). Mathematical Modeling of Chimeric TCR Triggering Predicts the Magnitude of Target Lysis and Its Impairment by TCR Downmodulation. *J. Immunol.*, 184(8):4284–4294.

Jang, I. K. and Gu, H. (2003). Negative regulation of TCR signaling and T-cell activation by selective protein degradation.

Jenkins, M. R., Rudd-Schmidt, J. A., Lopez, J. A., Ramsbottom, K. M., Mannering, S. I., Andrews, D. M., Voskoboinik, I., and Trapani, J. A. (2015). Failed CTL/NK cell killing and cytokine hypersecretion are directly linked through prolonged synapse time. *J. Exp. Med.*, 212(3):307 LP – 317.

Jensen, M. C., Popplewell, L., Cooper, L. J., Digiusto, D., Kalos, M., Ostberg, J. R., and Forman, S. J. (2010). Antitransgene rejection responses contribute to attenuated persistence of adoptively transferred CD20/CD19-specific chimeric antigen receptor redirected T cells in humans. *Biol. Blood Marrow Transplant.*, 16(9):1245–1256.

Jeon, M.-S., Atfield, A., Venuprasad, K., Krawczyk, C., Sarao, R., Elly, C., Yang, C., Arya, S., Bachmaier, K., Su, L., Bouchard, D., Jones, R., Gronski, M., Ohashi, P., Wada, T., Bloom, D., Fathman, C., Liu, Y.-C., and Penninger, J. M. (2004). Essential Role of the E3 Ubiquitin Ligase Cbl-b in T Cell Anergy Induction. *Immunity*, 21(2):167–177.

Jordan, M. S., Boesteanu, A., Reed, A. J., Petrone, A. L., Holenbeck, A. E., Lerman, M. A., Naji, A., and Caton, A. J. (2001). Thymic Selection of Cd4+Cd25+ Regulatory T Cells Induced by an Agonist Self-Peptide. *Nat Immunol*, 2(4):301–306.

June, C. H., Ledbetter, J. A., Gillespie, M. M., Lindsten, T., and Thompson, C. B. (1987). T-Cell Proliferation Involving the CD28 Pathway Is Associated with Cyclosporine-Resistant Interleukin 2 Gene Expression. *Mol Cell Biol*, 7(12):4472–4481.

Kappler, J. W., Roehm, N., and Marrack, P. (1987). T cell tolerance by clonal elimination in the thymus. *Cell*, 49(2):273–280.

Kassiotis, G., Zamoyska, R., and Stockinger, B. (2003). Involvement of Avidity for Major Histocompatibility Complex in Homeostasis of Naive and Memory T Cells. *J. Exp. Med.*

Kermack, W. and McKendrick, A. (1927). A contribution to the mathematical theory of epidemics. *Proc. R. Soc. London. Ser. A*, 115(772):700 LP – 721.

Kershaw, M. H., Westwood, J. A., Parker, L. L., Wang, G., Eshhar, Z., Mavroukakis, S. A., White, D. E., Wunderlich, J. R., Canevari, S., Rogers-Freezer, L., Chen, C. C., Yang, J. C., Rosenberg, S. A., and Hwu, P. (2006). A Phase I Study on Adoptive Immunotherapy Using Gene-Modified T Cells for Ovarian Cancer. *Clin Cancer Res*, 12(20 Pt 1):6106–6115.

Killeen, N., Stuart, S. G., Littman, D. R., Kileen, N., Stuart, S. G., Littman, D. R., and Killeen, N. (1992). Development and function of T cells in mice with a disrupted CD2 gene. *Embo J.*

Kim, S. T., Touma, M., Takeuchi, K., Sun, Z.-Y. J., Dave, V. P., Kappes, D. J., Wagner, G., and Reinherz, E. L. (2010). Distinctive CD3 Heterodimeric Ectodomain Topologies Maximize Antigen-Triggered Activation of $\alpha\beta$ T Cell Receptors. *J. Immunol.*, 185(5):2951–2959.

King, P. D., Sadra, A., Han, A., Liu, X. R., Sunder-Plassmann, R., Reinherz, E. L., and Dupont, B. (1996). CD2 signaling in T cells involves tyrosine phosphorylation and activation of the Tec family kinase, EMT/ITK/TSK. *Int Immunol*, 8(11):1707–1714.

Kirsch, K. H., Georgescu, M.-M., Shishido, T., Langdon, W. Y., Birge, R. B., and Hanafusa, H. (2001). The Adapter Type Protein CMS/CD2AP Binds to the Proto-oncogenic Protein c-Cbl through a Tyrosine Phosphorylation-regulated Src Homology 3 Domain Interaction. *J. Biol. Chem.*, 276(7):4957–4963.

Kisielow, P., Blüthmann, H., Staerz, U. D., Steinmetz, M., and von Boehmer, H. (1988). Tolerance in T-cell-receptor transgenic mice involves deletion of nonmature CD4+8+ thymocytes. *Nature*, 333:742.

Kjer-Nielsen, L., Clements, C. S., Purcell, A. W., Brooks, A. G., Whisstock, J. C., Burrows, S. R., McCluskey, J., and Rossjohn, J. (2003). A Structural Basis for the Selection of Dominant $\alpha\beta$ T Cell Receptors in Antiviral Immunity. *Immunity*, 18(1):53–64.

Kloss, C. C., Condomines, M., Cartellieri, M., Bachmann, M., and Sadelain, M. (2013). Combinatorial Antigen Recognition with Balanced Signaling Promotes Selective Tumor Eradication by Engineered T Cells. *Nat Biotechnol*, 31(1):71–75.

Kochenderfer, J. N., Dudley, M. E., Kassim, S. H., Somerville, R. P., Carpenter, R. O., Maryalice, S. S., Yang, J. C., Phan, G. Q., Hughes, M. S., Sherry, R. M., Raffeld, M., Feldman, S., Lu, L., Li, Y. F., Ngo, L. T., Goy, A., Feldman, T., Spaner, D. E., Wang, M. L., Chen, C. C., Kranick, S. M., Nath, A., Nathan, D. A. N., Morton, K. E., Toomey, M. A., Rosenberg, S. A., Stetler-Stevenson, M., Yang, J. C., Phan, G. Q., Hughes, M. S., Sherry, R. M., Raffeld, M., Feldman, S., Lu, L., Li, Y. F., Ngo, L. T., Goy, A., Feldman, T., Spaner, D. E., Wang, M. L., Chen, C. C., Kranick, S. M., Nath, A., Nathan, D. A. N., Morton, K. E., Toomey, M. A., and Rosenberg, S. A. (2015). Chemotherapy-refractory diffuse large B-cell lymphoma and indolent B-cell malignancies can be effectively treated with autologous T cells expressing an anti-CD19 chimeric antigen receptor. *J. Clin. Oncol.*, 33(6):540–549.

Kowolik, C. M., Topp, M. S., Gonzalez, S., Pfeiffer, T., Olivares, S., Gonzalez, N., Smith, D. D., Forman, S. J., Jensen, M. C., and Cooper, L. J. N. (2006). Cd28 Costimulation Provided through a Cd19-Specific Chimeric Antigen Receptor Enhances in Vivo Persistence and Antitumor Efficacy of Adoptively Transferred T Cells. *Cancer Res.*, 66(22):10995–11004.

Koyasu, S., Lawton, T., Novick, D., Recny, M. a., Siliciano, R. F., Wallner, B. P., and Reinherz, E. L. (1990). Role of interaction of CD2 molecules with lymphocyte function-associated antigen 3 in T-cell recognition of nominal antigen. *Proc. Natl. Acad. Sci. U. S. A.*

Krangel, M. S. (1987). Endocytosis and recycling of the T3-T cell receptor complex. The role of T3 phosphorylation. *J. Exp. Med.*

Kristensen, N. N., Madsen, A. N., Thomsen, A. R., and Christensen, J. P. (2004). Cytokine production by virus-specific CD8+T cells varies with activation state and localization, but not with TCR avidity. *J. Gen. Virol.*

Krogsgaard, M., Li, Q. J., Sumen, C., Huppa, J. B., Huse, M., and Davis, M. M. (2005). Agonist/Endogenous Peptide-MHC Heterodimers Drive T Cell Activation and Sensitivity. *Nature*, 434(7030):238–243.

Krummel, M. F. and Allison, J. P. (1995). CD28 and CTLA-4 Have Opposing Effects on the Response of T Cells to Stimulation. *J. Exp. Med.*, 182(2):459–465.

Kuhns, M. S., Girvin, A. T., Klein, L. O., Chen, R., Jensen, K. D. C., Newell, E. W., Huppa, J. B., Lillemeier, B. F., Huse, M., Chien, Y.-h., Garcia, K. C., and Davis, M. M. (2010). Evidence for a functional sidedness to the $\alpha\beta$TCR. *Proc. Natl. Acad. Sci.*, 107(11):5094 LP – 5099.

Kurts, C., Kosaka, H., Carbone, F. R., Miller, J. F. A. P., and Heath, W. R. (1997). Class I–restricted Cross-Presentation of Exogenous Self-Antigens Leads to Deletion of Autoreactive CD8+ T Cells. *J. Exp. Med.*, 186(2):239 LP – 245.

Lafferty, K. J. and Cunningham, A. J. (1975). A new analysis of allogeneic interactions. *Aust. J. Exp. Biol. Med. Sci.*

Lamers, C. H. J., Sleijfer, S., Van Steenbergen, S., Van Elzakker, P., Van Krimpen, B., Groot, C., Vulto, A., Den Bakker, M., Oosterwijk, E., Debets, R., and Gratama, J. W. (2013). Treatment of Metastatic Renal Cell Carcinoma with Caix CAR-Engineered T Cells: Clinical Evaluation and Management of on-Target Toxicity. *Mol Ther*, 21(4):904–912.

Lanitis, E., Poussin, M., Klattenhoff, A. W., Song, D., Sandaltzopoulos, R., June, C. H., and Powell, D. J. (2013). Chimeric Antigen Receptor T Cells with Dissociated Signaling Domains Exhibit Focused Antitumor Activity with Reduced Potential for Toxicity in Vivo. *Cancer Immunol. Res.*, 1(1):43–53.

Lauritsen, J. P., Christensen, M. D., Dietrich, J., Kastrup, J., Odum, N., and Geisler, C. (1998). Two distinct pathways exist for down-regulation of the TCR. *J. Immunol.*

Leach, D. R., Krummel, M. F., and Allison, J. P. (1996). Enhancement of Antitumor Immunity by CTLA-4 Blockade. *Science (80-.).*, 271(5256):1734 LP – 1736.

Lee, D. W., Kochenderfer, J. N., Stetler-Stevenson, M., Cui, Y. K., Delbrook, C., Feldman, S. A., Fry, T. J., Orentas, R., Sabatino, M., Shah, N. N., Steinberg, S. M., Stroncek, D., Tschernia, N., Yuan, C., Zhang, H., Zhang, L., Rosenberg, S. A., Wayne, A. S., and Mackall, C. L. (2015). T cells expressing CD19 chimeric antigen receptors for acute

lymphoblastic leukaemia in children and young adults: A phase 1 dose-escalation trial. *Lancet*, 385(9967):517–528.

Lee, K. H., Dinner, A. R., Tu, C., Campi, G., Raychaudhuri, S., Varma, R., Sims, T. N., Burack, W. R., Wu, H., Wang, J., Kanagawa, O., Markiewicz, M., Allen, P. M., Dustin, M. L., Chakraborty, A. K., and Shaw, A. S. (2003). The Immunological Synapse Balances T Cell Receptor Signaling and Degradation. *Science (80-.).*, 302(5648):1218–1222.

Lees, J. R., Charbonneau, B., Swanson, A. K., Jensen, R., Zhang, J. F., Matusik, R., and Ratliff, T. L. (2006). Deletion is neither sufficient nor necessary for the induction of peripheral tolerance in mature CD8+T cells. *Immunology*.

Leitner, J., Herndler-Brandstetter, D., Zlabinger, G. J., Grubeck-Loebenstein, B., and Steinberger, P. (2015). CD58/CD2 Is the Primary Costimulatory Pathway in Human CD28- CD8 T Cells. *J. Immunol.*, 195(2):477–487.

Leupin, O., Zaru, R., Laroche, T., Muller, S., and Valitutti, S. (2000). Exclusion of Cd45 from the T-Cell Receptor Signaling Area in Antigen-Stimulated T Lymphocytes. *Curr Biol*, 10(5):277–280.

Lever, M., Lim, H.-S., Kruger, P., Nguyen, J., Trendel, N., Abu-Shah, E., Maini, P. K., Van der Merwe, P. A., and Dushek, O. (2016). Architecture of a Minimal Signaling Pathway Explains the T-Cell Response to a 1 Million-Fold Variation in Antigen Affinity and Dose. *Proc. Natl. Acad. Sci.*, 113(43):E6630–E6638.

Li, J., Nishizawa, K., An, W., Hussey, R. E., Lialios, P. E., Salgia, R., Sunder-Plassmann, R., and Reinherz, E. L. (1998). A cdc15-like adaptor protein (CD2BP1) interacts with the CD2 cytoplasmic domain and regulates CD2-triggered adhesion. *EMBO J.*

Li, Y.-C., Chen, B.-M., Wu, P.-C., Cheng, T.-L., Kao, L.-S., Tao, M.-H., Lieber, A., and Roffler, S. R. (2010). Cutting Edge: Mechanical Forces Acting on T Cells Immobilized via the TCR Complex Can Trigger TCR Signaling. *J. Immunol.*, 184(11):5959 LP – 5963.

Liang, Y., Cucchetti, M., Roncagalli, R., Yokosuka, T., Malzac, A., Bertosio, E., Imbert, J., Nijman, I. J., Suchanek, M., Saito, T., Wülfing, C., Malissen, B., and Malissen, M.

(2013). The lymphoid lineage–specific actin-uncapping protein Rltpr is essential for costimulation via CD28 and the development of regulatory T cells. *Nat. Immunol.*, 14:858.

Liddy, N., Bossi, G., Adams, K. J., Lissina, A., Mahon, T. M., Hassan, N. J., Gavarret, J., Bianchi, F. C., Pumphrey, N. J., Ladell, K. I., Gostick, E., Sewell, A. K., Lissin, N. M., Harwood, N. E., Molloy, P. E., Li, Y., Cameron, B. J., Sami, M., Baston, E. E., Todorov, P. T., Paston, S. J., Dennis, R. E., Harper, J. V., Dunn, S. M., Ashfield, R., Johnson, A., McGrath, Y., Plesa, G., June, C. H., Kalos, M., Price, D., Vuidepot, A., Williams, D. D., Sutton, D. H., and Jakobsen, B. K. (2012). Monoclonal TCR-redirected tumor cell killing. 18(6).

Ligocki, A. J., Brown, J. R., and Niederkorn, J. Y. (2015). Role of interferon-γ and cytotoxic T lymphocytes in intraocular tumor rejection. *J. Leukoc. Biol.*, 99(5):735–747.

Lillemeier, B. F., Mörtelmaier, M. A., Forstner, M. B., Huppa, J. B., Groves, J. T., and Davis, M. M. (2009). TCR and Lat are expressed on separate protein islands on T cell membranes and concatenate during activation. *Nat. Immunol.*, 11:90.

Lim, W. A. and June, C. H. (2017). The Principles of Engineering Immune Cells to Treat Cancer.

Lindstein, T., June, C. H., Ledbetter, J. A., Stella, G., and Thompson, C. B. (1989). Regulation of lymphokine messenger RNA stability by a surface-mediated T cell activation pathway. *Science (80-.).*, 244(4902):339 LP – 343.

Linette, G. P., Stadtmauer, E. A., Maus, M. V., Rapoport, A. P., Levine, B. L., Emery, L., Litzky, L., Bagg, A., Carreno, B. M., Cimino, P. J., Binder-Scholl, G. K., Smethurst, D. P., Gerry, A. B., Pumphrey, N. J., Bennett, A. D., Brewer, J. E., Dukes, J., Harper, J., Tayton-Martin, H. K., Jakobsen, B. K., Hassan, N. J., Kalos, M., and June, C. H. (2013). Cardiovascular Toxicity and Titin Cross-Reactivity of Affinity-Enhanced T Cells in Myeloma and Melanoma. *Blood*, 122(6):863–871.

Liu, B., Zou, F., Lu, L., Chen, C., He, D., Zhang, X., Tang, X., Liu, C., Li, L., and Zhang, H. (2016). Chimeric Antigen Receptor T Cells Guided by the Single-Chain Fv of a Broadly Neutralizing Antibody Specifically and Effectively Eradicate Virus Reactivated

from Latency in Cd4(+) T Lymphocytes Isolated from Hiv-1-Infected Individuals Receiving Suppressive. *J. Virol.*, 90(21):9712–9724.

Liu, H., Rhodes, M., Wiest, D. L., and Vignali, D. A. (2000). On the Dynamics of TCR:Cd3 Complex Cell Surface Expression and Downmodulation. *Immunity*, 13(5):665–675.

Liu, X., Jiang, S., Fang, C., Yang, S., Olalere, D., Pequignot, E. C., Cogdill, A. P., Li, N., Ramones, M., Granda, B., Zhou, L., Loew, A., Young, R. M., June, C. H., and Zhao, Y. (2015). Affinity-tuned ErbB2 or EGFR chimeric antigen receptor T cells exhibit an increased therapeutic index against tumors in mice. *Cancer Res.*, 75(17):3596–3607.

Lo, A. S., Ma, Q., Liu, D. L., and Junghans, R. P. (2010). Anti-Gd3 Chimeric Sfv-Cd28/T-Cell Receptor Zeta Designer T Cells for Treatment of Metastatic Melanoma and Other Neuroectodermal Tumors. *Clin Cancer Res*, 16.

Long, A. H., Haso, W. M., Shern, J. F., Wanhainen, K. M., Murgai, M., Ingaramo, M., Smith, J. P., Walker, A. J., Kohler, M. E., Venkateshwara, V. R., Kaplan, R. N., Patterson, G. H., Fry, T. J., Orentas, R. J., and Mackall, C. L. (2015). 4-1BB Costimulation Ameliorates T Cell Exhaustion Induced by Tonic Signaling of Chimeric Antigen Receptors. *Nat Med*, 21(6):581–590.

Ma, W., Trusina, A., El-Samad, H., Lim, W. A., and Tang, C. (2009). Defining Network Topologies That Can Achieve Biochemical Adaptation. *Cell*, 138(4):760–773.

Martelli, M. P., Lin, H., Zhang, W., Samelson, L. E., and Bierer, B. E. (2000). Signaling via LAT (linker for T-cell activation) and Syk/ZAP70 is required for ERK activation and NFAT transcriptional activation following CD2 stimulation. *Blood*, 96(6):2181 LP – 2190.

Martin, S. and Bevan, M. J. (1998). Transient alteration of T cell fine specificity by a strong primary stimulus correlates with T cell receptor down-regulation. *Eur. J. Immunol.*

Martin-Blanco, N., Blanco, R., Alda-Catalinas, C., Bovolenta, E. R., Oeste, C. L., Palmer, E., Schamel, W. W., Lythe, G., Molina-París, C., Castro, M., and Alarcon, B. (2018). A window of opportunity for cooperativity in the T Cell Receptor. *Nat. Commun.*, 9(1):2618.

Martínez-Martín, N., Risueño, R. M., Morreale, A., Zaldívar, I., Fernández-Arenas, E., Herranz, F., Ortiz, A. R., and Alarcón, B. (2009). Cooperativity Between T Cell Receptor Complexes Revealed by Conformational Mutants of CD3 epsilon. *Sci. Signal.*, 2(83):ra43 LP – ra43.

Mason, D. (1998). A very high level of crossreactivity is an essential feature of the T- cell receptor.

Maude, S. L., Laetsch, T. W., Buechner, J., Rives, S., Boyer, M., Bittencourt, H., Bader, P., Verneris, M. R., Stefanski, H. E., Myers, G. D., Qayed, M., De Moerloose, B., Hiramatsu, H., Schlis, K., Davis, K. L., Martin, P. L., Nemecek, E. R., Yanik, G. A., Peters, C., Baruchel, A., Boissel, N., Mechinaud, F., Balduzzi, A., Krueger, J., June, C. H., Levine, B. L., Wood, P., Taran, T., Leung, M., Mueller, K. T., Zhang, Y., Sen, K., Lebwohl, D., Pulsipher, M. A., and Grupp, S. A. (2018). Tisagenlecleucel in Children and Young Adults with B-Cell Lymphoblastic Leukemia. *N. Engl. J. Med.*, 378(5):439–448.

Maus, M. V., Plotkin, J., Jakka, G., Stewart-Jones, G., Rivière, I., Merghoub, T., Wolchok, J., Renner, C., and Sadelain, M. (2016). An MHC-Restricted Antibody-Based Chimeric Antigen Receptor Requires TCR-like Affinity to Maintain Antigen Specificity. *Mol. Ther. — Oncolytics*, 3:16023.

Mckeithan, T. W. (1995). Kinetic Proofreading in T-Cell Receptor Signal Transduction. *Proc. Natl. Acad. Sci.*, 92(11):5042–5046.

Meinl, E., Lengenfelder, D., Blank, N., Pirzer, R., Barata, L., and Hivroz, C. (2000). Differential requirement of ZAP-70 for CD2-mediated activation pathways of mature human T cells. *J. Immunol.*

Michel, F., Attal-Bonnefoy, G., Mangino, G., Mise-Omata, S., and Acuto, O. (2001). CD28 as a Molecular Amplifier Extending TCR Ligation and Signaling Capabilities. *Immunity*, 15(6):935–945.

Milstein, O., Tseng, S. Y., Starr, T., Llodra, J., Nans, A., Liu, M., Wild, M. K., Van Der Merwe, P. A., Stokes, D. L., Reisner, Y., and Dustin, M. L. (2008). Nanoscale increases in CD2-CD48-mediated intermembrane spacing decrease adhesion and reorganize the immunological synapse. *J. Biol. Chem.*, 283(49):34414–34422.

Minguet, S., Swamy, M., Alarcón, B., Luescher, I. F., and Schamel, W. W. A. (2007). Full Activation of the T Cell Receptor Requires Both Clustering and Conformational Changes at CD3. *Immunity*, 26(1):43–54.

Moingeon, P., Chang, H. C., Wallner, B. P., Stebbins, C., Frey, A. Z., and Reinherz, E. L. (1989). CD2-mediated adhesion facilitates T lymphocyte antigen recognition function. *Nature*, 339:312–314.

Monach, P. A., Meredith, S. C., T.Siegel, C., and Schreiber, H. (1995). A unique tumor antigen produced by a single amino acid substitution. *Immunity*, 2(1):45–59.

Monjas, A., Alcover, A., and Alarcón, B. (2004). Engaged and bystander T cell receptors are down-modulated by different endocytotic pathways. *J. Biol. Chem.*

Monks, C. R. F., Freiberg, B. A., Kupfer, H., Sciaky, N., and Kupfer, A. (1998). Three-dimensional segregation of supramolecular activation clusters in T cells. *Nature*.

Morgan, R. A., Yang, J. C., Kitano, M., Dudley, M. E., Laurencot, C. M., and Rosenberg, S. A. (2010). Case Report of a Serious Adverse Event Following the Administration of T Cells Transduced with a Chimeric Antigen Receptor Recognizing Erbb2. *Mol Ther*, 18(4):843–851.

Mueller, D. L., Jenkins, M. K., and Schwartz, R. H. (1989). An Accessory Cell-Derived Costimulatory Signal Acts Independently of Protein Kinase C Activation to Allow T Cell Proliferation and Prevent the Induction of Unresponsiveness. *J Immunol*, 142(8):2617–2628.

Murphy, M. A., Schnall, R. G., Venter, D. J., Barnett, L., Bertoncello, I., Thien, C. B. F., Langdon, W. Y., and Bowtell, D. D. L. (1998). Tissue Hyperplasia and Enhanced T-Cell Signalling via ZAP-70 in c-Cbl-Deficient Mice. *Mol. Cell. Biol.*, 18(8):4872–4882.

Murtaza, A., Kuchroo, V. K., and Freeman, G. J. (1999). Changes in the Strength of Co-Stimulation through the B7/CD28 Pathway Alter Functional T Cell Responses to Altered Peptide Ligands. *Int. Immunol.*, 11(3):407–416.

Naramura, M., Jang, I.-K., Kole, H., Huang, F., Haines, D., and Gu, H. (2002). c-Cbl

and Cbl-b regulate T cell responsiveness by promoting ligand-induced TCR down-modulation. *Nat. Immunol.*, 3(12):1192–1199.

Naramura, M., Kole, H. K., Hu, R.-J., and Gu, H. (1998). Altered thymic positive selection and intracellular signals in Cbl-deficient mice. *Proc. Natl. Acad. Sci. U. S. A.*, 95(26):15547–15552.

Nishizawa, K., Freund, C., Li, J., Wagner, G., and Reinherz, E. L. (1998). Identification of a proline-binding motif regulating CD2-triggered T lymphocyte activation. *Immunol. Approv.*

Nurieva, R. I., Zheng, S., Jin, W., Chung, Y., Zhang, Y., Martinez, G. J., Reynolds, J. M., Wang, S. L., Lin, X., Sun, S. C., Lozano, G., and Dong, C. (2010). The E3 ubiquitin ligase GRAIL regulates T cell tolerance and regulatory T cell function by mediating T cell receptor-CD3 degradation. *Immunity*.

Oliveira, M. I., Gonçalves, C. M., Pinto, M., Fabre, S., Santos, A. M., Lee, S. F., Castro, M. A. A., Nunes, R. J., Barbosa, R. R., Parnes, J. R., Yu, C., Davis, S. J., Moreira, A., Bismuth, G., and Carmo, A. M. (2012). Cd6 Attenuates Early and Late Signaling Events, Setting Thresholds for T-Cell Activation. *Eur. J. Immunol.*, 42(1):195–205.

Ott, P. A., Hu, Z., Keskin, D. B., Shukla, S. A., Sun, J., Bozym, D. J., Zhang, W., Luoma, A., Giobbie-Hurder, A., Peter, L., Chen, C., Olive, O., Carter, T. A., Li, S., Lieb, D. J., Eisenhaure, T., Gjini, E., Stevens, J., Lane, W. J., Javeri, I., Nellaiappan, K., Salazar, A. M., Daley, H., Seaman, M., Buchbinder, E. I., Yoon, C. H., Harden, M., Lennon, N., Gabriel, S., Rodig, S. J., Barouch, D. H., Aster, J. C., Getz, G., Wucherpfennig, K., Neuberg, D., Ritz, J., Lander, E. S., Fritsch, E. F., Hacohen, N., and Wu, C. J. (2017). An immunogenic personal neoantigen vaccine for patients with melanoma. *Nature*, 547:217.

Pageon, S. V., Tabarin, T., Yamamoto, Y., Ma, Y., Nicovich, P. R., Bridgeman, J. S., Cohnen, A., Benzing, C., Gao, Y., Michael, D., Tungatt, K., Dolton, G., Sewell, A. K., Price, D. A., Acuto, O., Parton, R. G., Gooding, J. J., Rossy, J., Rossjohn, J., and Gaus, K. (2016). Functional role of T-cell receptor nanoclusters in signal initiation and antigen discrimination. *Proc. Natl. Acad. Sci.*, 113(37):E5454—-E5463.

Palmer, E. and Naeher, D. (2009). Affinity threshold for thymic selection through a T-cell receptor–co-receptor zipper. *Nat. Rev. Immunol.*, 9:207.

Park, J. R., Digiusto, D. L., Slovak, M., Wright, C., Naranjo, A., Wagner, J., Meechoovet, H. B., Bautista, C., Chang, W. C., Ostberg, J. R., and Jensen, M. C. (2007). Adoptive Transfer of Chimeric Antigen Receptor Re-Directed Cytolytic T Lymphocyte Clones in Patients with Neuroblastoma. *Mol Ther*, 15(4):825–833.

Paster, W., Bruger, A. M., Katsch, K., Grégoire, C., Roncagalli, R., Fu, G., Gascoigne, N. R. J., Nika, K., Cohnen, A., Feller, S. M., Simister, P. C., Molder, K. C., Cordoba, S.-p., Dushek, O., and Malissen, B. (2015). A THEMIS:SHP1 complex promotes T-cell survival. *EMBO J.*, 34(3):393–409.

Pegram, H. J., Lee, J. C., Hayman, E. G., Imperato, G. H., Tedder, T. F., Sadelain, M., and Brentjens, R. J. (2012). Tumor-Targeted T Cells Modified to Secrete Il-12 Eradicate Systemic Tumors without Need for Prior Conditioning. *Blood*, 119(18):4133–4141.

Pentcheva-Hoang, T., Egen, J. G., Wojnoonski, K., and Allison, J. P. (2004). B7-1 and B7-2 Selectively Recruit CTLA-4 and CD28 to the Immunological Synapse. *Immunity*, 21(3):401–413.

Pielak, R. M., O'donoghue, G. P., Lin, J. J., Alfieri, K. N., Fay, N. C., Low-Nam, S. T., and Groves, J. T. (2017). Early T Cell Receptor Signals Globally Modulate Ligand:Receptor Affinities During Antigen Discrimination. *Proc Natl Acad Sci U S A*.

Porter, D. L., Hwang, W.-T., Frey, N. V., Lacey, S. F., Shaw, P. A., Loren, A. W., Bagg, A., Marcucci, K. T., Shen, A., Gonzalez, V., Ambrose, D., Grupp, S. A., Chew, A., Zheng, Z., Milone, M. C., Levine, B. L., Melenhorst, J. J., and June, C. H. (2015). Chimeric antigen receptor T cells persist and induce sustained remissions in relapsed refractory chronic lymphocytic leukemia. *Sci. Transl. Med.*, 7(303):303ra139–303ra139.

Potter, T. A., Grebe, K., Freiberg, B., and Kupfer, A. (2001). Formation of supramolecular activation clusters on fresh ex vivo CD8⁺ T cells after engagement of the T cell antigen receptor and CD8 by antigen-presenting cells. *Proc. Natl. Acad. Sci.*, 98(22):12624 LP – 12629.

Prévost-Blondel, A., Roth, E., Rosenthal, F. M., and Pircher, H. (2000). Crucial Role of TNF-alpha in CD8 T cell-Mediated Elimination of 3LL-A9 Lewis Lung Carcinoma Cells In Vivo. *J. Immunol.*, 164(7):3645–3651.

Proulx-Giraldeau, F., Rademaker, T. J., and Francois, P. (2017). Untangling the Hairball: Fitness-Based Asymptotic Reduction of Biological Networks. *Biophys. J.*, 113(8):1893–1906.

Pulè, M. A., Straathof, K. C., Dotti, G., Heslop, H. E., Rooney, C. M., and Brenner, M. K. (2005). A Chimeric T Cell Antigen Receptor That Augments Cytokine Release and Supports Clonal Expansion of Primary Human T Cells. *Mol Ther*, 12(5):933–941.

Purbhoo, M. A., Irvine, D. J., Huppa, J. B., and Davis, M. M. (2004). T cell killing does not require the formation of a stable mature immunological synapse. *Nat. Immunol.*, 5(5):524–530.

Rapoport, A. P., Stadtmauer, E. A., Binder-Scholl, G. K., Goloubeva, O., Vogl, D. T., Lacey, S. F., Badros, A. Z., Garfall, A., Weiss, B., Finklestein, J., Kulikovskaya, I., Sinha, S. K., Kronsberg, S., Gupta, M., Bond, S., Melchiori, L., Brewer, J. E., Bennett, A. D., Gerry, A. B., Pumphrey, N. J., Williams, D., Tayton- Martin, H. K., Ribeiro, L., Holdich, T., Yanovich, S., Hardy, N., Yared, J., Kerr, N., Philip, S., Westphal, S., Siegel, D. L., Levine, B. L., Jakobsen, B. K., Kalos, M., and June, C. H. (2015). Ny-Eso-1-Specific TCR-Engineered T Cells Mediate Sustained Antigen-Specific Antitumor Effects in Myeloma. *Nat Med*, 21(8):914–921.

Redmond, W. L., Marincek, B. C., and Sherman, L. A. (2005). Distinct Requirements for Deletion versus Anergy during CD8 T Cell Peripheral Tolerance In Vivo. *J. Immunol.*, 174(4):2046 LP – 2053.

Reinherz, E. L., Meuer, S., Fitzgerald, K. A., Hussey, R. E., Levine, H., and Schlossman, S. F. (1982). Antigen recognition by human T lymphocytes is linked to surface expression of the T3 molecular complex. *Cell*, 30(3):735–743.

Reis e Sousa, C. (2006). Dendritic cells in a mature age. *Nat. Rev. Immunol.*, 6:476.

Reth, M. (1989). Antigen receptor tail clue [5].

Riedhammer, C. and Weissert, R. (2015). Antigen Presentation, Autoantigens, and Immune Regulation in Multiple Sclerosis and Other Autoimmune Diseases. *Front. Immunol.*, 6:322.

Rizvi, N. A., Hellmann, M. D., Snyder, A., Kvistborg, P., Makarov, V., Havel, J. J., Lee, W., Yuan, J., Wong, P., Ho, T. S., Miller, M. L., Rekhtman, N., Moreira, A. L., Ibrahim, F., Bruggeman, C., Gasmi, B., Zappasodi, R., Maeda, Y., Sander, C., Garon, E. B., Merghoub, T., Wolchok, J. D., Schumacher, T. N., and Chan, T. A. (2015). Mutational landscape determines sensitivity to PD-1 blockade in non–small cell lung cancer. *Science (80-.).*, 348(6230):124 LP – 128.

Rock, K. L., Reits, E., and Neefjes, J. (2016). Present Yourself! By MHC Class I and MHC Class II Molecules. *Trends Immunol.*, 37(11):724–737.

Roep, B. O. and Peakman, M. (2012). Antigen Targets of Type 1 Diabetes Autoimmunity. *Cold Spring Harb. Perspect. Med.*, 2(4):a007781.

Roncagalli, R., Hauri, S., Fiore, F., Liang, Y., Chen, Z., Sansoni, A., Kanduri, K., Joly, R., Malzac, A., Lähdesmäki, H., Lahesmaa, R., Yamasaki, S., Saito, T., Malissen, M., Aebersold, R., Gstaiger, M., and Malissen, B. (2014). Quantitative proteomics analysis of signalosome dynamics in primary T cells identifies the surface receptor CD6 as a Lat adaptor–independent TCR signaling hub. *Nat. Immunol.*, 15:384.

Roybal, K. t., Rupp, L. j., Morsut, L., Walker, W. j., Mcnally, K. a., Park, J. s., and Lim, W. a. (2016). Precision Tumor Recognition by T Cells with Combinatorial Antigen-Sensing Circuits. *Cell*, 164(4):770–779.

Rudolph, M. G., Stanfield, R. L., and Wilson, I. A. (2006). HOW TCRS BIND MHCS, PEPTIDES, AND CORECEPTORS. *Annu. Rev. Immunol.*, 24(1):419–466.

Ryan, K. R., McCue, D., and Anderton, S. M. (2005). Fas-mediated death and sensory adaptation limit the pathogenic potential of autoreactive T cells after strong antigenic stimulation. *J. Leukoc. Biol.*

Sagiv-Barfi, I., Czerwinski, D. K., Levy, S., Alam, I. S., Mayer, A. T., Gambhir, S. S., and Levy, R. (2018). Eradication of spontaneous malignancy by local immunotherapy. *Sci. Transl. Med.*, 10(426).

Sahin, U., Derhovanessian, E., Miller, M., Kloke, B.-P., Simon, P., Löwer, M., Bukur, V., Tadmor, A. D., Luxemburger, U., Schrörs, B., Omokoko, T., Vormehr, M., Albrecht, C., Paruzynski, A., Kuhn, A. N., Buck, J., Heesch, S., Schreeb, K. H., Müller, F., Ortseifer, I., Vogler, I., Godehardt, E., Attig, S., Rae, R., Breitkreuz, A., Tolliver, C., Suchan, M., Martic, G., Hohberger, A., Sorn, P., Diekmann, J., Ciesla, J., Waksmann, O., Brück, A.-K., Witt, M., Zillgen, M., Rothermel, A., Kasemann, B., Langer, D., Bolte, S., Diken, M., Kreiter, S., Nemecek, R., Gebhardt, C., Grabbe, S., Höller, C., Utikal, J., Huber, C., Loquai, C., and Türeci, Ö. (2017). Personalized RNA mutanome vaccines mobilize poly-specific therapeutic immunity against cancer. *Nature*, 547(7662):222–226.

Salio, M., Valitutti, S., and Lanzavecchia, A. (1997). Agonist-Induced T Cell Receptor Down-Regulation: Molecular Requirements and Dissociation from T Cell Activation. *Eur. J. Immunol.*, 27(7):1769–1773.

Samelson, L. E., Harford, J. B., and Klausner, R. D. (1985). Identification of the components of the murine T cell antigen receptor complex. *Cell*, 43(1):223–231.

San Jose, E., Borroto, A., Niedergang, F., Alcover, A., and Alarcón, B. (2000). Triggering the TCR complex causes the downregulation of nonengaged receptors by a signal transduction-dependent mechanism. *Immunity*, 12(2):161–170.

Sanchez-Lockhart, M., Graf, B., and Miller, J. (2008). Signals and Sequences That Control CD28 Localization to the Central Region of the Immunological Synapse. *J. Immunol.*

Sanchez-Lockhart, M. and Miller, J. (2006). Engagement of CD28 Outside of the Immunological Synapse Results in Up-Regulation of IL-2 mRNA Stability but Not IL-2 Transcription. *J Immunol*.

Sanchez-Madrid, F., Krensky, A. M., Ware, C. F., Robbins, E., Strominger, J. L., Burakoff, S. J., and Springer, T. A. (1982). Three distinct antigens associated with human T-lymphocyte-mediated cytolysis: LFA-1, LFA-2, and LFA-3. *Proc Natl Acad Sci U S A*, 79(23):7489–7493.

Sanders, M., Makgoba, M., June, C., Young, H., and Shaw, S. (1989). Enhanced respon-

siveness of human memory T cells to CD2 and CD3 receptor-mediated activation. *Eur. J. Immunol.*

Sasada, T., Yang, H., and Reinherz, E. L. (2002). CD2 Facilitates Differentiation of CD4 Th Cells Without Affecting Th1/Th2 Polarization. *J. Immunol.*

Savoldo, B., Ramos, C. A., Liu, E., Mims, M. P., Keating, M. J., Carrum, G., Kamble, R. T., Bollard, C. M., Gee, A. P., Mei, Z., Liu, H., Grilley, B., Rooney, C. M., Heslop, H. E., Brenner, M. K., and Dotti, G. (2011). Cd28 Costimulation Improves Expansion and Persistence of Chimeric Antigen Receptor-Modified T Cells in Lymphoma Patients. *J Clin Invest*, 121(5):1822–1826.

Schadendorf, D., Hodi, F. S., Robert, C., Weber, J. S., Margolin, K., Hamid, O., Patt, D., Chen, T.-T., Berman, D. M., and Wolchok, J. D. (2015). Pooled Analysis of Long-Term Survival Data From Phase II and Phase III Trials of Ipilimumab in Unresectable or Metastatic Melanoma. *J. Clin. Oncol.*

Schamel, W. W. A., Arechaga, I., Risueño, R. M., van Santen, H. M., Cabezas, P., Risco, C., Valpuesta, J. M., and Alarcón, B. (2005). Coexistence of multivalent and monovalent TCRs explains high sensitivity and wide range of response. *J. Exp. Med.*, 202(4):493–503.

Schmidt, A., Oberle, N., and Krammer, P. (2012). Molecular Mechanisms of Treg-Mediated T Cell Suppression .

Schönrich, G., Kalinke, U., Momburg, F., Malissen, M., Schmitt-Verhulst, A. M., Malissen, B., Hämmerling, G. J., and Arnold, B. (1991). Down-regulation of T cell receptors on self-reactive T cells as a novel mechanism for extrathymic tolerance induction. *Cell*, 65(2):293–304.

Schuster, S. J., Svoboda, J., Chong, E. A., Nasta, S. D., Mato, A. R., Anak, Ö., Brogdon, J. L., Pruteanu-Malinici, I., Bhoj, V., Landsburg, D., Wasik, M., Levine, B. L., Lacey, S. F., Melenhorst, J. J., Porter, D. L., and June, C. H. (2017). Chimeric Antigen Receptor T Cells in Refractory B-Cell Lymphomas. *N. Engl. J. Med.*, page NEJMoa1708566.

Schwartz, R. H. (2003). T cell anergy. *Annu. Rev. Immunol.*, 21(1):305–334.

Selvaraj, B. Y. P., Dustin, M. L., and Silber, R. (1987). DEFICIENCY OF LYMPHOCYTE FUNCTION-ASSOCIATED ANTIGEN 3 (LFA-3) IN PAROXYSMAL NOCTURNAL HEMOGLOBINURIA Membrane Anchor Functional Correlates and Evidence for a Phosphatidylinositol Many cell surface glycoproteins are anchored to the membrane via a hydro-. 166(October).

Shao, T., Shi, W., Zheng, J.-y., Xu, X.-x., Lin, A.-f., Xiang, L.-x., and Shao, J.-z. (2018). Costimulatory Function of CD58/CD2 Interaction in Adaptive Humoral Immunity in a Zebrafish Model.

Sherman, E., Barr, V., Manley, S., Patterson, G., Balagopalan, L., Akpan, I., Regan, C., Merrill, R., Sommers, C., Lippincott-Schwartz, J., and Samelson, L. (2011). Functional Nanoscale Organization of Signaling Molecules Downstream of the T Cell Antigen Receptor. *Immunity*, 35(5):705–720.

Shirasu, N., Shibaguci, H., Kuroki, M., Yamada, H., and Kuroki, M. (2010). Construction and Molecular Characterization of Human Chimeric T-Cell Antigen Receptors Specific for Carcinoembryonic Antigen. *Anticancer Res.*, 30(7):2731–2738.

Singh, N. J., Chen, C., and Schwartz, R. H. (2006). The impact of T cell intrinsic antigen adaptation on peripheral immune tolerance. *PLoS Biol.*, 4(11):1957–1969.

Singh, N. J. and Schwartz, R. H. (2003). The Strength of Persistent Antigenic Stimulation Modulates Adaptive Tolerance in Peripheral CD4+ T Cells. *J. Exp. Med.*, 198(7):1107–1117.

Singleton, K., Parvaze, N., Dama, K. R., Chen, K. S., Jennings, P., Purtic, B., Sjaastad, M. D., Gilpin, C., Davis, M. M., and Wulfing, C. (2006). A Large T Cell Invagination with CD2 Enrichment Resets Receptor Engagement in the Immunological Synapse. *J. Immunol.*

Skånland, S. S., Moltu, K., Berge, T., Aandahl, E. M., and Tasken, K. (2014). T-Cell Co-Stimulation through the Cd2 and Cd28 Co-Receptors Induces Distinct Signalling Responses. *Biochem J*, 460(3):399–410.

Smith, K., Seddon, B., Purbhoo, M. A., Zamoyska, R., Fisher, A. G., and Merkenschlager, M. (2001). Sensory adaptation in naive peripheral CD4 T cells. *J. Exp. Med.*

Sousa, J. and Carneiro, J. (2000). A mathematical analysis of TCR serial triggering and down-regulation. *Eur. J. Immunol.*, 30(11):3219–3227.

Sperling, A. I., Auger, J. A., Ehst, B. D., Rulifson, I. C., Thompson, C. B., and Bluestone, J. A. (1996). CD28/B7 interactions deliver a unique signal to naive T cells that regulates cell survival but not early proliferation. *J. Immunol.*

Stachlewitz, R. F., Hart, M. a., Bettencourt, B., Kebede, T., Schwartz, A., Ratnofsky, S. E., Calderwood, D. J., Waegell, W. O., and Hirst, G. C. (2005). A-770041, a novel and selective small-molecule inhibitor of Lck, prevents heart allograft rejection. *J. Pharmacol. Exp. Ther.*, 315(1):36–41.

Stamou, P., de Jersey, J., Carmignac, D., Mamalaki, C., Kioussis, D., and Stockinger, B. (2003). Chronic Exposure to Low Levels of Antigen in the Periphery Causes Reversible Functional Impairment Correlating with Changes in CD5 Levels in Monoclonal CD8 T Cells. *J. Immunol.*, 171(3):1278–1284.

Stefanová, I., Hemmer, B., Vergelli, M., Martin, R., Biddison, W. E., Germain, R. N., Stefanova, I., Hemmer, B., Vergelli, M., Martin, R., Biddison, W. E., and Germain, R. N. (2003). TCR ligand discrimination is enforced by competing ERK positive and SHP-1 negative feedback pathways. *Nat. Immunol.*, 4(3):248–254.

Stewart-Jones, G., Wadle, A., Hombach, A., Shenderov, E., Held, G., Fischer, E., Kleber, S., Nuber, N., Stenner-Liewen, F., Bauer, S., Mcmichael, A., Knuth, A., Abken, H., Hombach, A. A., Cerundolo, V., Jones, E. Y., and Renner, C. (2009). Rational Development of High-Affinity T-Cell Receptor-Like Antibodies. *Proc. Natl. Acad. Sci.*, 106(14):5784–5788.

Stinchcombe, J. C., Bossi, G., Booth, S., and Griffiths, G. M. (2001). The Immunological Synapse of CTL Contains a Secretory Domain and Membrane Bridges. *Immunity*, 15(5):751–761.

Stinchcombe, J. C., Majorovits, E., Bossi, G., Fuller, S., and Griffiths, G. M. (2006). Centrosome polarization delivers secretory granules to the immunological synapse. *Nature*, 443:462.

Su, J. R., Kyung, M. J., Hyun, S. Y., Tae, W. K., Sol, K., Jun, C., and Eun, Y. C. (2009). Cognate CD4 help is essential for the reactivation and expansion of CD8 memory T cells directed against the hematopoietic cell-specific dominant minor histocompatibility antigen, H60. *Blood*.

Sun, Z.-Y. J., Kim, K. S., Wagner, G., and Reinherz, E. L. (2001). Mechanisms Contributing to T Cell Receptor Signaling and Assembly Revealed by the Solution Structure of an Ectodomain Fragment of the CD3epsilon-gamma Heterodimer. *Cell*, 105(7):913–923.

Sykulev, Y., Joo, M., Vturina, I., Tsomides, T. J., and Eisen, H. N. (1996). Evidence that a single peptide-MHC complex on a target cell can elicit a cytolytic T cell response. *Immunity*, 4(6):565–571.

Tafuri, A., Alferink, J., Möller, P., Hämmerling, G. J., and Arnold, B. (1995). T cell awareness of paternal alloantigens during pregnancy. *Science (80-.).*

Tan, M. P., Gerry, A. B., Brewer, J. E., Melchiori, L., Bridgeman, J. S., Bennett, A. D., Pumphrey, N. J., Jakobsen, B. K., Price, D. A., Ladell, K., and Sewell, A. K. (2015). T cell receptor binding affinity governs the functional profile of cancer-specific CD8+ T cells. *Clin. Exp. Immunol.*, 180(2):255–270.

Tanchot, C., Lemonnier, F. A., Pérarnau, B., Freitas, A. A., and Rocha, B. (1997). Differential Requirements for Survival and Proliferation of CD8 Naïve or Memory T Cells. *Science (80-.).*, 276(5321):2057 LP – 2062.

Tham, E. L., Shrikant, P., and Mescher, M. F. (2002). Activation-Induced Nonresponsiveness: A Th-Dependent Regulatory Checkpoint in the CTL Response. *J. Immunol.*

Tibaldi, E. V. and Reinherz, E. L. (2003). CD2BP3, CIN85 and the structurally related adaptor protein CMS bind to the same CD2 cytoplasmic segment, but elicit divergent functional activities. *Int. Immunol.*

Till, B. G., Jensen, M. C., Wang, J., Chen, E. Y., Wood, B. L., Greisman, H. A., Qian, X., James, S. E., Raubitschek, A., Forman, S. J., Gopal, A. K., Pagel, J. M., Lindgren,

C. G., Greenberg, P. D., Riddell, S. R., and Press, O. W. (2008). *Adoptive Immunotherapy for Indolent Non-Hodgkin Lymphoma and Mantle Cell Lymphoma Using Genetically Modified Autologous Cd20-Specific T Cells*, volume 112.

Tobar, J. A., Gonzalez, P. A., and Kalergis, A. M. (2004). Salmonella Escape from Antigen Presentation Can Be Overcome by Targeting Bacteria to Fc Receptors on Dendritic Cells. *J. Immunol.*

Topp, M. S., Gökbuget, N., Zugmaier, G., Degenhard, E., Goebeler, M.-E., Klinger, M., Neumann, S. A., Horst, H. A., Raff, T., Viardot, A., Stelljes, M., Schaich, M., Köhne-Volland, R., Brüggemann, M., Ottmann, O. G., Burmeister, T., Baeuerle, P. A., Nagorsen, D., Schmidt, M., Einsele, H., Riethmüller, G., Kneba, M., Hoelzer, D., Kufer, P., and Bargou, R. C. (2012). Long-term follow-up of hematologic relapse-free survival in a phase 2 study of blinatumomab in patients with MRD in B-lineage ALL. *Blood*, 120(26):5185 LP – 5187.

Torres, P. S., Alcover, A., Zapata, D. A., Arnaud, J., Pacheco, A., Martin-Fernandez, J. M., Villasevil, E. M., Sanal, O., and Regueiro, J. R. (2003). TCR Dynamics in Human Mature T Lymphocytes Lacking CD3 . *J. Immunol.*

Träger, U., Sierro, S., Djordjevic, G., Bouzo, B., Khandwala, S., Meloni, A., Mortensen, M., and Simon, A. K. (2012). The Immune Response to Melanoma Is Limited by Thymic Selection of Self-Antigens. *PLoS One*, 7(4):e35005.

Trendel, N., Kruger, P., Nguyen, J., Gaglione, S., and Dushek, O. (2019). Adaptation of CD8+ effector T cell responses to persistent antigen over a wide range of affinity is overcome by costimulation. *Manuscr. Submitt.*

Tseng, S.-Y., Waite, J. C., Liu, M., Vardhana, S., and Dustin, M. L. (2008). T Cell-Dendritic Cell Immunological Synapses Contain TCR-Dependent CD28-CD80 Clusters That Recruit Protein Kinase C theta. *J. Immunol.*, 181(7):4852–4863.

Turtle, C. J., Hanafi, L.-A., Berger, C., Gooley, T. A., Cherian, S., Hudecek, M., Sommermeyer, D., Melville, K., Pender, B., Budiarto, T. M., Robinson, E., Steevens, N. N., Chaney, C., Soma, L., Chen, X., Yeung, C., Wood, B., Li, D., Cao, J., Heimfeld, S., Jensen, M. C., Riddell, S. R., and Maloney, D. G. (2016a). CD19 CAR–T cells of defined

CD4+:CD8+ composition in adult B cell ALL patients. *J. Clin. Invest.*, 126(6):2123–2138.

Turtle, C. J., Hanafi, L. A., Berger, C., Hudecek, M., Pender, B., Robinson, E., Hawkins, R., Chaney, C., Cherian, S., Chen, X., Soma, L., Wood, B., Li, D., Heimfeld, S., Riddell, S. R., and Maloney, D. G. (2016b). Immunotherapy of non-Hodgkin's lymphoma with a defined ratio of CD8+ and CD4+ CD19-specific chimeric antigen receptor-modified T cells. *Sci. Transl. Med.*, 8(355).

Utzny, C., Coombs, D., Müller, S., and Valitutti, S. (2006). Analysis of peptide/MHC-induced TCR downregulation: Deciphering the triggering kinetics. *Cell Biochem. Biophys.*

Valitutti, S., Müller, S., Cella, M., Padovan, E., Lanzavecchia, A., Muller, S., Cella, M., Padovan, E., and Lanzavecchia, A. (1995). Serial Triggering of Many T-Cell Receptors by a Few Peptide-Mhc Complexes. *Nature*, 375(6527):148–151.

Valitutti, S., Müller, S., Salio, M., Lanzavecchia, A., Valitutti, B. S., Müller, S., Salio, M., and Lanzavecchia, A. (1997). Degradation of T Cell Receptor (TCR)–CD3-zeta Complexes after Antigenic Stimulation. *J. Exp. Med*, 185(10):1859–1864.

van den Berg, H. A., Ladell, K., Miners, K., Laugel, B., Llewellyn-Lacey, S., Clement, M., Cole, D. K., Gostick, E., Wooldridge, L., Sewell, A. K., Bridgeman, J. S., and Price, D. A. (2013). Cellular-level versus receptor-level response threshold hierarchies in T-cell activation. *Front. Immunol.*, 4(September):250.

Van der Merwe, P. A., Barclay, A. N., Mason, D. W., Davies, E. A., Davis, S. J., Morgan, B. P., Tone, M., Krishnam, A. K., and Ianelli, C. (1994). Human Cell-Adhesion Molecule CD2 Binds CD58 (LFA-3) with a Very Low Affinity and an Extremely Fast Dissociation Rate but Does Not Bind CD48 or CD59. *Biochemistry*.

Van der Merwe, P. A. and Dushek, O. (2011). Mechanisms for T Cell Receptor Triggering. *Nat Rev Immunol*, 11(1):47–55.

van Mierlo, G. J. D., Boonman, Z. F. H. M., Dumortier, H. M. H., den Boer, A. T., Fransen, M. F., Nouta, J., van der Voort, E. I. H., Offringa, R., Toes, R. E. M., and Melief, C. J. M.

(2004). Activation of Dendritic Cells That Cross-Present Tumor-Derived Antigen Licenses CD8⁺ CTL to Cause Tumor Eradication. *J. Immunol.*, 173(11):6753 LP – 6759.

Varma, R., Campi, G., Yokosuka, T., Saito, T., and Dustin, M. L. (2006). T Cell Receptor-Proximal Signals Are Sustained in Peripheral Microclusters and Terminated in the Central Supramolecular Activation Cluster. *Immunity*, 25(1):117–127.

Veillette, A., Bookman, M. A., Horak, E. M., and Bolen, J. B. (1988). The CD4 and CD8 T cell surface antigens are associated with the internal membrane tyrosine-protein kinase p56lck. *Cell*, 55(2):301–308.

Viola, A. and Lanzavecchia, A. (1996). T Cell Activation Determined by T Cell Receptor Number and Tunable Thresholds. *Science (80-.).*, 273(5271):104–106.

von Essen, M., Menné, C., Nielsen, B. L., Lauritsen, J. P. H., Dietrich, J., Andersen, P. S., Karjalainen, K., Ødum, N., and Geisler, C. (2002). The CD3 gamma leucine-based receptor-sorting motif is required for efficient ligand-mediated TCR down-regulation. *J. Immunol.*

von Essen, M., Nielsen, M. W., Bonefeld, C. M., Boding, L., Larsen, J. M., Leitges, M., Baier, G., Odum, N., and Geisler, C. (2006). Protein kinase C (PKC) alpha and PKC theta are the major PKC isotypes involved in TCR down-regulation. *J. Immunol.*

Wallace, D. L. and Beverley, P. C. (1990). Phenotypic changes associated with activation of CD45RA+ and CD45RO+ T cells. *Immunology*, 69(3):460–467.

Wang, H. Y., Altman, Y., Fang, D., Elly, C., Dai, Y., Shao, Y., and Liu, Y. C. (2001). Cbl Promotes Ubiquitination of the T Cell Receptor Zeta through an Adaptor Function of Zap-70. *J. Biol. Chem.*

Wang, Y., Becker, D., Vass, T., White, J., Marrack, P., and Kappler, J. W. (2009). A Conserved CXXC Motif in CD3ϵ Is Critical for T Cell Development and TCR Signaling. *PLOS Biol.*, 7(12):e1000253.

Watanabe, K., Terakura, S., Martens, A. C., Van Meerten, T., Uchiyama, S., Imai, M., Sakemura, R., Goto, T., Hanajiri, R., Imahashi, N., Shimada, K., Tomita, A., Kiyoi, H.,

Nishida, T., Naoe, T., and Murata, M. (2015). Target Antigen Density Governs the Efficacy of Anti–CD20-CD28-CD3zeta Chimeric Antigen Receptor–Modified Effector CD8+ T Cells. *J. Immunol.*, 194(3):911–920.

Wherry, E. J. (2011). T cell exhaustion. *Nat. Immunol.*, 12:492.

Wild, M. K., Cambiaggi, A., Brown, M. H., Davies, E. A., Ohno, H., Saito, T., and Van der Merwe, P. A. (1999). Dependence of T cell antigen recognition on the dimensions of an accessory receptor-ligand complex. *J. Exp. Med.*, 190(1):31–41.

Wolchok, J. D., Chiarion-Sileni, V., Gonzalez, R., Rutkowski, P., Grob, J.-J., Cowey, C. L., Lao, C. D., Wagstaff, J., Schadendorf, D., Ferrucci, P. F., Smylie, M., Dummer, R., Hill, A., Hogg, D., Haanen, J., Carlino, M. S., Bechter, O., Maio, M., Marquez-Rodas, I., Guidoboni, M., McArthur, G., Lebbé, C., Ascierto, P. A., Long, G. V., Cebon, J., Sosman, J., Postow, M. A., Callahan, M. K., Walker, D., Rollin, L., Bhore, R., Hodi, F. S., and Larkin, J. (2017). Overall Survival with Combined Nivolumab and Ipilimumab in Advanced Melanoma. *N. Engl. J. Med.*, 377(14):1345–1356.

Wong, P., Barton, G. M., Forbush, K. A., and Rudensky, A. Y. (2001). Dynamic tuning of T cell reactivity by self-peptide-major histocompatibility complex ligands. *J Exp Med*.

Xu, C., Gagnon, E., Call, M. E., Schnell, J. R., Schwieters, C. D., Carman, C. V., Chou, J. J., and Wucherpfennig, K. W. (2008). Regulation of T cell receptor activation by dynamic membrane binding of the CD3epsilon cytoplasmic tyrosine-based motif. *Cell*, 135(4):702–713.

Yang, H. and Reinherz, E. L. (2006). CD2BP1 Modulates CD2-Dependent T Cell Activation via Linkage to Protein Tyrosine Phosphatase (PTP)-PEST. *J. Immunol.*, 176(10):5898 LP – 5907.

Yokosuka, T., Kobayashi, W., Sakata-Sogawa, K., Takamatsu, M., Hashimoto-Tane, A., Dustin, M. L., Tokunaga, M., and Saito, T. (2008). Spatiotemporal Regulation of T Cell Costimulation by TCR-Cd28 Microclusters and Protein Kinase C Θ Translocation. *Immunity*, 29(4):589–601.

Zacharakis, N., Chinnasamy, H., Black, M., Xu, H., Lu, Y.-C., Zheng, Z., Pasetto, A., Langhan, M., Shelton, T., Prickett, T., Gartner, J., Jia, L., Trebska-McGowan, K., So-

merville, R. P., Robbins, P. F., Rosenberg, S. A., Goff, S. L., and Feldman, S. A. (2018). Immune recognition of somatic mutations leading to complete durable regression in metastatic breast cancer. *Nat. Med.*, 24(6):724–730.

Zah, E., Lin, M.-y. M.-Y., Silva-Benedict, A., Jensen, M. C., and Chen, Y. Y. (2016). T Cells Expressing CD19 / CD20 Bispecific Chimeric Antigen Receptors Prevent Antigen Escape by Malignant B Cells. *Cancer Immunol. Res.*

Zanders, E. D., Lamb, J. R., Feldmann, M., Green, N., and Beverley, P. C. (1983). Tolerance of T-cell clones is associated with membrane antigen changes. *Nature*, 303(5918):625–627.

Zhao, Z., Condomines, M., van der Stegen, S. J. C., Perna, F., Kloss, C. C., Gunset, G., Plotkin, J., and Sadelain, M. (2015). Structural Design of Engineered Costimulation Determines Tumor Rejection Kinetics and Persistence of CAR T Cells. *Cancer Cell*, 28(4):415–428.

Zhong, X. S., Matsushita, M., Plotkin, J., Riviere, I., and Sadelain, M. (2010). Chimeric Antigen Receptors Combining 4-1BB and CD28 Signaling Domains Augment PI3 Kinase/Akt/Bcl-XI Activation and CD8+ T Cell-Mediated Tumor Eradication. *Mol Ther*, 18(2):413–420.

Zhu, D.-M., Dustin, M. L., Cairo, C. W., Thatte, H. S., and Golan, D. E. (2006). Mechanisms of Cellular Avidity Regulation in CD2–CD58-Mediated T Cell Adhesion. *ACS Chem. Biol.*, 1(10):649–658.

Zimmerman, A. W., Joosten, B., Torensma, R., Parnes, J. R., Van Leeuwen, F. N., and Figdor, C. G. (2006). Long-Term Engagement of CD6 and Alcam Is Essential for T-Cell Proliferation Induced by Dendritic Cells. *Blood*, 107(8):3212–3220.

Zinkernagel, R. M. and Doherty, P. C. (1974). Restriction of in vitro T cell-mediated cytotoxicity in lymphocytic choriomeningitis within a syngeneic or semiallogeneic system. *Nature*.